THE UNIVERSITY *of* EDINBURGH

A global study of lake surface water temperature (LSWT) behaviour and the tuning of a 1-dimensional model to determine the LSWTs of large lakes worldwide

Aisling Layden

Doctor of Philosophy – The University of Edinburgh - 2014

Declaration

This thesis has been composed by myself and all work reported herein is my own work except where otherwise stated

Aisling Layden

Acknowledgements

I gratefully acknowledge that this work is funded by the European Space Agency under contract 22184/09/I-OL. I wish to thank my supervisors Dr Chris Merchant and Dr Roy Thompson and research associate, Dr Stuart MacCallum for their invaluable support. I also wish to acknowledge Georgy Kirillin, the author of *FLake* lake model for his advice and Simon Hook for supplying the lake surface temperature observation from the Inland Water Body Project (IWBP).

Finally, a very appreciative thank you to my family and friends for their support and encouragement.

Abstract

Lake surface water temperatures (LSWTs) of 246 globally distributed large lakes were derived from Along-Track Scanning Radiometers (ATSR) for the period 1991 to 2011. These LSWTs, derived in a systematic manner, presents an ideal opportunity to study LSWT behaviour on a global scale. In this thesis, the annual cycles of lake-mean LSWTs derived from these data quantify the responses of large lakes' surface temperatures to the annual cycle of forcing by solar radiation and the ambient air temperature.

Minimum monthly net surface solar irradiance (netSSI) strongly influences minimum LSWTs of non-seasonally ice covered lakes (where lake-mean LSWT remains above 1 $^{\circ}$C throughout the annual cycle), explaining $\geq$ 0.88 (R^2_{adj}) of the inter-lake variation in both hemispheres. In some regions, for seasonally ice covered lakes (where lake-mean LSWT remains below 1 $^{\circ}$C for part of the annual cycle) the minimum monthly netSSI is a better predictor than latitude, of the length of the frozen period, which shows the importance of local cloud climatological conditions. Additionally, at lake locations between 1° S to 12° N, the netSSI, shown to peak twice annually, is reflected in the LSWT annual cycle.

The summer maximum LSWTs of lakes from 25° S to 35° N show a linear decrease with increasing altitude; -3.76 $\pm$ 0.17 $^{\circ}$C km^{-1} (R^2_{adj} = 0.95), marginally lower than the corresponding air temperature -4.15 $\pm$ 0.24 $^{\circ}$C km^{-1} (R^2_{adj} = 0.95) decrease with altitude. The start and end of the period where the lake-mean LSWT is greater than 4 $^{\circ}$C shows strong correlation with the spring and autumn 0 $^{\circ}$C air temperature crossing days, (R^2_{adj} = 0.74 and 0.80 respectively).

The temporally and spatially resolved LSWT observations allows for a greater practical understanding of LSWT behaviour of large lakes. For example, lakes with a greater LSWT annual range have more observed variability in the LSWT extremes, highlighting that they may be more responsive to changes in the climate than lakes with a low annual range. The nighttime LSWT trends show stronger

warming than day-night trends in the all regions, except Europe. The lake centre LSWT trends and absolute values can be generally considered representative of the lake-mean LSWT trends and absolute values.

The observed LSWT time series are used to tune a 1-dimensional thermodynamic lake model, *FLake*. By tuning *FLake* using only 3 basic lake properties, shown by myself to have the most influence over LSWTs (depth, snow and ice albedo and light extinction co-efficient), the daily mean absolute differences for 244 lakes is reduced from 3.38 $\pm$ 2.74 $^{\circ}$C (untuned model) to 0.85 $\pm$ 0.61 $^{\circ}$C (tuned model). The effect of wind speed, lake depth, albedo and light extinction co-efficient on LSWTs is demonstrated throughout the tuning process. The modelled summer LSWT response to changes in ice-off is strongly affected by lake depth and latitude explaining 0.50 ($R^2_{adj,}$ p = 0.001) of the inter-lake variation in summer LSWTs. Lake depth alone explains 0.35 ($p = 0.003$) of the variation, highlighting the sensitivity of the summer LSWTs of deeper lakes to changes in the ice-off.

Statistically significant summer/ maximum month modelled LSWT trends, from 1979-2011 are presented for lakes where the modelled LSWTs are strongly supported by observed LSWTs over the period of available observed LSWTs. For these lakes, the trends show LSWT warming of between 0.73 – 2.10 $^{\circ}$C for 29 lakes in northern temperate regions over the 33 year period (1979 – 2011). The modelled regional trends of all lakes over the same period show least warming in Africa of 0.30 $^{\circ}$C and the greatest warming in Europe, 1.35 $^{\circ}$

Acronyms

ARC-Lake	ATSR Reprocessing for Climate: Lake Surface Water Temperature & Ice Cover
(A)ATSR	(Advanced) Along-Track Scanning Radiometers
AVHRR	Advanced Very High Resolution Radiometer
CERES	Clouds and the Earth's Radiant Energy System
CRU	Climate Research Unit
DJF	December, January and February
DYRESM	Dynamic Reservoir Simulation Model
EBAF	Energy Balanced and Filled
ECMWF	European Centre for Medium-Range Weather Forecasts
ERA	ECMWF Interim Re-analysis
ESA	European Space Agency
FLake	Freshwater Lake Model
GLWD	Global Lakes and Wetlands Database
ILEC	International Lake Environment Committee Foundation
IWBP	Inland Water Body Project
JAS	July, August and September
JFM	January, February and March
JJA	June, July and August
LC	Lake centre
LM	Lake-mean
LSWT	Lake Surface Water Temperature
MAD	Mean Absolute Difference
NAVOCEANO	Naval Oceanographic Office
MINLAKE	Minnesota Lake Model
MyLake	Multi-year Lake simulation model
NH	Northern Hemisphere
NWP	Numerical Weather Prediction
SH	Southern Hemisphere

SSI	Surface Solar Irradiance
SSRD	Shortwave Solar Downward Radiation
SSTs	Sea Surface Temperatures
TCC	Total Cloud Cover
TDS	Total Dissolved Solids
TOA	Top of Atmosphere

Chapter 1 Introduction

1.1 Importance of understanding LSWT behaviour

Lake Surface Water Temperature (LSWT) is the most important factor in determining lake ecological conditions, influencing water chemistry and biological processes (Horne and Goldman 1994). Changes in the length of the ice cover period have important ecological implications. Increased summer LSWTs as a result of a longer period of solar radiation exposure may also increase the risk of algae blooms and cause a later ice-on date. Changes in the length of the ice cover period affect the timing of mixing of the surface water with deeper waters. This strongly influences nutrient cycling and primary production (Wetzel 1975). Knowledge of the timing and length of the lake surface ice free period is also important for commercial (fishing and transportation) and lake recreational activities (Williams 1965).

Reconstructing LSWTs is important from an ecological perspective. For example, the on-set of stratification occurs when the LSWT of a freshwater lake rises to above 4 $^{\circ}$C in Spring. The date of the on-set of stratification can have a bearing on the summer temperature. In summer when winds are generally low, and water temperature is high, an increase in the summer LSWTs can cause a more rapid decrease in oxygen than at lower temperatures. Furthermore, the metabolic rates of fish increase warmer water (Francis-Floyd and Florida Cooperative Extension 1992). These effects can result in fish kills and fish migration, with continued warming resulting in decreased primary production and reduced fish stocks (Vincent 2009). This suggests that LSWTs are important both in terms of accuracy and in terms of changes over time.

The extent of ice cover on lakes is a sensitive indicator of global change and also a factor in global change (Launiainen and Cheng 1998). Changes in the length of the ice cover period affect local climatic feedbacks, for example a shorter ice cover

period allows for a longer time for surface heat exchange with the atmosphere (Ashton 1986). This is particularly important in areas where there is a high concentration of lakes such as Canada (Pour *et al* 2012). For large lakes such as Great Bear and Great Slave, the lakes can alter the local climate through lake-effect storms and can impact on fluxes of heat, moisture and momentum (Long *et al* 2007). Shallow lakes, particularly those with a large surface area, such as Lake Balaton are more sensitive to atmospheric events (Voros *et al* 2010).

1.2 Background; Dynamic nature of LSWTs

Limnology, originally defined as 'the oceanography of lakes', by Forel in the 1800s, encompasses a multi-disciplinary scientific approach to the study of inland waters. The dynamic and variable nature of inland waters demanded the separation of the study of lakes from oceans. While ocean mixing regimes are predominantly driven by persistent wind patterns and a temperature gradient from low to high latitudes, for lakes, the individual lake characteristics such as depth, surface area, salinity, surrounding topography and altitude have an important effect on the lake mixing regimes. The process of mixing drives the temperature distribution throughout the lake and therefore the lake characteristics greatly affect the LSWT cycle.

1.2.1 Lake characteristics and LSWTs

Although LSWTs respond to the local meteorological conditions and climatic events, the response can be strongly affected by the individual lake characteristics. Lake characteristics vary greatly among lakes, even among lakes within the same group of lakes. For example, in the African Great Lakes, Lake Victoria has a mean depth of 40 m deep, while Lake Tanganyika has a mean depth of 570 m. The mean depth refers to the average depth of water across the entire lake. The depth difference causes the two lakes to have very different mixing regimes. Lake Tanganyika never fully mixes from top to bottom, mixing to a maximum depth of

approximately 90-100 m, while Lake Victoria mixes completely once per year, as shown in Figure 1.

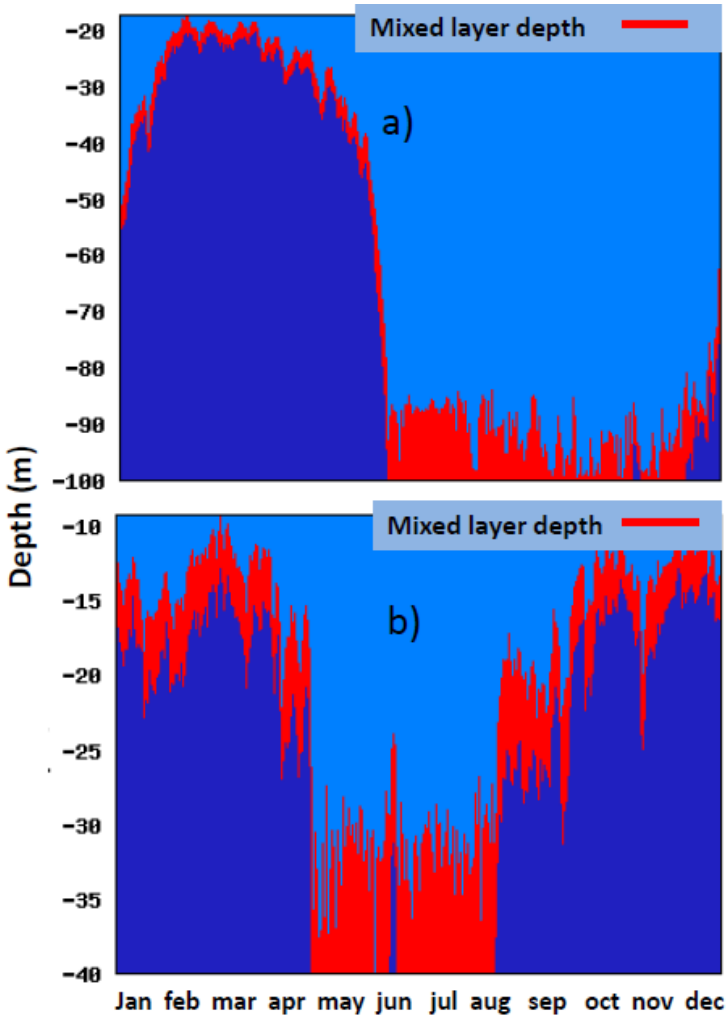

Figure 1 Mixed layer depth of two African Great Lakes a) Lake Tanganyika (6.1° S and b) Lake Victoria (1.4° S), showing that Lake Tanganyika mixes to a fraction of its depth of 570 m (90-100 m) for 5-6 months of the year while the shallower lake, lake Victoria completely mixes (depth 40 m) for 3-4 months of the year. The mixed layer depths are determined using a version of the *FLake* model (Kirillin *et al* 2011) which calculates lake temperature and mixing patterns for the perpetual hydrological year (2005/2006)

The different mixing regimes of these two lakes do not greatly affect the LSWT cycle, as the LSWT annual range in tropics is generally small. The effect of different mixing regimes on the LSWT is more pronounced in temperate regions where there is a greater range in the LSWT annual cycle. Figure 2 shows the annual lake-mean LSWT (mean of the LSWT across the entire surface) cycle of 3 North

American lakes located within 0.2° of latitude of each other; Lake Winnebago, with a mean depth of 5 m and Lake Ontario and Lake Michigan, with mean depths of 86 m and 85 m. As a result of the depth difference, Lake Winnebago freezes for two months of the year, while the LSWTs for Lake Ontario and Lake Michigan do not drop below 2 °C. The summer LSWT of the shallow lake is 2 °C greater and peaks earlier than the 2 deeper lakes and the LSWT cools more rapidly in autumn.

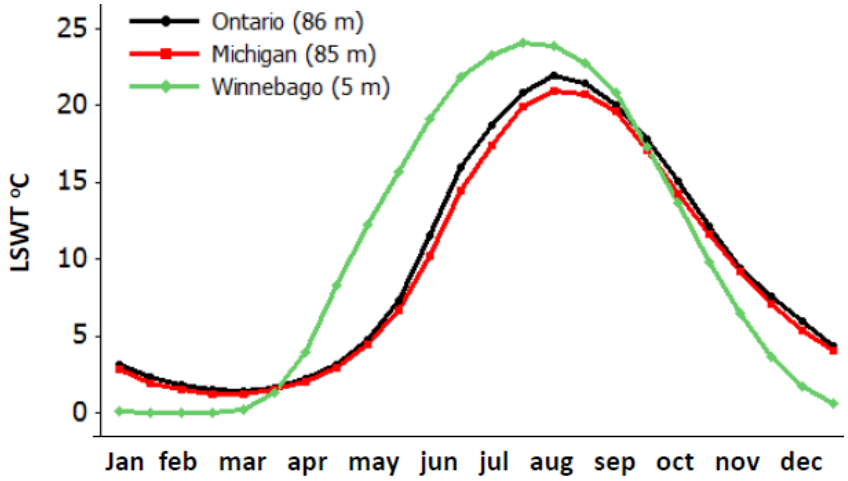

Figure 2 Lake-mean LSWT annual cycle (ARC-Lake) for 3 North American lakes at same latitude but with different depths shows that the surface of the shallow lake (Lake Winnebago) freezes for 2 months of the year while the minimum LSWT of two deep lakes remains above 2 °C.

Salinity is another highly variable lake characteristic. It affects the temperature at which water density is at a maximum, which affects the timing of density induced mixing. Mixing in turn influences the timing of LSWT cooling and of ice-on. The watershed and watershed runoff patterns are strongly influenced by the topography and can affect the LSWT. For example, high latitude lakes with mountainous surrounding can have a large influx of cooler ice melt water in late spring/ summer, which may have a cooling effect on the LSWT. There is also lake-to-lake variation in the availability and concentration of scavenging phases in lakes, for example, detrital particle and phytoplankton. These phases compete for light, oxygen and nutrients, causing large variability in the pattern of trace element distribution and behaviour (Lerman *et al* 1995a) and can greatly affect lake temperature. As a result

there is also large inter-lake and inter-seasonal variability in primary production and water turbidity. Light penetration also depends on lake depth, with shallow lakes often having poorer light penetration due to the clouding from lake bottom sediments. A clouded or turbid lake surface has less light penetration than a more transparent lake surface, and will therefore retain more heat in the surface layer. The extent of ice cover which varies greatly from lake to lake affects primary production. Primary production intensifies in lakes where there is less ice cover (Bernhardt *et al* 2012). Altitude is an important consideration for lakes, with higher altitude lakes having a colder climate with a longer ice cover period, as shown in Figure 3. Figure 3 shows the large difference in the lake-mean LSWT annual range and the maximum LSWT between a high altitude lake (Lake Oling) at 34.9° N and a low altitude lake (Lake Weishan) at 34.6° N. Lake Oling freezes for 4-5 months of the year while the minimum LSWT for Lake Weishan remains above 1 °C. Altitude also affects light absorption (Wetzel 1975) and at higher altitudes water contains less dissolved gases due to lower barometric pressures (Horne and Goldman 1994), resulting in less effective natural convective and thermal heat transfer processes.

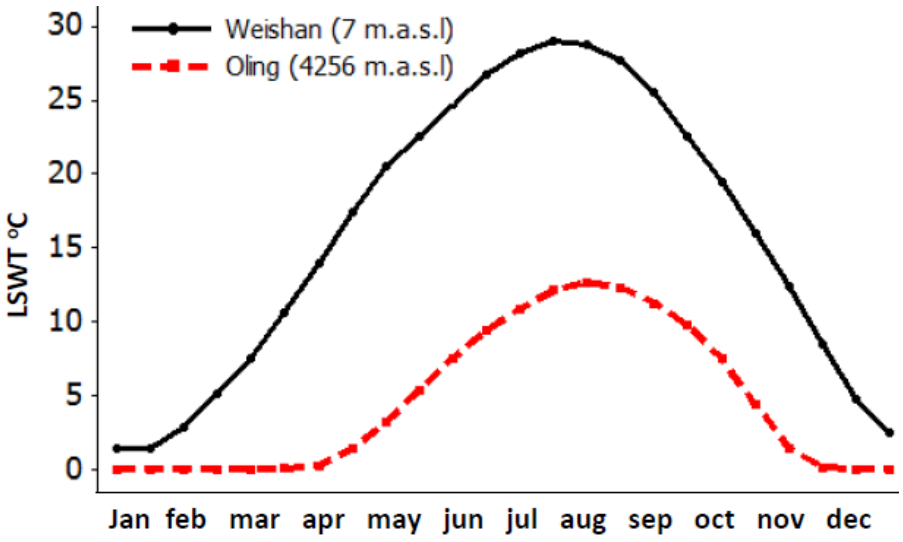

Figure 3 Lake-mean LSWT annual cycle (ARC-Lake) for 2 Asian lakes at the same latitude (~35° N) but at different altitudes showing that for the high altitude lake (Lake Oling) the surface freezes for 4-5 months of the year and reaches a maximum LSWT of 12.5 °C. For the low altitude lake (Lake Weishan), the minimum LSWT remains above 0 °C and the maximum LSWT reaches 29 °C

While the extent of ice cover varies greatly, both inter-annually and from lake–to-lake, the snow and ice albedo (referred to as albedo) also varies greatly. Albedo depends on the type of snow or ice and it varies with latitude, with higher latitudes generally having higher albedos (Manabe and Stouffer 1980). The albedo decay rates can vary substantially. The decay rates are higher for shallower snow packs and become increasingly higher over the melt period. Albedo studies on lake snow and ice are very scarce. For a small northern hemispheric lake, decay rates were shown to remain below 0.05 day^{-1} during the non-melt period and generally exceed 0.05 day^{-1} during ice melt period (Henneman and Stefan 1999). The rate of ice decay and melt is strongly affected by changes in the ice structure due to penetration from rain and melt snow or runoff (Livingstone and Adrian 2009). The extent and length of time of ice cover directly affects light penetrations through the surface water (light extinction coefficient).

The dynamic effect of climate, lake characteristics and the surrounding catchment area on LSWTs highlights the level of knowledge required to understand the highly variable LSWT behaviour of lakes.

1.3 Aim of study

1.3.1 LSWT climatological behaviour

My first research aim is to use the ATSR Reprocessing for Climate: Lake Surface Water Temperature & Ice Cover (ARC-Lake) observations, available for the period from August 1991 to December 2011) (MacCallum and Merchant 2012), to add to the understanding of the lake surface water temperature (LSWT) annual cycle (climatological) behaviour of large lake worldwide.

To meet this aim, in chapter 2, I quantify the global scale responses of the LSWT annual cycle of the large lakes to annual cycles of solar radiation (section 2.5) and air temperature (section 2.6). In section 2.7 of this chapter, for lakes that have a

lake-mean seasonal ice cover, I introduce new terminology; the climatological LSWT cold phase (the length of time the lake-mean LSWT remains below 1 °C), the LSWT open water phase (the length of time the lake-mean LSWT remains above 4 °C; the temperature at which the density of freshwater is at a maximum) and the warming and cooling intervening phases (the length of time taken for the lake-mean LSWT to warm from 1 °C to 4 °C and to cool from 4 °C to 1 °C. I refer to these as the LSWT phases. The inter-lake variability in the start and end of these LSWT phases are quantified through their dependency on the day air temperature rises above 0 °C (0 °C air warming day) or on the day air temperature drops below 0 °C (0 °C air cooling day). I extend this relationship to include lake characteristics (lake depth, surface area, altitude and distance from coast), to better explain the inter-lake variation of these phases.

1.3.2 Expanding our knowledge of LSWTs worldwide by tuning a 1-dimensional model.

Secondly, my aim is to evaluate if a 1-dimensional freshwater lake model (*FLake*) tuned with ARC-Lake LSWT observations can be used to expand our knowledge on LSWT behaviour in terms of the LSWT climatology and changes over time.

To achieve the second aim, I tune the 1-dimensional lake model *FLake* with the full time series of the ARC-Lake lake-mean LSWTs (excluding the final year which is used to independently test the tuned model), using a range of lake depth factors and a range of light extinction co-efficient and albedo (snow and ice) values. The tuned model is selected on the basis of the lowest bias of several (normalised and equally weighted) features in the annual LSWT cycle. Once tuned, the model will be evaluated to assess if tuning improves the modelled LSWTs and if the tuned model is suitable for determining long term LSWT changes globally. Chapters 3 - 6 address this aim.

1.4 Classification of lakes

For the purpose of the analysis carried out in this thesis, I divide all lakes into 2 distinct categorises. Lakes with a lake-mean LSWT climatology (determined using twice-a-month ARC-Lake LSWT timeseries observations, collapsed into one annual cycle) remaining below 1 $^{\circ}$C for part of the seasonally cycle are referred to as seasonally ice covered lakes (160 lakes). All other lakes are referred to as non-seasonally ice covered lakes (86 lakes). There is no latitudinal boundary between seasonally and non-seasonally ice covered lakes, as factors other than latitude can determine if a lake surface will freeze, such as depth and altitude, as shown in Figure 2 and Figure 3. Regional climate influences are also a factor; lakes in North America freeze at a lower latitude than lakes in Europe. Shallow low altitude lakes in North America are generally seasonally ice covered from ~ 42.5° N, and from ~ 45° N in Europe. Some deep lakes at higher latitudes in both regions (North America and Europe) do not have seasonal ice cover (lake-mean) due to their depth. For example Lake Geneva with a mean depth of 154 m, Lake Constance (90 m) and Lake Superior (147 m), located between 46.4 – 47.7 $^{\circ}$N have a minimum lake-mean LSWT in excess of 1 $^{\circ}$C. Although southern hemispheric lakes with ARC-lake observations extend to 55° S, none have seasonally ice cover. This is due to a more moderate southern hemispheric climate in mid latitude lakes.

Various lake classification systems have been derived for lakes, typically on the trophic state (measure of nutrient status), optical properties or mixing classifications. Most classifications relate to a specific lake characteristic and/ or regionally based, for example, classifications based on the optical properties have been derived for lakes in Estonia and South Finland (Arst and Reinart 2009) and for highly turbid productive waters (Sun *et al* 2012). Tropic level classifications have been based on near surface concentrations of chlorophyll (Carlson 1977) and a chlorophyll classification scheme based on phytoplankton biomass was determined for Northern and Western European lakes (Carvalho *et al* 2009). Over 100 lakes of various types in South East Estonia, were used in developing a trophic state index

based on 3 lake properties (total phosphorus and chlorophyll a, and water transparency) (Milius and Starast 1997). The thermal classification of lakes, classified on the basis of latitude and altitude (Hutchinson and Loffler 1956) was later revised to account for the effect of depth on mixing (Lewis 1983). This classification system is reproduced in Figure 4. In this thesis, I occasionally describe lakes with reference to these classifications. A description of these classifications is detailed by Lewis (1983). There are a few very deep lakes in this study that do not fit into this classification system. Some permanently stratified tropical lakes; Lake Malawi, Lake Tanganyika and Lake Kivu (Boehrer and Schultze 2008; Descy *et al* 2012) do not mix completely at any stage during the annual cycle due to their great depth, setting them apart from the warm monomictic lakes (lakes that mix from top to bottom once per year) shown in Figure 4.

As a result of the great range in latitudes of non-seasonally ice covered lakes (48° N to 55° S and the absence of the minimum LSWT restriction from ice cover, the inter-lake variation (reported as Kelvin squared, K^2) in the annual range of monthly LSWTs is almost 3 times greater (62 K^2) than in seasonally ice covered lakes (22 K^2). Consequentially, there is also more variation in Lewis's mixing classifications for non-seasonally ice covered lakes than for seasonally ice covered lakes.

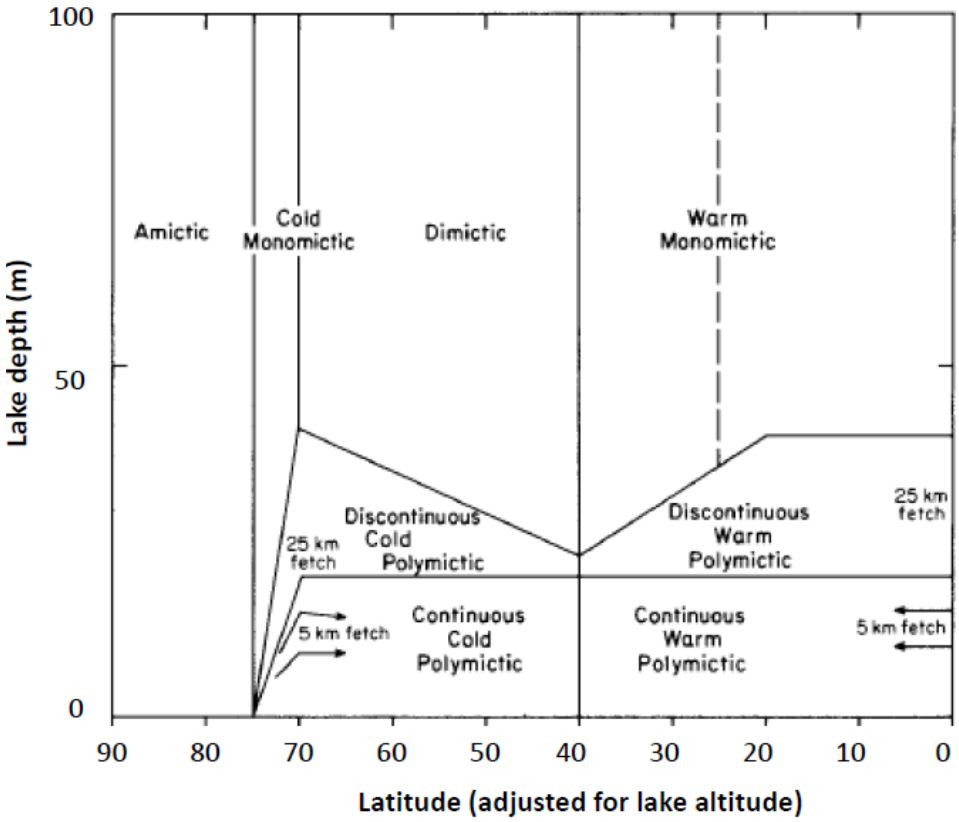

Figure 4 Mixing classification of lakes in relation to depth and latitude (adjusted for lake altitude), reproduced from Lewis (1983). Latitude is adjusted for by 0.27 $^{\circ}$C 100m^{-1} at 0° increasing to 2.4 $^{\circ}$C 100 m^{-1} at 90°. Polymictic lakes are lakes that do not develop thermal stratification due to their shallow depth and as a result they mix from top to bottom throughout the ice-free period. Dimitic lakes are seasonally ice covered that mix from the surface to bottom twice each year. A full description of these mixing classifications are available from Lewis (1983).

1.5 Recent studies of LSWTs

There have been numerous types of studies carried out on LSWTs globally. To my knowledge, remotely sensed LSWTs have not been previously analysed on a global scale to explore their climatological behaviour and dependencies. There are some regional scale climatology studies, the most substantial of which were carried out on North American lakes using *in situ* data from numerous sources. Ice phenology events were determined in this region using climate, geography and lake bathymetry (Williams and Stefan 2006). Williams *et al* (2004) found that the timing of ice-off on 143 North American freshwater lakes, was more strongly related with the spring air temperature (mean air temperature from February to June), $R^2 = 0.78$,

than with latitude ($R^2 = 0.59$). The autumn air temperature (mean air temperature from September to December) and latitude explained a similar fraction of the variation in the timing of 0.73 and 0.71 (R^2), respectively. A consistent but less significant relationship was shown, between the ice phenology events (ice-on and ice-off) and mean depth and surface area. This study (Williams *et al* 2004), also showed that a sliding mean air temperature for a fixed period before ice-on and ice-off was a poor indicator of events. A 1 $^{\circ}$C rise in air temperature was shown to cause the ice-on date to occur ~ 5 days later and the ice-off date ~ 6 days earlier. A follow-on study confirmed that the linear regression model best explained ice-off but that a log transform model best explained ice-on (Williams and Stefan 2006). Many other smaller scale or regional studies show the response of ice-on and ice-off dates to various features in the air temperatures cycle. A study on 63 Finnish lakes lying between 60° -70° N, showed that the mean temperature of individual months for up to five months before ice-on show significant correlation with ice-on timing (Palecki and Barry 1986). This study also showed regional variation in the regression coefficients. This variation was attributed to latitude and distance from coast (Palecki and Barry 1986). A study on 196 Swedish lakes, spanning 13° of latitude, showed that ice-off had a nonlinear relationship with the mean annual air temperature (Weyhenmeyer *et al* 2004). This possibly highlights regional differences, as Williams and Stefan (2006) showed that a linear regression model best explained ice-off in North American lakes. Livingston (1999) found that the ice-off on Lake Baikal is related to both the mean air temperature during the thawing phase (April) and to the month of minimum air temperature (February). This latter relationship is presumed to be due to the dependency of the ice thickness on the minimum month air temperature. Brown and Duguay (2010) suggest that the ice-on is predominantly controlled by summer and autumn air temperature.

Several other LSWTs studies are focussed on trends, the most significant of these is a long term trend analysis of historical records from a variety of sources, extending from 1846 to 1995 (Magnuson *et al* 2000). In this study, the ice-on and ice-off dates of a high latitude lake in Europe and a low latitude lake in North America

were shown to reflect the climate conditions of the 2 months preceding the events. For Lake Kallavesi, in Finland, 62.8° N, the ice-on dates reflect the October to November prevailing climate, while further south, Lake Michigan, 44.8° N, the ice-on reflects the January to February climate. Similarly the ice-off dates for Lake Kallavesi reflect the climatic conditions for April to May, while ice-off timing reflect the climatic conditions of the two previously months, February to March. In the same study, an analysis of all North American and Eurasian lakes indicated that the ice cover period shortened by 12 days over a century, due to a combination of later ice-on dates (5.7 $\pm$ 2.4 days 100 years^{-1}) and earlier ice-off dates (6.3 days $\pm$ 1.6 days 100 years^{-1}). This translates to an increase in air temperature of approximately 1.2 °C per century. Over the same period (100-150 years), in a study on Canadian lakes, the decrease in lake ice cover was attributed to the effect of global warming. At many locations in Canada, the day the mean daily air temperature falls below 0 °C in autumn and rises above 0 °C in spring explained greater than half the variation in the ice-on and ice-off timing (Duguay *et al* 2006). A 100 year analysis on Lake Superior using two primary timeseries records, showed that the open water temperatures have risen by ~3.5 °C, with most of this warming occurring the last 3 decades (Austin and Colman 2008).

More recent trend analysis from satellite observations purport to show rapid warming of nighttime LSWTs from 1985-2009 of 0.05 $\pm$ 0.01 °C yr^{-1}, across 167 globally distributed lakes (Schneider and Hook 2010). Six large lake in North America located between 38-40° N show an average warming of 0.11 $\pm$ 0.02 °C yr^{-1} from 1992-2008 (Schneider and Hook 2010). However, satellite observations only allow for a relatively short term trend analysis. Therefore trends using less than 30 years (climate period) of LSWTs may be reflecting some inter-annual variability.

Several separate studies have been carried out deriving LSWTs using MODIS (Moderate Resolution Imaging Spectroradiometer) on specific lakes over short periods of time for example, Great Salt Lake is examined between 2000 and 2007 (Crosman and Horel 2009), Lake Victoria for 2009 (Muhindo and Gidudu 2012),

Great Bear and Great Slave Lakes from 2002-2010 (Kang and Duguay 2011) and Lake Vanern and Lake Vattern for 2001 -2003 (Reinart and Reinhold 2008).

For the studies outlined in this section, there is much variation in the air temperature shown to best explain the timing of ice-on/ice-off; mean seasonal, mean of 1-5 preceding months, minimum month and the day air temperature fell below/ rose above 0 °C. This possibly highlights regional differences where other factors may have varying influences on LSWTs. It is also possible that comparing results from different studies can lead to inconsistent results due to the use of LSWTs from different sources.

1.5.1 Comparing LSWTs from different sources

Comparing the absolute LSWT values or trends from different sources can lead to disparities due to differences in the spatial and temporal resolution and in the method of LSWT retrieval or measurements. For example, the strong diurnal LSWT cycle for Lake Victoria (MacIntyre *et al* 2002) cannot be observed due to the relatively low temporal resolution of ARC-Lake LSWTs. *In situ* LSWT measurement locations in areas close to the land may not be retrievable using satellite data due to proximity to land. Lake specific influences, such as inflow from the catchment area and ice albedo can be difficult to ascertain and therefore model, causing inaccuracies in the modelled results.

Absolute LSWT differences arise due to the sub-micron surface (skin) temperature (radiometric measurements) versus the upper mixed layer (bulk) temperature (*in situ* measurements). At nighttime, in the absence of solar heating, the skin temperature detected by remote sensing is generally cooler than the bulk temperature, measured by *in situ* means. The biases associated with the skin and bulk temperature difference (skin effect), are generally in the order of 0.2 K (Donlon *et al* 2002). These biases can cause disparities between the observed and *in situ* LSWTs in diurnal studies, particularly in summer months where the skin effect

is larger. For example, for Lake Tahoe on 7th June 2001, the diurnal surface temperature range is wider (~6 °C) than the diurnal bulk temperature range, (~ 5 °C) (Hook *et al* 2003). Wind speed and solar radiation cause variability in the skin effect. At wind speeds > 6 m/s, the skin effect is well characterised but shows greater variability at low wind speeds due to greater stratification (Donlon *et al* 2002). The daytime variability in the solar radiation cycle introduces more variability in the skin effect (Hook *et al* 2003).

While observed LSWTs and LSWTs from buoy measurements may be considered robust, as they generally involve instrument calibration, hand measured *in situ* LSWTs may be less robust due to variation in equipment sensitivity and accuracy, methods and equipment calibration. LSWTs derived using different methods but from the same observation instruments have also shown to give rise to disparities. In the 'State of the Climate Report 2011' (Hook *et al* 2012), ARC-Lake trends and LSWT trends derived under the Inland Water Body Project (IWBP) showed regional differences, despite both being derived using ATSRs. These differences show disparities in the magnitude of warming in some regions and whether warming has actually occurred in other regions. This adds ambiguity and doubt to the certainty and extent of LSWT changes globally.

1.6 Application of ARC-Lake observed LSWTs

To meet the aims of this study (outlined in section 1.3), I use ARC-Lake LSWT observations.

1.6.1 ARC-Lake observed LSWTs

LSWTs of 246 globally distributed large lakes, principally those with surface area > 500 km^2 (Herdendorf 1982; Lehner and Doll 2004) were generated from the three ATSRs, (MacCallum and Merchant 2012). This series of ATSRs; ATSR1, ATSR2 and AATSR (Advanced ATSR), on board the European Space Agency (ESA) satellite ENVISAT, measured the earth's surface temperature over a 20 year period,

from August 1991 to December 2011. The length of the time series varies for the 246 lakes, depending on instrument coverage. One hundred and nineteen (119) lakes have continuous LSWT observations for 20 years (all 3 ATSR instruments, from August 1991 to December 2011), 113 have 16 years of continuous LSWT observations (2 ATSR instruments), and 14 lakes have 8-9 years of continuous LSWT observations (1 ATSR instrument). Observations are made at a spatial resolution of ~ 1 km at nadir and averaged to 0.05° cells (~5 km). The full resolution of 0.05° cells which results in a possible 25 observations per cell greatly increases the likelihood of LSWT retrieval, which is important in areas where cloud cover persists. The temporal resolution of LSWT retrievals averages < 1 week. Each 0.05° cell has an uncertainty in the order of 0.4 K (relative standard deviation).

A target lake is identified on the basis of the geographical co-ordinates of a pixel in the ATSR imagery. A land/water mask (fixed in time) reconciling the global lakes and wetlands database (GLWD) polygon area and Naval Oceanographic Office data (NAVOCEANO) was developed specifically to define lake boundaries used in the ARC-Lake project (MacCallum and Merchant 2012). Valid LSWTs are estimated only for pixels that are effectively free from cloud (clear-sky). An algorithm based on Bayes' theorem (Merchant *et al* 2008) is employed for assigning a clear-sky probability to each pixel. The effectiveness of the lake product retrieval algorithms is assessed using two methods of data validation: analysis of the performance for case study images at full ATSR resolution and quantitative point comparisons with *in situ* observations. A match-up data set from *in situ* temperature data consisting of 52 observation locations covering 18 of the lakes was constructed. The majority of these lakes are located in North America or northern Europe but also include an African and Oceanic lake. The difference between the instruments ranged from a mean of -0.34 °C to -0.09 °C (day) and -0.18 °C to +0.06 °C (night) (MacCallum and Merchant 2012).

The uncertainty in LSWT observations (~0.4 K per cell) is higher than for sea surface temperatures (SSTs) derived using ATSR instruments, ~0.2 K, primarily

due to factors such as altitude, emissivity and continentality of air masses. LSWT retrieval uncertainties may be larger than the average uncertainty where cloud (and perhaps aerosols) are present or if there is failure in cloud detection. The relative sparseness of the validation match-up (between LSWT retrieval and *in situ* data) compared with SST match-up prevents a reliable quantification of the retrieval uncertainties associated with cloud detection errors (MacCallum and Merchant 2010).

Of the 263 lakes originally targeted, 15 lakes are omitted due to a low rate of successful observation retrievals and 1 lake (Lake Natron) due to large seasonal variation in the surface area. The location of the 246 lakes, extending from 55° S to 69° N, classified by surface area is shown in Figure 5.

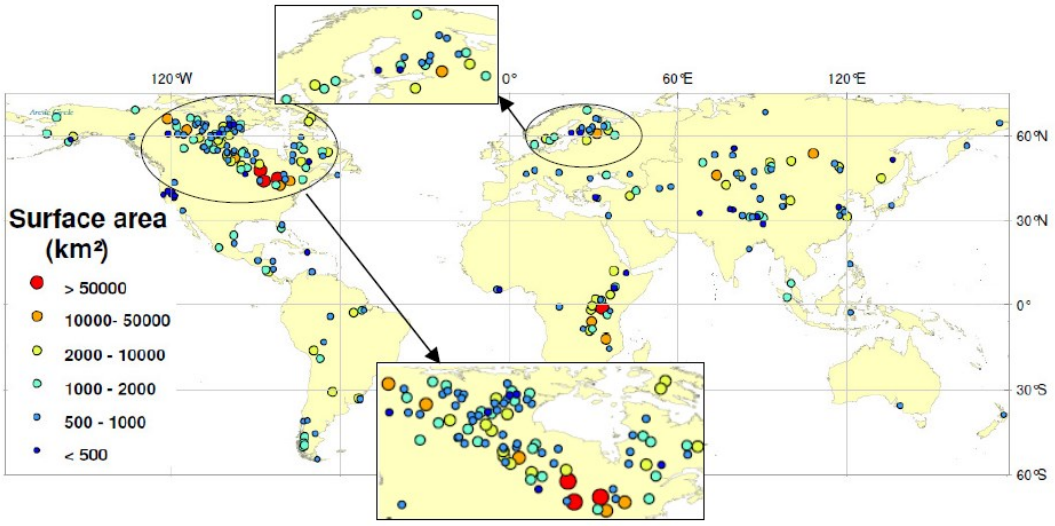

Figure 5 Location of 246 observed lakes colour coded by surface area (obtained using polygon area in GLWD) showing zoomed inset of North America and Northern Europe

1.6.2 How can ARC-Lake LSWTs add to the knowledge of LSWT behaviour?

The globally available set of spatially resolved observations for a wide number of lakes, derived in a systematic manner, such as ARC-Lake observed LSWTs, has the

potential to greatly add to the understanding of the global LSWT behaviour. ARC-Lake LSWT trends and features in the LSWT cycle will be examined in a consistent manner. For example the ice-on and ice-off dates will be examined in relation to the day air temperature drops below 0 °C or on the day air temperature rises above 0 °C. It is therefore expected that an analysis of these data will allow like-for-like comparison to be made, avoiding the spatial, temporal and methodological disparities outlined in section 1.5.1.

Due to the high effective heat capacity per unit area of lake water (Wetzel 1975), the synoptic variability of air temperature is lessened in lake temperatures, resulting in less extreme LSWTs. This allows the frequency of observations available (the average temporal resolution is < 1 week), to support a useful quantification of the lake surface water temperature (LSWT) variability in lakes. Temporal and spatial investigations of this data set would also answer some relevant questions on the LSWT behaviour of large lakes, such as, are lake-centre LSWTs representative of lake-mean LSWTs? Are nighttime LSWTs warming faster than day-night average LSWTs? Does the observed inter-annual variability in the summer LSWTs vary with latitude or regionally? Furthermore, the observed LSWTs can be used to tune a lake model, the model can then be run over a longer time period, to determine longer term LSWT changes. This helps address the issue surrounding the relatively short term LSWT observation trends.

LSWTs are important from an ecological perspective, both in terms of accuracy and in terms of changes over time, as outlined in section 1.1. Small changes in lake temperatures can have an ecological effect (Vincent 2009). As the uncertainty in the LSWT observations is relatively low (~0.4 K per cell) and the observations are derived in a systematic manner, the absolute changes over time are expected to be highly representative. Therefore the observed LSWT timeseries could be usefully applied in ecological studies.

1.7 *FLake* lake model

A 1-dimensional model which is computationally efficient and incorporates the meteorological components necessary to determine LSWTs, are the basis of the model selection. *FLake* lake model meets these requirements.

FLake is a 1-dimensional thermodynamic lake model (made available from Kirillin, 2010), capable of predicting the vertical temperature structure and mixing conditions of a lake. This model is a two-layer parametric representation of the evolving temperature profile of a lake and is based on the net heat and kinetic energy budgets (Mironow 2008) and can also be used as a lake parameterisation scheme in numerical weather prediction (NWP). The minimum set of input data required for a 1-dimensional thermal and ice model are included in *FLake*. These are the meteorological forcing data (shortwave and long wave radiation, wind speed, air vapour pressure and air temperature), an estimation of turbidity and basic bathymetric data (Lerman *et al* 1995b). Air temperature, humidity, cloud cover (which controls the amount of incident radiation) and wind speed are the variables that determine the net heat flux between a lake and the atmosphere; (Livingstone and Adrian 2009), all of which are considered in *FLake.* In the *FLake* model, the upper mixed layer is treated as homogeneous, while the structure of the thermocline (the stratified layer below the upper mixed layer), is parameterised through a self-similarity representation of the temperature profile, $\upsilon(\zeta)$, using time (T) and depth (z) as illustrated in Figure 6.

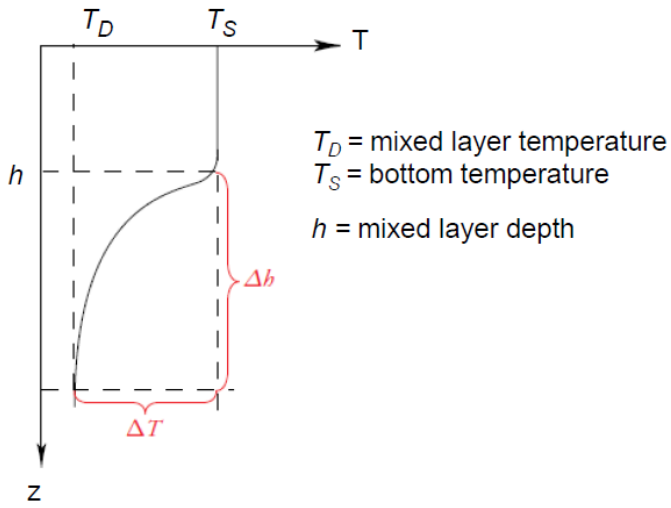

Figure 6 Schematic representation of the temperature profile in the upper mixed layer and in the thermocline, reproduced from Killirin (2003). The self-similarity representation of the temperature profile is determined using dimensionless co-ordinates, $\zeta = (z-h)/\Delta h$, and $\upsilon = [T(z)-T_D]/\Delta T$

Models based on the concept of self-similarity, are considered to be only fairly accurate (Dutra *et al* 2010). There have been few modelling studies carried out that use both the *FLake* model and observations (Voros *et al* 2010; Bernhardt *et al* 2012; Pour *et al* 2012). The findings of two of these studies show consistent biases between the modelled and observed LSWTs (overestimation of the open water LSWTs and underestimation of the ice cover period). These biases form the basis for further investigations in chapters 4 and 5. Despite these biases, *FLake* is considered to be a reliable model for studying LSWTs and ice phenology and is considered suitable for global application for ice covered lakes (Bernhardt *et al* 2012).

Although self-similarity models are considered to be only fairly accurate, the model will be tuned, therefore model accuracy is not critical when choosing a model for use in a tuning study. The process of tuning *FLake* is expected to greatly reduce the consistent biases shown between the modelled and observed LSWTs (overestimation of the open water LSWTs and underestimation of the ice cover

period), in the previous *FLake* studies. Furthermore, the biases in features of the LSWT annual cycle will be measured and reported for each lake, quantifying the level of agreement with observed LSWTs. Although initially validated for cold freshwater lakes, it is expected that *FLake* is globally applicable and is also suitable for tuning LSWTs for deep tropical lakes and saline lakes (investigated in chapters 4 and 5). Additionally, *FLake* requires relatively little lake specific knowledge, and is therefore less resource intensive when modelling 100's of lakes.

It is the intention of this tuning study to minimise the modelled LSWT biases, by tuning the model with the observed LSWTs for each lake, aiming for an average daily mean absolute difference (MAD) of ≤ 1 $^{\circ}$C, across all lakes. An MAD of ≤ 1 $^{\circ}$C is possibly accurate enough for a global scale study. A lower MAD target may not be achievable for this tuning study which comprises of lakes with a wide range of geographical and physical characteristics.
A version of *FLake* model (Kirillin *et al* 2011) is also available which calculates lake temperature and mixing patterns for the perpetual hydrological year (2005/2006). This version requires only mean depth, geographical co-ordinates and an estimate of water transparency, while incorporating the same lake physics as the *FLake* model used in the tuning study. This version of *FLake* was used in Figure 1 to demonstrate the mixed layer depth Lake Tanganyika and Lake Victoria.

In chapter 3, I show that 3 basic lake properties in *FLake,* have the most influence over the modelled LSWTs; lake depth, the reflectivity of snow and ice (albedo) and light penetration through the water surface (light extinction co-efficient). Tuning the lakes using these 3 properties, minimises the amount of lake specific knowledge that would otherwise be required to model LSWTs.

1.7.1 Other LSWT models

There are a number of other 1-dimensional simulation models, capable of determining the vertical temperature structure and mixing conditions of a lake at

various depths and on various timescales. For example, DYRESM (Dynamic Reservoir Simulation Model), MINLAKE (Minnesota Lake Model) and MyLake (Multi-year Lake simulation model).

MINLAKE is considered a good predictor of regional scale surface temperatures, thermocline depths and duration of stratification, with relatively modest model input requirements (Kamari 2001). In MINLAKE, the lake is subdivided into layers of variable thickness and other aspects of water quality are determined, such as, settling of particles, and several biological and chemical processes related to primary productivity (Riley and Stefan 1987). As a result MINLAKE is less computationally efficient than *FLake*. MyLake, was shown to have a good level of sensitivity and certainty (Saloranta and Andersen 2007). MyLake also models water quality, computing the phosphorus-phytoplankton dynamics. This increases the model computation time. DYRESM is a hydrodynamic model and like *FLake*, it is widely used globally. It uses a layer concept, in which the lake is modelled as a system of dynamic horizontal layers of changing depths, reducing the stability problem associated with fixed layers (Imerito 2013). Although layer concept is relatively simple, it is only modestly efficient. Additionally DYRESM requires detailed knowledge on lake morphometry e.g. number and heights of inlets and outlets.

1.7.2 What can be gained from the tuning of *FLake*?

The tuned model can be used to assess LSWT behaviour, in a way that cannot be done using the LSWT observations. For example, by changing the albedo (which strongly influences the timing of ice-off), the inter-lake variability of the effect of ice-off on the summer LSWTs can be examined. The tuned model can be run for a longer time period, using the complete available timeseries of the meteorological forcing data used in the tuning process. Allowing longer term LSWT trends to be considered, addresses the issue of having relatively short term LSWT observational

data. Lastly, the values for the optimal LSWT regulating properties (lake depth, albedo and light extinction co-efficient) determined from the tuning process are expected to provide a basis for improving LSWTs modelled in *FLake*.

1.8 Layout of thesis

Chapter 2 This chapter addresses aim 1, as described in section 1.3.1. I quantify the global scale responses of the LSWT annual cycle in terms of solar radiation and air temperature. I quantify the inter-lake variability in the start and end of the open water and cold phases in terms of their dependency on the 0 $^{\circ}$C air temperature days and extend this relationship to lake depth, surface area, altitude and distance from coast.

Chapter 3 Chapters 3-6 address aim 2. The main aim of chapter 3 is to discuss the use of *FLake* in the tuning study and to discuss the 3 LSWT regulating properties (lake depth, albedo and light extinction co-efficient) used in the tuning process. I also suggest the need to apply a wind speed scaling to the model meteorological forcing data, to better represent wind speeds over water.

Chapter 4 The aim is to successfully tune *FLake* for all seasonally ice-covered lakes (160 lakes) using the lake-mean observed LSWTs. Through a series of trials, I apply a range values/ factors to the LSWT regulating properties and apply wind speed scalings to the wind forcing data. I describe the metrics by which I tune the model and how they relate to the LSWT regulating properties.

Chapter 5 The aim is to successfully tune *FLake* for all non-seasonally ice-covered lakes (86 lakes) using the lake-mean observed LSWTs, using a similar approach as outlined for chapter 4.

Chapter 6 Having established in chapters 4 and 5 that the tuned model LSWTs are substantially closer to the observed LSWTs by means of the tuning metrics, in

chapter 6, I assess how well the tuned model (run for a period of 33 years, the length of time of available model forcing data) represents both the regional and lake-specific long term summer trends. I also investigate the meteorological drivers of LSWT trends, using air temperature and shortwave solar downward radiation.

Chapter 7 In this final chapter, new findings and supportive evidence in the LSWT behaviour (climatological and changes over time) from chapters 2-6 are drawn together and discussed. Some of these findings give rise to suggestions for further study in this area.

1.9 Notes on conventions used in this thesis

All regression values from analysis carried out within this thesis are reported as adjusted R^2 (R^2_{adj}) values, which consider the ratio of the number of observations to the number of predictors. R^2_{adj} are shown as fractions. Throughout this study, the dispersion of biases/ values between lakes is characterised using $\pm$ 2 standard deviation (σ), encompassing ~95% of the data. When presenting regional trends, the error bars (level of uncertainty) are calculated using 2 standard errors, giving a confidence level of ~95%.

Chapter 2 Global climatology of LSWTS of large lakes by remote sensing

2.1 Introduction

Lakes act as integrators for the many factors affecting their temperature (Schneider *et al* 2009), such as local climatic conditions (air temperature, wind speed, and surface solar irradiance), air temperature having most influence (Livingstone and Adrian 2009). Lake temperature response to air temperature can be affected by physical lake characteristics (morphometry and altitude) (Brown and Duguay 2010), inflow from streams and land run-off (Williams 1965). There is a need for a global scale understanding of the climatic and lake characteristic drivers of LSWT climatology. Due to the high effective heat capacity per unit area of lake water (Wetzel 1975), the synoptic variability of air temperature is lessened in lake temperatures, resulting in less extreme LSWTs. This allows the frequency (average of < 1 week) of global scale observations available from remote sensing to support a useful quantification of LSWT variability. Given climate change predictions of increases in the frequency and magnitude of air temperature extremes in the 21st century (IPCC 2012), determining the global scale response of LSWTs and the timing of ice phenology events (ice-on and ice-off dates) to ambient air temperatures is highly important in their prediction. Ice-on and ice-off is a good indicator of climate variability and climate change (Duguay *et al* 2006) and have been considered for use as an index for climate change (Palecki and Barry 1986; Lenormand *et al* 2002). Latitude is strongly related to air temperature and has been considered as a proxy for air temperature in many LSWT studies (Weyhenmeyer *et al* 2004). As a result, latitude is also strongly related to LSWTs, though this can vary with region and with season. For example, in the tropics, minimum LSWTs correlate with latitude (Lewis 1996), while at higher latitudes, the presence and extent of lake ice cover can significantly alter the relationship between LSWT and latitude. Lake location can also affect the response of LSWTs to changes in ambient air temperatures over time. At 38° to 40° N, summer LSWT warming was shown to

be approximately twice that of the minimum air temperature (Austin and Colman 2008; Schneider *et al* 2009), while for Lake Malawi at 12° S, the winter LSWTs track the minimum air temperature (Vollmer *et al* 2005). Unlike lake latitude which is fixed, changes in the ambient air temperature have the potential to be used to predict changes in the timing of the phase transition days. The response of LSWTs to ambient air temperature is affected by other geographical and physical factors such as lake altitude, continentality, depth and the presence and extent of lake ice cover. Altitude and topography of high mountainous areas can promote distinctive weather patterns over lakes differentiating them from the weather pattern over lakes with low lying surrounding (Thompson *et al* 2009). Altitude-dependent light intensity and quality can influence LSWTs (Wetzel 1975). Continentality influences the inter-annual LSWT variability, with lakes relatively close to the coast showing considerably less variability due to the moderating oceanic effect (Thompson *et al* 2009). The temporal and spatial extent of ice cover also has a feedback effect on the local climate through changes in albedo and heat flux (Williams and Stefan 2006), with reduced ice cover resulting in increased evaporation (Brown and Duguay 2010).

In this chapter, I present a satellite-based climatology of LSWT of large lakes, including the geographical distributions of the annual cycle (section 2.3). I interpret the annual cycles of large lakes relative to the annual cycle in forcing of lakes from solar irradiance (section 2.5) and ambient air temperature cycle (section 2.5). I consider the effect of altitude on LSWTs and on ambient temperature. For lakes that have a lake-mean seasonal ice cover, I quantify the inter-lake variability of the start and end of the LSWT cold and open water phases (described in section 1.3.1) through their dependency on the day the air temperature rises above 0 °C (0 °C air warming day) or on the day the air temperature drops below 0 °C (0 °C air cooling day). I also attempt to explain more of the inter-lake variation of the start and end of the phases using lake physical characteristics; lake depth, surface area, altitude and distance from coast.

In the final section of this chapter, I examine the ARC-Lake LSWT trends and absolute values and compare them with observed LSWTs from the Inland Water Body Project (IWBP).

2.2 LSWT format, lake distribution and salinity

2.2.1 LSWT format

The ARC-Lake LSWTs of 246 globally distributed large lakes derived from ATSR instruments as described in chapter 1, section 1.6.1, are used in this climatological study. I use the lake-mean (the mean of the LSWTs for the entire lake surface) LSWT climatology (collapsing the available LSWT time series into one annual cycle) for each of the 246 lakes. I use an average of the daytime and nighttime observations, referred to as daily observations (or to day-night observations when discussed in context to nighttime observations). Daytime and nighttime observations are flagged on the basis of the solar zenith angle ($< 90^{\circ}$ = daytime, $\geq 90^{\circ}$ = nighttime). To fit the purpose of the different analyses, I use climatological data at a range of temporal resolutions; daily LSWTs (interpolated), twice a month LSWTs and monthly LSWTs.

2.2.2 Global distribution of lake size and origin

Lakes of known origin (ILEC 1999; LakeNet 2003) are categorized in terms of lake number and surface area for temperate and tropical lakes, Table 1. Due to its size, the Caspian Sea (accounting for one third of the surface area of all large lakes in this study) is not considered. The majority of lakes with unavailable lake origin (38% of lakes) are smaller lakes, accounting for only 11% of the total lake surface area. Almost two-thirds of all the observed large lakes are located between 40° to 70° N. The cluster of East African rift lakes make up a significant portion of the tropical lakes, as shown in chapter 1, Figure 5. Lake origin plays a significant part

in the global distribution and surface area of large lakes. Tectonically formed lakes are globally well distributed, while glacial lakes exist mainly in temperate regions at latitudes above 40° N. A small number of glacial lakes are found at equivalent latitudes in the southern hemisphere but are typically 5 times smaller in surface area. Table 1 highlights the surface area contribution that tectonic lakes make to the tropical large lakes (94%). The importance of the tectonically formed Great African Lakes is evident both in terms of lake depth and area, accounting for six of the eight deepest tropical lakes.

Lake origin	Temperate lakes, n = 203 (of known origin, n =132)		Tropical lakes, n = 42 (of known origin, n = 19)	
	Number (%)	surface area (%)	Number (%)	surface area (%)
Coastal, Fluvatile & Volcanic	11	4	35	6
Glacial	72	82	0	0
Tectonic*	17	14	65	94

*excluding the Caspian Sea

Table 1 Lake origin of temperate (132 lakes) and tropical lakes (19 lakes) in terms of lake number percentage and surface area percentage, showing that tectonic lakes account for most of the surface area of tropical lakes of known origin

2.2.3 Lake salinity

Salinity is a measure of the concentration of dissolved salts in a water body. A total 64 of the 246 lakes are considered saline or a mix of saline and freshwater (S/F). Salinity data from the ILEC World Lake Database (http://wldb.ilec.or.jp/), LakeNet (http://www.worldlakes.org/) and Herdendorf (1982), was obtained for 53 of these lakes. There is no available salinity data for the remaining 11 lakes.

Lakes with a total dissolved solids (TDS) content exceeding 3 g/l are considered saline (Williams 1962), although 6 of the 10 S/F lakes have a TDS of or below this value. The salinity values of these 64 lakes range from 0.5 g/l for Lake Razelm (S/F) (Vadineanu *et al* 1997) to 340 g/l for the Dead sea (Horita 2009). Over half of

the saline and S/F lakes (36 of 64 lakes) are in Asia. The most saline of these Asian lakes (>155 g/l) are at altitudes in excess of 4000 m a.s.l. or below sea level; Lake Kara-bogaz-gol (next to the Caspian sea) and the Dead sea are located at 22 m and 404 m below sea level respectively. The most saline lake in Europe is Lake Manych-Gudilo, 42 g/l (Matishov *et al* 2007), and the coastal lake of Bras d'or with a salinity value of 25 g/l is most saline North American lake.

2.3 Climatological characteristics

I demonstrate the variation in the observed LSWT annual range and summer climatological LSWTs (temporal resolution of twice a month) with latitude on a global scale. The global distribution of the annual LSWT range, Figure 7, shows as expected, a strong relationship with latitude. Lakes from 23.5° N to 23.5° S have the lowest LSWT annual range, generally < 7.5 °C. The annual LSWT range widens with increasing latitude, peaking at latitudes of 45° to 50° N. Beyond 50° N, a longer and more widespread seasonal freezing of lake surfaces causes a decrease in LSWT range, as shown in Figure 7. The variation in the LSWT range with latitude shows good consistency in North America and Europe. In Asia, the presence of high altitude lakes, confound the relationship between the LSWT range and latitude. All 13 lakes with altitudes exceeding 4000 m a.s.l., are located in Asia between 29° to 38° N (Figure 7). While > 90% of North American and European lakes are below 500 m a.s.l., only 51% of Asian lakes are below 500 m a.s.l.

Figure 8 shows the global distribution of the summer LSWTs at latitudes > 23.5° N/ S. As there is no pronounced summer in the tropics (23.5° S to 23.5° N) and the LSWTs remain high throughout the annual cycle, Figure 8 shows the mean annual LSWT in tropics. Summer LSWTs are determined using JAS LSWTs at latitudes > 23.5° N and January, February and March (JFM) LSWTs at latitudes > 23.5° S to reflect the warmest months of the LSWT cycle. There is typically a 1 month lag between the warmest months of the air temperature cycle (June, July and August at

latitudes > 23.5° N and December, January and February at latitudes > 23.5° S) and the warmest months of the LSWT cycle. For this reason the mean JAS LSWTs at latitudes > 23.5° N and JFM LSWTs at latitudes > 23.5° N represent the warmest months of the LSWT cycle. Higher altitude lakes have lower summer LSWTs, as evident for high altitude Asian lakes, Figure 8. High altitude lakes also have a smaller annual LSWT range. From 23.5° S to 23.5° N the mean LSWT range for lakes at altitudes < 1000 m a.s.l., is 25.3 °C to 29.9 °C. Within this region, the higher altitude lakes; Lake Tana at 1786 m a.s.l., Lake Poopo at 3679 m a.s.l. and Lake Titicaca at 3827 m a.s.l. (shown in Figure 8) have lower respective mean LSWTs of 21.9 °C, 13.4 °C and 12.6 °C. The LSWT cycle of a low altitude and high altitude lake at similar latitudes, shown in chapter 1, Figure 3, demonstrates the effect that lake altitude has on the LSWT cycle and annual range.

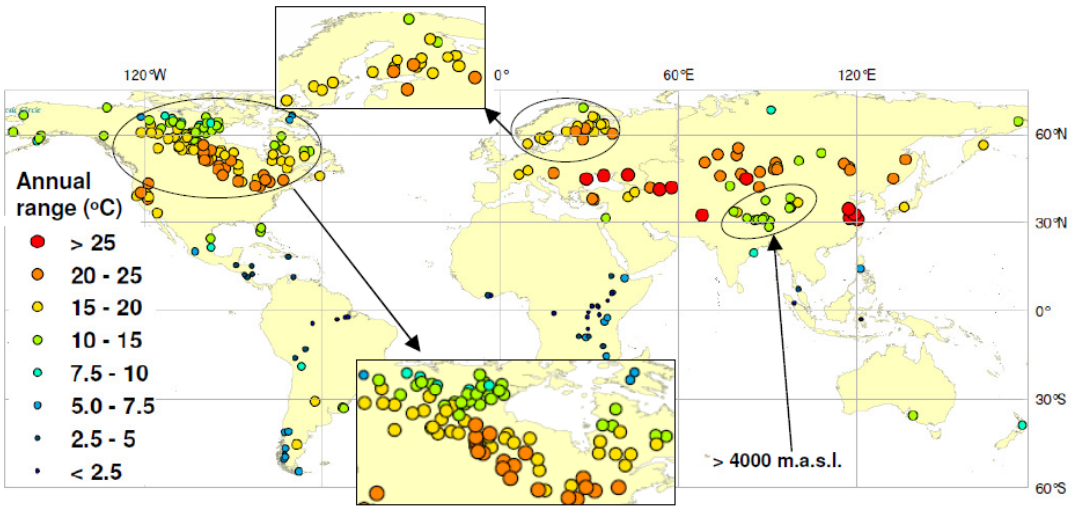

Figure 7 Global distribution of the observed annual LSWT range with zoomed inset of North America and Northern Europe, showing the strong relationship between the LSWT range and latitude in North America and showing the lower LSWT range for tropical lakes and high altitude Asian lakes

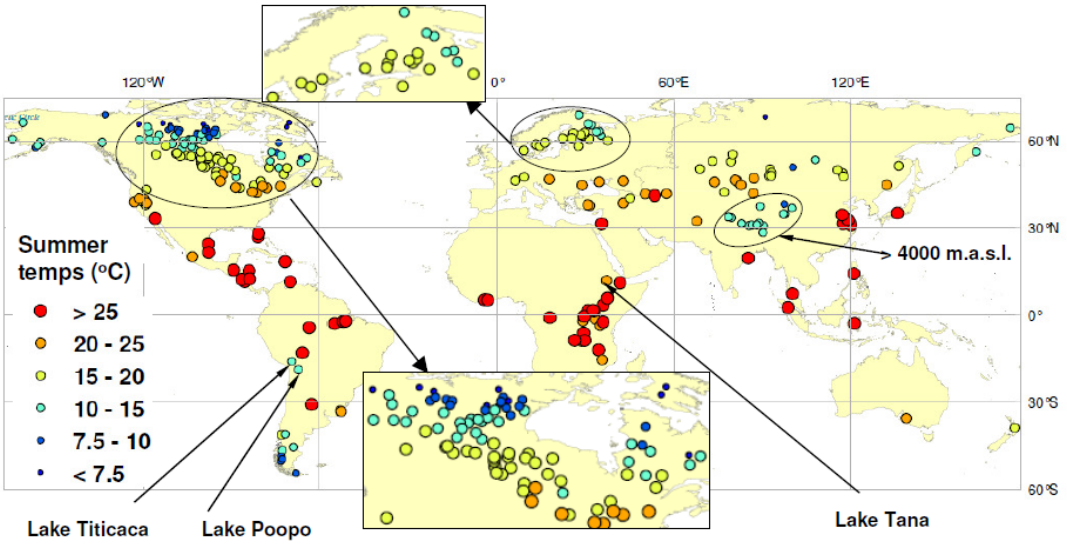

Figure 8 Global distribution of the observed mean hemispheric summer LSWTs (JAS > 23.5° N, JFM > 23.5° S) and the mean annual LSWT for 23.5° S to 23.5° N (with zoomed inset of North America and Northern Europe) showing the decrease in summer LSWTs with increasing latitude in North America and the lower summer LSWTs of high altitude lakes Asian (> 4000 m a.s.l.)

2.4 LSWT Climatological assessment

Figure 9a and b, show the observed annual LSWT cycle (temporal resolution of twice a month) for lakes at altitudes < 2000 m a.s.l. (n = 231) in latitudinal zones of 10° (for example, the 20° S zone is an average of LSWTs from 15° to 25° S). Throughout the annual cycle, LSWTs in temperate regions in both hemispheres decrease with increasing latitude and have a higher LSWT range than in equatorial and high latitude regions, Figure 9a and b. Lakes from 45° N (from the 50° N latitudinal zone) northward generally remain frozen for several months of the year. Within the latitudinal zones 0-50°, the mean annual LSWT decreases with latitude at a rate of 0.44 $\pm$ 0.02 °C per 1° latitude in the northern hemisphere (R^2_{adj} = 0.91) and at similar a rate of 0.40 $\pm$ 0.04 °C in the southern hemisphere (R^2_{adj} = 0.93). There is a notable difference between the 20° N and 30° N minimum LSWT (January): there are 11 lakes in the 30° N zone, 6 of which are located in eastern Asia (China and Japan). Harsher winters in this region result in a minimum LSWT ~13 °C lower than North American lakes at the same latitude, decreasing the overall

mean minimum LSWT in the 30° N zone, Figure 9a. In the southern hemisphere, no large lakes exist from 19° to 31°, contributing to the large difference in the 20° S and 30° S minimum LSWT (July), Figure 9b.

The observed LSWT climatology is compared with a simple LSWT parametric climatology model, Figure 9c and d. Developed by Straskraba (1980), this parametric fit was based on the annual surface temperature variations of 38 lakes of medium depth, spanning 0° to 70° N at altitudes of < 2000 m a.s.l., using an atmospheric transmission factor of 0.6. The parametric fit and observed data produce a similar pattern of the hemispheric annual cycle and the extreme LSWT response to latitude is comparable. At lower latitudes in both hemispheres there is little or no change in the maximum (summer) observed and parametric LSWTs with latitude, Figure 9a-9d. At the highest latitudinal zones (from 40° to 70° N and from 30° to 50° S), both the maximum observed and parametric LSWTs decrease with latitude. The minimum (winter) LSWT from 50° S to 50° N is strongly correlated with latitude, for both the observed data and parametric fit. The observed data, however, show the limitations of a parametric fit based on relatively fewer lake observations. The parametric LSWTs do not correctly predict freezing lake conditions, as shown by the 50° N, Figure 9c. *In situ* data supports the observed data, for example, Lake Hovsgol in Mongolia located at 51° N and 1640 m a.s.l. freezes from November to mid-June and Lake Winnipeg in Canada, located at 52° N and 214 m a.s.l. freezes from November to March (ILEC 1999). For most latitudinal zones Figure 9a- 9d, the parametric fit and observed annual range data are within $\pm$ 3 °C of each other. The exceptions are latitudinal zones 30° N, 40° S and 50° S, where the LSWT annual ranges differ by +9 °C, -12 °C and -13 °C respectively. In the 40° S latitudinal zone, the observed data yields an annual mean LSWT range of 8 °C, which is substantially lower than the parametric fit range of 20 °C. *In situ* data supports the observed LSWT data. For example, the LSWT range from *in situ* climatology for New Zealand's Lake Taupo (-39° S) and Argentina's Lake Nahuel Huapi (-41° S) are 9.4 °C (Gibbs 2010) and 9 °C (ILEC 1999)

respectively, corresponding well with the corresponding LSWT observations of 8.6 °C and 6.5 °C. At the 30° N latitudinal zone, the observed data yields an annual mean LSWT range (21 °C) substantially higher than the parametric fit range (12 °C). A review of lakes between 25° N -35° N yielded *in situ* annual LSWT ranges for three lakes; Lake Tai at 31° N (28 °C), Lake Chao at 32° N (27 °C) and Lake Biwa at 35° N (21 °C) (ILEC 1999). The *in situ* data are comparable to the observed data range for these three lakes; 26.2 °C, 26.2 °C and 19.6 °C respectively.

As shown, where notable differences occur between the observed data and parametric fit, comparison with *in situ* data supports the observed data, highlighting the limitations of the globally applied parametric fit and supporting the use of the ARC-Lake data in global scale studies.

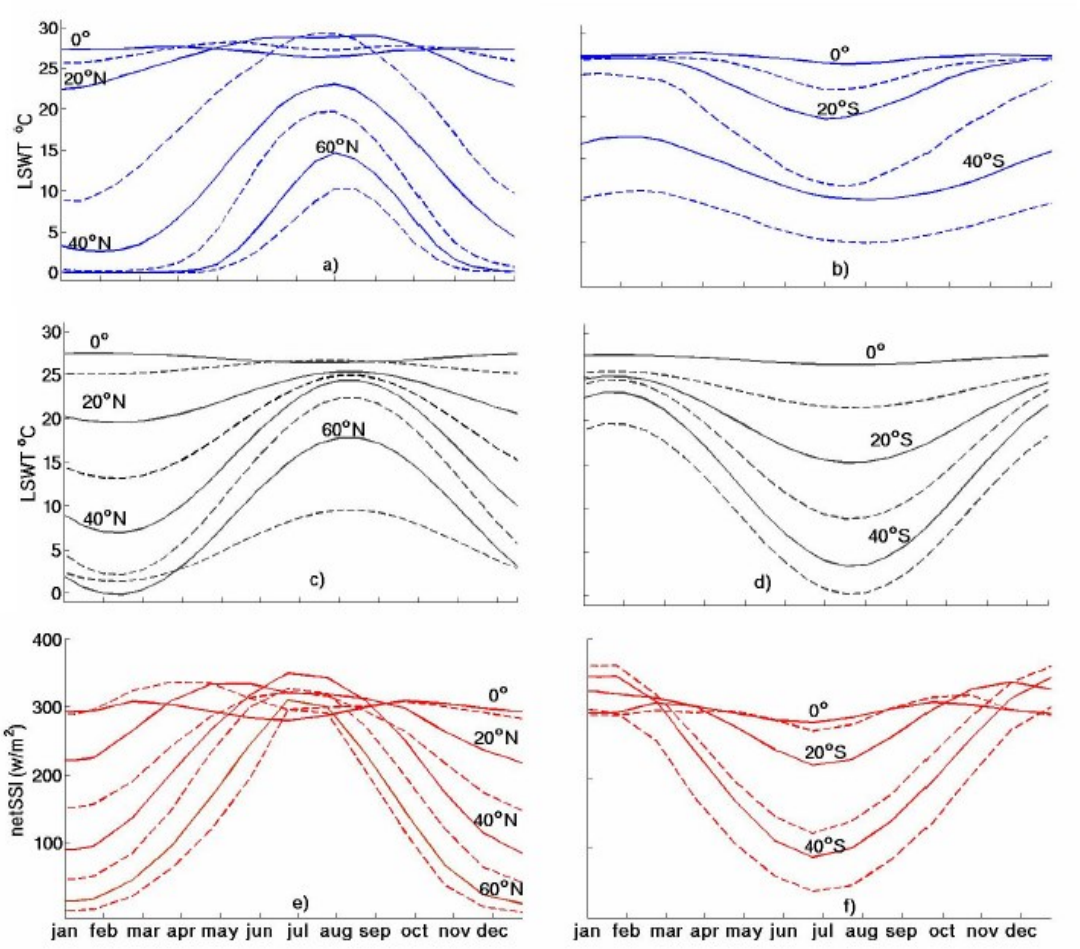

Figure 9 Observed and parameterized annual LSWT (< 2000 m a.s.l.) cycles and solar radiation cycles by 10° latitudinal zones from 70° N to 50° S. a) observed LSWT northern hemisphere (NH) n = 200 and b) observed LSWT southern hemisphere (SH) n = 31, c) parameterized LSWT for NH and d) parameterized LSWT for SH; c and d re-plotted from (Straskraba 1980) e) net surface solar irradiance (netSSI) (NH) and f) netSSI (SH); based on interpolated mean monthly observations from March 2000 to October 2005. Solids line represents even 10° latitudinal zones (labelled), broken lines odd 10° latitudinal zones (unlabelled).

2.5 LSWT responses to solar radiation

2.5.1 LSWT and solar radiation extremes

Air temperature, determined by the exchange of radiant energy between the sun, the earth's surface and the atmosphere, is driven by solar radiation, the principal source of energy to the earth's surface (Ritter 2006). LSWTs exhibit some degree of variation that corresponds to the seasonal cycle of solar radiation at a given latitude (Lerman *et al* 1995a). This is evident from the broad similarity, with time lag, of the hemispheric annual LSWT cycle Figure 9a and b) and the hemispheric net surface solar irradiance (netSSI) climatology (Figure 9e and f). The incoming and reflected monthly shortwave radiation data are derived from the Energy Balanced and Filled (EBAF) data set (resolution 1° x 1°) from the Clouds and the Earth's Radiant Energy System (CERES) project (Loeb *et al* 2009).

The minimum netSSI (at the lake centre grid references of all lakes < 2000 m a.s.l.) is strongly correlated with latitude throughout both hemispheres; decreasing with increasing latitude at a marginally higher rate in the southern hemisphere, 5.1 ± 0.3 W/m^2 per 1° latitude than in the northern hemisphere; 4.8 ± 0.1 W/m^2 per 1° latitude ($R^2_{adj} \geq 0.96$). Similarly, the corresponding minimum LSWT decreases at a rate of 0.46 ± 0.04 $^{\circ}$C per 1° latitude ($R^2_{adj} = 0.94$) in the southern hemisphere and 0.44 ± 0.03 $^{\circ}$C per 1° latitude ($R^2_{adj} = 0.79$) in the northern hemisphere. Consequentially, there is a strong correlation between the monthly minimum netSSI (> 60 W/m^2) and minimum LSWT in both hemispheres ($R^2_{adj} \geq 0.88$), for lakes < 2000 m a.s.l., as shown in Table 2. From 45° N northwards, the minimum netSSI decreases to below 60 W/m^2, at which point the lake-mean LSWT approaches ~0 $^{\circ}$C, confounding the relationship between minimum netSSI and minimum LSWT. Globally and regionally, the minimum monthly netSSI of seasonally ice covered lakes are well correlated with the length of the cold phase, explaining 0.73 (R^2_{adj}) of the variation in North America lakes (93 lakes) while latitude explains 0.67 of the variation.

Variable	Region	Number of records	R^2 adjusted	Standard error (ºC)	Constant	Coefficient of Variable (ºC W/m^2) $^{-1}$
Minimum netSSI	NH (0º-45º N)	61	0.88	3.9	-7.37	0.121
	SH (0º -55º S)	31	0.90	3.1	+1.94	0.086

Table 2 Linear regression of minimum observed LSWT versus minimum netSSI for lakes < 2000 m a.s.l. where the minimum netSSI > 60 W/m^2 (from 0° to 45° N and from 0° to 55° S), showing that the minimum month netSSI is a very strong predictor ($R^2_{adj} \geq 0.88$) of the variation in the minimum LSWTs

The maximum netSSIs are poorly correlated with the maximum LSWTs in both hemispheres. As shown in Figure 9e and f, while the maximum netSSI show little change with latitude, the length of time that the netSSI levels are at a maximum decreases with increasing latitude. This directly affects the amount of heat absorbed through the lake surface in summer. As a result, the variation in the maximum LSWTs is better explained by latitude than netSSI, explaining 0.67 of the inter-lake variation in the northern hemisphere and 0.82 in the southern hemisphere.

2.5.2 LSWT response to equatorial insolation cycle

Between latitudes of 5° S and 10° N, top of atmosphere (TOA) solar radiation peaks twice a year, exhibiting two solar maxima and minima. The maxima occur towards the end of March and the end of September and the deeper minimum occurs during the hemispheric winter (Lewis 1987). Lewis determines the hemispheric divide to be at 3.4° N, the latitude at which the annual range of monthly TOA irradiance is at a minimum. The annual cycle of the total incoming shortwave solar radiation at all observed lake locations (21 lakes) within this range show the presence of two annual solar maxima and minima, the timing of the maxima ($\pm$ 1 month), and the occurrence of the deeper minimum in the hemispheric winter (considering the hemispheric divide to be at 3.4° N). In further agreement with Lewis (1987), the annual range of incoming solar radiation is at a minimum for lakes closest to the hemispheric divide and increases at lake locations to the north and south.

Considering the reduction of shortwave radiation to the earths' surface due to cloud cover, which varies greatly depending on time of year and latitude, the two annual peaks in netSSI extremes are present at lake locations between latitudes from 9° S and 12° N but with varying amplitude (not shown). The range of annual netSSI varies across these locations and is at a minimum at 2° S, south of which the deeper minimum netSSI generally occurs during the southern hemispheric winter. Northwards of 2° S it occurs in either hemispheric winter and the first annual maximum is dominant over the second maximum. The twice annual netSSI peaks are reflected in the LSWT cycle of all lakes (n = 16) from 1° S to 12° N, with the first annual maximum dominating the second annual maximum for 14 of the 16 lakes. The LSWT annual cycle for 6 lakes spaced throughout this region (from 1° S to 12° N) and the netSSI cycle at the corresponding latitude are shown in Figure 10. As expected, the LSWT maxima and minima lag the netSSI maxima and minima. With an optimal lag (ranging from 2 weeks - 6 weeks) applied to each lake, the variation in the netSSI cycle explain 0.76–0.97 (R^2_{adj}) of the variation in the LSWT cycle for 5 of the 6 lakes, as shown in Figure 10b and d The LSWT cycle for Lake Turkana shows a poor correlation with the netSSI cycle. The range in the annual monthly LSWTs is at a minimum at 2° S (not shown), reflecting that of the minimum netSSI range.

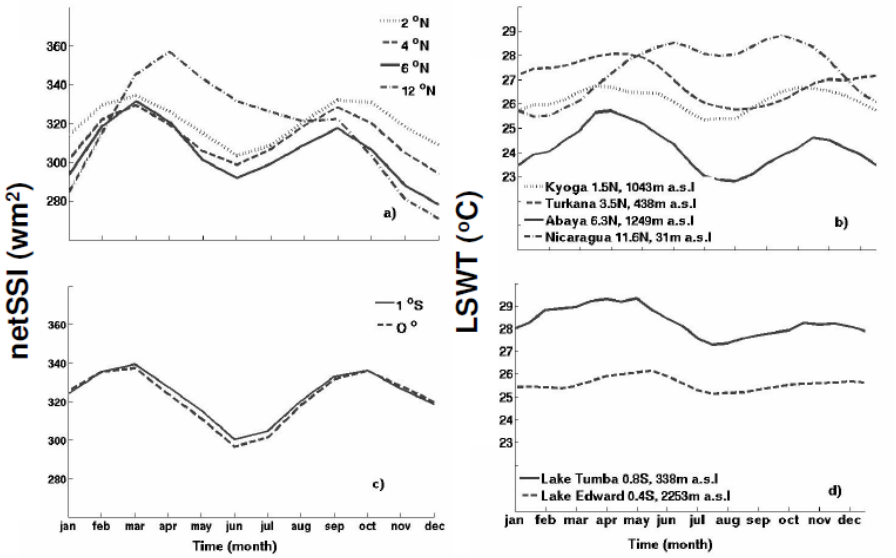

Figure 10 Annual cycle of net surface solar irradiance and LSWTs at lake locations from 1° S to 12° N; a) netSSI NH, b) LSWT NH, c) netSSI SH, d) LSWT SH, showing that the dual netSSI maxima and minima is reflected in the LSWT cycle.

2.5.3 Timing of peak LSWT

The timing of the netSSI extremes are determined from the calculated TOA daily solar heat flux at every 1° latitude and CERES 5-year reflected TOA shortwave radiation climatology (interpolated from monthly to daily). LSWT extreme timings extracted from the lake-mean daily climatological data are compared with the netSSI extreme timings to determine the LSWT/netSSI lag at each latitudinal band.

The range in latitude over which a true LSWT/netSSI lag can be defined is limited to regions where there is a strong seasonal cycle but no seasonal ice cover (non-seasonally ice covered lakes > 25° N/ S, 38 lakes). In the southern hemisphere, this range of latitudes is greater (30° S to 50° S zones) than in the northern hemisphere (30° N to 40° N zones). This is due to the predominately Mediterranean climate at lake locations 35° S to 55° S, which is considerably milder than the harsher moist continental climate from 35° S to 55° N (Strahler and Strahler 1989). Figure 11 shows a 38 day increase (day 69-31) and 43 day increase (day 71-28) in the

minimum and maximum LSWT/netSSI lag from the 30° S to 50° S latitudinal zones. There is a 23 day increase in the minimum lag between the 30° N and 40° N latitudinal zones, and no increase in the maximum lag, Figure 11.

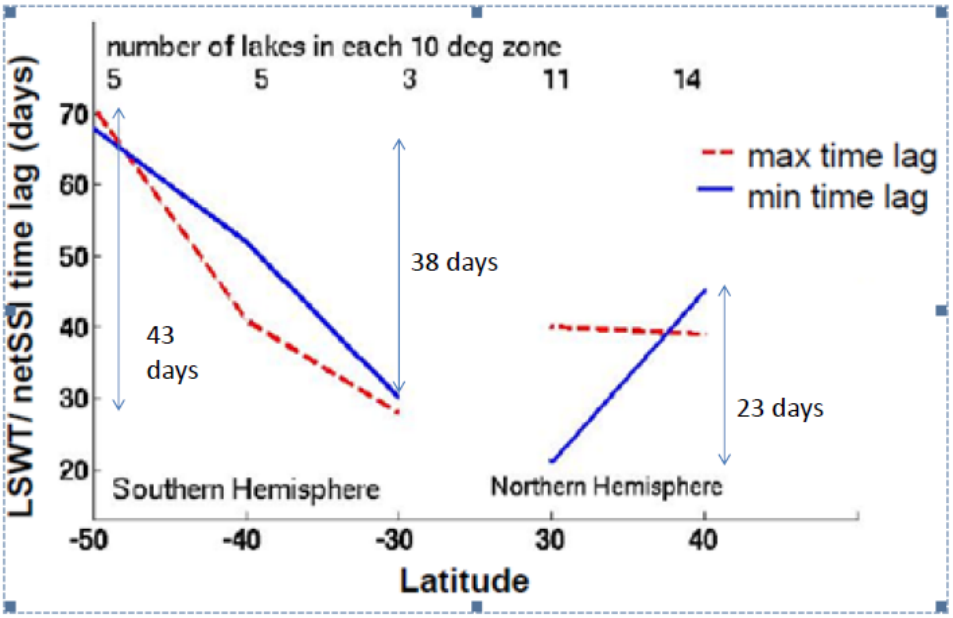

Figure 11 Zonal (10°) time lag between netSSI and LSWT extremes from 30° S to 50° S and 30° N to 40° N, showing a 38 day and 43 day increase in the minimum and maximum LSWT/netSSI lag from the 30° to 50° S and a 23 day increase in the minimum lag between the 30° and 40° N

2.6 LSWT and air temperature relationship

In this section, I consider the effect that latitude and altitude have on the relationship between monthly LSWT and air temperature climatological extremes. I use air temperature from the CRU timeseries version 3.1 (Jones and Harris 2008) data set, from January 1992 to December 2009 (0.5° x 0.5° resolution) at the lake centre grid references, collapsed into a monthly climatology. The relationship between the zonal-mean LSWT and air temperature extremes from 60° S to 70° N (in 10° latitude zones) is shown in Figure 12a. The LSWT extremes are warmer than the air temperature extremes, in latitudinal zones 60° S to 60° N, with the maximum LSWT exceeding the air temperature by 0.7 °C to 2.9 °C across this

region. The corresponding minimum temperature range is considerably greater due to seasonal ice cover at higher latitudes. Across latitudinal zones where minimum LSWTs generally remain above freezing (from 40° S to 30° N), the LSWT and air temperature extreme differences are similar; 1.2 °C to 2.9 °C for maximum temperature and 1.4 °C to 3.0 °C for minimum temperature.

The effect of altitude on the zonal LSWT and air temperatures is also shown in Figure 12a. The high average lake altitude in the 30° to 40° N zone (2335 m a.s.l.), results in lower zonal maximum temperatures than those in the 40° to 50° N zone (average altitude of 434 m a.s.l.). In Figure 12b, the altitude variation between zones is adjusted for on the basis of a strong correlation between maximum temperature (air and LSWT) and altitude, over latitudes from 25° S to 35° N. The maximum air temperature and LSWT show no evidence of a relationship with latitude across the 20° S to 30° N zones (25° S to 35° N). Within this region (66 lakes), the maximum LSWT strongly correlates with altitude, changing by -3.76 $\pm$0.17 °C km^{-1} (R^2_{adj} = 0.95), Figure 13a. Lake altitudes range from -474 to 5007 m a.s.l. and include 11 of the 13 highest altitude lakes (> 4000 m a.s.l.). This adjustment (-3.76 °C km^{-1}) is applied to the LSWT extremes (Figure 12b, solid lines), with the exception of the minimum LSWT of lakes with seasonal ice cover. The maximum air temperature strongly correlates with altitude changing by -4.15 $\pm$0.23 °C km^{-1} (R^2_{adj} = 0.95), Figure 13b. Although based on a limited region and considers only maximum temperatures, this adjustment fulfils the purpose of minimizing the effect of altitude on temperatures, allowing for a clearer view of the LSWT and air temperature relationship with latitude. Lakes at latitudes beyond 25° S to 35° N are of low altitude, averaging < 500 m a.s.l. and therefore will not be substantially affected by the adjustment.

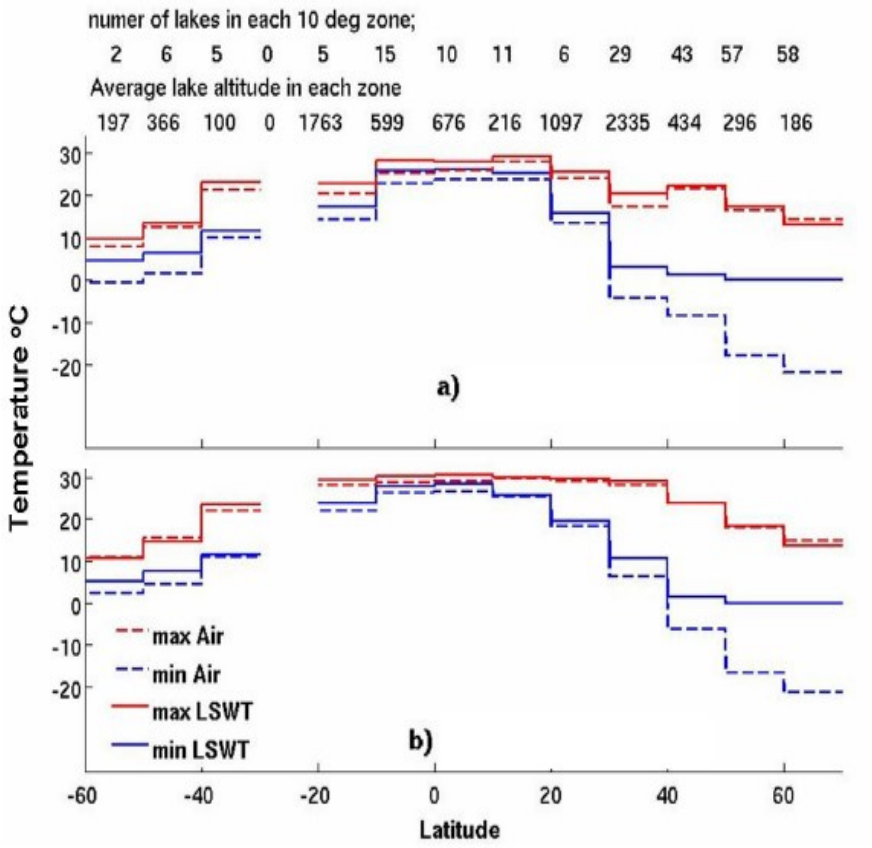

Figure 12 Monthly climatological air temperature and LSWT extremes averaged across lakes in 10° latitudinal zones (n = 246) a) no altitude adjustment b) adjusted for altitude (LSWTs by -3.76 °C km^{-1}, and air temperature by -4.15 °C km^{-1})

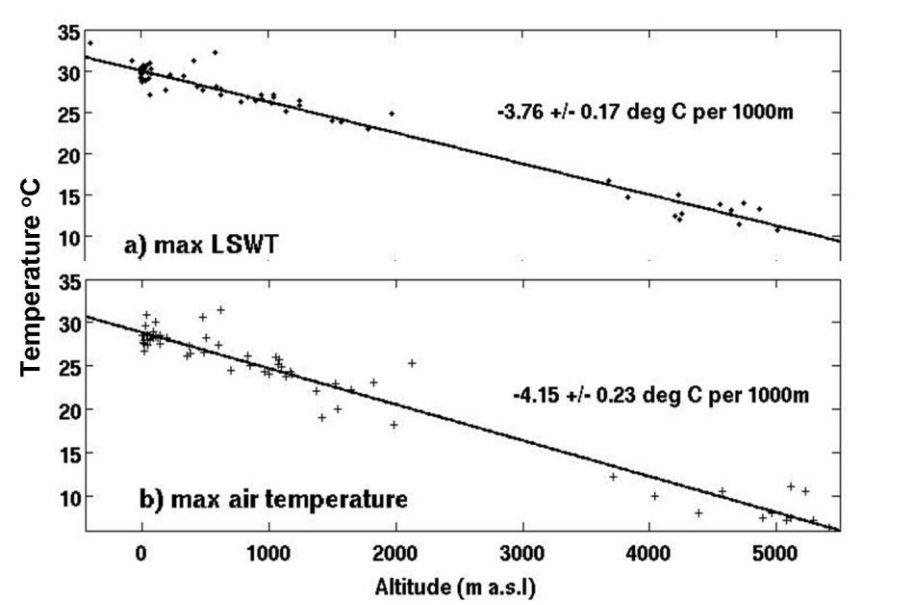

Figure 13 Regression of maximum temperature with altitude at lake location from 25° S to 35° N (n = 66) ranging from -474 to 5007 m a.s.l. a) maximum LSWT b) maximum air temperature

2.6.1 Studies of the LSWT relationship with altitude

An LSWT lapse rate (the rate of decrease of temperature with increase in altitude) of 4.3 °C km^{-1} (R^2 = 0.83) determined for 161 lakes of Papua New Guinea, ranging from 0-3800 m a.s.l. (Vyverman and Sabbe 1995), compares well with LSWT adjustment rate used in this study. A study on small temperate lakes clustered on the Swiss Plateau yielded lapse rates of 3.7–5.5 °C km^{-1} (Livingstone and Lotter 1998) and up to 6.9 °C km^{-1} in July (Livingstone *et al* 1999). The large lakes in the global dataset appear to be less strongly coupled to the air temperature lapse rate (6.5 °C km^{-1}) than the Swiss plateau lakes.

2.6.2 LSWT-air temperature difference with altitude

With the applied altitude adjustment, the LSWTs exceed the air temperatures by 0.5 °C to 1.7 °C for maximum temperature, by 0.7 °C to 1.9 °C for minimum temperature and by 0.8 °C to 1.8 °C for mean temperature. As a result of the larger altitude

adjustment rate for air temperature (0.4 °C km^{-1} higher than the adjustment for LSWT), the difference in maximum LSWT and air temperature is lessened with altitude. At 500 m a.s.l., the LSWT-air temperature difference is greater by 1.9 °C than at 1800 m a.s.l.. This is determined using lakes from 20° S to 30° N (where maximum air temperature and LSWTs show no relationship with latitude) and where the lake and air temperature altitudes are within 5% of each other. For the 6 lakes meeting these conditions (ranging from 12° S to 20° N), a strong LSWT-air temperature difference and altitude relationship is observed from March to June and over the altitude range 500 to 1800 m a.s.l. Lake altitude accounts for 0.78- 0.83 (R^2_{adj}) of the variation in the temperature difference, with differences decreasing by 1.9 °C with increasing altitude from 500 to 1800 m a.s.l. The netSSI for most tropical lakes is at its maximum in March Figure 9e and f and Figure 10a and c), indicating the variation of LSWT-air temperature difference with altitude is strongest following maximum netSSI. Altitude explains 0.33 (R^2_{adj}) of the temperature difference in July (statistically insignificant, $p = 0.14$) and drops to 0.00-0.10 from August through to February (with the exception of November). A slightly higher proportion of the variation in explained in November (0.20), possibly because this month follows the second annual netSSI maximum. A study carried out on out by Livingstone and Lotter (1998) on lakes in the Swiss Plateau (located at ~ 47° N), showed a similar decrease in the summer (June to September) LSWT-air temperature differences (1.8 °C) with increasing altitude (from 500 to 2000 m a.s.l.).

The greater range in the LSWT and air temperatures in temperate regions of the northern hemisphere, as evident from Figure 12b, is primarily due to regional climatic hemispheric differences in temperate regions. Most of the lakes in the 35° to 55° S zones are located in Chile, Argentina and Oceania and have a Mediterranean climate with an air temperature range of ~7 °C. Many regions with lake observations between 35° to 55° N have a moist continental climate with air temperature ranges of ~31 °C (Strahler and Strahler 1989). As a result the observed

temperate LSWT ranges are much lower in the Southern hemisphere. For example, for Lake Taupo, 39° S the observed LSWT range is 8.6 °C, while for Clear Lake and Walker Lake at 39° N, the LSWT range is 17.4 °C and 18.4 °C respectively.

2.7 The relationship of temperature dependent LSWT phases with air temperature and lake characteristics

A typical seasonal cycle of lake-mean LSWT for a dimictic lake is shown in Figure 14. Here, new terminology is introduced that is used in the assessment of the timing of features of this seasonal cycle in relation to ambient 0 °C air temperature and lake characteristics. The seasonal cycle can be broken down into four phases: a cold phase and an open water phase, separated by two intervening phases (warming and cooling). As illustrated in Figure 14, the boundaries of these phases are defined by the day of the year on which the lake-mean LSWT transitions through 1 °C and 4 °C. I term these dates as 1 °C and 4 °C warming and cooling days, collectively, termed as the LSWT phase transition days. I examine the timing of the LSWT phase transition days in relation to the day on which the air temperature increases from below to above 0 °C in Spring (0 °C air warming day) and decreases from above to below 0 °C in autumn (0 °C air cooling day). Collectively these are referred to as the air temperature transition days.

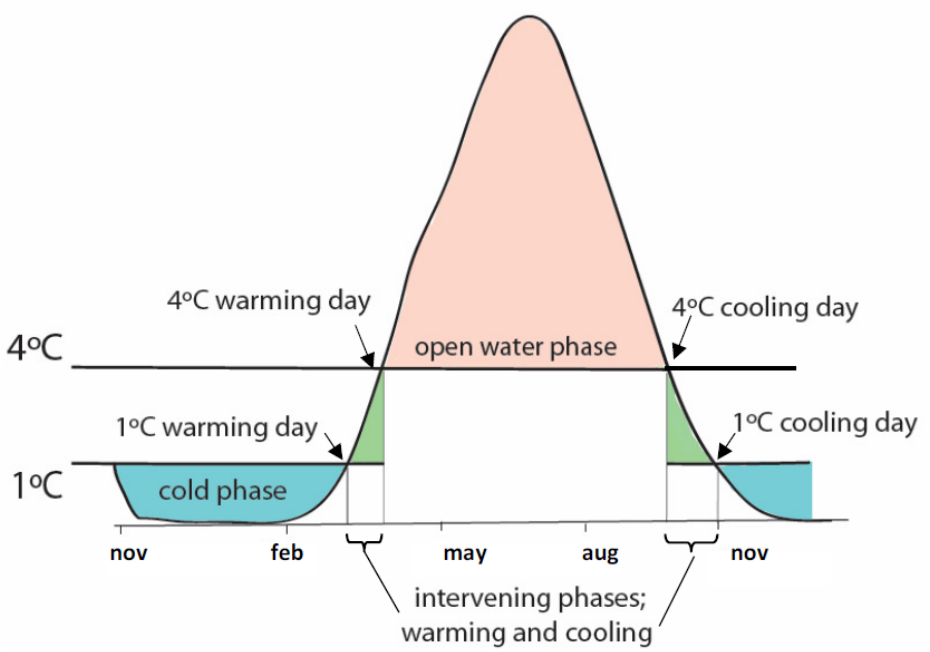

Figure 14 The climatological temperature dependent LSWT phases; cold phase, open water phase and intervening phase for lakes with a seasonal ice cover

2.7.1 LSWT phases of freshwater lakes

As illustrated in Figure 14 the start of the cold phase is marked by the day the lake-mean LSWT drops to below 1 °C in autumn (1 °C cooling day) and ends on the day it increases to above 1 °C in spring (1 °C warming day). Although the temporal frequency of satellite data are not high enough to precisely detect the first 0 °C day, interpolating to the 1 °C day is possibly a more effective indicator of ice-on/off for lake-mean LSWTs of large lakes. Typically while much of a large lakes' surface may be frozen, some parts will freeze and thaw earlier or later or remain unfrozen, yielding a mean LSWT greater than 0 °C, which may not be representative of the majority of the lake. For this reason, the cold phase is considered the period during which at least part of the lake surface is likely to be ice covered. As shown in Figure 15a and b, the cold phase transition days (1 °C cooling and warming days) show a good consistency with *in-situ* measurements of ice-on and ice-off days for 21 Eurasian and North American lakes (Benson and Magnuson 2000; Layman

2001) at locations close to lake centre over a varying time-span from 1955-2004. The observed 1 °C cooling and warming days for the 21 lakes are on average 3.3 and 2.0 days earlier than the average *in-situ* ice-on and ice-off days.

The open water phase starts on the day the lake-mean LSWT heats to above 4 °C in spring (4 °C warming day) and ends on the day the LSWT cools to below 4 °C in autumn (4 °C cooling day), Figure 14. During this phase the lake is considered to be completely ice free. A study on the Great lakes, showed that while both open water and ice are present within a lake, the range of surface temperatures will not normally exceed 4 °C (Reinart and Reinhold 2008). The start of this phase follows spring turnover, where the increasing density of warming water (from 0 °C to 4 °C) causes surface water to sink and mix with deeper waters, breaking up any remaining ice cover. When the LSWT cools to 4 °C in autumn (the same temperature as the lake bottom), the temperature (and therefore the density) of the lake is uniform and water mixes readily (autumn turnover). After turnover, the rate at which cooling and surface ice formation occurs is a function of the lake heat storage capacity, often showing a relationship with lake depth (Pour *et al* 2012). During the open water phase, the mixing and stratification patterns are highly dependent on individual lake characteristics such as lake depth and surface area, lake location (latitude and altitude) (Lewis 1983) and on other factors such as local wind conditions and salinity (Boehrer and Schultze 2008). Lake morphometry is a factor in the ice-on/off timing as it affects wind fetch, water circulation and heat storage (Pour *et al* 2012).

Changes in the length of the cold phase and open water phase have important climatic, ecological and commercial implications. For example, a shorter cold phase, (indicative of a shorter ice cover period) has a climate feedback effect by reducing the period of high albedo (from snow or ice), allowing for a longer time for surface heat exchange with the atmosphere (Ashton 1986). The longer period of solar radiation penetration increases photosynthesis, having ecological

consequences (Williams 1965) and results in warmer summer LSWTs. Warmer summer LSWTs increases the risk of algae blooms and cause a later ice-on date. Knowledge of the timing and length of the open water phase is also important for commercial (fishing and transportation) and lake recreational activities (Williams 1965).

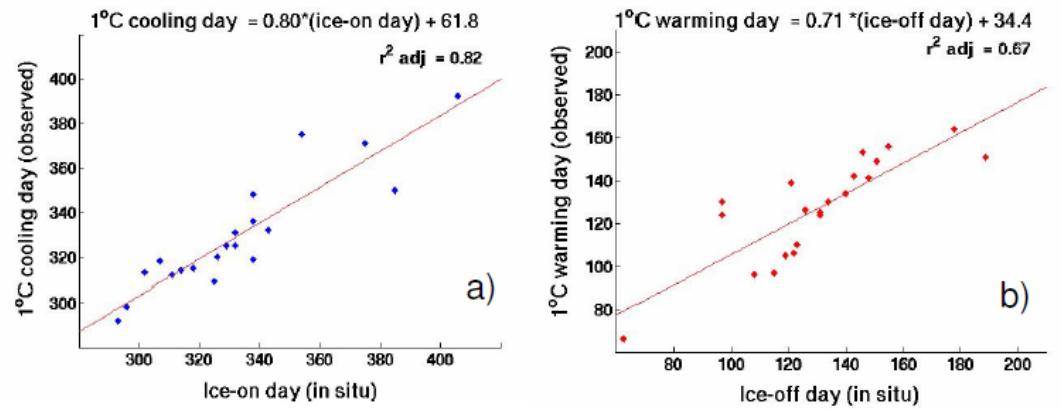

Figure 15 LSWT climatological day of year for cooling to 1 °C (1 °C cooling day) and warming to 1 °C (1 °C warming day) versus *in situ* ice-on and ice-off data a) 1 °C cooling versus ice-on day b) 1 °C warming versus ice-off day

Figure 16 displays the start and end of the cold phase for 160 seasonally ice covered lakes, spanning from 29° N to 69° N. The lengthening of the cold phase (earlier 1 °C cooling day and later 1 °C warming day) with increasing latitude is evident in North American and European lakes, Figure 16a and b. The mild partly maritime climate has a shortening effect on the cold phase in northern Europe with later cooling dates and earlier warming dates than North American lakes at corresponding latitudes. The effect of lake altitude confounds the relationship between the cooling and warming days and latitude. High altitude lakes have earlier cooling and substantially later warming than low altitude lakes, as demonstrated in chapter 1, Figure 3. Salinity lowers the temperature at which water density is at a maximum and the temperature at which water freezes, changing the physical properties of water on which these lake phases are dependent. For example, water with a typical ocean salinity value of 35 practical salinity units (psu, ~ 35 g/l), the

water freezes at ~ -2 °C (Boehrer and Schultze 2008). For this reason, this analysis is applied to freshwater lakes at low altitude.

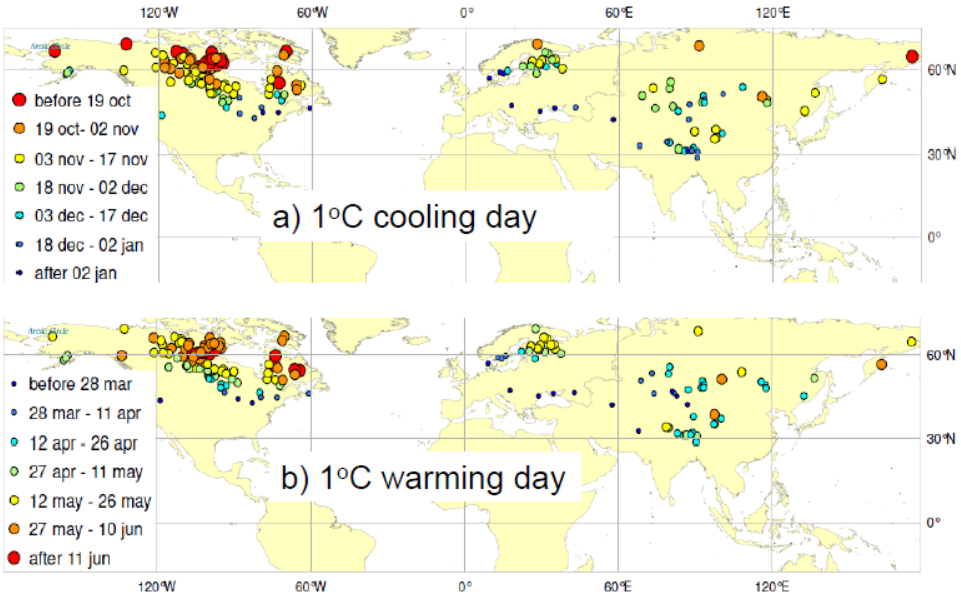

Figure 16 The cooling and warming climatology dates of 160 seasonally ice covered lakes from 29° N to 69° N a) 1 °C cooling day b) 1 °C warming day

Omitting high altitude (> 700 m a.s.l.) and saline lakes, the 1 °C cooling and warming days of lakes (n = 122) change with latitude at a similar rate; 2.2 ± 0.6 days per 1° latitude (R^2_{adj} = 0.34) and 2.3 ± 0.5 days per 1° latitude (R^2_{adj} = 0.40) respectively, increasing the length of the cold phase by 4.5 ± 0.9 days per 1° latitude (0.42). Similarly, the length of the corresponding open water phase shortens by 5.2 ± 0.9 days per 1° latitude (0.55). Across the Northern hemisphere, there is a 3 month period over which the cold phase of seasonally ice covered lakes start and end. The climatological cold phase starts (1 °C cooling day) first with Lake Garry, Canada, at 66° N on 6 October and lastly, Lake Vattern, northern Europe at 58° N on 10 February. The climatological cold phase ends (1 °C warming day) first with Lake Razelm, Europe, at 44.8° N on 01 March and lastly, Lake Payne, Canada, at 59.4° N on 20 June. Lake Pya at 66° N, is the last lake to end its cold phase in Europe. This lake, although at a higher latitude then Lake Payne, has an earlier end to its cold phase (16 May), demonstrating the shorter cold phases of European lakes.

2.7.2 Dependence of LSWT phases on air temperature

The relationship between air temperature and ice-on/off dates is long established (Brown and Duguay 2010) and statistically, air temperature can explain 60% to 70% of the variance in ice-off (Livingstone and Adrian 2009). Many regional studies have been carried out correlating ice phenology events with air temperatures as discussed in chapter 1, section 1.5. I regress the 1 °C and 4 °C warming days with the 0 °C air warming day and the 1 °C and 4 °C cooling days with the 0 °C air cooling day for non-saline lakes < 700 m a.s.l. (122 lakes) globally and regionally (North America, Europe and Asia). Daily climatological ECMWF re-analysis (ECMWF 2009) T2 (2 m air temperature) data, closest to the lake grid reference point for years 1991 to 2010 with an applied 14-day moving average were used in this analysis. The regression equations (constant and air temperature day coefficient) reported in Table 3 to Table 6 are suitable for the prediction of the LSWT phases and phase transition days for large non-saline lakes < 700 m a.s.l., in North America, Europe and Asia, lying within 42° N to 69° N, within a surface area of 100 to 32,000 km^2 and depths ranging from < 1-680 m. The physical and geographical information for the 122 lakes are shown in Appendix I.

Globally and regionally (with exception to Europe), the air temperature transition days have a substantially stronger relationship with the LSWT phase transition days than latitude. Globally, the air temperature transition days explain 0.65 and 0.60 (R^2_{adj}) of the inter-lake variation in the timing of the 1 °C cooling and warming days, (Table 3), whilst latitude explains only 0.34 and 0.40 of the variation. The length of time the air temperature remains below 0 °C explains 0.70 of the variance in the length of the cold phase whilst latitude explains only 0.42. Similarly, for the timing of the 4 °C cooling and warming days, air temperature transition days explain more of the variation (R^2_{adj} = 0.74 and 0.80), Table 4, than latitude (0.42 and 0.54). The length of time the air temperature remains above 0 °C explains 0.85 of the variance in the length of the open water phase whilst latitude explains only 0.55.

Air temperature also explains more of the variation in the 4 °C days and the length of the open water phase than the 1 °C days and the length of the cold phase, as shown in Table 3 and Table 4. A better relationship between the 4 °C days and air temperature is sensible. As the phase transition days are lake-mean values, at a lake-mean LSWT of 1 °C, parts of a large lake are ice free and responding to ambient air temperatures while other parts of lake will be ice covered. The extent of lake ice cover which will vary from lake to lake confounds the inter-lake relationship between the 1 °C days and air temperature. Additional factors during warming, such as the insulating effect of overlying snow, affect the timing of the ice melt (Dutra *et al* 2010), further confounding the relationship with air temperature.

As shown in Table 4, globally and regionally (Asia and North America), air temperature shows a stronger relationship with the 4 °C warming day than the 4 °C cooling day. This is expected as the rate of cooling has a higher dependency on the effective heat storage capacity of the lake. In Europe, air temperature explains a consistently low amount of the inter-lake variation in the timing of all 4 LSWT phase transition days (0.30 -0.32). Regional differences are expected due to localized climate system and influences. For example, in North America the inflow of colder water due to ice melt at high latitudes, may affect the relationship between air temperature and the 1 °C and 4 °C warming days. Additionally, the limnic ratio (the ratio between the total lake area and the total documented regional area), expressed as a percentage (Lerman *et al* 1995a) varies regionally; 0.2% in Asia, 1.1% in Europe and 1.7% in North America.

Phase transition day	Air temperature transition day	Region	Number of lakes	R^2 adjusted	Standard error (days)	Constant	Air temperature Transition day coefficient $(days/day)^{-1}$
1 °C cooling day	Air temp < 0 °C (day)	Global	122	0.65	14.5	18.6	1.01
		Europe	22	0.30	21.6	111.0	0.73
		Asia	9	0.22*	18.9	120.1	0.69
		N.Amer	91	0.71	11.6	-2.7	1.08
1 °C warming day	Air temp > 0 °C (day)	Global	122	0.60	14.5	53.0	0.73
		Europe	22	0.30	19.0	56.4	0.69
		Asia	9	0.67	11.0	39.3	0.75
		N.Amer	91	0.58	13.3	59.2	0.68

Table 3 Global and regional linear regression results of 1 °C phase transition days versus air temperature transition days for non-saline lakes below 700 m a.s.l., located from 42° to 69° N, with surface areas of 100 to 32,000 km^2 and depths ranging from 0-680 m

Phase transition day	Air temperature transition day	Region	Number of lakes	R^2 adjusted	Standard error (days)	Constant	Air temperature transition day coefficient $(days/day)^{-1}$
4 °C cooling day	Air temp < 0 °C (day)	Global	122	0.74	9.7	48.4	0.85
		Europe	22	0.32	13.7	166	0.48
		Asia	9	0.61	11.5	51.2	0.85
		N.Amer	91	0.81	7.7	18.4	0.96
4 °C warming day	Air temp > 0 °C (day)	Global	122	0.80	12.7	36.8	1.05
		Europe	22	0.30	19.5	69.6	0.71
		Asia	9	0.82	13.2	-0.2	1.34
		N.Amer	91	0.86	9.9	34.6	1.07

Table 4 Global and regional linear regression results of 4 °C phase transition days versus air temperature transition days for non-saline lakes below 700 m a.s.l., located from 42° N to 69° N, with surface areas of 100 to 32,000 km^2 and depths ranging from 0-680 m

2.7.3 Relationship of LSWT phases with lake physical characteristics

Expanding the regression with air temperature to include distance from coast (Wessel and Smith 1996) and lake physical characteristics (depth, altitude and surface area) obtained from Herdendorf (1982), Lehner and Doll (2004), the ILEC World Lake Database (http://wldb.ilec.or.jp/), LakeNet (http://www.worldlakes.org/) and (Kourzeneva *et al* 2012) helps to further explain the timing of the LSWT phase transition days of the 122 lakes.

Globally, air temperature is shown to explain 0.60-0.65 and 0.74-0.80 (R^2_{adj}) of the variation in 1 °C and 4 °C phase transition days respectively (Table 3 and Table 4). Expanding this regression (stepwise) to include lake characteristics contributes a small but statistically significant improvement to the explanation of the global inter-lake variation. Regionally, statistically significant relationships with the phase transition days were found for depth but not for lake surface area, indicating that depth may be a more suitable characteristic for estimating the effective heat storage capacity. Lake depth explains a further 0.02-0.09 of the inter-lake variation in the LSWT phase transition days in North America, accounting for more of the variation in the cooling days (0.04-0.09) than the warming days (0.02-0.03). The contribution that lake characteristics make to the regional R^2_{adj} values is shown by the difference between the R^2_{adj} values in Table 3 and 4 and those in Table 5.

Similarly, in Europe depth accounts for more of the variation in the 1 °C and 4 °C cooling days (0.10-0.12) than in the 4 °C warming day (0.07). Depth does not explain any of the variation in the 1 °C warming day in Europe. This demonstrates the stronger dependency of the rate of cooling than the rate of warming on the effective heat storage capacity of the lake. Depth results in a later cooling day, by 2-4 days/10 m in North America and 5-8 days/10 m in Europe and a later warming day of 2-3 days/10 m in North America 6 days/10 m (4 °C warming day) in Europe. In contrast, while lake depth does not explain any of the variation in the cooling

days in Asia, it explains a further 0.09 in the 4 °C warming day. Its effect is small, causing later warming by < 0.5 day/10 m.

Lake altitude explains a further 0.05 of the variation in both the 1 °C and 4 °C warming days in North America causing a later 1 °C warming day (3.5 days/ 100 m a.s.l.) and 4 °C warming day (1.3 days/ 100 m a.s.l.), across the range of altitudes, 0- 700 m a.s.l., Table 5. This is expected as LSWTs at higher altitudes are cooler and warm later than lakes at lower altitudes, as shown in chapter 1, figure 3. There is no statistically significant relationship between altitude and the LSWT phase transition days in European and Asian lakes.

In Europe, distance from coast replaces air temperature in the stepwise regression for all four phase transition days, explaining more of the inter-lake variation (0.36-0.57) than air temperature (0.30-0.32). Lakes further from the coast show a later 1 °C and 4 °C cooling day and an earlier 1 °C and 4 °C warming day. The opposite would be expected, as inland lakes have harsher winters due a greater distance from the moderating effect of the ocean (Thompson *et al* 2009). Latitude, when added to the stepwise regression, also replaces distance from coast for all 4 transition days (not shown). This suggests that distance from coast in Europe misleadingly acts as a proxy for latitude and air temperature. There is no relationship between distance from coast and the phase transition days in Asia and North America.

As well as air temperature and lake characteristics, other factors such as wind and snow depth are related to the timing of the LSWT phase transition days. The mechanical action of wind can prevent the formation of solid ice cover on the initial ice skim. Wind also can accelerate the ice-off process by breaking up ice and mixing it with warmer sub-surface water (Williams 1965). Overlying snow will have insulating effect, affecting the timing of the ice melt (Dutra *et al* 2010). Hence, consideration of other lake characteristic and meteorological factors may add to the explanation of the 1 °C and 4 °C cooling and warming days.

Phase transition day	Region	No. of lakes	R^2 Adj	Std error (days)	constant	Coefficients			
						Air temp 0 °C (days/ day)$^{-1}$	Depth (days/ m)$^{-1}$	Altitude (days/ m a.s.l.)$^{-1}$	Distance from coast days/arc degree)$^{-1}$
1 °C cooling day	Europe	22	0.51	18.1	280	-	0.761	-	6.05
	Asia	9	0.22*	19.0	120	0.694		-	-
	N.Amer	91	0.80	9.8	-3.8	1.07	0.357	-	-
1 °C warming Day	Europe	22	0.45	16.8	161	-	-	-	-5.52
	Asia	9	0.67	11.0	39.3	0.749	-	-	-
	N.Amer	91	0.65	12.1	42.8	0.722	0.176	0.0346	-
4 °C cooling day	Europe	22	0.46	12.1	280	-	0.461	-	3.78
	Asia	9	0.61	11.5	51.2	0.846		-	-
	N.Amer	91	0.85	6.8	17.8	0.948	0.202	-	-
4 °C warming Day	Europe	22	0.64	13.9	172	-	0.552	-	-6.18
	Asia	9	0.91	9.4	10.8	1.19	0.044	-	-
	N.Amer	91	0.89	8.6	24.6	1.09	0.274	0.0128	-

* not statistically significant p = 0.1

Table 5 Stepwise regression results of phase transition days versus air temperature transition days, depth, lake altitude, distance from coast and lake surface area for non-saline lakes below 700 m a.s.l., located from 42° N to 69° N, with surface areas of 100 to 32,000 km^2 and depths ranging from 0-680 m

LSWT Phase	Region	No. of lakes	R^2 adjusted	Std error (days)	Constant	Coefficients				
						Air temp 0 °C (days/ day)$^{-1}$	Depth (days/ m)$^{-1}$	Altitude (days/ m a.s.l.)$^{-1}$	Distance from coast days/arc degree)$^{-1}$	Area days/100 km^2)$^{-1}$
Intervening cooling (regressed with air temp)	Global	122	0.16	7.13	-29.83	+0.162				
	Europe	22	0.18	9.57	-54.52	+0.244				
	Asia	9	-	-	-	-				
	N.Amer	91	0.11	6.05	-21.11	+0.129				
Intervening cooling (regressed with air temp and lakes characteristics)	Global	122	0.24	6.77	-31.05	+0.164	+0.037	-	-	-
	Europe	22	0.42	8.09	-0.17	-	+0.300	-	+2.27	-
	Asia	9	-	-	-	-	-	-	-	-
	N.Amer	91	0.28	5.44	-21.57	+0.124	+0.155	-	-	-
Intervening warming (regressed with air temp)	Global	122	0.40	9.67	16.24	+0.321				
	Europe	22	-	-	-	-				
	Asia	9	0.85	5.26	-39.47	+0.593				
	N.Amer	91	0.45	9.69	-24.65	+0.386				
Intervening warming (regressed with air temp and lakes characteristics)	Global	122	0.47	9.02	-13.06	+0.328	+0.037	-0.019	-	-
	Europe	22	0.36	6.20	+8.95	-	+0.384	-	-	-
	Asia	9	0.93	3.61	-41.0	+0.585	-	-	-	+3.46
	N.Amer	91	0.51	9.15	-15.96	+0.365	-	-0.022	-	-

Table 6 Stepwise regression results of length of intervening phases vs air temperature transition days, depth, lake atitude, distance from coast and lake surface area for non-saline lakes below 700 m a.s.l, located from 42° N to 69° N, with surface areas of 100 to 32,000 km^2 and depths ranging from 0-680 m

2.7.4 Warming and cooling intervening phases

The cooling and warming intervening phase is the time taken for the LSWT to change between the cold and open water phases; to cool from 4 °C to 1 °C and warm from 1 °C to 4 °C, Figure 14. Globally and regionally (with exception to Europe) there is a stronger relationship between air temperature and the warming intervening phase than the cooling intervening phase (Table 6), again demonstrating the stronger relationship between air temperature and warming. Globally, the air temperature transition days explains 0.16 (R^2_{adj}) of the variation in the length of the cooling intervening phase and 0.40 of the length of the warming intervening phases. Other than the warming phase in Asia where air temperature and surface area explains 0.93 of the length of the warming intervening phase, the intervening phases are poorly explained by air temperature and lake characteristics. It is likely that the variations in the extent of lake ice cover at the 1 °C days (discussed in section 2.6.2), confounds the relationship between air temperature transition days and the length of the two intervening phases.

2.8 Observed LSWT trends and absolute values

To assess if the lake-mean LSWTs can be considered representative of the lake-centre LSWTs (and vice versa), I compare the ARC-Lake lake centre and lake-mean summer trends and absolute values. The availability of spatially resolute (0.05° x 0.05°) ARC-Lake observations allows for such an evaluation. This comparison allows assumptions (both general and specific to this tuning study) to be made about how the lake centre LSWTs (observations or *in situ* measurements) relate to the lake-mean LSWTs. For example, do changes in LSWTs recorded from a buoy in the centre of a lake reflect similar LSWT changes in the whole lake?

I also compare the ARC-Lake lake centre nighttime LSWT trends with LSWT trends from IWBP (Schneider and Hook 2010). For IWBP, only the lake centre

nighttime LSWTs are derived. The summer LSWT trends for IWBP lakes are determined using the JAS LSWTs means for lakes at latitudes from 23.5° N pole-ward and from equator to 23.5° S and JFM LSWT means at latitudes from 23.5° S pole-ward and from equator to 23.5° N. To avoid the cloudy wet season in the tropics, a dry-season metric was used (JFM) between the equator and 23.5° N and the JAS between the equator and 23.5° S (Schneider and Hook 2010). I apply the same latitude bounds to determine the ARC-Lake summer trends throughout. All trends in the remainder of this chapter refer to summer trends, unless stated otherwise.

2.8.1 ARC-Lake lake centre and lake-mean comparison

The lake-mean LSWT is the mean of the LSWTs across the entire lake surface, while the LSWT for the pixel closest to the geographical lake reference coordinates (Herdendorf 1982; Lehner and Doll 2004) is considered to be the lake centre LSWT. I assess the daily MADs and summer trend differences between the ARC-Lake lake-mean and lake centre LSWTs. The MAD between the lake centre and the lake-mean LSWTs is low, averaging 0.17 $\pm$ 0.31 °C across all lakes with an observed time series of $\geq$ 16 years (232 lakes). Figure 17 shows the lake centre and lake-mean time series data for 4 lakes in different regions. The LSWT cycle and LSWT extremes for these lakes are very comparable, although for Lake Nicaragua Figure 17b the lake centre maximum LSWTs are approximately 0.5 ºC warmer than the lake mean LSWTs.

The four largest temperate lakes, the Caspian Sea (378,000km^2), Lake Huron, Lake Michigan and Lake Superior which range from 57,000-82,000 km^2, have the largest lake centre and the lake-mean daily MADs, ranging from 0.81 to 1.30 °C. Across all 232 lakes, there is a correlation of 0.51 between the lake surface area and the MAD, Figure 18. Despite the larger MADs for the few largest lakes, the lake-mean summer trends (0.08 and 0.11 °C yr^{-1}) for the Caspian sea and Lake Superior are highly representative of the respective lake centre trends (0.08 and 0.11 °C yr^{-1}). For

Lake Michigan and Lake Huron the trends show slightly stronger warming for the lake centre (0.1 and 0.09 $^{\circ}$C yr^{-1}) than for the lake mean (0.07 $^{\circ}$C yr^{-1}).

For 159 lakes (69%), the lake centre summer LSWT trends are within $\pm$ 0.01 $^{\circ}$C yr^{-1} of the lake mean trends, Figure 19. The lakes with the poorest trend agreement are small (relatively) or small sinuous lakes. There were initially 21 lakes with poor agreement, 8 of which showed better agreement using co-ordinates that are physically more representative of the lake centre, these 8 lakes are shown in appendix IIa. In this appendix, the yellow symbols show the lake geographical reference coordinates and the red crosses show the LSWT pixel used for the trend comparison. Six (6) of these 8 lakes are not sinuous but elongated in shape and most of the lake body is well connected. It makes sense that for these lakes a central part of the lake may well represent the entire lake. The trend comparison for the other 13 small lakes, shown in appendix IIb showed no improvement by using a LSWT trend at a more centrally representative location. Many of these small lakes are sinuous or contain large areas of land and therefore areas within these lakes may be poorly connected. The shape and size of these areas can vary substantially and therefore how the area responds to influences from the surrounding catchment area will also vary. For these 13 lakes, I conclude that there is no central location where the lake centre trends are considered representative of the lake-mean trends. Despite this, the absolute values compare well. The MAD (between the lake centre and lake-mean) averages 0.18 $\pm$ 0.16 $^{\circ}$C over the 21 lakes and is comparable to the MAD for all lakes (0.17 $\pm$ 0.31 $^{\circ}$C). The lake-mean and lake centre LSWTs for one of these small lakes, Lake Paijanne in Finland, is shown in Figure 17a.

As shown in Figure 19, there are 10 lakes that show lake centre and lake-mean summer LSWT trend differences of greater than $\pm$ 0.05 $^{\circ}$C yr^{-1}. All 10 lakes are small lakes and are included in the 13 lakes with poor agreement trend agreement, appendix IIb. These 10 relatively smaller lakes are also substantially shallower (average depth of 14 m and average surface area of 960 km^2) than the lakes with

lake-mean lake centre trend differences within $\pm$ 0.01 $^{\circ}$C yr^{-1} (average depth = 33 m and average surface area = 6100 km^2).

In conclusion, with the exception of very large lakes, the absolute LSWT values recorded at the lake centre, *in situ* or remotely can be considered representative of the lake-mean absolute values. With exception to small sinuous lakes, the lake centre trends can be considered representative of the lake mean trends for all lakes.

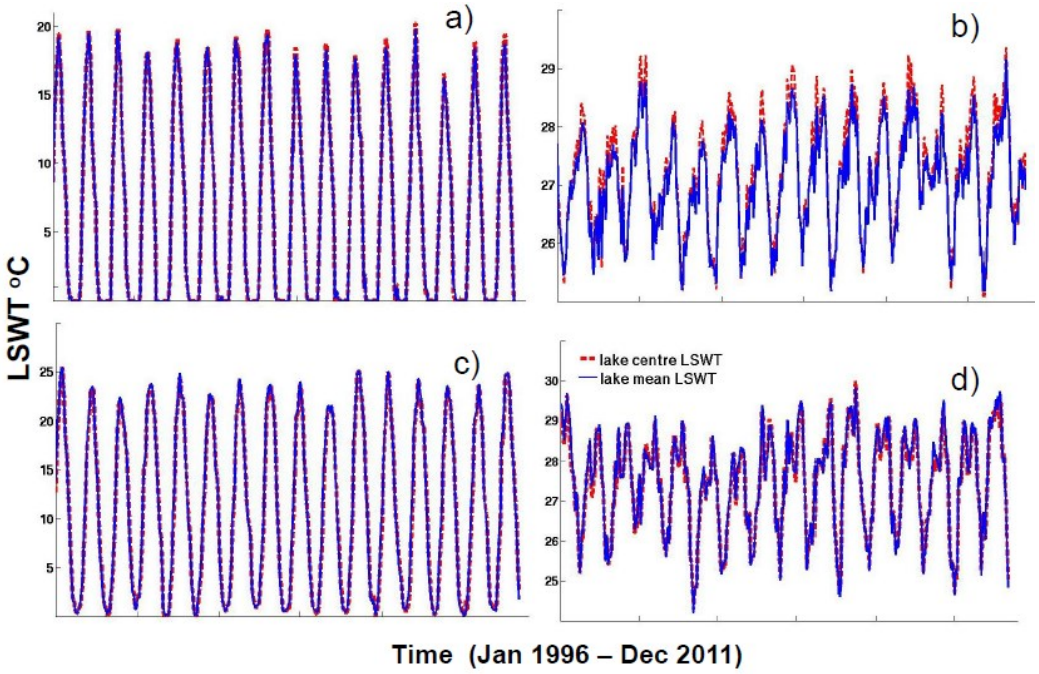

Figure 17 Lake centre and lake-mean LSWT time series for 4 lakes at varying latitudes a) Lake Paijanne, Europe, 61.7° N b) Lake Nicaragua, Central America, 11.6° N c) Lake Erie, North America, 42.3° N and d) Lake Turkana, Africa, 3.5° N

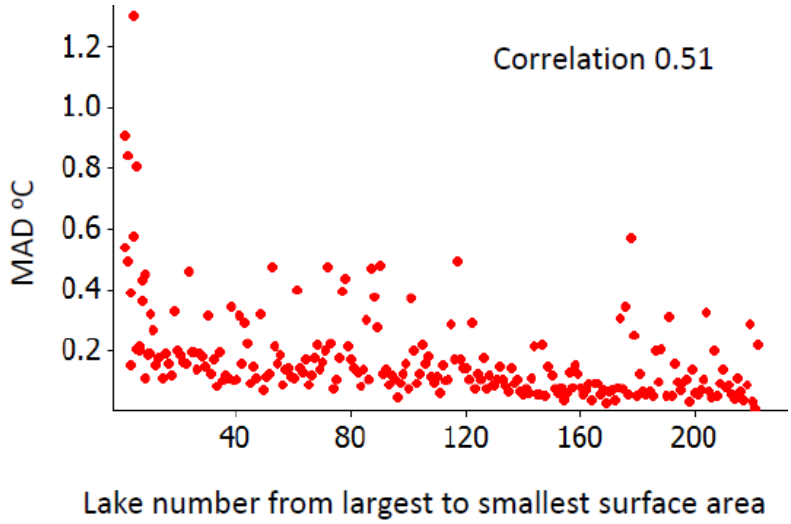

Figure 18 Daily MADs between the ARC-Lake lake-mean and lake centre LSWTs for the 232 lakes with ≥ 16 years of LSWT observations, showing that larger lakes have a bigger lake mean lake centre LSWT MAD. The MAD and lake surface areas have a correlation of 0.51.

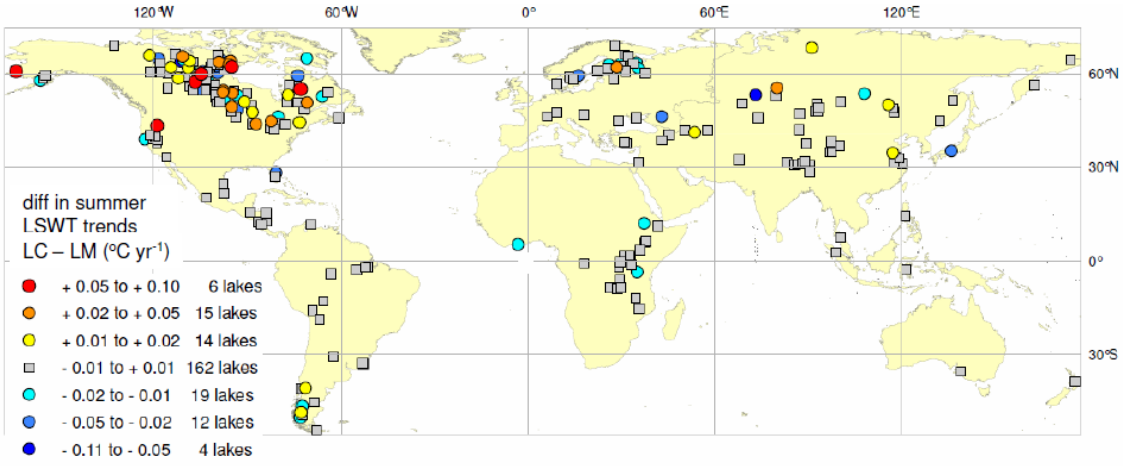

Figure 19 The summer trend LSWT difference, lake centre (LC) – lake-mean (LM), for 232 lakes with an observed time series of ≥ 16 years

2.8.2 ARC-Lake and IWBP LSWT comparison

The regional differences between the ARC-Lake and IWBP LSWT trends (the magnitude of warming in some regions and whether warming has actually occurred in other regions) in the State of the Climate report 2011, discussed in chapter 1, section 1.5.1, has been attributed to the different LSWT time periods and retrieval

methods employed in observed LSWT retrieval. In this report, the IWBP summer LSWT trends span 27 years (1985 to 2011) of lake centre nighttime LSWTs. The ARC-Lake trends span only a maximum 20 years, from 1992 to 2011 of lake-mean day/night average LSWTs. The LSWT observations from IWBP use AVHRR (Advanced Very High Resolution Radiometer) and ATSR instruments. Although both sets of observations employ the ATSR instruments, the methods of retrieval are different as described in the State of the Climate report. The IWBP LSWT data consist of lake centre, nighttime LSWT observations, while for ARC-Lake the entire lake is observed using a fixed (in time) land/water mask and an algorithm (Merchant *et al* 2008) based on Bayes' theorem for assigning a clear-sky probability to each pixel. AVHRR Pathfinder product was used to identify and exclude cloud pixels IWBP use a different method of cloud detection (Schneider and Hook 2010).

There are 114 IWBP lakes and 119 ARC-Lake with 20 year trends (1992 – 2011), with 71 lakes common to both sets of observations over the 20 year period. For these 71 lakes, using the nighttime lake centre trends, I determine the regional trends of ARC-Lake and IWBP LSWTs, eliminating some of the differences between the sets of observations. The LSWT lake-centre coordinates for the IWBP LSWT are very close to the lake-centre reference co-ordinates for ARC-Lake LSWT. The average absolute difference in the coordinates is $0.16 \pm 0.44^{\circ}$ for latitude and $0.18 \pm 0.50^{\circ}$ for longitude. The regional IWBP and ARC-Lake trends of these 71 common lakes are shown in Table 7. Individually, the trends for these lakes are reasonably well correlated (0.62), Figure 20. The mean regional trends and the uncertainty of these trends are shown in Figure 21. The paired t-test P-value of 0.049 shows that the ARC-Lake and IWBP trends in Europe are statistically different, although marginally. It is evident that the mean trends in all regions and are higher for IWBP trends, Figure 21, particularly in Europe, where the nighttime IWBP trend is double the corresponding ARC-Lake nighttime trend.

Figure 22a and b show the individual lake centre night time summer trends from 1992 to 2011, for all IWBP lakes (114) and all ARC-Lake with 20 year trends (119). This figure shows some comparable regions, although the ARC-Lake trends shows greater cooling trends in higher latitudes in North and South America and less extreme warming in northern Europe. Both sets of observations show that the strongest warming has occurred in Europe and North America and the least warming (with exception to South America) in Africa and Asia, Table 7. In South America (only 4 common lakes), ARC-Lake show a slight cooling while the IWBP show a warming similar to that in Asia and in Africa, although trends are statistically indistinguishable.

Region	Number of lakes	Trend ˚C yr^{-1}		
		IWBP LC night	ARC-Lake LC Night	ARC-Lake LC Day-night
Africa	7	0.02± 0.02	0.02± 0.02	0.01 ± 0.01
Asia	27	0.02± 0.02	0.02± 0.01	0.01 ± 0.01
Europe	10	0.08± 0.04	0.04± 0.02	0.05 ± 0.02
North America	23	0.06± 0.02	0.05± 0.02	0.04 ± 0.02
South America	4	0.02± 0.01	0.00± 0.02	0.00 ± 0.02

Table 7 IWBP and ARC-Lake LC nighttime and ARC-Lake LC day-night average regional summer trend comparison using the 71 common lakes, from 1992-2011 (20 years) uncertainty of the trends (95% confidence level) showing that the IWBP nighttime trends are warmer in all regions than the ARC-Lake nighttime trends

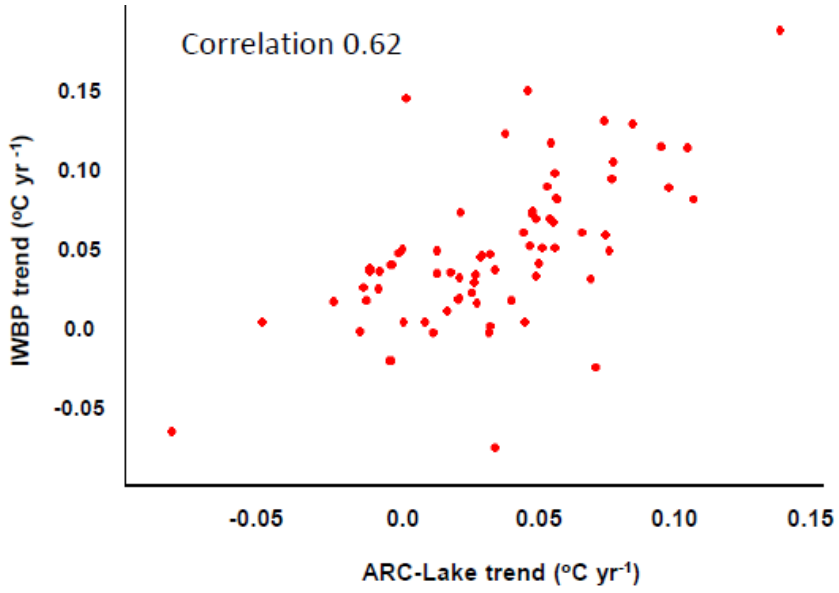

Figure 20 ARC-Lake and IWBP summer nighttime lake centre observed LSWT trends, for the 71 lakes common to both sets of observations

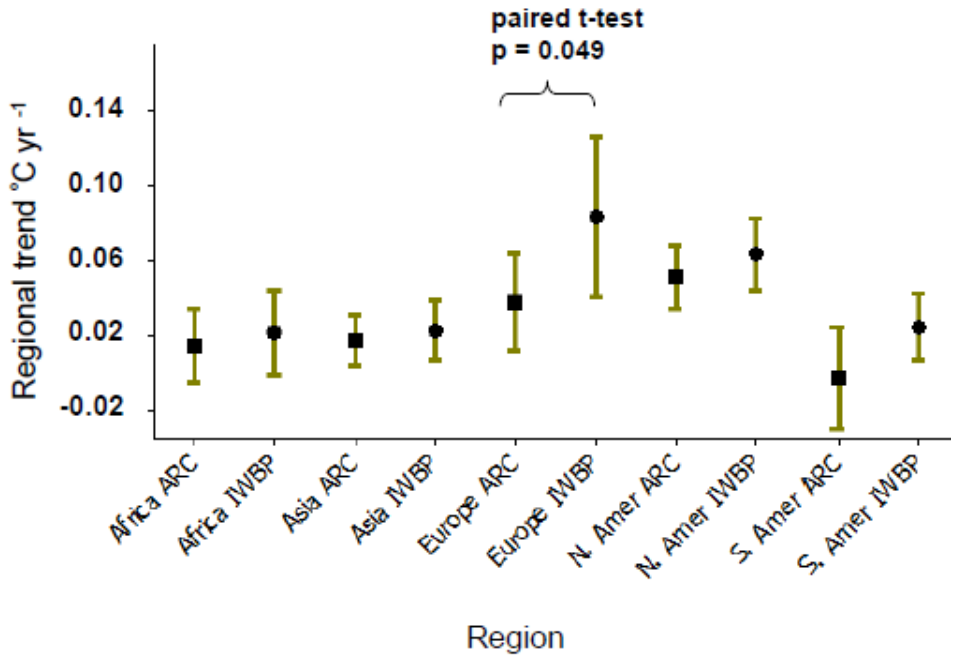

Figure 21 Regional ARC-Lake and IWBP lake centre nighttime trends (71 lakes) and the uncertainty of the trends (95% confidence level) represented by the error bars. The paired t-test for Europe show that the trends are statistically different, although marginally. ARC trends are marked by a square and IWBP trends by a circle

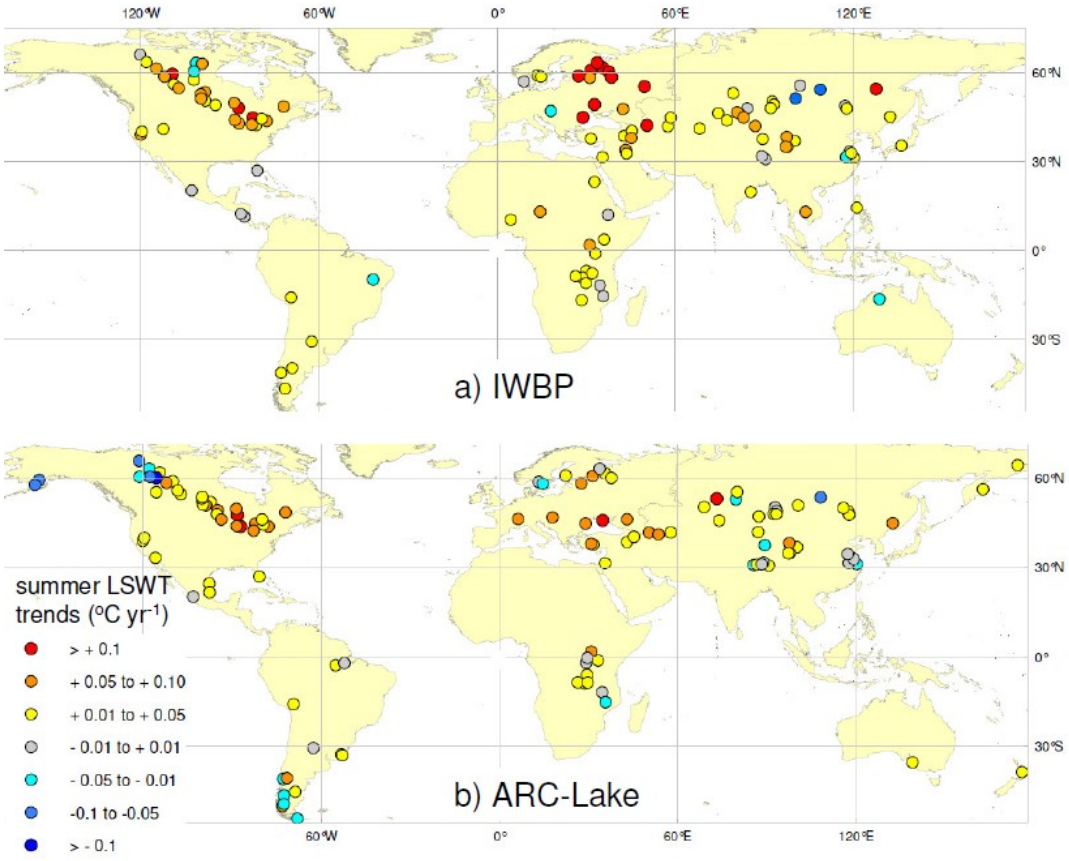

Figure 22 Summer nighttime lake centre LSWT observed trends a) IWBP (114 lakes, 1992 – 2011) b) ARC (119 lakes, 1992 to 2011), showing some regional comparison, with ARC-Lake trends show greater cooling trends in higher latitudes in North and South America and less extreme warming in northern Europe

2.8.2.1 Nighttime v's daytime temperature trends

As shown in Table 7, the ARC-Lake nighttime LSWT trends are warming slightly more rapidly than the day-night average trends in North America, Africa and Asia and slightly less rapidly in Europe. However, regionally the trends are statistically indistinguishable, Figure 23b, and individually, they are well correlated (0.91), Figure 23a.

There is evidence to show that while nighttime air temperatures were warming more rapidly than day-night air temperatures, in recent decades the air temperature diurnal minimum and maximum trends have been comparable. This indicates that the LSWT diurnal extreme trends may not be reflecting air temperature diurnal

extreme trends. The HadEX2 dataset from 1901-1951 and from 1961-2010 show that nighttime trends have warmed more rapidly than daytime trends (Vose *et al* 2005; Donat *et al* 2013; Revadekar *et al* 2013) but show more comparable trends in recent decades. A global study covering the equivalent of 71% of the total global land area shows agreement in the more rapid minimum air temperature warming from 1950–2004 but from 1979–2004 this study shows highly comparable increases in minimum and maximum temperature of 0.295 $^{\circ}$C dec^{-1} and 0.287 $^{\circ}$C dec^{-1} (Vose *et al* 2005). It is possible that lake characteristics and other meteorological factors play a role in how the LSWT diurnal extremes respond to air temperature diurnal extremes.

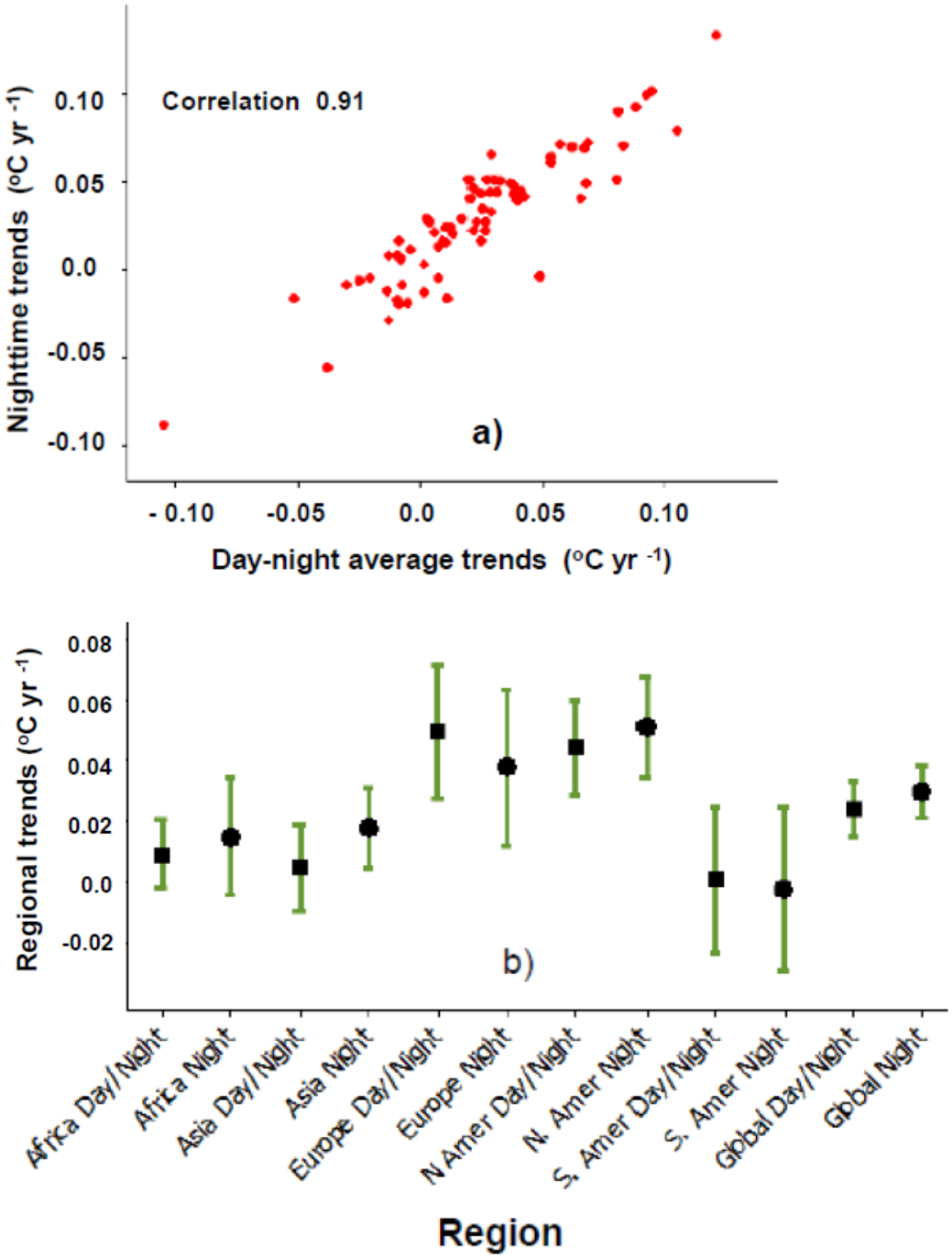

Figure 23 ARC-Lake summer nighttime versus day-night average lake centre observed LSWT trends, for the 71 lakes with 20 years of observations
a) individual trends b) regional trends

2.9 ARC-Lake LSWT summer trends

I present the ARC-Lake summer trends for all 232 lakes with 16-20 years of observations and for the 119 lakes with 20 years of observations, Figure 24. The trends based on 20 years (1992-2011) of observations show more rapid warming globally and regionally in Africa and Europe than the trends based on 16-20 years of observations (1992/1996-2011). In North America, the ARC-Lake 20 year trends show an average of warming of +0.03 $^{\circ}$C yr^{-1}, while the 16-20 year trends show virtually no change. The cooling or stabilising of the global summer and winter air temperatures in the last decade (Jones *et al* 2013) may have greater leverage, causing the less extreme trends over the shorter period of observations. Regionally, with exception to North America, the average trend and the range of uncertainties are statistically indistinguishable. The difference in trends is primarily due to the summer cooling of many lakes in Canada with the shorter period of observations. Fifty eight (58) of the 79 lakes in Canada have only 16 years of observations, 39 of which show summer cooling. Only 3 of the 21 lakes with 20 years of observations show cooling. The comparison between trends using 20 years of observation versus 16-20 years of observations highlights the importance of using longer term data when evaluating trends. More of the inter-annual variation will be filtered out over a longer time period, capturing realistic climatic trends.

The individual summer trends for all 232 lakes over the 16-20 year period Figure 25, show strong cooling trends in Northern Canada. This cooling can be partly explained by a later 4 $^{\circ}$C warming day (the day the lake-mean LSWT exceeds 4 $^{\circ}$C in spring) trend. The 4 $^{\circ}$C warming day trends explain 0.50 (R^2_{adj}, p = 0.000) of the inter-lake variation in the summer trends of lakes in Canada (79 lakes) and latitude explains 0.26 (p = 0.000) of the variation.

While the majority of lakes show a lengthening in the open water phase (the length of time the LSWT remains above 4 $^{\circ}$C) over the 16-20 year period, some Northern Canadian and central Asian lakes, show a shortening in the open water phase by 0.25 to 1.0 days yr^{-1}, Figure 26a. The shorter open water phase for these lakes occur

as a result of a later 4 °C warming day trends, Figure 26b, of +0.25 to +1.0 days yr^{-1}. As shown in Figure 25, the summer LSWTs for these lakes show cooling trends, indicating the effect of a later a warming day trend.

For all lakes, the 1 °C warming day trends, although not statistically significant related to the summer LSWT trends. Both the 1 °C and 4 °C warming day trends shows a later warming of +0.25 to +1.0 days yr^{-1} for the majority of lakes in North America and Asia, Figure 27 and Figure 26b.

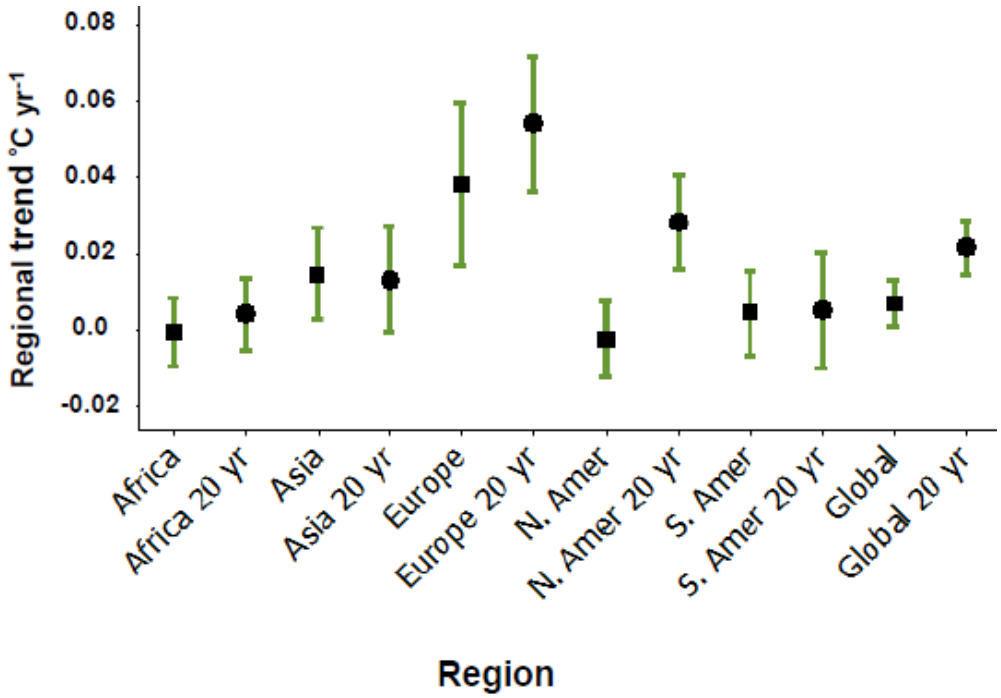

Figure 24 Regional ARC-Lake lake-mean day-night average trends with the uncertainty of the trends represented by the error bars (95% confidence level) for all lakes with 16-20 years (232) of observations (marked by black square) and for lakes with only 20 years (119) of observations. In North America the trends are statistically different causing global statistically different trends.

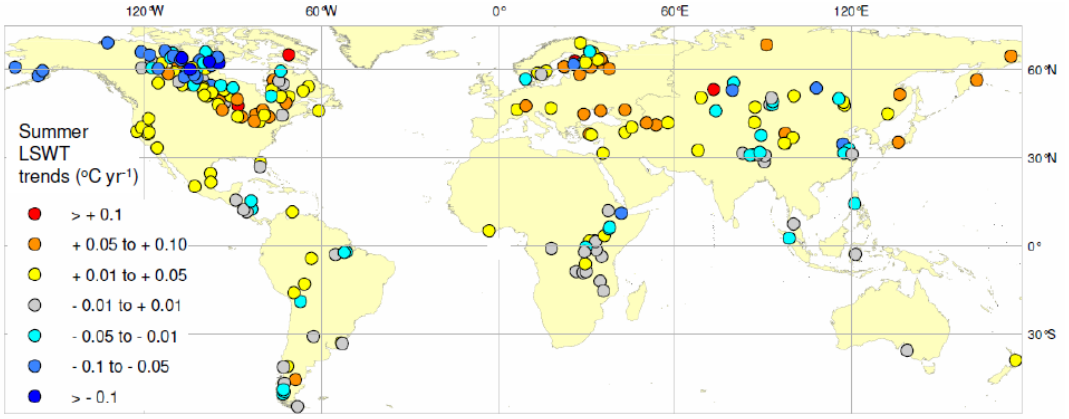

Figure 25 Summer ARC-Lake lake-mean day-night average trends for all lakes with 16-20 years of observations (232) showing cooling trends in Canada and in central Asia

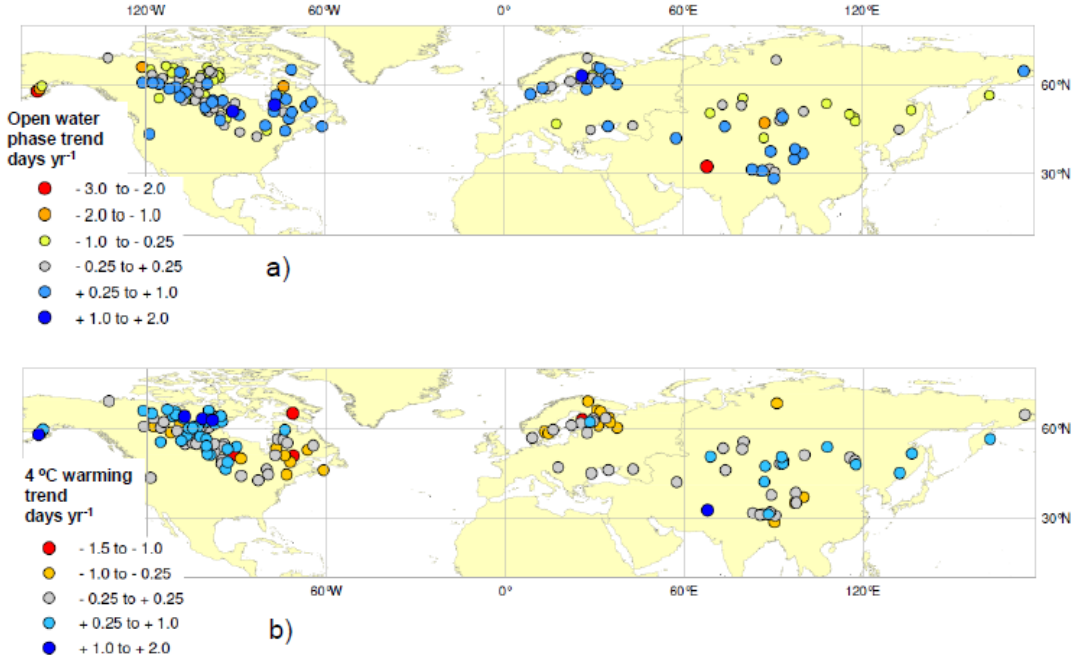

Figure 26 Open water phase and 4 ˚C warming day ARC-Lake lake-mean trends for all lakes with 16-20 years of observations (232) showing that the shorter open water phase caused by the later 4 ˚C warming day for lakes in Northern Canada and in central Asia a) Open water phase trends b) 4 ˚C warming day trends

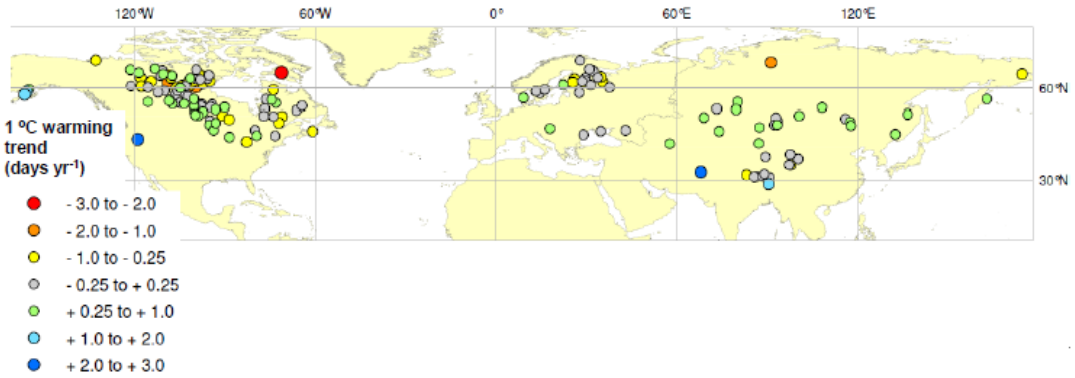

Figure 27 1°C warming day ARC-Lake lake-mean trends for all lakes with 16-20 years of observations (232) showing later warming trends of 0.25 to 1.0 days yr^{-1} for many North American and Asian lakes

2.10 Summary and conclusions

Global LSWT climatology of 246 lakes has been explored using up to 20 years of available satellite observations from ARC-Lake. LSWT climatologies have been used to quantify, on a global scale, the responses the annual cycle of large lakes' temperatures to the annual cycle of surface temperatures to the annual cycle of solar radiation and the ambient meteorological conditions. For all lakes < 2000 m a.s.l., the minimum LSWT decrease with latitude, in the northern and southern hemispheres were shown to be strongly driven by minimum netSSI. Globally and regionally (with exception to Europe), the minimum netSSI is a stronger predictor of the length of the cold phase of lakes than latitude. The observed LSWT annual cycles with time lag were shown to be strongly related to the netSSI annual cycles in tropical lakes, despite the small temperature variations and lack of seasonality. Globally, considering all 246 lakes, the LSWT zonal (10°) monthly extremes closely track air temperature extremes. The changes in lake altitude are demonstrated to drive the changes in the maximum LSWT–air temperature difference of tropical lakes.

The typical annual LSWT cycle for dimictic lakes is defined by 4 phases (cold, open-water, and two intervening phases), the boundaries of which are marked by the days on which the LSWT passes through temperatures of 1 °C and 4 °C. The air

temperature transition days are better estimators of the 4 °C cooling and warming days than of the 1 °C cooling and warming days, Table 3 and Table 4. Complications due to the presence and extent of ice at the 1 °C lake-mean boundary confound the relationship between the 1 °C transition days and air temperature.

Globally and regionally (with the exception of Europe), air temperature shows a stronger relationship with LSWT warming (1 °C and 4 °C warming days and the warming intervening phase) than with LSWT cooling (1 °C and 4 °C cooling days and the cooling intervening phase), further supporting that lake warming is more strongly related with air temperature. Lake depth explains more of the inter-lake variation in the 1 °C and 4 °C cooling days than in the 1 °C and 4 °C warming days, further supporting that lake-mean depth is a good indicator of the effective heat capacity of large lakes.

In Europe, air temperature is a poor predictor of the phase transition days. The effect of the distance from coast on the LSWT transition days is masked by the opposite (and stronger) effect of air temperature/ latitude.

Globally and regionally (Asia and North America), the 4 °C air temperature transition days have an approximate 1:1 relationship with the 4 °C phase transition days, explaining 0.61-0.86 in the 4 °C phase transition days. The equations outlined in Table 3 to Table 6 are suitable for the prediction of the LSWT transition days and phases of large non-saline lakes < 700 m a.s.l. in North America, Europe and Asia, lying within 42° to 69° N, with depth from>1 to 680 m and within surface areas of 100 to 32,000 km^2.

I demonstrated that for the majority of lakes, the LSWT trends and absolute values at the lake centre are representative of the lake-mean LSWT trends and absolute values, with exception to the absolute values of 4 largest temperate lakes and to the LSWT trends for 13 relatively small poorly connected lakes (appendix IIb).

The ARC-Lake and IWBP LSWT summer nighttime trends for common lakes with observations from 1992 to 2011 were shown to be reasonably well correlated (0.62). Regionally, both datasets agree that the strongest warming has occurred in Europe and North America and the least change has occurred in Africa, Asia and South America. In Europe, the average IWBP trend show warming twice that of the average ARC-Lake trend.

Finally, presenting the ARC-Lake summer trends for all lakes with 16-20 years of observations, I show that there is considerably more cooling in the summer trends for lakes with the shorter observation period (16 years). The cooling trends predominately in Northern Canada may be partly attributed a reduced heating time of the lake caused by a later warming day trend.

Chapter 3 Use of *FLake* in the tuning study

3.1 Introduction

In chapter 2, I demonstrated the global coherence of the ARC-Lake lake-mean climatology observations. In the next two chapters (chapters 4 and 5), I use the LSWT timeseries observations (1992 to 2010) of the same 246 large lakes to tune the modelled LSWTs from the lake model, *FLake*. For the purpose of this tuning study the 246 lakes are categorized into seasonally and non-seasonally ice covered lakes, as described in chapter 1, section 1.4. The tuning process for seasonally ice covered lakes (160 lakes) is dealt with in chapter 4 and in chapter 5 for non-seasonally ice covered lakes (86 lakes). In this chapter, I discuss the use of *FLake* (section 3.2) and the meteorological forcing data (section 3.3) in the tuning study. I introduce the role that wind plays in LSWTs and review whether wind speeds measured over land are representative of those over water (section 3.4). I suggest two wind speed scalings to apply to the model forcing wind speed data to better represent over-water wind speeds.

3.2 *FLake* lake model

FLake, as discussed in chapter 1, section 1.7, is a computationally efficient model and includes the important aspects of lake physics. It is therefore ideal for use in this tuning study which requires multiple runs for each lake in order to find the optimal modelled LSWT.

3.2.1 *FLake* parameters and properties

Many lake specific model parameters and lake properties can be considered in *FLake.* Through preliminary runs of *FLake* lake model, I selected 3 basic lake properties that have the most influence over the modelled LSWTs; lake depth, the

reflectivity of snow and ice (albedo) and light penetration through the water surface (light extinction co-efficient).

3.2.1.1 Preliminary trials using *FLake*

Preliminary runs of *FLake* lake model (carried out on 7 seasonally ice covered lakes), showed that lake depth **(*d*)**, albedo; snow and ice **(*α*)** and light extinction coefficient **(*κ*)** values, exerted a large influence on the modelled LSWT cycle. The lakes assessed in the preliminary trials are the first 7 lakes listed in chapter 4, Table 11. When running *FLake*, it is recommended to use the mean depth of the lake and the model default albedo value (0.60 for snow and white ice and 0.10 for melting snow and blue ice). I demonstrate using Lake Athabasca, and Lake Ladoga, Figure 28 and Figure 29, that adjusting the values *d*, *α* and *κ*, the modelled LSWTs become substantially closer to the observed LSWTs. For Lake Athabasca, an increase in the modelled albedo (higher reflectivity) results in a later ice-off date, closely corresponding to the observed ice-off date, Figure 28a. In Figure 28b, I show that by using a lower depth, the ice-on day is brought forward corresponding more closely to the observed LSWTs. Lowering the light extinction coefficient (greater transparency), the greater transmission of surface heat to lower layers result in a lower and more representative maximum LSWT, Figure 28b. The modelled LSWTs, combining all 3 adjusted properties compared with the observed LSWTs, are shown in Figure 28c. For Lake Ladoga, Figure 29, I show the effect of the adjusted *d*, *α* and *κ* values on the modelled LSWT. From herein, I refer to *d*, *α* and *κ* as the LSWT regulating properties.

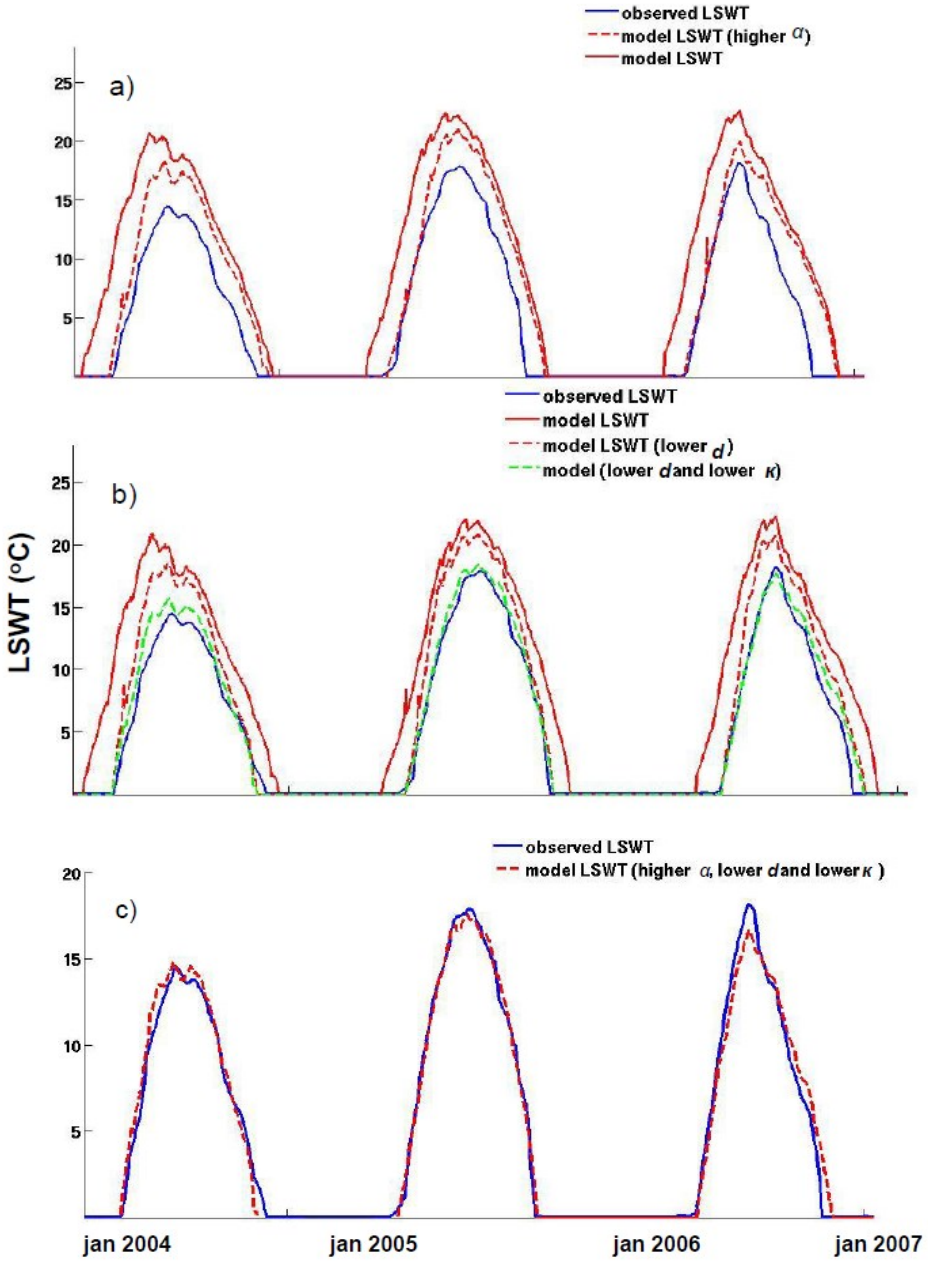

Figure 28 Preliminary modelled runs for Lake Athabasca showing that adjustments to d, α and κ can greatly improve the modelled LSWTs a) shows that a higher α causes a later and more timely thawing date b) shows that a lower d causes an earlier and more timely freezing date and a lower κ value (greater transparency) reduces the maximum LSWT and c) shows that the combined effect of the adjusted d, α and κ produces LSWTs that are highly comparable to the observed LSWTs.

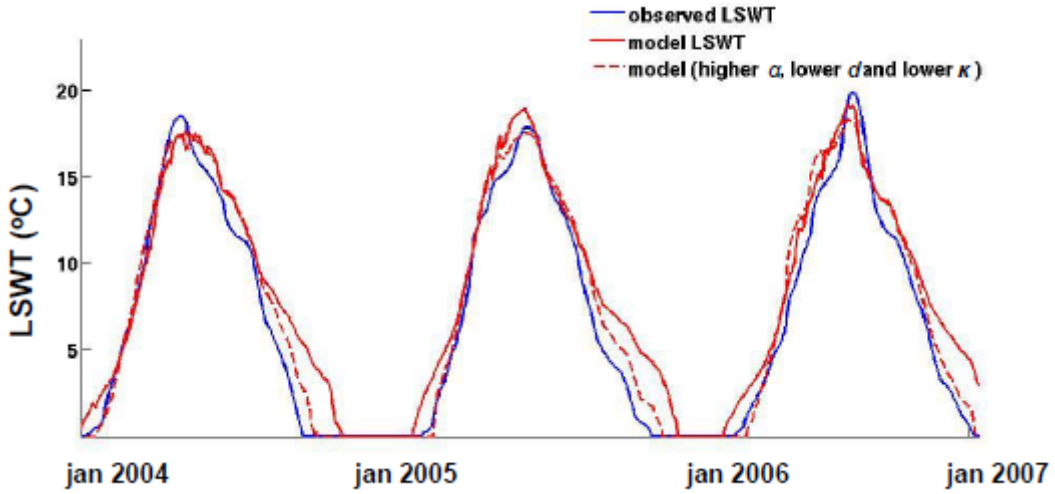

Figure 29 Preliminary modelled runs for Lake Ladoga showing how d, α and κ alterations produce modelled LSWTs that are closer to the observed LSWTs.

3.2.1.2 LSWT regulating properties.

I tune the LSWTs of individual lakes using these 3 LSWT regulating properties, by applying a range of values/ factors to each property, as described in this section.

Lake depth (*d*); The mean depth (Z_d1) is the recommended depth value for *FLake*. Lake depth information was obtained from Herdendorf (1982), the ILEC World Lake Database (http://wldb.ilec.or.jp/), LakeNet (http://www.worldlakes.org/) and (Kourzeneva *et al* 2012). Where only maximum depth is available, I calculated the mean depth using the average maximum-to-mean depth ratio of lakes with known maximum and mean depths. I found this ratio to be 3.5 for seasonally ice covered lakes and 3.0 for non-seasonally ice covered lakes. I apply a range of effective depth (Z_d) factors to the lake-mean depth (Z_d1: Z_d6), ranging from 0.3 to 2.5 times the mean depth, Table 8. For lakes with no depth information, I initially apply a depth of 5 m. Applying depths to lakes with no depth information further discussed in chapters 4 and 5.

Light extinction coefficients (κ); I apply two methods for deriving light extinction coefficients. For the initial investigative work on trial lakes, the light extinction coefficients values are derived from Secchi disk depth data (κ_{sd}), as described in the next chapter. Much of the Secchi disk depth data are obtained from the ILEC database (ILEC 1999).

For the tuning of all lakes, I use an alternative method, as many lakes do not have available Secchi disk depth data. I apply a range of 10 optical water types which essentially describe the attenuation process of oceans and its changes with turbidity (Jerlov 1976). These consist of 5 optical water types for open ocean, type I, IA, IB, II and III; type I being the most transparent and type III being least transparent and 5 coastal ocean types (1, 3, 5, 7 and 9) (Jerlov 1976). The spectrums for these 10 ocean types are divided (0.18, 0.54, 0.28) into three wavelengths; 375 nm, 475 nm and 700 nm, respectively. The 10 ocean types are renamed herein as κ_{d1} to $\kappa_{d10,}$ the values for which are shown in Table 8.

Albedo (α); the model default albedo value is 0.60 for snow and white ice and 0.10 for melting snow and blue ice, I refer to this as $\alpha 1$. On the basis of the modelled biases highlighted in chapter 1, section 1.7, I apply 3 additional albedos of higher values ($\alpha 2$: $\alpha 4$), shown in Table 8, when tuning of seasonally ice-covered lakes. A higher albedo causes more of the incoming radiation to be reflected, causing a later (and more timely) ice-off. Albedo when discussed throughout this study refers to snow and ice albedo.

Lake depth	Light extinction coefficient				albedo	Snow & white ice Albedo	Melting snow & blue ice albedo
	κ_d	375nm	475nm	700nm			
Z_{d1}	$\kappa_{d\,1}$	0.038	0.018	0.56	α1	0.60	0.10
	$\kappa_{d\,2}$	0.052	0.025	0.57	α2	0.80	0.60
Z_{d2} (Z_{d1}* 0.75)	$\kappa_{d\,3}$	0.066	0.033	0.58	α3	0.80	0.40
Z_{d3} (Z_{d1}* 0.50)	$\kappa_{d\,4}$	0.122	0.062	0.61	α4	0.60	0.30
Z_{d4} (Z_{d1}* 1.50)	$\kappa_{d\,5}$	0.22	0.116	0.66			
	$\kappa_{d\,6}$	0.80	0.17	0.65			
Z_{d5} (Z_{d1}* 0.30)	$\kappa_{d\,7}$	1.10	0.29	0.71			
Z_{d6} (Z_{d1}* 2.50)	$\kappa_{d\,8}$	1.60	0.43	0.80			
	$\kappa_{d\,9}$	2.10	0.71	0.92			
	$\kappa_{d\,10}$	3.00	1.23	1.10			

Table 8 Lake depth, light extinction coefficient and albedo factor/ values be to applied for the tuning of 246 lakes. $\kappa_{d\,1}$ to $\kappa_{d\,5}$ represent Jerlov's 5 optical water types for open ocean and lakes $\kappa_{d\,6}$ to $\kappa_{d\,10}$ represent the 5 optical water types for coastal ocean

The range of values/ factors for the LSWT regulating properties depend on the lake type. For examples, for non-seasonally ice covered lakes, only lake depth and light extinction coefficient are applied, as albedo is irrelevant where ice cover is not part of the LSWT cycle.

3.2.1.3 Lake model properties

Properties that are lake-specific but have less influence on the LSWT than the 3 LSWT regulating properties, are referred to as lake model properties. Some model properties for example, c_relax_C and fetch (defined in this section), can affect LSWT but to a lesser extent. Additionally, the strong relationship between c_relax_C and lake depth and between wind fetch and lake dimensions or surface area, allow for a realistic determination of these values for these properties. The lake model properties are retained throughout the investigative and tuning process.

c_relax_C; is a relaxation time scale for the temperature profile in the thermocline. The default c_relax_C value of 0.003 was found to be too low to adequately readjust the temperature profile of deep lakes (Kirillin 2010), weakening the predicted stratification and affecting the LSWT. For lakes with mean depths < 5 m, the c_relax_C is set to 10^{-2}, and decreases with increasing depth, to a setting of 10^{-5} for mean depths > 50 m, as recommended by Kirillin (2010).

fetch; I determine the lake wind fetch to be the square root of the product of lake length and breadth measurements. These measurements are available for 205 of the 246 lakes. The calculated fetch of these 205 lakes are found to be strongly related to surface area, Equation 1 ($R^2_{adj} = 0.84$, $p = 0.001$). I use Equation 1 to determine the fetch of the remaining 41 lakes with no available dimensions.

Equation 1: fetch = 39.9 + 0.00781 area

latitude; the latitude of the lake centre reference co-ordinates (Herdendorf 1982; Lehner and Doll 2004)

Starting conditions; These parameters provide *FLake* with the lake specific initial temperature and mixing conditions. Other than shortening the model spin-up time, the starting conditions have no influence over the modelled LSWTs thereafter. The starting conditions are;

temperature of upper mixed layer
bottom temperature
mixed layer depth
ice thickness
temperature at air-ice interface

A good estimation of the starting conditions for each lake were obtained from the *FLake* model based on the hydrological year 2005/2006. (Kirillin *et al* 2011). The model was run for all lakes and the lake starting conditions were extracted.

3.2.1.4 Fixed model parameters

I refer to the model parameters that remain fixed throughout the investigative and tuning process, across all lakes, as fixed model parameters. These are;

icewater_flux
inflow from the catchment
heat flux from sediments
variation in the light extinction coefficient

icewater_flux; Kirillin (2010) suggests icewater_flux (heat flow from water to ice) values of ~3-5 W/m^{-2}. When modelled with values 3 and 5 W/m^{-2}, the effect on the LSWTs of 7 randomly chosen seasonally ice covered lakes is negligible. Extending the range of icewater_flux values to 2 and 10 W/m^{-2} the effect on the LSWT was very small, yielding daily mean absolute difference (MAD) values of between 0.05 - 0.08 $^{\circ}C$ across the 8 lakes. As there is very little available icewater_flux information on lakes and this parameter has a comparatively low effect on LSWTs, I apply an icewater_flux value of 5 W/m^{-2} across all lakes.

heat flux from sediments; It is reasonable to discount heat flux from sediments, as it has a negligible effect on the LSWT for deeper lakes (where there is no geothermal source).

inflow from the catchment; Although inflow of water from the catchment can affect the LSWTs for some lakes, the extent of the affect varies greatly from lake to lake, depending on factors such as the height and location of the inflow point/ area, the lake size and depth and the surrounding topography all. The preliminary trials showed that the modelled LSWTs can be adequately tuned using the 3 LSWT regulating properties, section 3.2.1.1. On this basis, the inflow from the catchment region is not expected to improve the tuning of the model. Furthermore, inflow data is not readily available for the majority of lakes.

variation in the light extinction coefficient: seasonal variation in the light extinction coefficient depends on factors such as, lake trophic level, on lake depth and wind strength for shallow lakes (strong winds can stir up lake bottom sediments, making shallow lakes more turbid). The effect of light extinction coefficient on the LSWT will therefore vary throughout the year will vary from lake to lake. For this study, light extinction coefficient is kept constant throughout the annual cycle. For all lakes, irrespective of the different lake conditions, the effect of the light extinction coefficient is more pronounced in summer when solar radiation is at its highest. For this reason, light extinction coefficient is one of the LSWT regulating properties as discussed in section 3.2.1.2 and is tuned by its effect on the maximum LSWT.

As a result, the schemes for catchment inflow, heat flux from sediments and the annual variation in the light extinction coefficient are not used in the tuning study.

3.3 Model forcing data

FLake is forced with meteorological data. I use ECMWF Interim Re-analysis (ERA) data provided by ECMWF (ECMWF 2009) at grid points close to the lake centre (0.7° x 0.7° resolution). Table 9 shows the ERA data components and the conversion used to fit *FLake* input requirements. The lake centre coordinates and the corresponding ERA coordinates are recorded in Appendix III. As the ERA data are available at a lower resolution (0.7° x 0.7°) than the observed LSWTs (0.05° x 0.05°), I use the ERA data at the grid point closest to the lake centre, as it is expected to represent the meteorological conditions of the whole lake. Additionally, the altitude of the meteorological conditions close to the lake centre is likely to be representative of the altitude of the lake.

ERA data components and description	Flake input format
SSRD; 3 hourly shortwave solar downward radiation, cumulative over 12 hour forecasts (W/m^{-2})	Mean SSRD W/m^{-2}
T2; 6 hourly air temperature at 2 metres (K)	Mean daily T2 ($^{\circ}C$)
D2; 6 hourly dewpoint at 2 metres (K) Equation 2	**Equation 2;** vapour pressure (hPa) $= P(z)*10^{(7.5(dewpoint / (237.7+dewpoint))}$ Where P(z) = P(sea level)*exp(-z/H). P(*z*)= pressure at height *z*, P(sea level)= sea level pressure (~1013 mb), z = height in metres, H= scale height (~7 km) http://www.gorhamschaffler.com/humidity_formulas.htm
U10 and V10; 6 hourly wind components at 10 meters (m/s) (Equation 3)	**Equation 3;** wind speed (m/s); $= sqrt (V10^2 + U10^2)$
TCC; 6 hourly total cloud cover	Mean daily TCC

Table 9 ERA data component description and *FLake* input format

3.4 The role of wind in LSWT

Wind speed is a major factor in determining LSWTs and over large areas of water it can be considerably stronger than wind measured over land (Stephens 2000; Resio *et al* 2008). The effect that wind can have on LSWT throughout the annual cycle is illustrated in Figure 30. The mechanical action of wind and current can prevent solid ice cover formation on the initial ice skim and can also accelerate the ice-off process by breaking up ice and mixing it with warmer sub-surface water (Williams 1965), shortening the ice cover period. Exposure of solid ice cover to strong winds promotes ice growth prolonging the ice cover period (Brown and Duguay 2010). Strong winds can drive lake mixing in deep lakes affecting the rate at which heat exchange occurs between the surface water and the atmosphere and the surface

water and deeper waters, strongly influencing the mixed layer depth and the LSWT. This is particularly true for tropical lakes (Lewis 1996) where smaller temperature (and density) differences between the mixed layer and the bottom layer of lake (hypolimnion) offer less of a buffer against wind mixing forces than for lakes where the temperature difference is greater. Wind speed is one of the 5 model forcing data components, Table 9. As most long-term wind measurements are observed over land, the ERA wind speed may not be wholly representative of wind speeds over large lakes.

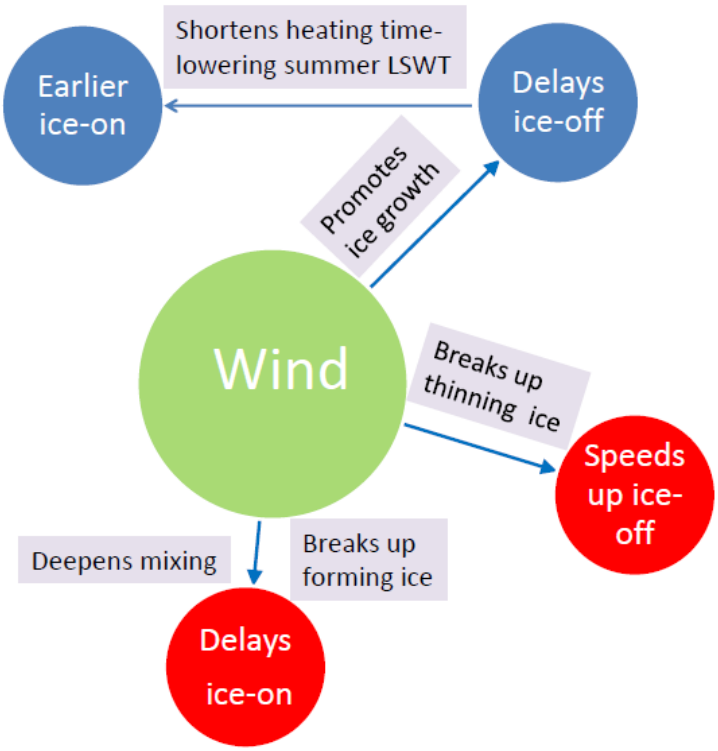

Figure 30 Schematic showing the effects that wind can have on the timing of ice-on and ice-off (red circles indicate a lessening of the ice cover period and blue circles indicate a lengthening). The grey boxes explain the cause of the wind effect on ice-on/ ice-off.

3.4.1 Over-water wind speed scaling

As most long-term wind measurements are observed over land, attempts have been made to correlate wind speeds measured over land (U_{land}) with those measured over water (U_{water}). The prediction of wind speeds over water is generally simpler than

over land due to the flattened topography of water (Stephens 2000). Where the fetch is long enough for the development of a marine boundary layer (> 16 km), U_{water} is suggested to be related non-proportionally to U_{land} (Resio *et al* 2008). Hsu (1988) suggests the following adjustment;

Equation 4; $U_{water} = 1.62 + 1.17\ U_{land}$

For fetches <16 km, the atmospheric boundary layer is said to be in transition and is not fully adjusted to the over water regime. In this case, a factor of 1.2 is considered a reasonable wind speed scaling (Resio *et al* 2008).

The majority of lakes considered in this study have fetches $\geq$ 16 km. There are also few smaller lakes with fetches < 16 km. I carry out the trial work applying wind speed scalings to the ERA wind speed timeseries to assess which better represents U_{water}. I use the unadjusted wind speed (*u1*), wind speed factored by 1.2 (*u2*) and wind speed suggested by Hsu (1988) (*u3;* Equation 4*)*. The tuning trials using wind speed scalings for the seasonally and non-seasonally ice covered lakes are discussed in chapter 4 and 5, respectively.

3.4.2 Modelling lake centre or lake-mean

FLake, initially validated as a stand-alone one-dimensional model requiring lake-mean properties and parameters, represents the LSWTs of the whole lake. In chapter 2, I found that for the majority of lakes, the observed lake-mean LSWTs (and therefore the LSWTs from the tuned model) are representative of the lake centre LSWTs. I find that there is good agreement between observed lake-mean and lake centre summer trends for the majority the lakes, indicating that the modelled LSWT trends can also be considered representative of the lake centre trends. For some smaller and more sinuous lakes, the lake centre trends are not representative of the lake-mean trends, as discussed in detail in section 2.8.1.

3.5 Conclusion

In this chapter, I demonstrated through the preliminary trials, how lake depth, snow and ice albedo and light extinction co-efficient (LSWT regulating properties) can greatly influence the modelled LSWTs, bringing the modelled LSWTs substantially closer to the observed LSWTs. I discussed the possible need to apply wind speed scalings to the ERA wind speed timeseries to better represent over-water wind speeds. As literature suggests that land based wind measurements, may not be representative of wind speeds over water, I carry out the tuning trials (in chapter 4 and 5) using 3 wind speeds. I apply the ERA unadjusted wind speed *(u1)*, the ERA wind speed factored by 1.2 (*u2*) and the wind speed suggested by Hsu (1988) (*u3)*.

Chapter 4 Tuning of seasonally ice covered lakes

4.1 Introduction

In the introduction, I highlighted the relatively short term availability of observational LSWTs. In this chapter, I begin to address this need by using the lake-mean observed LSWT data from 160 seasonally ice-covered lakes to tune the lake-mean LSWT from *FLake* lake model, with the aim to better represent LSWTs. In chapter 6, I evaluate the longer term LSWT timeseries from the tuned model. The tuning of LSWT for all other lakes (86 lakes non-seasonally ice-covered lakes are covered in chapter 5. The tuning process is carried out separately for these two lake types as the tuning of the start and end of the cold phase of seasonally ice covered lakes uses controls that are not applicable to non-seasonally ice coved lakes.

While all 246 lakes are located from 55° S- 69° N, the seasonally ice covered lakes are located from 29° N - 69° N, at altitudes from -12 to 5000 m a.s.l., and have lake-mean depths ranging from 1 to 680 m, surface areas of 100-32,000 km^2 and salinity values up to 155 g/l. Preliminary *FLake* trials carried out on 7 lakes identify lake depth (d), albedo (α) and light extinction coefficient (κ) as the lake properties most affecting the modelled LSWT (section 3.2.1.1). In this chapter, I also show that wind speed is an important factor in determining the LSWTs. Prior to tuning the 160 lakes, I carry out trials to help understand the modelled LSWT response to wind and to the LSWT regulating properties and to assess a range of values/factors for these properties.

In trial 1, I assess the ERA wind speed; *u1* (unscaled) and two scaled wind speeds (*u2*, *u3*), defined in chapter 3, using the recommended/ default LSWT regulating properties to find the most appropriate over-water (U_{water}) wind speed scaling. In trial 2, I apply a range of LSWT regulating properties values/ factors (giving a possible 80 combinations of d, α and κ) for each wind speed scaling. In this chapter,

I report and discuss the results from the trials (section 4.4 and 4.5), the tuning results of all 160 lakes (section 4.6 - 4.8) and the results of independent assessment of the tuned model (section 4.9).

For each lake, I use 4 tuning metrics to select the optimal combination of the LSWT regulating properties, *d*, α and *κ*. The tuning metrics show the comparability of the modelled and the observed LSWTs over the tuning period. Figure 31 summarises the tuning process for the 160 seasonally ice covered lakes. The aim of the tuning study is to obtain an average (across all lakes) daily MAD value of below 1.0 °C. As discussed in chapter 1, section 1.7, an MAD of $\leq$ 1 °C is possibly accurate enough for a global scale study. A lower MAD target may not be achievable for this tuning study which comprises of lakes with a wide range of geographical and physical characteristics.

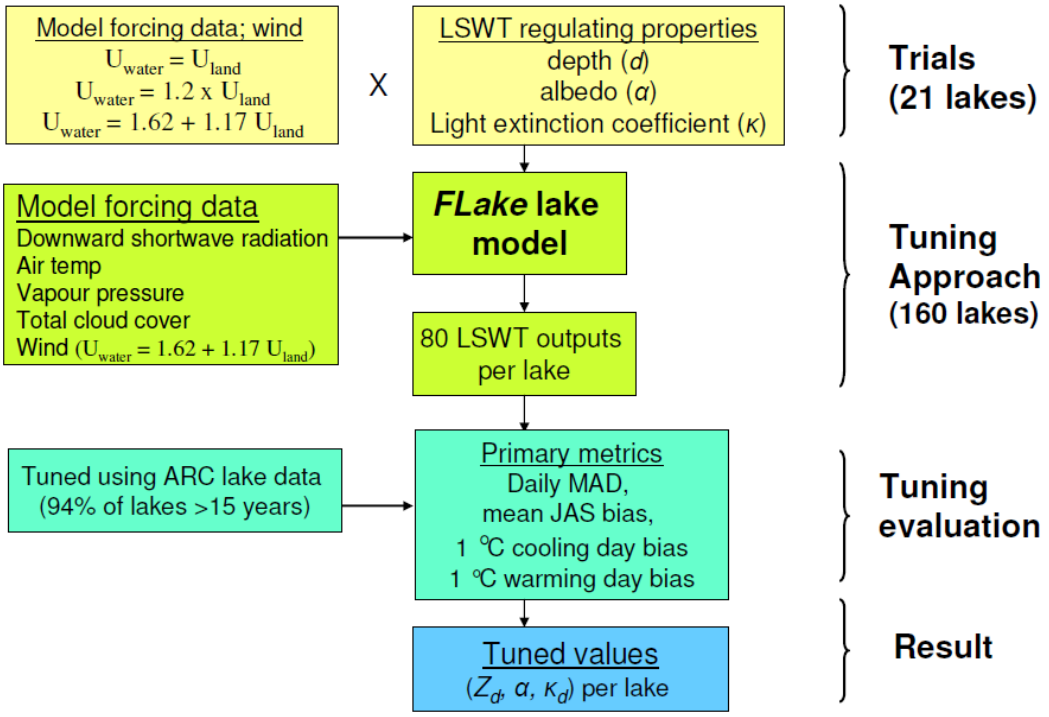

Figure 31 Tuning approach overview for seasonally ice covered lakes

4.2 Metrics

4.2.1 Primary metrics

The closeness of the modelled to the observed LSWTs is measured using 4 primary metrics (normalized and equally weighted), which are the basis of selecting the optimal LSWT model for each lake. These metrics measure the effect that the LSWT regulating properties d, α and κ have on the modelled LSWT. The relationship between the LSWT regulating properties and the primary metrics is summarised in Table 1.

LSWT regulating properties	Relationship with metric	primary metrics
d, α and κ	All LSWT regulating properties contribute to the comparability of the modelled and observed LSWT	**Equation 5**; Daily MAD (°C) $= \sum (abs(x_i^{mod} - x_i^{obs})) / N$; ^{mod} = daily modelled LSWTs ^{obs} = daily observed LSWTs N = sample size
κ	κ affects irradiance transmission of surface water, which is more notable in summer months	**Equation 6**; Mean JAS LSWT bias (°C) $= (\bar{x}_i^{mod\_jas} - \bar{x}_i^{obs\_jas})$ $^{mod\_jas}$ = mean modelled JAS LSWT $^{obs\_jas}$ = mean observed JAS LSWT
d	d alters heat storage capacity affecting timing of the start of the cold phase (the day that the LSWT drops to below 1 °C)	1 °C cooling day bias (days)
α	α alters ice/snow reflectance affecting the end of the cold phase (the day that the LSWT increases to above 1 °C)	1 °C warming day Bias (days)

Table 10 Relationship between the LSWT regulating properties and primary metrics, showing the equations for determining MAD and the JAS LSWT bias

4.2.2 Secondary metrics

Secondary metrics, namely, $inter_{jas}$, var_{jas}, the 4 °C cooling and warming day biases (days) are used in evaluating the modelled LSWTs but are not used in selecting the optimal modelled LSWT.

***Inter*$_{jas}$** calculates the fraction of the observed JAS LSWT inter-annual variability explained by the tuned model, *inter*$_{jas}$ *(*R^2_{adj}*)*;

Equation 7; $inter_{jas} = 1 - ((1 - r^2)(N - 1) / (N - P - 1))$

N = sample size (number of years with JAS LSWTs)
P = total number of regressors

$$r^2 = \frac{N\sum (x_i^{obs\_jas}\, x_i^{mod\_jas}) - \sum (x_i^{obs\_jas}) \sum (x_i^{mod\_jas})}{(N\sum (x_i^{mod\_jas\ 2}) - \sum (x_i^{mod\_jas})^2)\,(N\sum (x_i^{obs\_jas\ 2}) - \sum (x_i^{obs\_jas})^2)}$$

***var*$_{jas}$** calculates the variation in the observed JAS LSWT (Kelvin squared, K^2).

Equation 8; $var_{jas} = \sum (x_i^{obs\_jas} - \bar{x})^2 / (N - 1)$

4 °C warming and 4 °C cooling day; The 4 °C warming day (the day that the LSWT rises to above 4 °C in spring/ summer) and the 4 °C cooling day (the day that the LSWT drops to below 4 °C in autumn/ winter) mark the start and end of the open water mixing phase in freshwater lakes. Water warming from 0 to 3.98 °C, the temperature at which freshwater density is at a maximum, will mix, causing surface water to sink and mix with deeper waters, breaking up any remaining ice cover, marking the start of the open water phase. As the LSWT cools in autumn/ winter, water will sink and mix with deeper waters until it reaches 3.98 °C, at which point the cooler (and less dense) overlying water will no longer sink and mix, ending the open water phase. The 4 °C warming and cooling days are useful in determining the length of the open water phase of freshwater lakes.

4.3 Trial lakes

In a series of trials, I chose 21 lakes that are broadly representative of the range of lake characteristics, lake depth (*d*), albedo (α), and light extinction coefficient (κ),

of seasonally ice covered lakes and have available Secchi disk depth data. Secchi disk depth data is used to derive light extinction coefficients values in the first trial. I determine an appropriate range of values/ factors to be applied to d, α and κ for the tuning of the LSWTs in *FLake*. The suitability of the 3 wind speed scalings for seasonally ice covered lakes is assessed during these trials.

Of the 160 seasonally ice covered lakes, shown in Figure 33, the 21 trial lakes are marked by squares. The lake name, location and characteristics of the trial lakes, outlined in Table 11, encompass a wide range of lake characteristics. The trial lakes are located from 44° N - 69° N, at altitudes from 11 to 1640 m a.s.l. and have lake-mean depths ranging from 4 to 138 m, surface areas of 550 to 30,000 km^2 and light extinction coefficient values of 0.06 – 5.31 derived from Secchi disk depth (κ_{sd}).

4.3.1 Light extinction coefficients derived from Secchi disk depth

Secchi disk depth data are available for all 21 trials lakes and is used to derive light extinction coefficients values. Many studies have been carried out deriving κ values from Secchi disk depths (Poole and Atkins 1929; Holmes 1970; Bukata *et al* 1988; Monson 1992; Armengol *et al* 2003). Figure 32 compares 5 methods relating κ values to Secchi disk depths. This comparison covers a range of different water conditions, from coastal turbid waters (Holmes 1970) and eutrophic water (tested 1 km from a dam in the Sau reservoir, Spain) (Armengol *et al* 2003) to a range of North American lakes of different trophic levels (Monson 1992). Irrespective of the water state, for Secchi disk depths > 10 m, as shown in Figure 32, all 5 studies show a good comparison between Secchi disk depths and κ.

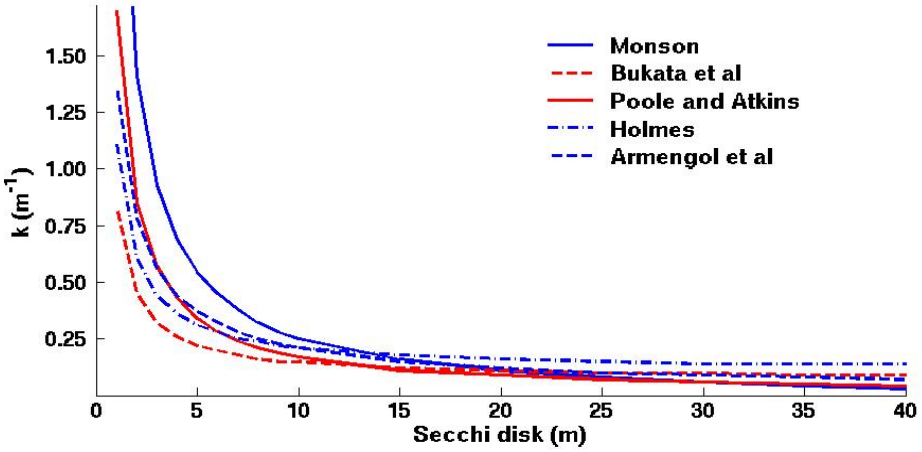

Figure 32 A comparison of 5 methods relating light extinction coefficients to Secchi disk depths, showing that all method compare well at Secchi disk depths > 10 m

From Secchi disk depths of 10 m to 1 m the range of results between studies become increasingly large. Bukata et al (1998) showed that the following formula (Equation 9), based on *in situ* optical measurements from many stations, adequately described Lake Huron, Lake Superior and Lake Ontario, for Secchi disk depths from 2 to 10 m;

Equation 9; $\kappa_{sd} = 0.757*S^{-1} + 0.07$

where S^{-1} = inverse Secchi disk depth (m). Of the 5 studies, this formula produces the lowest (most transparent) κ values, and possibly more likely to represent open water conditions of large lakes.

For Secchi disk depths outside the 2-10m range (less than 2 m and greater than 10 m) the Poole and Atkins (1929) formula is applied. This formula (Equation 10) is used as it is considered to serve as a universal relation between light extinction coefficient and Secchi disk depth data and provides sufficiently accurate estimations of light extinction coefficients in waters with all degrees of turbidity (Sherwood 1974).

Equation 10; κ_{sd} =1.7/ Secchi disk depth

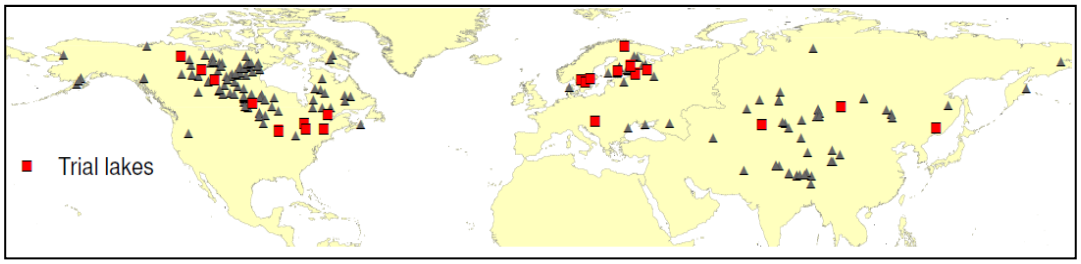

Figure 33 Location of the 160 seasonally ice covered lakes, with red square showing the 21 trial lakes

ARC ID	Lake name	Lat	Lon	Altitude (m a.s.l.)	surface area (km^2)	Mean depth (m)	κ_{sd}
9	Great bear	65.91	-121.3	157	30000	72	0.06
11	Great slave	62.09	-114.37	158	28000	41	0.13
13	Winnipeg	52.12	-97.25	217	24000	13	0.45
16	Ladoga	60.84	31.39	11	17500	52	0.32
17	Balkhash	45.91	73.95	329	17500	7	0.2
18	Onega	61.9	35.35	56	9500	30	0.29
23	Athabasca	59.1	-109.96	212	8000	26	0.26
29	Vanern	58.88	13.22	45	5500	27	0.16
45	Khanka	44.94	132.42	64	4000	5	1.7
59	Hovsgol	51.02	100.48	1640	2500	138	0.68
95	Vattern	58.33	14.57	91	2000	39	0.12
144	Inari	69.04	27.83	126	1200	14	0.12
157	Paijanne	61.71	25.49	95	1100	17	0.22
158	Saintjean	48.66	-72.02	97	1100	11	5.31
163	Malaren	59.44	16.19	18	1000	12	0.29
165	Champlain	44.45	-73.27	35	1000	23	0.2
195	Pielinen	63.16	29.71	113	1000	10	0.28
198	Nipissing	46.24	-79.92	212	900	5	1.59
236	Simcoe	44.47	-79.42	233	750	15	0.17
310	Balaton	46.88	17.83	126	550	4	2.98
340	Winnebago	44.02	-88.42	229	550	5	1.7

Table 11 Location, altitude, surface area, depth and light extinction coefficient of trial lakes.

4.4 Trial 1, the modelled effect of wind, depth and albedo on LSWT

The aim of this trial is to quantify how close the untuned modelled LSWT is to the observed LSWT and to evaluate the effect of wind speed scaling on the modelled LSWT. The untuned model is run with the recommended settings; default albedo and mean depth. For each of the 21 lakes, I model the LSWT using the mean depth (Z_d1), the default albedo ($\alpha 1$; snow and white ice= 0.60 and melting snow and blue ice = 0.10) and light extinction coefficient values derived from Secchi disk data (κ_{sd}) for 3 different wind speed scalings, *u1*, *u2, u3*. The primary metrics (MAD, JAS LSWT bias, 1 °C cooling day bias and 1 °C warming day bias; as described in section 4.1.1) are used to measure the accuracy of the modelled LSWT.

4.4.1 The effect of wind on LSWT

Using the fixed LSWT regulating properties with the unscaled wind speed (*u1*), the modelled LSWT shows that *FLake* consistently (for all lakes) overestimates the JAS LSWT by 3.71± 3.51 °C, Table 12. The length of the cold phase is under-estimated (the length of time the LSWT remains below 1 °C) by an average of 39 days, starting 12 days later and ending 27 days earlier than observations, Table 12. The trial using (*u2* and *u3*), show that *u3,* the highest wind speed scaling is the most suitable wind speed. Wind scaling, *u3* in place of *u1* reduces the mean difference in JAS LSWT by 50% from 3.71 to 1.87 °C and the mean daily MAD by 35% from 3.07 to 2.02 °C, Table 12. The higher wind speed scaling also reduces the difference in the length of the average cold phase (when compared to the observed cold phase) by 18 days (from 39 to 21 days). This scaling also causes an earlier (more timely) 1 °C cooling day, presumed to be due to an increase in the rate of the heat exchange with the atmosphere. The higher scaling also promotes ice-growth during solid ice cover causing a later (more timely) 1 °C warming day. The improvement that the higher wind speed scaling makes to the modelled LSWT for Lake Simcoe is

demonstrated in Figure 34. The panel on this figure shows the MAD and JAS LSWT average over the 19 year tuning period for the 3 wind scalings.

Trial 1	*u1*	*u2*	*u3*
MAD (°C)	3.07 ±2.25	2.66 ±1.93	2.02 ±1.30
Mean JAS bias (°C)	3.71 ±3.51	3.07 ±3.41	1.87 ±2.93
1 °C cooling day bias (days)	12.0 ±39.6	7.9 ±33.3	1.0 ±30.5
1 °C warming day Bias (days)	- 27.1 ±29.7	- 23.6 ±22.7	- 20.3 ±18.4

Table 12 The effect of wind speed scalings on untuned modelled LSWTs of the 21 trial lakes, showing the spread of differences across lakes, 2σ

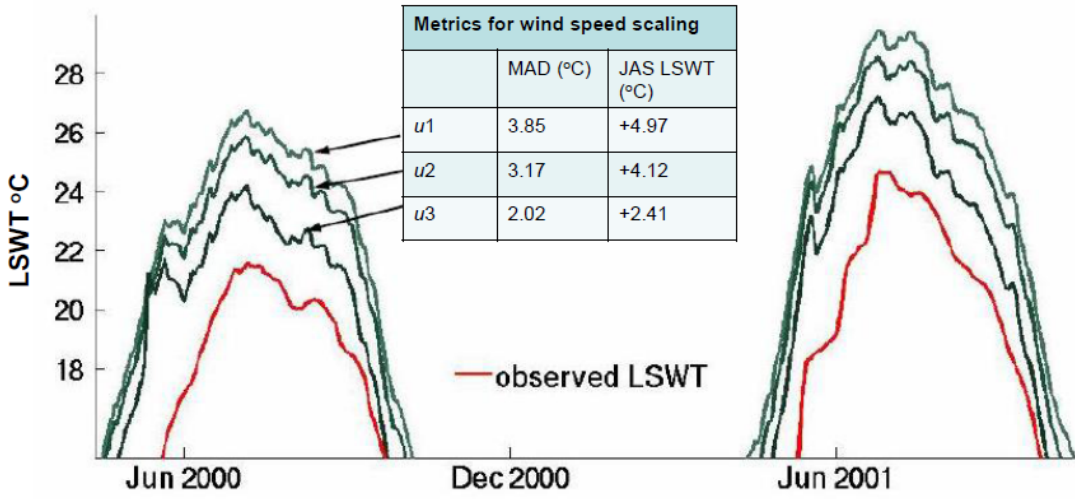

Figure 34 Effect of wind speed scalings on modelled LSWT for Lake Simcoe, Canada, showing that the *u3* scaling halves the daily MAD and JAS LSWT bias

4.4.2 The effect of the 1 °C warming day on JAS LSWT

The modelled LSWTs are greatly improved by applying the highest wind speed scaling, *u3,* Table 12, however, the 1 °C warming day still occurs too early and the mean JAS LSWT remains overestimated. I show that by applying a higher albedo

these two biases can be improved. I also find that the timing of the 1 °C warming day affects the JAS LSWT and the 1 °C cooling day of deep high latitude lakes. This finding is significant in understanding the role that lake characteristics can play in the response of lakes to changes in the climate.

When modelled with *u3*, the 1 °C warming day of the 21 trial lakes occurs, on average, 20 days too early. The snow cover module is not considered in this version of *FLake* and therefore the insulating effect that snow has on the underlying ice is not considered. It is possible that this is the reason for the earlier 1 °C warming day. These observations have been noted in other studies. Earlier ice-off days of an average of 6 days, were observed in a study comparing *FLake* LSWTs with MODIS observational data on 4 sites on Great Bear and Great Slave (Pour *et al* 2012). A study on 38 small lakes in Germany, showed that although the length of the ice cover period modelled in *FLake* was correlated with *in-situ* measurements, it was underestimated in most cases (Bernhardt *et al* 2012). As snow cover is not considered in *FLake*, the snow and ice albedo are set to the same default value. It is possible that the default albedo ($\alpha 1$) maybe too low, overestimating the surface absorption of short-wave radiation, leading to earlier warming and overestimated mean JAS LSWTs. Pour et al (2012) also found that *FLake* produced relatively warmer LSWTs in the open water phase for all 4 sites assessed. To assess if albedo can be adjusted to model a more timely 1 °C warming day and an improved JAS LSWT bias, I repeated the *u3* trial using a higher albedo, keeping all other parameters the same.

The results show that a higher albedo (snow and white ice = 0.80 and melting snow and blue ice = 0.60) delays the 1 °C warming day by 27 $\pm$ 12.6 days and decreases the mean JAS LSWT bias by half, to 0.98 $\pm$ 2.51 °C across the 21 lakes. The LSWTs for Great Bear and Great Slave lakes modelled with high and low albedo values shown in Figure 35, clearly show the effect that the later warming day has on the modelled JAS LSWT.

There is no correlation between the modelled JAS LSWT decrease and the length of the delay in the 1 °C warming day across the 21 lakes, meaning that not all trial lakes respond in the same way to a change in the 1 °C warming day. Over the 21 lakes, the range in the length of the delay in the 1 °C warming day, is quite consistent (18 of the 21 lakes show a delay of 22-34 days), while the range in the JAS LSWT decrease is highly variable, from 0.0 – 4.26 °C. Lake depth and latitude cause much of this variation. There is a statistically significant relationship between the amount of decrease in the modelled JAS LSWT (due to the change in the 1 °C warming day) and the increase in depth and lake latitude, together (using stepwise regression), accounting for 0.50 (R^2_{adj}, p = 0.001) of the JAS LSWT decrease. Separately, depth accounts for 0.35 (p = 0.003) of the JAS LSWT decrease and latitude for 0.26 (p= 0.01). Great Slave (62° N and 41 m in depth) and Great Bear (66° N and 72 m in depth), both deep, high latitude lakes, showed a JAS LSWT decrease of 4.26 °C and 3.40 °C as a result of postponing the 1 °C warming day by 28 and 32 days. Meanwhile, a similar delay in the 1 °C warming day (29 and 32 days) for Winnebago (44° N) and Khanka (45° N) both with depths of 5 m, resulted in only a small JAS LSWT decrease of ~0.1 °C. The magnitude of a JAS LSWT increase in response to an earlier 1 °C warming day is therefore greater for deep high latitude lakes, demonstrating a positive ice albedo feedback (on JAS LSWTs) for deep and high latitude lakes. The relationship between the amount of the JAS LSWT decrease per week of earlier 1 °C warming day, shown in Figure 36, clearly demonstrates the greater JAS LSWT change for deeper higher latitude lakes.

A study on Lake Superior, a deep lake, (average depth = 147 m) supports this finding (Austin and Colman 2007). A JAS LSWT warming trend (of 2.5 °C from 1979 to 2006) for Lake Superior which is substantially in excess of the air temperature warming trend, was found to be as a result of a longer warming period, caused by an earlier ice-off date of ~0.5 day yr^{-1}. The JAS LSWT trend of 2.5 °C from 1979 to 2006 in this study (Austin and Colman 2007) show similar warming to the ARC-Lake JAS LSWT trend of 2.2 °C from 1992-2011.

The modelled results also show that depth is a major factor in how the decrease in the JAS LSWTs affect the 1 °C cooling day. While the decrease in the JAS LSWT (as a result of the higher albedo) explains 0.25 ($R^2_{adj,}$ p= 0.012) of the inter-lake variation in the difference in the modelled 1 °C cooling day, depth explains 0.42 ($R^2_{adj,}$ p= 0.001) of the variation, causing an earlier 1 °C cooling day. For Great Slave (41 m depth) the modelled JAS LSWT decrease of 4.26 °C, resulted in an earlier 1 °C cooling day of 3.4 days, while for Great Bear which is deeper (72 m), the smaller JAS LSWT decrease of 3.40 °C had a bigger effect on the 1 °C cooling day, 7.6 days earlier. For the deepest lake in the trials, Lake Hovsgol (138 m at an altitude of 1640 m a.s.l.), the decrease of 2.60 °C had the largest effect on 1 °C cooling day, causing it to occur 12.8 days earlier.

This demonstrates that in addition to the greater positive ice albedo feedback on JAS LSWTs for deeper and high latitude lakes as a result of an earlier 1°C warming day, the higher JAS LSWT also contributes to the positive ice albedo feedback by causing a later 1°C cooling day. This demonstrates the sensitivity of the whole LSWT cycle of deep high latitude lakes, to changes in the timing of ice-off. This can also be extended to deep high altitude seasonally ice covered lakes, as lake at high altitudes have a longer ice cover period than lakes at low altitudes. For very deep lakes, such as Lake Hovsgol at 1640 m a.s.l., a delay of ~ 4 weeks in the 1 °C warming day results in a cooler JAS LSWT (by 2.6 °C) and an earlier 1 °C cooling day of ~2 weeks. The link between albedo and the LSWT regulating properties is illustrated in Figure 37.

The findings demonstrate that the modelled LSWTs sensibly relate to the modelled lake characteristics. For a shallow lake, the time required to heat up a lake (after ice melt) is shorter due to the lower heat storage capacity than that of a deeper lake. A delay in the 1 °C warming day, shortening the lake warming period, may not prevent a shallow lake reaching its full heating capacity but may prevent of a deep lake from reaching its maximum heat storage capacity. At higher latitudes, the warming period of northern hemispheric lakes become increasingly shorter as

demonstrated in chapter 2, Figure 16. With increasing latitude, deep lakes increasingly fall short of reaching their maximum heat storage, resulting in a lower JAS LSWT. As a result, deep and high latitude (or high altitude lakes) any changes to the 1°C warming day will affect JAS LSWT, highlighting their sensitivity to changes in ice-off.

The affect that depth has on the JAS LSWT is apparent when comparing lakes at the same altitude and latitude but with different depths. For example, Lake Nipigion, located in Canada at 49.8° N, has a mean depth of 55 m and an average JAS LSWT of 4.4 °C lower (15.4 °C) than that of Lake Manitoba (19.8 °C), Canada, located at 50.8 ° N but with a mean depth of only 12m.

The modelled 1 °C warming day, the mean JAS LSWT and the 1 °C cooling day biases in *FLake* can be substantially improved by applying a higher snow and ice albedo. A range of higher (than the default) albedo values are tested in trial 2 to provide a better representation of 1 °C warming day.

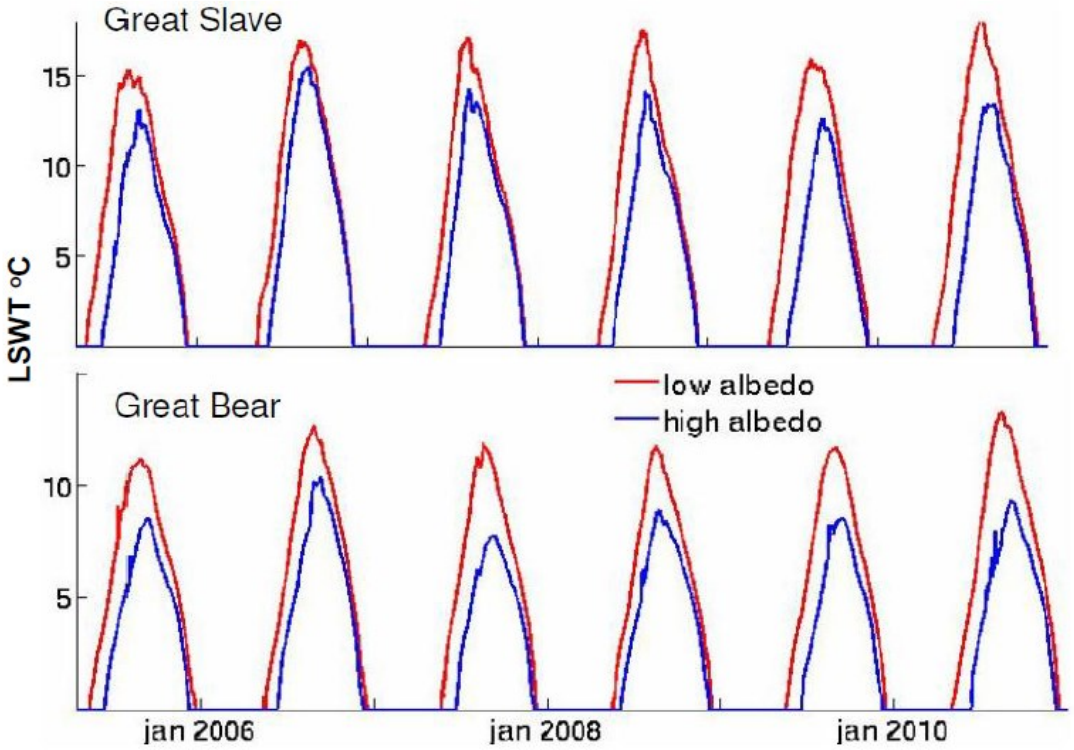

Figure 35 Trial 1 *u3* LSWTs for Great Bear and Great Slave modelled with low albedo (default albedo) and high albedo (snow and white ice = 0.80 and melting snow and blue ice = 0.60) demonstrates the that the higher albedo (blue line) causes a later ice-off and lower JAS LSWT

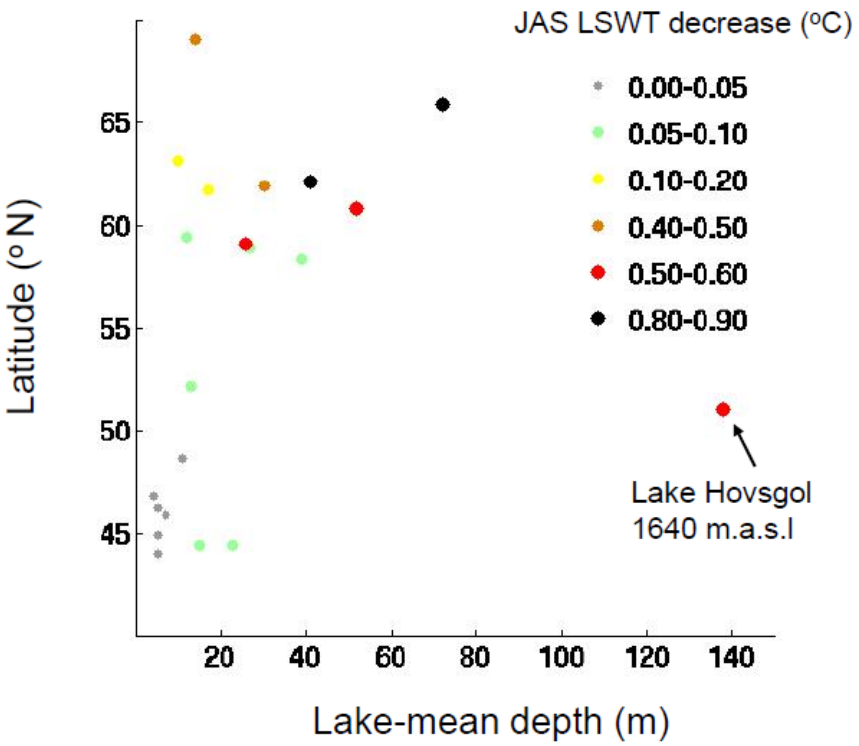

Figure 36 The JAS LSWT decrease (shown as °C decrease per week of later 1 °C warming day) caused by a higher albedo for the 21 trial lakes shown with respect to lake depth and latitude. This figure shows that high latitude and deep lakes show largest JAS LSWT decrease with later 1 °C warming day, signifying that the LSWT of high latitude and deep lakes are more responsive to changes in the 1 °C warming day.

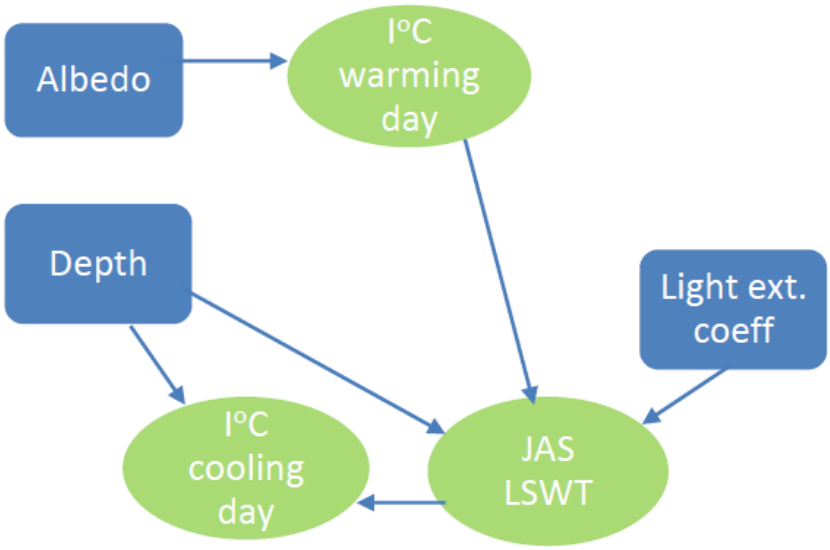

Figure 37 Schematic linking the LSWT regulating parameters (blue squares) with LSWT phases (green circles)

4.4.3 The effect of depth on the 1 °C cooling day

The lake-mean depth used in trial 1 may not be suitable for all lakes. Although the mean 1 °C cooling day, modelled using *u3* shows a good improvement when compared to *u1* and *u2*, Table 12. Modelled using *u3*, the 1 °C cooling day of the four deepest lakes (41 -138m) occurs on average 22 days later than the observed 1 °C cooling day, indicating that the modelled LSWT is taking too long to cool. A shallow lake (which has a lower heat capacity than a deep lake), will cool more quickly, resulting in an earlier and more timely 1 °C cooling day. Similarly, 1 °C cooling day for the four shallowest lakes (< 5 m) occur, on average, 14 days earlier than the observed data, in this case a higher depth (which increases the heat capacity), results in a more timely (later) cooling day.

I repeat trial 1, for all 21 lakes, (using *u3*), halving the mean depth for lakes over 40m and multiplying the mean depth by 1.5 for lakes <5 m. This results in a more timely 1 °C cooling. The average 1 °C cooling day bias for the four deepest lakes (41 -138m) reduces from 22 days to 1 day and for the four shallowest lakes (< 5 m) it reduces from 14 days early to 11 days. As a result, in trial 2 I apply a range of 4 lake depth factors to all lakes allowing depths from 0.5 to 1.5 times the lake depth to be modelled for each lake.

It is possible that the deepening of shallow lakes in the tuning process is compensating for not having considered the 'heat flux from sediments' scheme in the model. In chapter 3, I outlined that the solar heating and heat capacity of lake sediments can be ignored for deeper lakes, for shallower lakes however retention of heat in the sediments will increase the heat storage capacity of the lake delaying the 1 °C cooling day.

Many deep lakes have 3 distinct layers, the upper mixed layer (epilimnion) and the underlying thermocline (metalimnion) and a third layer referred to as the bottom layer or hypolimnion. As *Flake* is based on a two-layer parametric representation of the evolving temperature profile and on integral energy budgets (Mironov 2008), it

is possible that for deep lakes the mean depth (mean of entire lake depth) is tuned to a shallower depth as it is more representative of the mean depth of the 2 upper lake layers.

Although lake depth is strongly related to the heat storage capacity of a lake, factors such as topography, altitude, bathymetry and surface area affect the rate at which heat is exchanged between the atmosphere and the surface water. Although these factors show considerable lake–to-lake variation (as shown for altitude and surface area of the ARC-Lake lakes, Appendix I), they are not considered in *FLake.* Adjustment of the lake depth may also compensate for effect that these factors have on the rate of the surface heat exchange.

4.5 Trial 2, tuning of the LSWT regulating properties

In trial 1, I established that wind speed scalings, depth and albedo can be altered to improve the fit of the model to the observed LSWT data. The aim of the trial 2 is to attribute an appropriate range of values/ factors to the lake depth and albedo and also to assess an alternative method for determining an appropriate κ value.
In trial 1, I used light extinction coefficient values derived from Secchi disk depth data (κ_{sd}), however Secchi disk depth data are not readily available for the majority of lakes. In this trial, I use an alternative method for determining an appropriate light extinction coefficient (κ) value. I apply all three winds speed scalings and assess how the different scalings affect the optimal LSWT regulating properties.

Light extinction coefficient; I apply a range of light extinction coefficient values for 5 open ocean types (type I, IA, IB, II and III; type 1 being the most transparent and type III being least transparent) (Jerlov 1976), as discussed in chapter 3, section 3.2.1.2, instead of the κ_{sd}. Ocean types I-III correspond to κ_{d1} to κ_{d5}, Table 13.

Depth;. In this trial, I apply the lake-mean depth (Z_{d1}) and 3 additional effective depth factors (Z_{d2}- Z_{d4}) ranging from 0.5 to 1.5 times Z_{d1}.

Albedo; In this trial, I apply 4 different albedo values, the lowest of which is the *FLake* default albedo (*α1*), the highest of which was assessed in section 4.4. (trial 1).

I model each lake using a range of depth adjustment factors and a range of values for albedo and light extinction coefficient, resulting in 80 (4 x 4 x 5) possible combinations, as shown in Table 13. I normalize the primary metrics results (equally weighted), section 4.2.1, selecting the most optimal set of LSWT regulating properties for each lake.

Trial	Light extinction coefficient				Albedo			Lake depth
	κ_d	375nm	475nm	700nm		Snow & white ice	Melting snow & blue ice	
2	κ_{d1}	0.038	0.018	0.56	α1	0.60	0.10	Z_{d1} (mean depth)
	κ_{d2}	0.052	0.025	0.57	α2	0.80	0.60	Z_{d2} (Z_{d1} *0.75)
	κ_{d3}	0.066	0.033	0.58	α3	0.80	0.40	Z_{d3} (Z_{d1} *0.50)
	κ_{d4}	0.122	0.062	0.61	α4	0.60	0.30	Z_{d4} (Z_{d1} *1.50)
	κ_{d5}	0.22	0.116	0.66				

Table 13 LSWT regulating property combinations for trial 2 for each of the wind speed scalings, *u1- u3,* showing 80 possible combinations (5 κ_d x 4 α x 4 Z_d) for each scaling

4.5.1 Trial 2 results; tuning of the LSWT regulating properties

Trial 2 results show that the tuning of the LSWT regulating properties yield marginally better for *u3.* For 20 of the 21 lakes, *u3* has a lower mean MAD value than for *u1* and *u2* and also has the lowest range of errors for 3 of the 4 primary metric results, (Table 14). The inter-play between wind and the 3 LSWT regulating properties in the tuning of the trials lakes is discussed in section. 4.4.1 (trial 1) and illustrated in chapter 3, Figure 30.

Use of *u3* is strongly supported by the results from trial 1 and by literature recommendations, as discussed in chapter 3. On this basis, the approach outlined in

Table 13, using *u3* (herein approach 1), is applied to all 160 lakes, reported in section 4.6.

Using approach 1, across all three wind speed scalings, the 1 °C cooling day For 1 of the 21 lakes, Lake Balaton, the 1 °C cooling day ranges from 14-18 days early across the 3 wind speed scalings and has JAS LSWTs of ~2.0 °C lower than the observed LSWTs. Lake Balaton is the shallowest of the trial lakes. It has a mean depth of 4 m and has the second highest light extinction coefficient, κ_{sd} = 2.98 (equivalent to a Secchi disk depth of ~0.57m). Despite being tuned to the maximum depth factor and maximum light extinction coefficients values, the early cooling day of Lake Balaton indicates that the depth is still too shallow and the low JAS LSWT indicates that the κ_d value is still too low to retain enough heat in the surface. As discussed in section 4.4.3 (trial 1), considering the heat flux from sediments for shallower lakes would increase the heat storage capacity of the lake and cause a delay in the 1 °C cooling day.

The results for Lake Balaton highlight the possible limitations of using approach 1 for the tuning of shallow lakes with high light extinction coefficients (more turbid). To address this, I consider an alternative optimisation approach (approach 2) for shallow lakes with high light extinction coefficients in section 4.6.

Trial 2 20 lakes (excluding lake Balaton)	*u1*	*u2*	*u3*
MAD (°C)	0.89± 0.62	0.88± 0.63	0.84± 0.51
Mean JAS bias (°C)	0.03± 1.32	0.16± 1.26	-0.12± 1.09
1 °C cooling day bias (days)	-0.7± 10.1	-2.6± 10.4	-1.6± 12.8
1 °C warming day Bias (days)	-0.4± 11.6	-0.3± 10.9	-0.2± 10.7

Table 14 Trial 2 metric results for the 3 wind speed scalings, showing the spread of differences across lakes, 2σ

4.5.2 Inter-play between wind and the LSWT regulating properties

The inter-play between the κ_d values, Z_d depth factors (and to a lesser extent the four α values) compensate for the different wind speed scalings, resulting in comparable results across all three wind speed scalings (Table 14).

The *u3* optimal LSWT regulating properties for 7 of the trial lakes resulted in a lower simulated κ_d, 6 lakes have a higher Z_d and 3 lakes have both a lower κ_d and a higher Z_d than for *u1*. It makes sense that at a higher wind speed scaling the κ_d would be lower and the Z_d would be greater. The higher wind speed (*u3*) causes more thorough mixing, deepening the mixed layer, possibly causing the cooler lake surface for Lake Simcoe, shown in Figure 34. In the tuning process, the cooler surface as a result of the higher wind speed is counteracted by a less transparent lake surface (higher κ_d), causing more heat to be retained in the surface layer, increasing the LSWT. A more rapid exchange of heat between the surface and atmosphere, due to a higher wind speed is also the possible cause of the earlier 1 $^{\circ}$C cooling day shown in Figure 34. A greater lake depth possibly counteracts the earlier 1 $^{\circ}$C cooling day, by slowing down the time taken to cool the lake, as shown for Lake Ladoga in Figure 38.

The results show that when modelled with *u1,* half (10) of the lakes are optimised with the maximum albedo (*α2*; snow and white ice = 0.80 and melting snow and blue ice = 0.60). A lower albedo is optimised for 3 of these 10 lakes using *u3*. In this case, the higher wind speed scaling, which prolongs the ice cover period, is counteracted by a lower albedo which causes an earlier 1 $^{\circ}$C warming day.

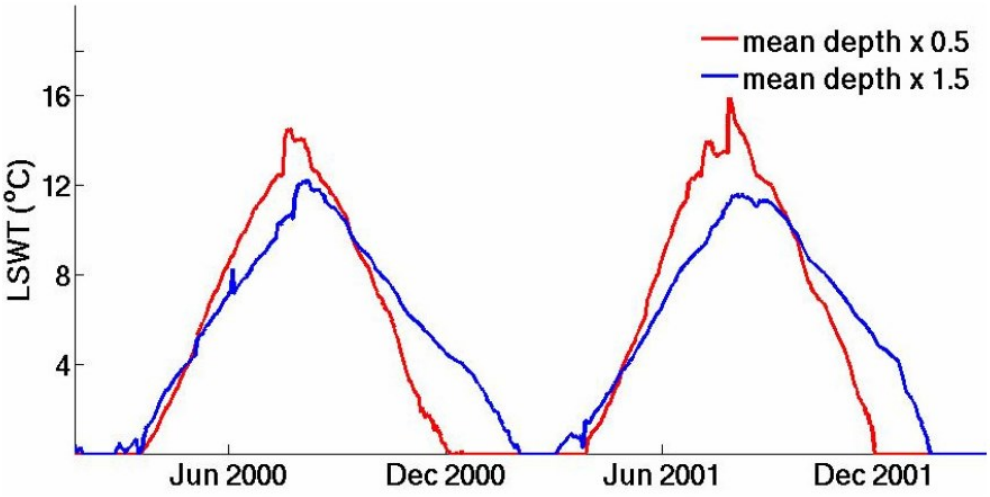

Figure 38 Effect of depth on LSWT for Lake Ladoga, Russia, showing that when modelled with a greater depth, the lake cools later and the maximum LSWT is lower

4.6 Tuning of all 160 lakes

I present the results of the tuning study, summarising and illustrating the primary and secondary metrics results for each lake. Firstly, I explain how I determine the depth of lakes that have no depth information.

4.6.1 Lakes with unknown depths

38 of the 160 lakes have no depth information, for these lakes I used an initial default value of 5 m. Applying the depth factors (Z_{d1}- Z_{d4}), allow a range of depths from 2.5 to 7.5 m to be evaluated. Where the results indicate that the 5 m input value is too low, the tuning is repeated using a depth of 16 m, which allows evaluation of depths from 8 to 24 m. A depth that is too low is characterized by an early 1 °C cooling day and a high JAS LSWT, as shown in Figure 38. This procedure allows a range of depths from 2.5 – 24 m to be considered for lakes with no available depth data.

For modelling very deep lakes, a "false depth" is recommended (Kirillin 2010). A false depth of 100 m is applied to Lake Baikal (mean depth of 680 m). For all other seasonally ice covered lakes, the mean depth does not exceed 138 m. The range of depth factors in the tuning process negates the need to apply a false depth to any other seasonally ice covered lake (other than lake Baikal).

4.6.2 Tuning results

The tuning approach 1 (trial 2 using *u3*; Table 13) is applied to all 160 lakes and yield results that are comparable to the observed LSWTs for 135 of the 160 lakes. The remaining 25 lakes (shallow lakes and/or lakes with high light extinction coefficients) are tuned using a modification of this approach (approach 2).

For 135 of the 160 lakes, approach 1 yield results comparable to the trial 2 results for the 20 lakes, as shown in Table 15. The tuned LSWT regulating properties and the corresponding primary metric results for each lake are shown in Appendix III. 90% of the lakes yield daily MAD values of $\leq$ 1.0 $^{\circ}$C and range from 0.44 to 1.92 $^{\circ}$C. The mean JAS LSWT for 95% of the lakes is within 1.0 $^{\circ}$C of the observed JAS LSWT and range from -1.37 to +1.96 $^{\circ}$C of the observed JAS LSWT. Using Lake Bras d'or, I demonstrate that *FLake* is suitable for tuning LSWTs for saline lakes.

For the remaining 25 lakes, (including trial lake; Lake Balaton), the tuned results from approach 1 yield comparatively poor results. The average depth of these 25 lakes is < 5 m and most have unknown transparencies, although the metric results indicate that these lakes are relatively turbid. The tuned LSWTs for these lakes show a 1 $^{\circ}$C cooling day $\geq$ 14 days earlier than the observed 1 $^{\circ}$C cooling day and/or a JAS LSWT value of $\geq$ 2 $^{\circ}$C lower than the observed JAS LSWTs. Similar to the results for Lake Balaton in trial 2, these results indicate that the modelled lakes require two possible adjustments; 1) a greater depth to increase the heat capacity, postponing the 1 $^{\circ}$C cooling day and, 2) lower transparency values (higher κ_d) to retain more surface heat increasing the JAS LSWT. The need to apply higher *d* factors and higher κ_d values is apparent from the tuned values for the 25 lakes. All

lakes were tuned with the highest depth factor, Z_{d4} and/or the highest light extinction coefficient, κ_{d5} (lowest transparency).

I modify approach 1 by including 3 greater depth factors (2, 2.5 and 4 times the mean depth), Z_{d5}: Z_{d7}, and 2 higher light extinction coefficient values (κ_{d6} and κ_{d7}), equivalent to coastal type 1 and 3 (Jerlov 1976). Albedo values remain the same. This approach (herein approach 2) for is applied to these 25 lakes substantially improving the 1 $^{\circ}$C cooling day and the JAS LSWT. A summary of the approach 2 results are shown in Table 15. The 1 $^{\circ}$C cooling day bias is on average 1.3 days (ranging from -8.0 to 5.4 days) later than the observed 1 $^{\circ}$C cooling day and the JAS LSWT is on average 0.34 $^{\circ}$C (ranging from -1.96 to +1.17 $^{\circ}$C) lower. The LSWT regulating properties and the corresponding primary metric results are recorded in Appendix III. One of the 25 lakes, Lake Istada, (a small lake of 127 km^2 and of unknown salinity), yields reasonably poor results with approach 1 and approach 2, showing a daily MAD and a mean JAS difference of ~2.0 $^{\circ}$C (approach 2).
The MAD metrics are better for approach 1 (average of 0.74 $^{\circ}$C) than for approach 2 (average of 1.11 $^{\circ}$C), as shown in Table 15. While 90% of the lakes yield daily MAD values of $\leq$ 1.0 $^{\circ}$C for approach 1, only 40% of lakes have daily MAD values of $\leq$ 1.0 $^{\circ}$C for approach 2, however 90% having MAD values of $\leq$ 1.5 $^{\circ}$C. The 1 $^{\circ}$C cooling and warming day biases are comparable for both approaches.

The results for all 160 lakes, column 3, Table 15, are highly comparable to the results for the 20 lakes trial lakes, column 4, Table 15. All primary metric results are displayed in Figure 39, the approach 2 results are marked by diamond symbols. With the exception to Northern Canada where the modelled JAS LSWTs are generally warmer than the observed LSWTs (Figure 39a), there are no obvious regional biases in the metrics results. The daily MADs are greater in Asia for lakes tuned with approach 2, than in the rest of the northern hemisphere, Figure 39b.
A summary of the secondary metrics, shown in Table 15, show that the fraction of inter-annual variability in the observed JAS LSWT explained by the model is highly comparable for the two approaches and that the observed JAS LSWT

variation are similarly comparable. The secondary metrics, although not used in the tuning process, show that the average length of the open water phase (the length of time the LSWT remains above 4 °C) is within 1 week of the observed open water phase. The start of the open water phase (4 °C warming day) occurs 6 days too early for approach 1 and the end of the phase (4 °C cooling day) occurs 7 days too late for approach 2, overestimating the open water phase by ~1 week. The open water phase of lakes is illustrated and discussed in chapter 2, section 2.7.

Trial 2	Approach 1 (135 lakes)	Approach 2 (25 lakes)	All lakes (160)	Trial (20 lakes)
Primary metrics				
MAD (°C)	0.74± 0.48	1.11± 0.56	0.80± 0.56	0.84± 0.51
Mean JAS bias (°C)	-0.01± 1.11	- 0.34±1.22	-0.06± 1.15	-0.12± 1.09
1 °C cooling day bias (days)	-1.0± 8.8	-1.3± 6.9	-1.08± 8.5	-1.6 ± 12.8
1 °C warming day Bias (days)	0.5± 12.6	- 0.5± 10.2	0.3± 12.3	-0.2± 10.7
Secondary metrics				
4 °C warming day bias (days)	-6.07± 17.8	0.52± 17.9	-5.04± 18.4	5.3± 15.9
4 °C cooling day bias (days)	2.6± 13.7	7.0± 15.4	3.3± 14.3	-3.9± 16.0
$Inter_{jas}$ (R^2_{adj})	0.48± 0.62	0.50± 0.62	0.50± 0.62	0.61± 0.52
var_{jas} (K^2)	0.70	0.71	0.70	0.92

Table 15 Metric results for tuning approach 1 and 2, for all 160 lakes and for trial lakes, showing the spread of differences across lakes, 2σ

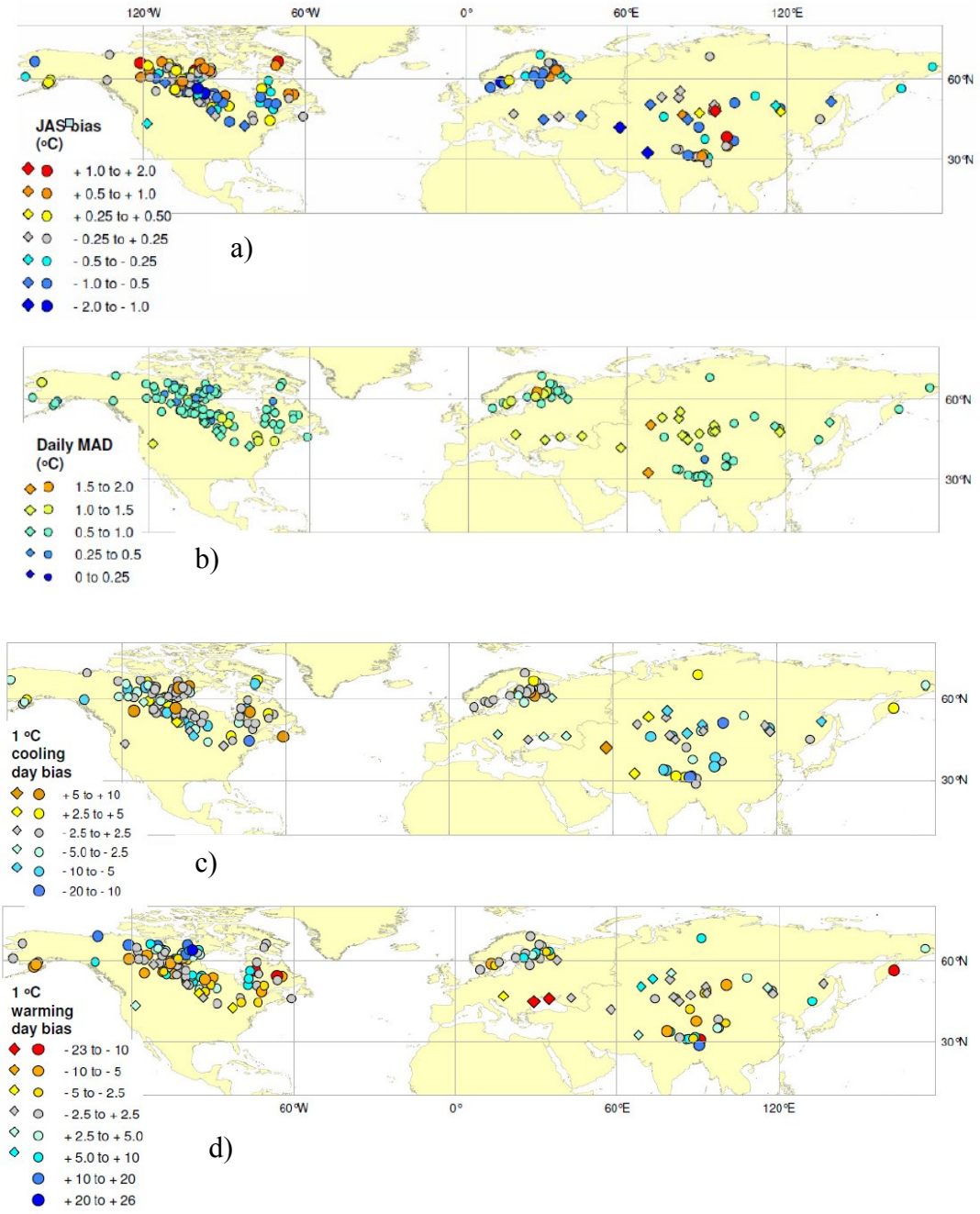

Figure 39 Primary metric results for all 160 lakes with seasonal ice cover. Approach 2 results are marked by diamond symbols a) JAS bias, b) MAD bias, c) 1 °C cooling day bias and d) warming day bias

Across all 160 lakes, the tuning of the 1 °C cooling day is a little better than the tuning of 1 °C warming day. This could indicate that albedo (or the albedo values; α_1- α_4) used in optimising the 1 °C warming day is slightly less effective than lake

depth (or the lake depth factors; Z_{d1}- Z_{d4}) used in optimising the 1 °C cooling day. For the 1 °C cooling day 78% of the biases are within 5 days of the observed biases and only 3 lakes have biases of > 10 days. For the 1 °C warming day 65% of the biases are within 5 days of the observed biases while 15 of the lakes have biases of > 10 days.

The success of the approach 1 tuning process, for 2 lakes (one North American and one European lake), is demonstrated in Figure 40. This figure compares the pre and post tuning LSWTs and the observed LSWTs for the 2 lakes, showing the tuned metric values (listed in Appendix III for each of the 246 lakes). The post tuning LSWTs and the observed LSWTs and the tuned metrics values (from Appendix III) are also shown for a saline and high altitude lake (Lake Ang-le-jen) modelled with approach 1 and a saline lake (Lake Ebi) modelled with approach 2, Figure 42. As neither depth nor light extinction coefficient/ Secchi disk depth data is available for Lake Ang-le-jen and Lake Ebi, there are no pre-tuning LSWTs for these lakes. This also demonstrates that LSWTs can be tuned irrespective of the lack of lake characteristic information.

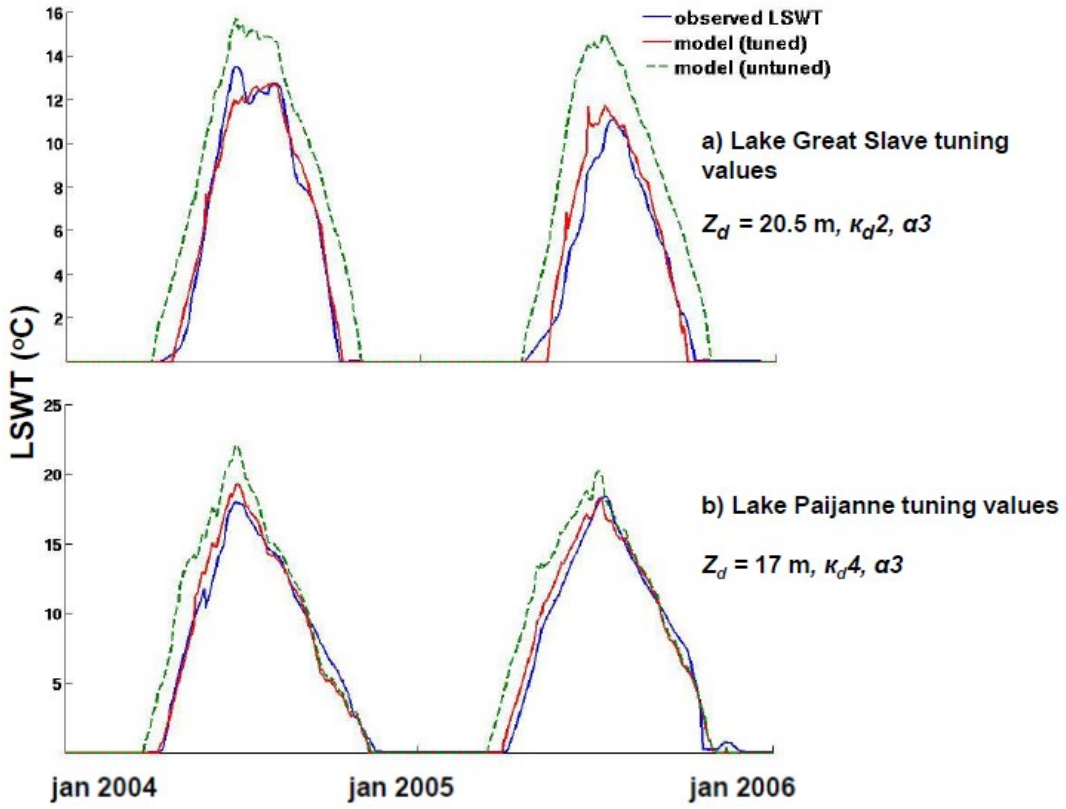

Figure 40 The pre and post-tuning and observed LSWTs for a North American and a European lake, showing the tuned metrics values (listed for all individual lakes in appendix III), demonstrating the success tuning process. Values for κ_d and α are shown in table 13

4.6.3 Tuned values for LSWTs regulating properties

The tuned values for the LSWT regulating properties, give an indication of how certain lakes types, for example deep lakes are represented in *FLake*. This information proves useful in obtaining improved modelled LSWT from *FLake*. It is evident from the tuned LSWT regulating properties for the 160 lakes that the model default albedo may be too low, the mean depth may only be suitable for lakes of medium depth and that if the light extinction coefficient value is not known, κ_{d4} and κ_{d5}, type II or III (Jerlov 1976) may be a good guesstimate.

The results of the tuning study highlight the importance of using an appropriate depth when modelling LSWTs using *FLake*. The effect of depth on the LSWT has been demonstrated through the trials carried out on the seasonally ice covered lakes. The results show that on average deep lakes (> 40 m) were tuned to depths of 0.7 times their mean depth, and shallow lakes (< 4 m) were tuned to effective depths 3.4 times their depth, Figure 41. For the shallow lakes, the factor is close to the maximum-to-mean lake depth ratio, 3.5 (of the 92 lakes with both maximum and mean depth data). As a rule of thumb the maximum depth may be considered a more suitable depth to use for shallow lakes when running Flake (without using the heat flux from sediments scheme). The inter-lake variation in the effective depth strongly reflects the variation in the mean depth, indicating that the effective depths are sensible. The effective and mean depth show a correlation of 0.75 (p= 0.000).

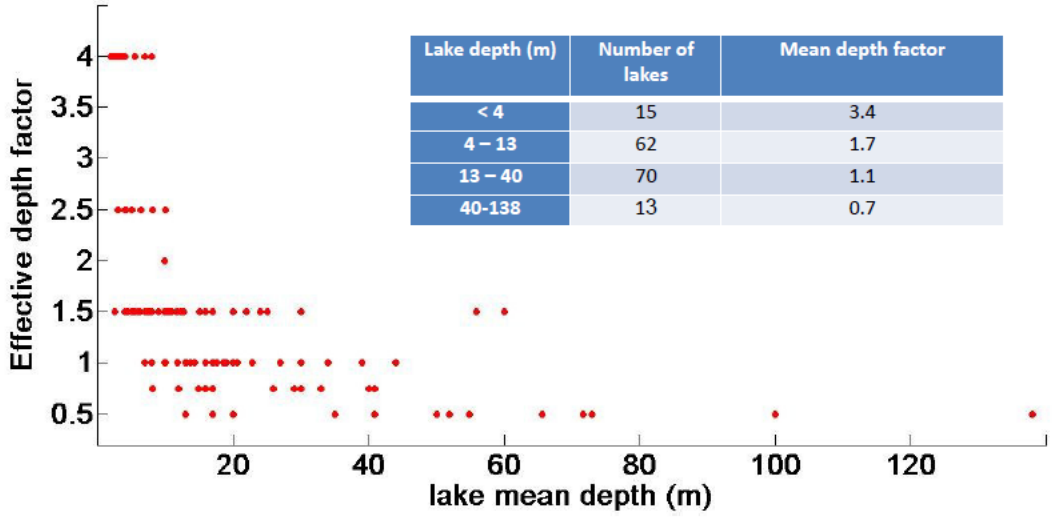

Figure 41 Tuned effective depth factor versus lake-mean depth, demonstrating that shallower lakes are tuned to a higher depth factor and deep lakes to a lower depth factor.

The 2 least transparent light extinction coefficients for open ocean κ_{d4} and κ_{d5}, (values shown in Table 8), were the tuned κ_d values for 64% of lakes. The 53 lakes tuned with κ_{d4} have an average depth of 17 m and the 50 lakes tuned with κ_{d5} have an average depth of 14 m, indicating that shallower lakes are tuned to a less

transparent κ_d value. This is sensible as the water clarity of a shallower lake is more affected by the lake bottom sediments than that of deeper lake.

Only 19% of the lakes were tuned to the default albedo, *α1,* (snow and white ice = 0.60 and melting snow and blue ice = 0.10). 64% of lakes were tuned to two higher albedos *α2* or *α3,* (snow and white ice = 0.80 and melting snow and blue ice = 0.60 for *α2* or 0.40 for *α3*), Table 13, indicating that the default albedo is too low.

Studies carried out on snow and ice albedo indicate that values for albedo are higher than the *FLake* default. Blue ice albedo values of 0.66 and snow values of 0.87 were obtained from ground-based observations of broadband, narrowband and bidirectional reflectance in Antarctica (Reijmer *et al* 2001). Although albedo generally increase with latitude, and the albedo values for Antarctica may not be applicable to lower latitude lakes, higher values (than the *FLake* default values) were also obtained on a Lake in Minnesota (~46° N), using radiation sensors. These showed the mean albedo of new snow to be 0.83 and the mean ice albedo (after snow melt) to be 0.38 (Henneman and Stefan 1999). These higher albedo values are comparable to the *α3* value.

4.7 Tuning of high altitude lakes

The average metric results and the spread of differences, for all 160 lakes, are presented for high altitude (14 lakes; 3200 to 5000 m a.s.l.) and low altitude lakes (146 lakes), in Table 16. The good comparison indicates that the geo-potential height (the altitude associated with the data measurement) for ERA data at the 0.7 ° x 0.7 ° grid reference co-ordinates is representative of the lake altitude, for the 160 lakes. Additionally, it demonstrates that the tuning approach either compensates for the effect that altitude has on heat transfer or else that this effect on the LSWT is minimal. The density of freshwater in *FLake* is determined at sea level (normal atmospheric pressure) (Mironow 2008). As a result of the lower density at high altitudes, the natural convective and thermal heat transfer processes are less effective. Although the variation of density (and therefore heat transfer) with

altitude is not considered for lakes in this study, which range from -12 to 5000 m a.s.l., the effect is shown to be minimal. The comparability of the observed and tuned LSWTs for two lakes, Lake Ang-le-jen, a high altitude lake (4863 m a.s.l.) and Lake Ebi a low altitude lake (166 m a.s.l.), is demonstrated in Figure 42. I discuss findings from the tuning of high altitude lakes in more detail in section 4.7.1.

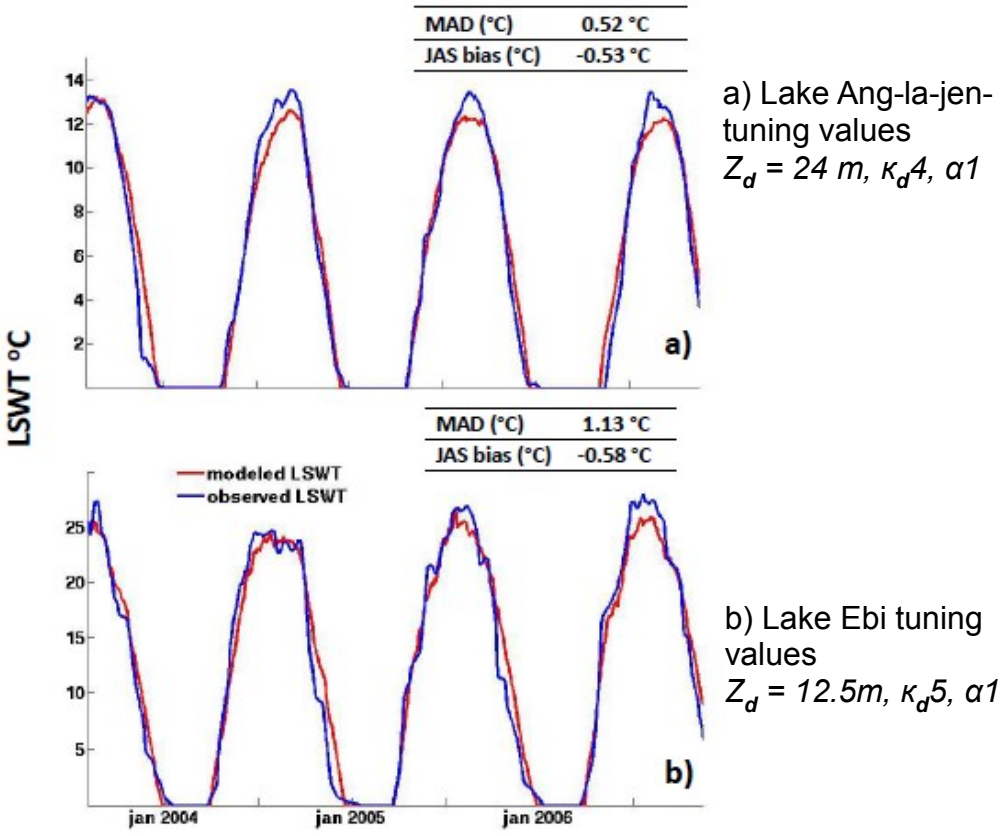

Figure 42 Observed LSWT versus tuned model LSWT for saline and high altitude lakes a) Lake Ang-le-jen, China (32° N, 4863 m a.s.l., salinity 155 g/l) modelled with approach 1 b) Lake Ebi, China (45° N, 166 m a.s.l., salinity 100 g/l) modelled with approach 2

4.7.1 High altitude versus low altitudes LSWT metrics results

Twelve (12) of the 14 high altitude lakes (3200 to 5000 m a.s.l) are also saline (ranging from 2-155 g/l). All other 146 lakes are located below 2000 m a.s.l. The mean daily MAD values for the 14 high altitude lakes is lower (0.61 °C) than for the

low altitude lakes (0.81 °C), Table 16. The average bias in the 1 °C and 4 °C cooling and warming days for the high and low altitude lakes are comparable (within 2 days of each other).

For high altitude lakes, the fraction of the observed JAS LSWT inter-annual variability (secondary metric) explained by the tuned model is considerably less ($inter_{jas}$ = 0.21) than for low altitude lakes (0.52), Table 16. The variability in the observed JAS LSWT for high altitude lakes (var_{jas}= 0.19) is almost 4 times lower than for low altitude lakes (0.75). Furthermore, the low var_{jas} in high altitude lakes can be explained by their high altitude and comparatively low latitude (28-32° N). For Asian seasonally ice covered lakes (located from 28 – 65° N), the var_{jas} increases with increasing latitudes explaining 0.40 (R^2_{adj}, p = 0.000) of the inter-lake variation. Altitude explains 0.26 (p=0.000) of the variation, with higher altitude lakes having a lower var_{jas}.

Primary metrics	Altitude >3200 m a.s.l. (14 lakes)	Altitude < 2000 m a.s.l. (146 lakes)
MAD (°C)	0.61± 0.24	0.81± 0.57
Mean JAS bias (°C)	0.06± 1.14	-0.07± 1.15
1 °C cooling day bias (days)	-3.1± 10.8	-0.9± 8.2
1 °C warming day bias (days)	0.9± 13.6	0.3± 12.1
Secondary metrics		
4 °C warming day bias (days)	-3.0± 11.6	-5.2± 18.9
4 °C cooling day bias (days)	5.2± 12.8	3.1± 14.4
$Inter_{jas}$ (R^2_{adj})	0.21± 0.46	0.52± 0.59
var_{jas} (K^2)	0.19	0.75

Table 16 Comparison of tuned model results for high and low altitude lakes showing the spread of differences across lakes, 2σ

4.8 Tuning of saline lakes

Salinity lowers the temperature at which water density is at a maximum, causing a longer mixing period and therefore can delay LSWT cooling and ice-on. As a result, of the prolonged surface cooling of saline lake, saline lakes freeze later than freshwater lakes.

Using Lake Bras d'or, I demonstrate that the use of *FLake* is suitable for tuning saline lakes and that light extinction coefficient compensates for the effect of salinity on the LSWT. The temperature at which water density is at a maximum (4 $^{\circ}$C), is substantially lower for saline lakes. For Lake Bras d'or (salinity value of ~ 26.2 g/l), this value is ~1.3 $^{\circ}$C. As a result, the surface of Lake Bras d'or takes longer to cool and freezes later than a freshwater lake. There are 3 model parameters in *FLake* that are directly related to salinity and are normally defaulted to the values for freshwater; freezing temperature, maximum density and temperature at which water density is at a maximum. I refer to these as the salinity parameters. I assess the suitability of the tuning approach by tuning Lake Bras d'or with and without adjusting these 3 salinity parameters to the salinity values for the lake. The results show that light extinction coefficient compensates for not having considered the effect of salinity in the tuning of Lake Bras d'or. Tuned using salinity parameters adjusted to the salinity of Lake Bras d'or, the lowest light extinction coefficient (κ_{d1}) value gives the optimal LSWT, while tuned using freshwater values) a higher κ_d value (κ_{d2}) gives the optimal LSWT. The other two LSWT regulating properties (depth and albedo) remain the same. The possible reason for this compensatory effect is that the higher light extinction coefficient (lower transparency) causes more heat to be retained in the surface layer, resulting in a higher LSWT, particularly in summer when the solar radiation is at its highest. The higher summer LSWT in turn results in a longer cooling period and a later freeze, resembling the cooling conditions for the saline lake. This suggests that if the modelled salinity of a lake is not known or not considered, the light extinction coefficient values can compensate for its effect on the tuned LSWT. Figure 43 demonstrates the good comparability between Lake Bras d'or tuned with and

without considering the effect of salinity. This also addresses the problem of having to tune saline lakes with no available salinity values.

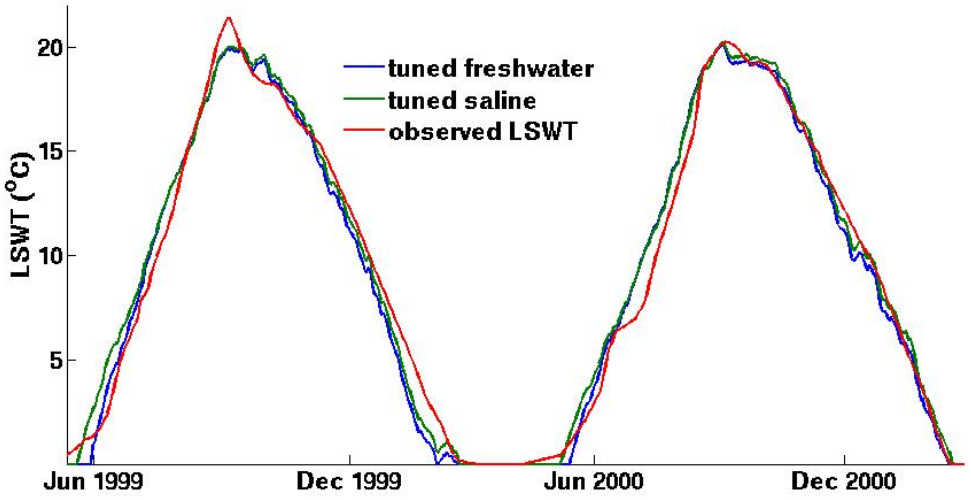

Figure 43 A comparison of saline and freshwater tuned model LSWTs and the observed LSWTs for Lake Bras d'or demonstrate that saline lakes can be tuned successfully. The tuned κ_d value for LSWTs modelled using the freshwater parameters of Lake Bras d'or (κ_{d2}) compensates for the modelled LSWTs tuned using the saline parameters (κ_{d1}), while the Z_d and α values remained the same

Freshwater parameter values were maintained throughout the tuning study for all lakes. Thirty seven (37) of the 160 seasonally ice covered lakes are saline, 30 of which range from < 3 g/l to 155 g/l and another 7 saline lakes have no available salinity values. The average metric results and the spread of differences for all 160 lakes are presented for saline lakes (37 lakes) and freshwater lakes (123 lakes) in Table 17 and discussed in section 4.8.1. The metrics results for saline and freshwater lakes compare well. This indicates that both tuning approaches (approach 1 and 2), result in representative LSWTs for saline lakes and that either the effect of salinity on the LSWT is small and/or it is minimised by the tuning approaches.

4.8.1 Saline versus freshwater LSWT metric results

The 1 °C and 4 °C warming and cooling days (LSWT phase transition days) are lake-mean thresholds indicative of freshwater lake-mean ice-on and ice-off (1 °C days) and start and end density induced mixing (4 °C days). For saline lakes, the LSWT phase transition days are a measure of how close (in time) the modelled transition days are to the observed LSWT transition days and are not appropriate to determine lake-mean phases.

The results for the saline and freshwater lakes are closely comparable, Table 17 (column 1 and 2), although the dispersion of errors among saline lakes is marginally higher than among freshwater lakes. The daily MADs for the saline lakes are on average 0.14 °C higher than for freshwater lakes. This is the same difference between the MAD results for Lake Bras d'or tuned using the freshwater and saline parameter values, Table 17 (column 3 and 4).

For freshwater lakes, the 4 °C cooling day occurs 4 days earlier than for saline lakes, this is the same difference between the freshwater and saline tuned 4 °C cooling day for Lake Bras d'or. Density induced mixing of freshwater lakes will begin earlier (when the LSWT drops to 4 °C) than in saline lakes (for example -1.3 °C for lake Bras d'or) explaining the earlier cooling of freshwater lakes.

The lower inter-annual variability in the observed JAS LSWT ($inter_{jas}$) of saline lakes (R^2_{adj} = 0.44) compared to freshwater lakes (0.51), can be attributed to a lower observed JAS LSWT variation (var_{jas}) in saline lakes, 0.51 K^2, compared to in freshwater lakes (0.76 K^2). There is a correlation between the between $inter_{jas}$ and var_{jas} of 0.31, meaning that, where there is less variability in the observed JAS LSWT, there will be proportionally less variability detected in the model. Additionally, for the freshwater and saline tuned models for Lake Bras d'or, the $inter_{jas}$ fractions are highly comparable (0.78 and 0.79), highlighting that the fraction of $inter_{jas}$ is not compromised by not considering salinity.

Primary metrics	Tuned results for 160 lakes using freshwater parameter values		Tuned results for Bras d'or	
	Saline (37 lakes)	Freshwater (123 lakes)	using freshwater parameter values	using saline parameter values
MAD (°C)	0.90± 0.69	0.76± 0.50	0.80	0.66
Mean JAS bias (°C)	-0.23± 1.14	-0.01± 1.14	-0.05	+0.04
1 °C cooling day bias (days)	-1.3± 9.7	-1.0± 8.3	-3.2	+1.4
1 °C warming day Bias (days)	0.0± 13.1	0.4± 12.0	+0.1	-0.9
Secondary metrics				
4 °C warming day bias (days)	4.9± 15.3	2.8± 13.9	-8.7	-7.7
4 °C cooling day bias (days)	-1.9± 21.1	-6.0± 19.1	-8.6	-4.7
$Inter_{jas}$ (R^2_{adj})	0.44	0.51	0.79	0.78
var_{jas} (K^2)	0.51	0.76	0.26	0.26

Table 17 Tuned model results for saline and freshwater lakes and Lake Bras d'or (tuned with freshwater and saline parameters), showing the spread of differences across lakes, 2σ

4.9 Independent evaluation of tuned model

The tuning period extends from 08 Aug 1991 to 31 December 2010. Observational ARC-Lake LSWT data and ERA data are also available for 2011. I independently evaluate the tuning process by forcing the tuned model with 2011 ERA data, determining the primary metrics using 2011 observational LSWT. I compare the metrics of this untuned year (2011) with two tuned years (1996 and 2010). 1996 is the first full year of data from ATSR2 and 2010 is the last year of tuned data from AATSR.

The mean metric results and the spread of differences across lakes for the tuned and untuned period are highly comparable for approach 1 across all 3 years, showing a marginally better MAD metrics for the untuned period. For approach 2, the MAD

results for the untuned year are more comparable with 2010 results than the 1996 results.

For the other 3 metrics in approach 2, the untuned year has a lower spread of differences across lakes than for 2010 and a marginally better JAS LSWT and 1 °C cooling day. The spread of differences across lakes for 1 °C warming day for the untuned year is wider than in 2010 but is better than for 1996, Table 18.
The 1 °C cooling and warming day approach 2 biases for 1996 and 2010 are less comparable than for approach 1. This may be because the approach 2 lakes are shallower, with the modelled effect of depth being less consistent than for deeper lakes.

Overall, the result of the modelled LSWTs for the untuned year (2011) compare well to the modelled results from the tuned years (1996 and 2010) showing that the model remains stable when run with ERA forcing data outside the tuning period.

Primary metrics	Approach 1			Approach 2		
	2011 Untuned	1996 Tuned (ATSR2)	2010 Tuned (AATSR)	2011 Untuned	1996 Tuned (ATSR2)	2010 Tuned (AATSR)
MAD (°C)	0.86± 0.68	0.89±0.74	0.87±0.71	1.59±1.04	1.33±0.79	1.66±0.95
Mean JAS bias (°C)	0.18±1.50	-0.33±1.79	0.28±1.44	0.12±1.71	0.17±1.19	0.28±1.81
1 °C cooling day bias (days)	11.1±23.8	5.1±25.6	8.5±21.4	10.9±18.7	-3.0±41.9	11.7±31.3
1 °C warming day bias (days)	7.4±19.7	12.1±19.7	6.5±19.8	9.33±21.6	13.2±18.2	1.0±32.54

Table 18 Results of independent evaluation of the tuning process with the spread of differences across lakes, 2σ, showing the untuned year (2011) with the first full year of data from ATSR2 (1996) and the last year of tuned data from AATSR (2010)

4.10 Conclusion

I conclude the LSWT tuning approaches for *FLake* for 160 seasonally ice covered lakes (including saline and high altitude lakes) substantially improve the modelled LSWTs. The post-tuning metrics for the trial lakes are highly representative of the post-tuning metrics of all lakes, Table 19. The tuning approach reduces the daily MAD and the spread of differences across lakes by ~75%, achieving the target of an average MAD value $\leq$ 1.0 $^{\circ}$C. This demonstrates that the tuned values for depth, light extinction coefficient and albedo, applying the *u3* wind speed scaling, produces a substantially more accurate modelled LSWT than using recommended/ default values.

The higher wind speed scaling was shown to cause greater mixing, cooling the JAS LSWTs, resulting in an earlier 1 $^{\circ}$C cooling day. The higher wind speed causes a delay the 1 $^{\circ}$C warming day (contributing to the lower JAS LSWT for deep lakes).

Primary metrics	Pre-tuning (21 trial lakes)	Post-tuning (20 trial lakes)	Post-tuning (160 lakes)
MAD ($^{\circ}$C)	3.07$\pm$ 2.25.	0.84$\pm$ 0.51	0.80$\pm$ 0.56
Mean JAS LSWT bias ($^{\circ}$C)	3.71$\pm$ 3.51	-0.12$\pm$ 1.09	-0.06$\pm$ 1.15
1 $^{\circ}$C cooling day bias (days)	12.0$\pm$ 39.6	-1.6$\pm$ 12.8	-1.08$\pm$ 8.5
1 $^{\circ}$C warming day Bias (days)	- 27.1$\pm$ 29.7	-0.2$\pm$ 10.7	+0.3$\pm$ 12.3

Table 19 Summary of pre and post-tuning metrics for the trial lakes and the post-tuning metrics for the 160 seasonally ice covered lakes showing the spread of differences across lakes, 2σ, showing that the post-tuning results for the 160 lakes are highly comparable to the post-tuning results for the trial lakes

In trial 2 where the 3 LSWT regulating properties are tuned, the inter-play between the LSWT regulating properties and wind in obtaining the optimal LSWT has been demonstrated, showing how the tuned results for the lower wind speed scaling, *u1,* are similar to the tuned results for the higher wind speed scaling, *u3.*

The tuned values for the LSWT regulating properties, were shown to be sensible and to give a good indication of how the modelled LSWTs can be improved for other lakes, without having to tune the model. This helps to address the modelled biases that appear to be a feature of *FLake*, as discussed in chapter 1, section 1.5. For example, a more suitable lake depth for seasonally ice covered lakes is obtained by using a lake depth of 0.7 times the mean depth for deep lakes (> 40 m) or by using the maximum depth for shallow lakes (< 4 m) instead of the mean depth. Shallow lakes tuned to a greater depth improves (delays) the 1 °C cooling day, compensating for not considering heat flux from sediments, which would also delay the 1 °C cooling day. For deep lakes it is possible that the mean depth is tuned to a shallower depth (causing an earlier and more timely the 1 °C cooling day) as it is more representative of the mean depth of the 2 upper lake layers represented by *FLake*.

I demonstrated that for deep high latitude lakes (or very deep lakes) changes in the timing of ice-off influence the whole LSWT cycle by affecting the JAS LSWT and the 1 °C cooling day. This finding is critical to our understanding of the effect of changes in the ice-off day on the LSWT cycle. For example, for very deep lakes, such as Lake Hovsgol (138 m), a delay of ~ 4 weeks in the 1 °C warming day results in a cooler JAS LSWT by 2.6 °C and an earlier 1 °C warming day of ~2 weeks.

The tuning approach is suitable for the saline and high altitude lakes. The slightly earlier 1 °C and 4 °C cooling day biases for freshwater lakes may be attributed to the higher temperature at which freshwater density is at a maximum, inducing an earlier mixing and earlier cooling than saline lakes. For high altitude lakes (3200 – 5000 m a.s.l.) all of which are located in Asia, the low observed variation in the JAS LSWT (var_{jas}) can be explained by their high altitude (0.26) and there low latitude (0.40).

Having demonstrated successful LSWT tuning the LSWTs for 160 seasonally ice covered lakes, in chapter 6 I evaluate for what purpose the tuned model is effective, examining long term modelled trends.

Chapter 5 Tuning of non-seasonally ice covered lakes

5.1 Introduction

In chapter 4, I showed how I tuned LSWTs from *FLake* for 160 seasonally ice covered lakes, meeting the average daily MAD target value of below 1.0 °C. In this chapter, I address the tuning of the modelled LSWTs for the 86 non-seasonally ice covered lakes (lakes with a lake-mean climatology above 1 °C all year), aiming to reduce the daily MAD to an average value of < 1.0 °C.

The non-seasonally ice covered lakes are located from 55° S to 48° N, at altitudes from -404 to 3827 m a.s.l., have lake-mean depths ranging from < 1 to 572 m, surface areas of 105 to 378,119 km^2 and salinity values up to 340 g/l. From ~40° N northward, the lake surface of the non-seasonally ice covered lakes generally have partial freezing in winter, the extent and duration of which varies greatly and depends on lake characteristics, climate and local weather conditions (Bernhardt *et al* 2012). Many lakes located at latitudes up to ~48° N are partially ice covered in winter but do not have a lake-mean climatology above 1 °C while none of the southern hemispheric lakes in the ARC-Lake dataset have a lake-mean cold phase, despite being located at latitudes up to 55° S. This hemispheric difference is due to higher latitude lakes in the Southern Hemisphere (located in Chile, Argentina and Oceania) having milder winters than Northern regions at the same latitudes, owing to a Mediterranean climate (Strahler and Strahler 1989). In the southern hemisphere, because there is less land mass and the continents are narrower, there is possibly a greater ocean influence on the climate. This could explain the milder southern hemispheric climate.

As ice cover is not part of the lake-mean LSWT cycle of these 86 lakes, snow and ice albedo is not relevant. Only two of the three LSWT regulating properties; lake depth (d) and light extinction coefficient (κ) are used in the LSWT tuning.

The annual LSWT range and extremes show much greater variation among non-seasonally ice covered lakes than among seasonally ice covered lakes and have a wider range of mixing regimes. While the maximum LSWT of seasonally ice covered lakes shows some variation, the minimum LSWT remains the same and these lakes have consistent features in their annual cycle such as ice-on and ice-off. It is expected that the variation in the LSWTs of non-seasonally ice covered lakes will result in less conclusive findings than the findings for seasonally ice covered lakes.

In a series of 4 trials (sections 5.4-5.7) on 14 non-seasonally ice covered lakes, I assess the modelled LSWTs using both fixed values and a range of values for the LSWT regulating properties (d and κ), with 3 different over-water wind speeds (U_{water}), the ERA unscaled wind speed *(u1)* and the two scaled wind speeds, *u2, u3*. From these trials, the most appropriate wind speed, range of depth factors, light extinction coefficient values are selected and assessed in the final trial, before applying to all 86 lakes. Results from the trials, the tuning results of all 86 lakes and the results of independent test on the tuned model are reported and discussed in this chapter. In chapter 6, I evaluate the longer term LSWT timeseries from the tuned model.

I use 3 primary metrics to select the optimal model combination of lake depth and light extinction coefficient for each lake. An overview of the tuning process for the non-seasonally ice covered lakes is shown in Figure 44.

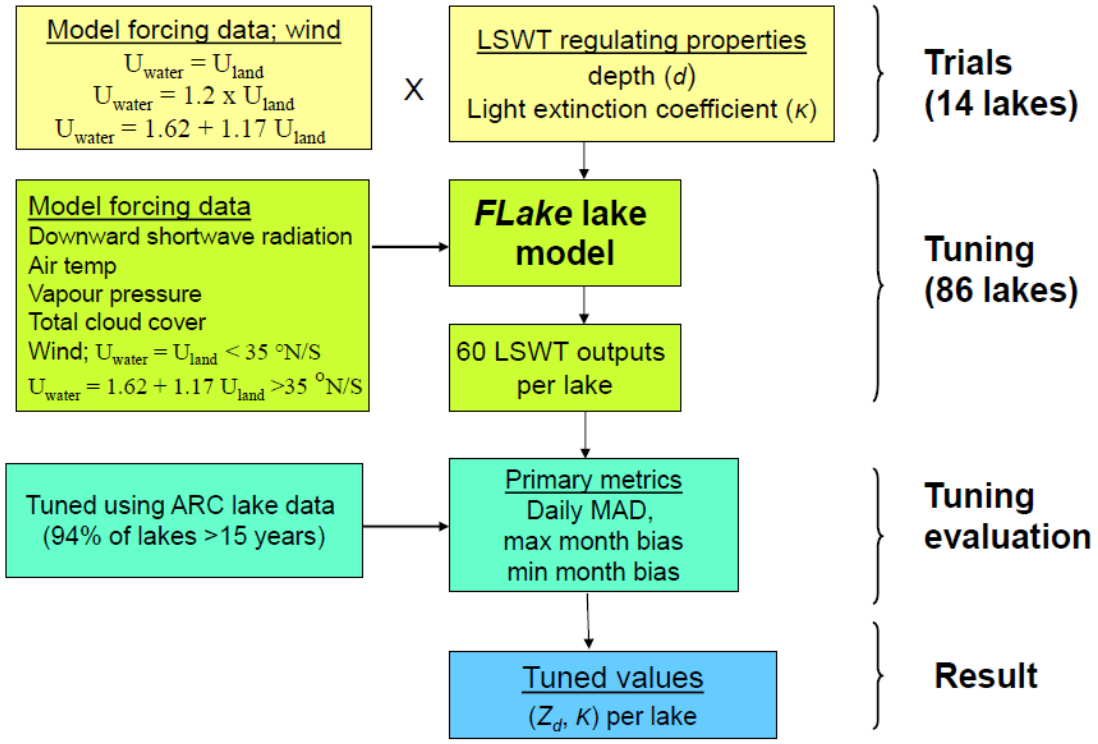

Figure 44 Tuning approach overview for non-seasonally ice covered lakes

5.2 Metrics

The metrics measure the closeness of the modelled to the observed LSWTs. The 3 primary metrics (normalized and equally weighted) are the basis of selecting the optimal modelled LSWT for each lake. The secondary metrics provide more information on how well the modelled LSWTs represent the observed LSWTs. These metrics (primary and secondary) are different to those used for seasonally ice covered lakes.

5.2.1 Primary metrics

The mth_{min} (and mth_{max}) measure the difference in the LSWT between the minimum (and maximum) observed month and the corresponding month of the modelled LSWT, exerting some control over the timing of the modelled monthly extreme

LSWTs. The daily MAD measures the daily mean absolute difference between the modelled and observed LSWTs, calculated as shown in chapter 4, Table 10.

For seasonally ice covered lakes, the start and end of the cold phase are strongly influenced by depth and albedo respectively. The primary metrics for non-seasonally ice covered lakes are more difficult to ascertain as there are no definitive stages in the LSWT cycle. However tuning using $mth_{\min}$ and $mth_{\max,}$ helping to align the timing of the extreme modelled LSWTs with the observed LSWT is important, particularly for tropical lakes where there is little variation in the annual cycle. Additionally, a change to the light extinction coefficient value has the biggest effect on the maximum LSWT, therefore the $mth_{\max}$ bias also indicates the appropriateness of κ values (this is discussed later in this chapter in section 5.5). The $mth_{\min}$ and $mth_{\max}$ are more appropriate measures than the winter and summer LSWTs, as non-seasonally ice-covered lakes cover a large range of latitudes (39° S to 48° N) and many tropical lakes do not have a pronounced seasonal cycle. While high latitude lakes have a strong seasonal cycle, with annual ranges in excess in 25 °C, some tropical lakes show annual variations as low as 2-3 °C and show evidence of a twice yearly solar maxima and minima, as shown in chapter 2, Figure 10.

5.2.2 Secondary metrics

Secondary metrics are used in evaluating the modelled LSWTs but are not used in selecting the optimal modelled LSWT.

***bias*$_{\mathbf{mth}}$** measures the bias of the mean month LSWT

Equation 11; $bias_{\mathrm{mth}} = \sum (x_i^{mod\_mth} - x_i^{obs\_mth})) / \mathrm{N}$

$^{mod\_mth}$ = mean month modelled LSWT

$^{obs\_mth}$ = mean month observed LSWT

N = sample size

***bias*$_{\mathbf{max}}$** measures the bias of the maximum month LSWT

Equation 12; $bias_{\max} = \sum (x_i^{mod\_max} - x_i^{obs\_max})) / N$

$^{mod\_max}$ = maximum month modelled LSWT

$^{obs\_max}$ = maximum month observed LSWT

***bias*$_{\mathbf{min}}$** measures the bias of the minimum month LSWT

Equation 13; bias$_{\mathbf{min}}$ $= \sum (x_i^{mod\_min} - x_i^{obs\_min})) / N$

$^{mod\_min}$ = minimum month modelled LSWT

$^{obs\_min}$ = minimum month observed LSWT

The difference between the ***bias*$_{\mathbf{max}}$** and ***bias*$_{\mathbf{min}}$** (secondary metric) and the ***mth*$_{\mathbf{max}}$** and ***mth*$_{\mathbf{min}}$** (primary metric) is that the secondary metrics measure the extreme biases (monthly) whereas the primary metrics measure the bias between the extreme monthly observed LSWTs and the modelled LSWT for the same month.

***inter*$_{\mathbf{max}}$** calculates the fraction of the observed maximum month inter-annual variability explained by tuned model $inter_{\max}$ (R^2_{adj});

Equation 14; $inter_{\max} = 1 - ((1 - r^2\ max)\ (N - 1) / (N - P - 1))$

P = total number of regressors

$$r^2\ max = \frac{N\sum (x_i^{obs\_max}\ x_i^{mod\_max}) - \sum (x_i^{obs\_max}) \sum (x_i^{mod\_max})}{(N\sum (x_i^{mod\_max^2}) - \sum (x_i^{mod\_max})^2)\ (N\sum (x_i^{obs\_max^2}) - \sum (x_i^{obs\_max})^2)}$$

***inter*$_{\mathbf{min}}$** calculates the fraction of the observed minimum month inter-annual variability explained by tuned model *inter*$_{\min}$ (R^2_{adj});

Equation 15; $inter_{\min} = 1 - ((1 - r^2\ min)\ (N - 1) / (N - P - 1))$

$$r^2 \min = \frac{N\sum (x_i^{obs\_min}\ x_i^{mod\_min}) - \sum (x_i^{obs\_min}) \sum (x_i^{mod\_min})}{(N\sum (x_i^{mod\_min2}) - \sum (x_i^{mod\_min})^2)\ (N\sum (x_i^{obs\_min2}) - \sum (x_i^{obs\_min})^2)}$$

***var*$_{\mathbf{min}}$** and ***var*$_{\mathbf{max}}$** calculate the variation in the observed minimum and maximum monthly LSWT (Kelvin squared, K^2);

Equation 16; $var_{\min} = \sum (x_i^{obs\_min} - \bar{x})^2 / (n - 1)$

Equation 17; $var_{\max} = \sum (x_i^{obs\_max} - \bar{x})^2 / (n - 1)$

5.3 Trial lakes

In a series of trials, I use 14 lakes that are broadly representative of the range of lake characteristics of non-seasonally ice covered lakes to determine an appropriate range of values/ factors to be applied to lake depth (d) and light extinction coefficient (κ) for the tuning of the LSWTs in *FLake*. As well representing the range of lake characteristics, the 14 trial lakes are also selected as they have Secchi disk depth data, which is used to derive light extinction coefficients values in the first trial, as was done so for the seasonally ice covered lakes in chapter 4. I also assess the suitability of the three wind speeds for non-seasonally ice covered lakes for these 14 lakes.

Of the 86 non-seasonally ice covered lakes, shown in Figure 45, the 14 trial lakes are marked by squares. The lake name, location and characteristics of the trial lakes, outlined in Table 20, encompass a wide range of lake characteristics. They are located from 39° S to 48° N at altitudes from 1 to 1620 m a.s.l.

In trial 1, I assess the modelled LSWT using fixed values for the LSWT regulating properties, with the 3 different U_{water} wind speed scalings, *u1- u3*. I assess the effect of 4 different depth factors in trial 2 and a range of 6 light extinction coefficient values in trial 3 across the 3 wind speeds scalings. Trial 4 combines trial 2 and 3 using a greater range of d and κ_{sd} values, totalling 60 possible combinations for each wind speed scaling. The combinations of the LSWT regulating properties for the trials are outlined in Table 21. For Lake Malawi which has a mean depth of 273 m and Lake Issykkul, 280 m, a "false depth" of 75 m is applied, as recommended (Kirillin 2010).

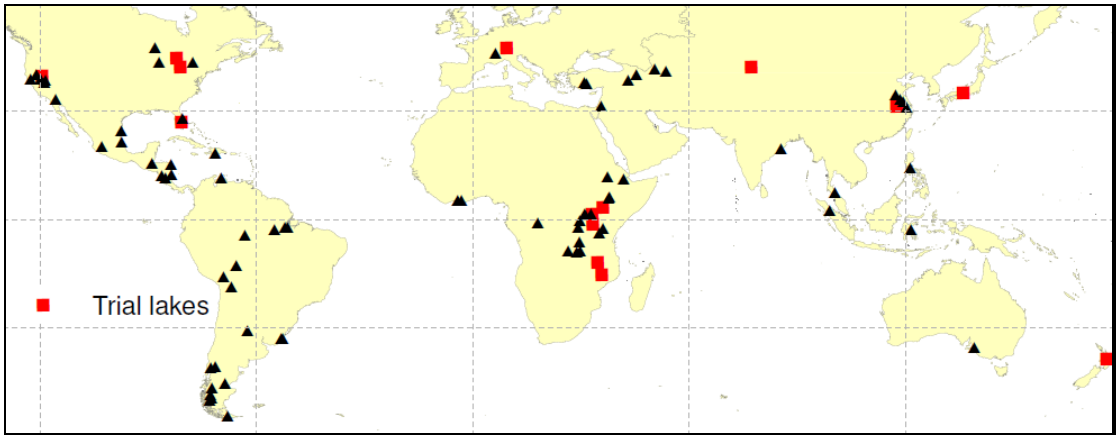

Figure 45 Location of non-seasonally ice covered lakes, with red square showing the 14 trial lakes

ARC ID	Lake name	Lat	Lon	Altitude (m a.s.l.)	surface area (km^2)	Mean depth (m)	κ_{sd}
3	Victoria	-1.30	33.23	1140	67075	40	1.70
5	Huron	44.78	-82.21	176	59757	59	0.13
10	Malawi	-11.96	34.59	485	29252	273	0.11
12	Erie	42.25	-81.16	174	25691	19	0.22
22	Turkana	3.53	36.08	438	7785	30	0.37
25	Issykkul	42.46	77.25	1619	6259	280	0.11
99	Kyoga	1.50	33.01	1043	1728	6	0.94
114	Okeeciiobee	26.95	-80.86	4	1437	3	3.40
233	Chao	31.57	117.57	1	768	3	4.25
256	Chilwa	-15.32	35.71	629	696	2	8.50
268	Biwa	35.25	136.08	69	659	41	0.19
295	Taupo	-38.81	175.9	395	600	91	0.12
352	Constance	47.65	9.28	431	516	90	0.15
411	Pyramid	40.03	-119.55	1161	448	60	0.30

Table 20 Location, altitude, surface area, depth and light extinction of 14 trial lakes.

Trial #	Light extinction coefficient				Lake depth	Number of combinations (for each wind speed scaling, *u1- u3*)
1 (untuned)	κ_{sd} (derived from Secchi disk depth)				Z_{d1} (mean depth)	1
2	κ_{sd}				Z_{d1} Z_{d2} (Z_{d1}* 0.75) Z_{d3} (Z_{d1}* 0.50) Z_{d4} (Z_{d1}* 1.50)	4 (4 Z_d)
3	κ_d	375nm	475nm	700nm	Z_{d1}	6 (6 κ_d)
	$\kappa_{d\,1}$	0.038	0.018	0.56		
	$\kappa_{d\,3}$	0.066	0.033	0.58		
	$\kappa_{d\,5}$	0.22	0.116	0.66		
	$\kappa_{d\,6}$	0.80	0.17	0.65		
	$\kappa_{d\,8}$	1.60	0.43	0.80		
	$\kappa_{d\,9}$	2.10	0.71	0.92		
4	κ_d	375nm	475nm	700nm	Z_{d1}	60 (10 κ_d * 6 Z_d)
	$\kappa_{d\,1}$	0.038	0.018	0.56		
	$\kappa_{d\,2}$	**0.052**	**0.025**	**0.57**	Z_{d2} (Z_{d1}* 0.75)	
	$\kappa_{d\,3}$	0.066	0.033	0.58	Z_{d3} (Z_{d1}* 0.50)	
	$\kappa_{d\,4}$	**0.122**	**0.062**	**0.61**	Z_{d4} (Z_{d1}* 1.50)	
	$\kappa_{d\,5}$	0.22	0.116	0.66		
	$\kappa_{d\,6}$	0.80	0.17	0.65	**Z_{d5} (Z_{d1}* 0.30)**	
	$\kappa_{d\,7}$	**1.10**	**0.29**	**0.71**	**Z_{d6} (Z_{d1}* 2.50)**	
	$\kappa_{d\,8}$	1.60	0.43	0.80		
	$\kappa_{d\,9}$	2.10	0.71	0.92		
	$\kappa_{d\,10}$	**3.00**	**1.23**	**1.10**		

Table 21 LSWT regulating property combinations for all trials (1-4) for each of the wind speeds, *u1- u3.* The 2 additional Z_d factors and 4 additional κ_d values introduced in trial 4 are highlighted in bold

5.4 Trial 1: The effect of wind speed on modelled LSWT

For each of the 14 lakes, I model the LSWT using lake-mean depth (Z_{d1}) and the light extinction coefficient values derived from Secchi disk data (κ_{sd}) with the 3 wind speed scalings. The κ_{sd} values are derived from Secchi disk depths, as discussed in chapter 4, section 4.3.1.

5.4.1 Trial 1: results and discussion

Four (4) non-seasonally ice covered trial lakes show smaller biases when modelled with the 2 lower wind speed scalings. Although the average metric results (MAD, mth_{min} and mth_{max}) for *u3* are closer to the observed LSWT than for *u1 and u2* (Table 22), 3 tropical lakes (Lake Turkana, Lake Malawi and Lake Kyoga) and 1 temperate lake (Lake Constance) show improved mth_{max} with *u1* or *u2*. Two (2) of these lakes (both tropical) also show an improved mth_{min} with *u1* or *u2*. Figure 46 shows that wind speed scaling *u1* better represents the LSWT for Turkana (3.5° N), while the LSWT for a temperate lake (Lake Biwa, 35.6° N) is better represented using *u3*. The suitability of the wind speed scaling for lakes at different latitudes is further evaluated in trial 2- 4.

Trial 1	*u1*	*u2*	*u3*
MAD (°C)	3.55± 3.20	3.11± 2.77	2.17± 1.93
mth_{max} (°C)	1.92± 5.05	1.39± 5.06	-0.42± 5.18
mth_{min} (°C)	3.71± 4.33	3.08± 4.16	1.47± 3.87

Table 22 The effect of wind speed scalings on untuned modelled LSWTs of the 14 trial lakes, with the spread of differences across lakes, 2σ, highlighting that any one wind speed may not be applicable for all lakes (While the average bias is improved with *u3*, the spread of biases across lakes for mth_{min} and mth_{max} show little change)

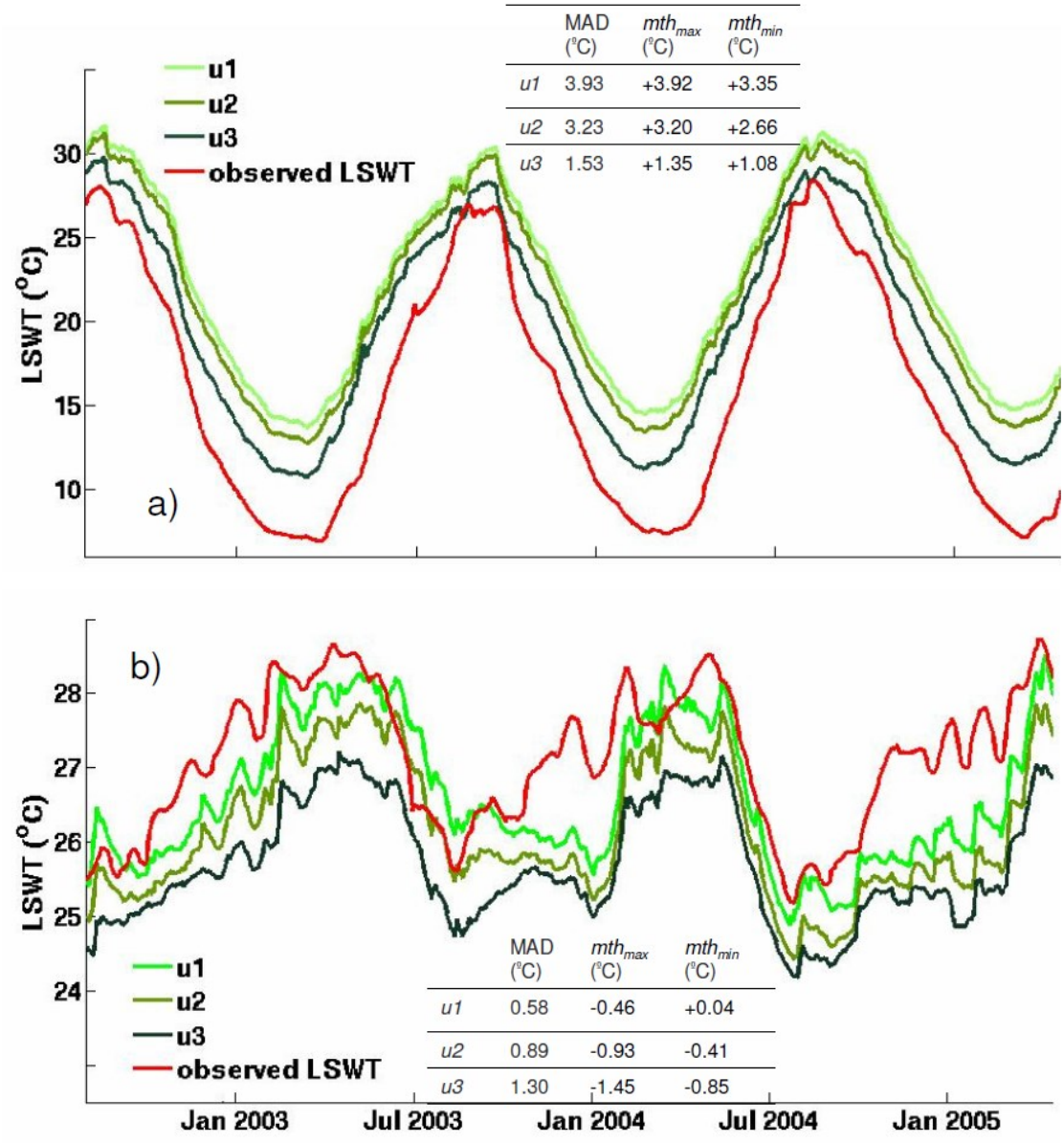

	MAD (°C)	mth_{max} (°C)	mth_{min} (°C)
u1	3.93	+3.92	+3.35
u2	3.23	+3.20	+2.66
u3	1.53	+1.35	+1.08

	MAD (°C)	mth_{max} (°C)	mth_{min} (°C)
u1	0.58	-0.46	+0.04
u2	0.89	-0.93	-0.41
u3	1.30	-1.45	-0.85

Figure 46 Effect of wind speed scaling on LSWT (trial 1) for a temperate lake a) Lake Biwa, Japan (35.6° N) and a tropical lake b) Lake Turkana, Africa (3.5° N) showing that the modelled LSWT for the temperate lake is better represented using *u3* and the modelled LSWT for the tropical lake is better represented using *u1*.

5.5 Trial 2: The effect of depth and wind on modelled LSWT

In trial 2, I assess a range of effective depth factors (the same factors applied to the seasonally ice covered lakes: Z_{d1}- Z_{d4}), applying all 3 wind speed scalings, giving a

total of 12 possible combinations. The results show that deep lakes are generally tuned with the lowest depth factor and shallow lakes with the highest factor, the suggested reasons for which are discussed in chapter 4, section 4.4.3. Only 2 of the 14 lakes are tuned to the recommended (mean) depth (Z_{d1}); Lake Turkana and Lake Victoria with mean depth of 30 m and 40 m, respectively.

Column 2 to 4 of Table 23 show the optimal results for effective depth for each wind speed scaling. Although the mean metric results are better for *u3,* the $mth_{\min}$ and $mth_{\max}$ spread of biases is not substantially better using any one scaling. Table 23, column 1, which shows the metric results for the optimal wind speed scaling and depth factor, shows improved $mth_{\min}$ and $mth_{\max}$ mean and biases. Six (6) of the 7 lakes located at latitudes > 35° N/ S show optimal tuning using *u3,* while 3 of the 4 lakes located < 12 ° N/ S are optimally tuned with *u1* and *u2*.

This highlights that a higher wind speed scaling may be more appropriate for higher latitude lakes and a lower wind speed scaling for lower latitude lakes. As winds can drive lake mixing in deep lakes, it strongly influences the mixed layer depth and the LSWT. The effect of wind on the LSWT is more pronounced in lakes where there is a smaller density difference between the maximum LSWT and the bottom stratified layer (hypolimnion), as a larger density gradient acts as a buffer against wind induced mixing. As density is non-linearly dependent on temperature, the density differences (as opposed to temperature differences), between the maximum LSWT and the hypolimnion is a better indicator of this buffering effect.

This shows that more wind energy is required to produce the same amount of mixing where the density differences between the maximum LSWT and the hypolimnion is larger. Although the density differences between the 2 layers are considered in *FLake*, it is possible that when forced with an underestimated wind speed, the effect of wind on the LSWT will be further reduced. As a result, higher latitudes lakes may show more representative LSWTs using a higher wind speed scaling.

For deep lakes, I assess the buffering effect against wind by determining the density differences (Haynes 2013) between the minimum monthly LSWT and the hypolimnion temperature. From the equator to approximately 40 ° (N/S), the steep decline in the minimum LSWT is reflected in the bottom temperature (Lewis 1996). The comparability between the minimum monthly LSWT (using ARC-Lake minimum monthly LSWT climatology) and the hypolimnion temperature (extracted from the version of *FLake* based on the hydrological year 2005/ 2006), for all deep (> 25 m) non-seasonally ice covered lakes (14 lakes) supports this, as demonstrated in Figure 47. The minimum monthly LSWT and the hypolimnion temperature are highly correlated (0.99, p = 0.000), showing a 1:1 relationship, (R^2_{adj} = 0.97, p = 0.000). At latitudes below 35° N/ S the density difference is lower (0.65×10^{-3} kg m^3) than those at latitudes above 35° N/S (1.49×10^{-3} kg m^3, indicating a stronger buffering effect against wind for high latitude lakes. This supports the explanation of why higher latitude lakes may show more representative LSWTs using a higher wind speed scaling.

The strong inter-lake comparison between the minimum monthly LSWT and the hypolimnion temperature also highlights that the minimum month LSWTs could be used to as a proxy for deep water lake temperatures. This could be confirmed by comparing to *in situ* hypolimnion temperature for the lakes shown in Figure 47.

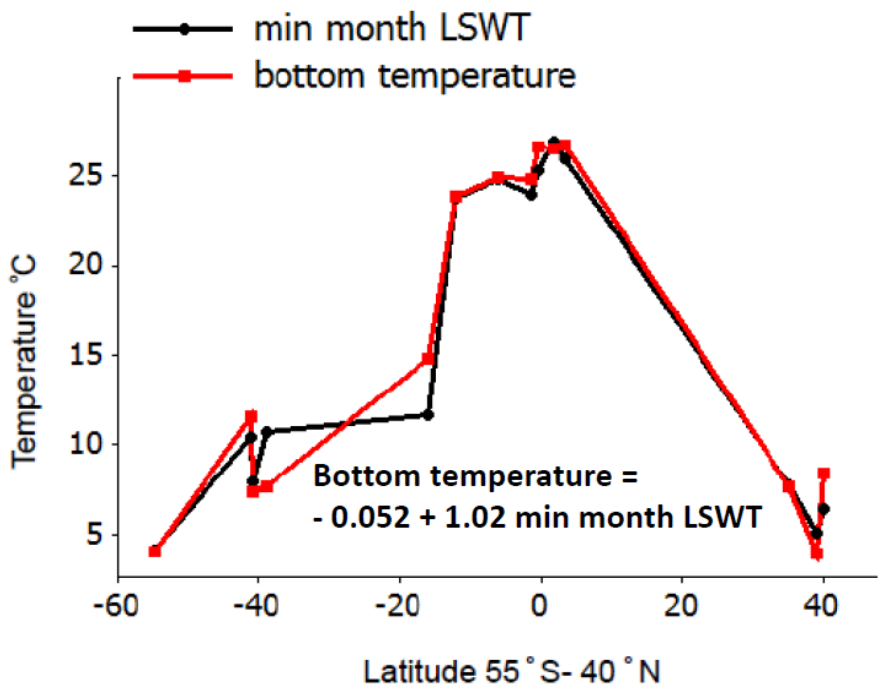

Figure 47 Lake bottom temperature during stratification and climatological minimum monthly LSWT of 14 deep (>25 m) non-seasonally ice covered lakes from 55° S to 40° N, showing the modelled equilibrium result (lake bottom temperatures obtained from *Flake* lake model, using perpetual hydrological year, 2005/2006) compared with observed minimum monthly climatology (1992-2011) LSWTs from ARC-Lake

Trial 2	Tuned Z_d with optimal wind speed scaling	Tuned depth		
		u1	*u2*	*u3*
MAD (°C)	1.86± 2.00	3.31± 3.35	2.89± 2.90	1.97± 1.82
mth_{max} (°C)	0.47± 3.25	1.95± 4.26	1.45± 4.18	-0.05± 4.58
mth_{min} (°C)	1.26± 2.69	3.32± 4.16	2.71± 4.06	0.84± 3.07

Table 23 Primary metric results for trial 2 showing the modelled LSWTs tuned with *Zd* using the optimal wind speed scalings (column 1) and using individual scalings, *u1-u3* (column 2-4), with the spread of differences across lakes, 2σ

5.5.1 Why depth doesn't compensate for wind for non-seasonally ice covered lakes

In chapter 4, section 4.5.2, I found that seasonally ice covered lakes when modelled with a higher wind speed (*u3*), had a greater tuned depth and/or a lower light extinction co-efficient value. This effect is not evident in the tuned results of the non-seasonally ice covered lakes. For these lakes the higher wind speed caused a more rapid heat exchange between the lake surface and the atmosphere, resulting in an earlier 1 °C cooling day. The increased heat capacity of a deeper lake counteracted the effect of the stronger winds, slowing down the time required to cool the lake.

The average metric result and the spread of differences across the 14 non-seasonally ice covered lakes, shown in column 2 - 4, Table 23, are only a marginal improvement on the trial 1 results, Table 22. Eight (8) of the 14 lakes (widely ranging in depth and latitude) were tuned with the same depth for all 3 wind speed scalings, demonstrating that there is no compensatory effect between depth and wind scaling for these 8 lakes. For the other 6 lakes, although the tuned depth changed with the wind scaling, the compensatory effect seen in the seasonally ice covered lakes is not apparent. This can possibly be explained by the fact that the majority of seasonally ice covered lakes have the same classification of mixing (dimitic), while the mixing regimes and annual LSWT range for non-seasonally ice covered lakes vary greatly.

Dimictic lakes remain frozen for several months of the year and have a pronounced seasonally cycle and a bottom temperature of 3.98 °C (freshwater deep lakes). Therefore increases in wind speed, for example, during the ice cover period will cause ice growth and delay 1 °C warming day across all seasonally ice covered lakes. Additionally, for seasonally ice covered lakes, the 1 °C warming and cooling days are definitive stages in the LSWT cycle and therefore are good measures of any compensatory effect. There is no such definitive stage in the LSWT cycle non-seasonally ice covered lakes.

The classification of non-seasonally ice covered lakes varies from permanently stratified (for example, Lake Malawi) to warm-monomictic (Lake Constance; mixes once per year in February or March and is stably stratified for rest of year) to shallow and continually mixing lakes such as Lake Chilwa (continuous warm polymictic). Additionally, for tropical lakes rapid heat gain after a brief cooling can cause the formation of a secondary thermocline on the surface (Lewis 1996) impeding wind mixing. The variation in the lake classification is mainly a consequence of the variation in latitude and therefore in the annual range of the LSWT. The trial lakes covered a wide range of latitudes from 39° S to 48° N. For example, Lake Biwa at 35.6° N has an annual range of ~20 °C and Lake Turkana at 3.5° N has an annual range of ~ 3 °C, Figure 46.

5.6 Trial 3: The effect of light extinction coefficient and wind on modelled LSWTs

In this trial, I assess a range of 6 light extinction coefficients values for each wind speed scaling, giving a total of 18 possible combinations. As the range of light extinction coefficient values derived from Secchi disk depth for the trial lakes (0.11 – 8.50) is wider than those for the seasonally ice covered trial lakes (0.06 – 5.31), I apply a wider range of light extinction coefficient values; 3 open ocean types (type I, IB and III) and 3 coastal ocean types (type 1, 5 and 7) (Jerlov 1976), type I being the most transparent and type 7 being least transparent. I rename these light extinction coefficients values κ_{d1}, κ_{d3}, κ_{d5}, κ_{d6}, κ_{d8} and κ_{d9}, Table 21.

The effect of light extinction on the LSWT is most apparent in the warmest months, when irradiance is at its maximum, as demonstrated in Figure 48, which shows the LSWT for Lake Geneva modelled with two different κ_d values (κ_{d2} and κ_{d6}). A comparison between the average $mth_{\max}$ spread of differences across lakes and wind speed scaling in Table 24 (column 2 to 4), and Table 22 show that by tuning using a range Jerlov's ocean κ_d values in place of the fixed κ_{sd} values substantial improves the $mth_{\max}$ spread of differences. The average $mth_{\max}$ spread of differences is reduced

from an average of ± 5.1 °C in trial 1 (fixed κ_{sd}) to ± 2.8 °C in trial 3. There is no improvement in the corresponding average mth_{min}, demonstrating that tuning the light extinction coefficient has substantially smaller effect on the minimum LSWT.

Similar to trial 2 findings, 5 of the 7 lakes located at latitudes > 35° N/ S are tuned with *u3* and 4 of the 7 lakes located < 35° N/ S are tuned using *u1*. The 5 lakes tuned with *u2* are scattered across a wide range of latitudes, with 3 lakes in the tropics and 2 in temperate regions, showing that some lakes in both regions showing better results with a wind scaling of 1.2 (*u2*).

Trial 3	Tuned κ_d and with optimal wind speed scaling	Tuned κ_d		
		u1	*u2*	*u3*
MAD (°C)	1.51±1.43	2.10± 2.22	1.97± 2.12	1.69± 1.45
mth_{max} (°C)	-0.84± 2.87	-0.40± 2.35	-0.63± 2.33	-1.24± 3.74
mth_{min} (°C)	1.04± 3.11	2.29± 4.76	1.85± 4.88	0.76± 3.56

Table 24 Primary metric results for trial 3 showing the modelled LSWTs tuned with k_d, and wind speeds scaling, *u1 -u3*, with the spread of differences across lakes, 2σ

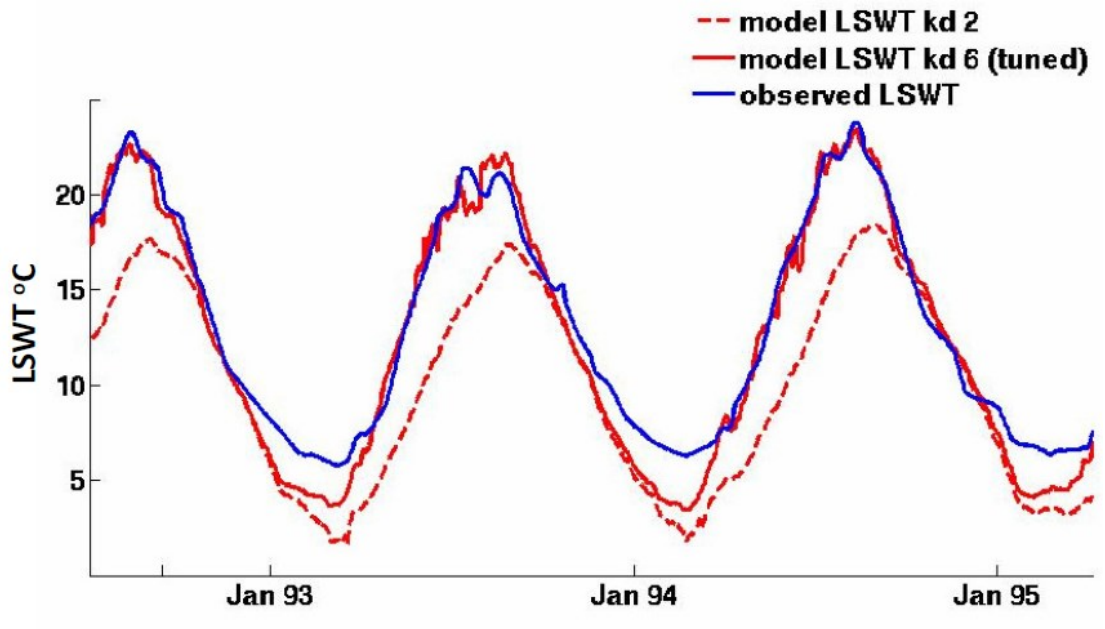

Figure 48 LSWTs for Lake Geneva modelled with two different κ_d values (κ_{d2} κ_{d6}) shows the substantially stronger effect of κ_d on the maximum LSWT (summer) than the minimum LSWT (winter)

5.6.1 Compensatory effect between wind and light extinction coefficients

There is a compensatory effect between wind and light extinction coefficients. Although 6 of the 14 lakes maintain the same κ_d values across all wind speed scalings, the remaining 8 lakes (tropical and higher latitude) tuned with *u3* have a higher κ_d value than when tuned with *u1*. This effect is also evident in the seasonally ice covered lakes. The higher wind speed causes more thorough mixing, deepening the mixed layer resulting in a cooler lake surface, demonstrated in Figure 46. In the tuning process, the cooler surface as a result of the higher wind speed scaling is counteracted by a less transparent lake surface (higher κ_d), causing more heat to be retained in the surface layer, increasing the LSWT.

5.7 Trial 4: tuning of all LSWT regulating properties

In this trial, I combine the tuning of depth (trial 2) and light extinction coefficient (trial 3) applying 2 additional Z_d factors and 4 additional κ_d values, covering a wider range of depths and covering the full range of Jerlov's (1976) open ocean (Type I, IA, IB, II and III) and coastal ocean types (Type 1, 3, 5,7 and 9), renamed $\kappa_{d1:}$ κ_{d10}. The 2 new additional Z_d factors and 4 additional κ_d values are highlighted in bold, Table 21, giving a total of 60 possible combinations for each wind speed scaling.

Trial 4	Tuned k_d, *Zd* with wind speed scaling *u1* below 35° N/ S and *u3* above 35° N/ S) (approach 3)	Tuned k_d		
		u1	*u2*	*u3*
MAD (°C)	0.96± 0.63	1.04± 0.65	1.07± 0.48	1.07± 0.74
mth_{max} (°C)	-0.44± 1.52	-0.33± 0.92	-0.15± 1.25	-0.85± 1.82
mth_{min} (°C)	-0.03± 1.48	0.10± 1.86	0.19± 1.27	-0.35± 1.32

Table 25 Primary metric results for trial 4 showing the modelled LSWTs tuned with k_d, *Zd* and wind speed scalings, *u1 -u3*, with the spread of differences across lakes, 2σ

Similar to the trial 2 and trial 3 findings, high latitude lakes generally show better results with wind speed scaling *u3* and lower latitudes lakes with scaling *u1*. In this trial, 5 of the 7 lakes at latitudes > 35° N/S and 5 of the 7 lakes located < 35° N/S show best results *u3* and *u1,* respectively. The remaining 4 lakes show better results with *u2*; similar to the previous trials these lakes are dispersed across the tropics and higher latitudes.

Table 25, column 1, shows the optimal results for 2 LSWT regulating properties using wind scaling, *u1* for lakes at latitudes < 35° N/ S and *u3* for lakes at latitudes > 35° N/ S. The average MAD and the spread of differences across the 14 lakes is 0.96 ± 0.63 °C, meeting the aim of reducing the average MAD to < 1 °C. This approach,

(herein approach 3) is used to tune all 86 non-seasonally ice covered lakes for depth (Z_d) and light extinction coefficient (κ_d).

Across the 14 trial lakes, approach 3 shows a substantial improvement on the trial 1 results (using the same wind scaling). The MAD is reduced 3-fold and the spread of distribution 4-fold from 2.76 $\pm$ 2.70 $^{\circ}$C to 0.96 $\pm$ 0.63 $^{\circ}$C).

5.8 Tuning results for all non-seasonally ice covered lakes

I apply tuning approach 3 to all 86 non-seasonally ice-covered lakes. The wind scaling applied is *u3* for lakes > 35° N/S and *u1* for lakes < 35° N/S. The mean depth information is required, but is not available for some lakes. I address how depths for these lakes are estimated in section 5.8.1, and present the approach 3 tuning results and in section 5.8.2.

5.8.1 False depth and lakes with unknown depths

Seven (7) of the 86 lakes have no depth information. For these lakes I use an initial default value of 5 m. Applying the range of Z_d factors to 5 m allow depths from 1.5 to 12.5 m to be assessed. If the results indicate that the 5 m input depth is too low (a high maximum LSWT), the tuning is repeated using a depth of 24 m. Applying the range of Z_d factors to 24 m allow depths from 7.2 to 60 m to be assessed, covering a total range of depths from 1.5 – 60 m for lakes with no available depth data. For lakes with only maximum depth values (9 lakes), a maximum-to-mean depth ratio of 3 (based on 63 lakes which have both maximum and mean lake depth) is used to determine the mean depth. A false depth of 200 m is used for all 5 lakes with mean depths > 200 m. This allows the tuned depth of a very deep lake to be no less than 60 m (lowest depth factor = 0.3, Table 21), exerting a sensible lower limit on the tuned depth of very deep lakes.

5.8.2 Tuning results for all lakes

The average daily MAD result for 84 of the 86 lakes is 0.96 °C, with a spread of differences of ± 0.66 °C (2σ), Table 26. This achieves the aim of reducing the average MAD to below 1 °C. The tuning approach is a substantial improvement on using the fixed LSWT regulating properties (*d* and *κ*), as show in Table 27. The primary metric results for 84 of the 86 lakes are very comparable to the results for the 14 trial lakes, showing that lakes used in the trial and the approach taken resulted in the successful LSWT tuning of the 84 non-seasonally ice covered lakes. I also demonstrate that *FLake* is suitable for tuning LSWTs for deep tropical lakes and saline lakes.

The tuned values for the LSWT regulating properties for all lakes and the corresponding primary and secondary metrics are shown in Appendix III. The daily MAD values are ≤ 1.0 °C for 71% of the lakes and the $mth_{\min}$ and $mth_{\max}$ values are within 1.0 °C of the observed LSWTs for ≥ 85% of the lakes. For 92% of lakes the mean monthly bias ($bias_{\mathrm{mth}}$), which is a secondary metric (not used to tune the modelled LSWTs), is < ± 1.0 °C. The primary metrics results for the 84 lakes are illustrated in Figure 49. Figure 49 shows that lakes with the largest daily MADs (> 1.60 °C) are located from ~ 30 to 50° N, the zone where the annual LSWT range is greatest. The $mth_{\max}$ biases are also greater in regions where the annual range is larger; in South America, from ~35 to 55° S and in Europe and Asia from ~30 to 50° N. Additionally, the model shows regional variability, over-estimating the $mth_{\max}$ bias in the South American region and under-estimating the bias in Europe and Asia, Figure 49.

Two of the 86 lakes yield highly unsatisfactory results. Lake Viedma, an Argentinian freshwater lake of unknown depth yielded a daily MAD of 3.1 °C and the Dead sea, a deep and highly saline lake (340 g/l) located in Asia at 404 m below sea level yielded a daily MAD of 4.1 °C. For the Dead Sea, a difference in the average maximum

month temperature between the observed LSWT (33 °C) and ERA T2 air temperature (25 °C), results in a negative modelled bias in the maximum month LSWT ($bias_{max}$) of 6.3 °C. Given the standard air temperature lapse rate (6.5 °C km^{-1}), altitude can explain the substantially lower air temperatures. The altitude of Dead Sea (-404 m a.s.l.), is lower by ~ 850 m a.s.l than the altitude of the meteorological data at the lake centre co-ordinates, 445 m a.s.l. (determined by interpolating surrounding cells using the orography data accompanying the ECMWF meteorological data).

For Lake Viedma, while the observed LSWTs range from 5-10 °C, the minimum ERA T2 air temperature remains well below 0 °C for many months of year, regularly reaching -8 °C, resulting in the negative modelled bias in the minimum month LSWT ($bias_{min}$) of 4.8 °C. This bias can be at least, partially explained by the difference in altitude of > 500 m a.s.l., between the altitude of Lake Viedma (297 m a.s.l.) and the altitude of meteorological data at the lake centre co-ordinates of 825 m a.s.l.

I conclude that for Lake Viedma and the Dead Sea, the geo-potential height (the altitude associated with the data measurement) of the ECMWF meteorological data is not representative. The tuning metrics results for these two lakes are shown in Appendix III but are excluded from the summary of results in Table 26. In this table, the metric results for these 84 lakes are shown for temperate lakes (>20° N/S) and tropical lakes (<20° N/S), column 2 and 3.

Table 26 shows that the fraction of the maximum and minimum observed inter-annual variability explained by the model is substantially greater for temperate lakes, ($inter_{max}$ = 0.49 and $inter_{min}$ = 0.37) than for tropical lakes ($inter_{max}$ = 0.07 and $inter_{min}$ = 0.13). This can be explained by a larger observed variance in the maximum and minimum LSWTs (var_{max} and var_{min}) in temperate lakes (4-5 times greater than the variance in tropical lakes), Table 26. Across all non-seasonally ice covered lakes the correlation between the observed variance (var_{max} and var_{min}) and the observed

variance detected in the model ($inter_{max}$ and $inter_{min}$) is 0.34 for maximum LSWTs and 0.69 for minimum LSWTs.

Primary metrics	All lakes (84)	Temperate lakes >20˚ N/S (44 lakes)	Tropical lakes < 20˚ N/S (40 lakes)
MAD (˚C)	0.96± 0.66	1.07± 0.66	0.84± 0.58
mth_{max} (˚C)	-0.21± 1.47	-0.36± 1.71	-0.03± 1.06
mth_{min} (˚C)	-0.08± 1.47	0.00± 1.57	-0.17± 1.36
Secondary metrics			
$bias_{mth}$ (˚C)	0.00± 1.09	+0.02± 1.30	-0.01± 0.80
$bias_{max}$ (˚C)	0.15± 1.60	-0.22± 1.61	0.56± 1.14
$bias_{min}$ (˚C)	-0.35± 1.66	-0.17± 1.77	-0.55± 1.45
$inter_{max}$ (R^2_{adj})	0.29± 0.63	0.49± 0.58	0.07± 0.31
$inter_{min}$ (R^2_{adj})	0.25± 0.49	0.37± 0.49	0.13± 0.37
var_{max} (K^2)	0.40	0.65	0.12
var_{min} (K^2)	0.43	0.69	0.15

Table 26 Metric results for all non-seasonally ice covered lakes with the spread of differences across lakes, 2σ, showing the results for temperate and tropical lakes

Primary metrics	Pre-tuning (14 trial lakes)	Post-tuning (14 trial lakes)	Post-tuning (84 lakes)
MAD (˚C)	3.55± 3.20	0.96± 0.63	0.96± 0.66
mth_{max} (˚C)	1.92± 5.05	-0.44± 1.52	-0.21± 1.47
mth_{min} (˚C)	3.71± 4.33	-0.03± 1.48	-0.08± 1.47

Table 27 Summary of pre and post-tuning metrics for the 14 trial lakes and the post-tuning metrics for the 84 seasonally ice covered lakes

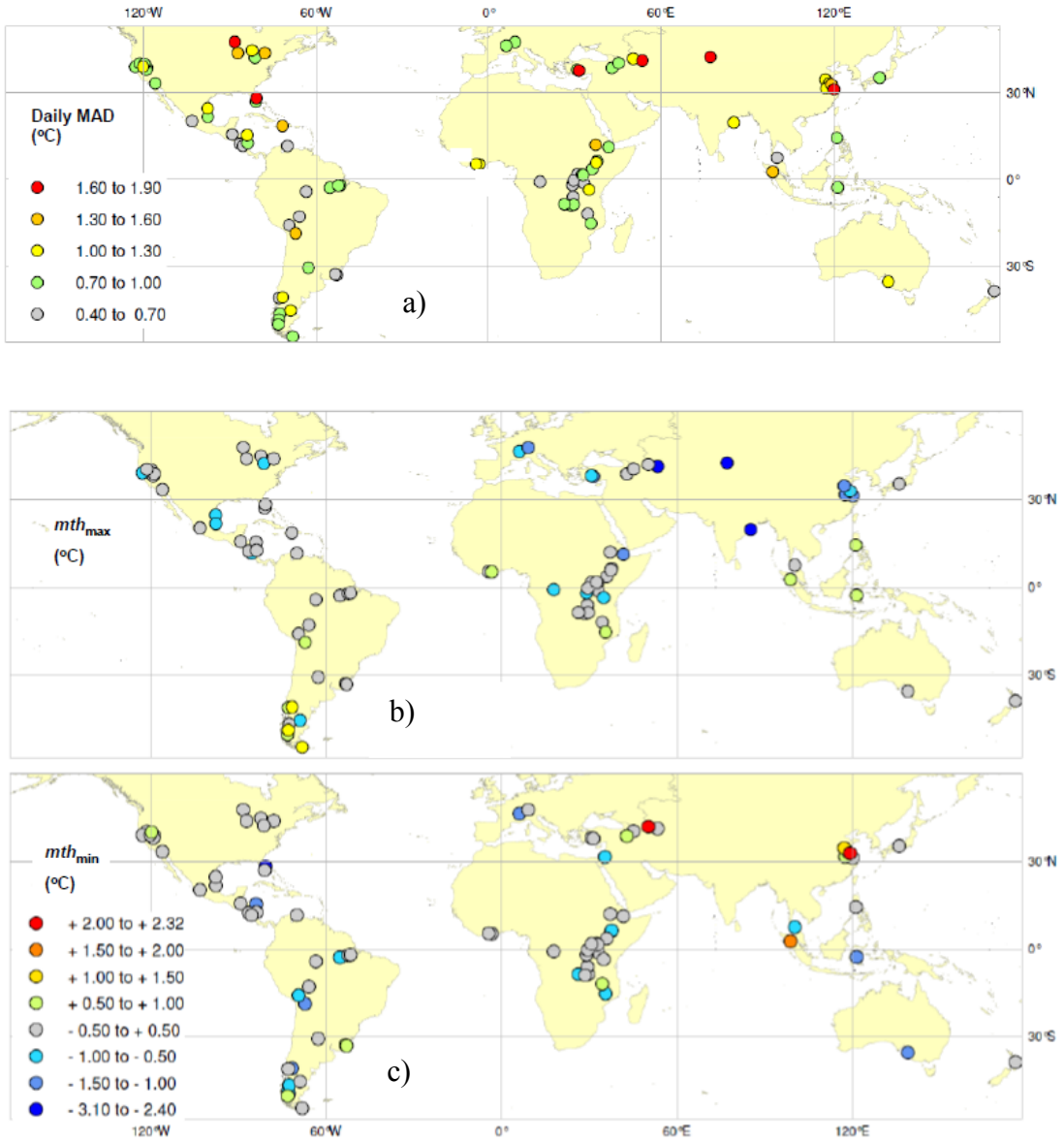

Figure 49 Primary metric results for the 84 lakes with non-seasonally ice cover lakes a) MAD, b) mth_{max} and c) mth_{min}

5.8.2.1 Tuning deep tropical lakes

Although, initially intended for modelling cold water lakes where the bottom temperature reaches 3.98 °C, I demonstrate (using Lake Malawi) that *FLake* is suitable for modelling deep tropical lakes. While Lake Malawi, located at 12° S, has a mean depth of 273 m, the tuned model uses an effective depth (Z_d) of 60 m. The observed LSWTs are substantially closer to the tuned model LSWTs than the LSWTs from the untuned model, as shown in Figure 50b. The daily MAD is 0.63 °C for the tuned model and 2.87 °C for the untuned model.

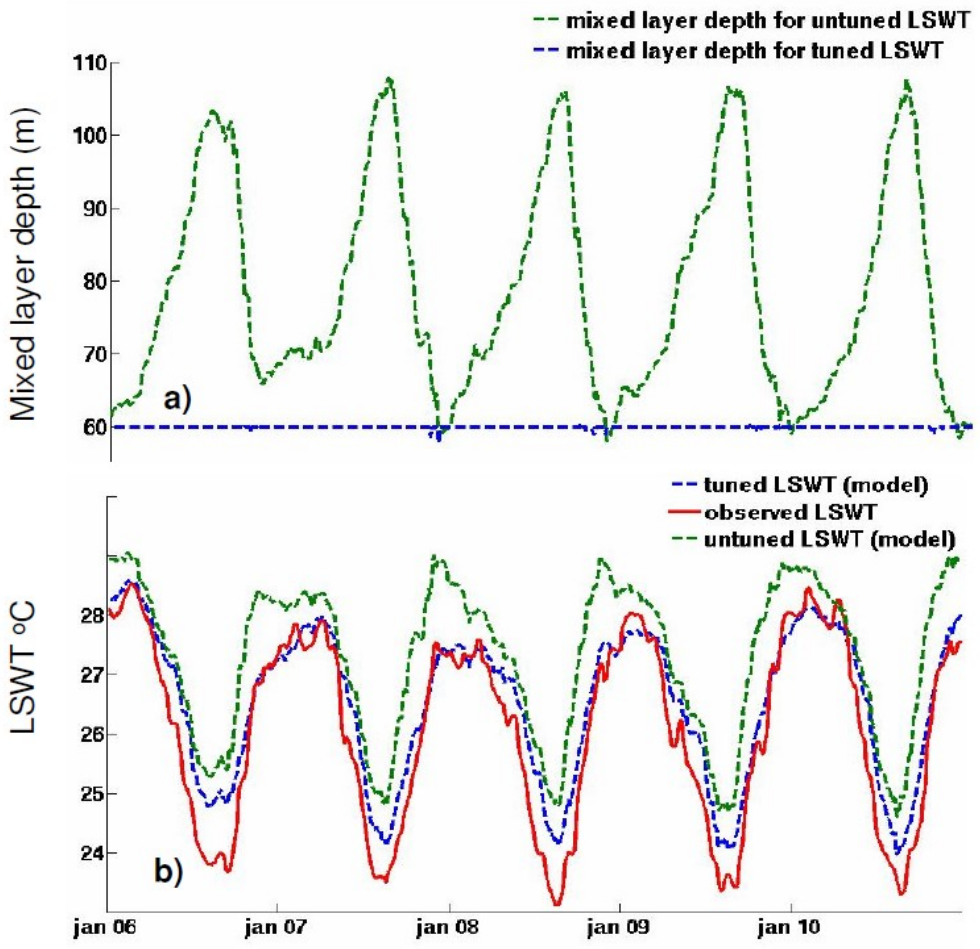

Figure 50 Comparison of tuned and untuned LSWTs and mixed layer depth for Lake Malawi a) mixed layer depth (tuned and untuned) b) LSWTs (observed, tuned and untuned) demonstrating that the tuned model produces LSWTs that compare well with the observed LSWTs but poorly represents the mixed layer depth.

Although, the mixed layer (top) depth and the LSWT are inter-dependent, the tuned mixed layer depth is not as reliable as the LSWT, as only the LSWT is tuned. Additionally, the effective depth may ultimately alter the mixed layer depth leading to non-representative mixed layer depth results, as is the case for Lake Malawi. *In-situ* measurements show that the mixed layer depth for Lake Malawi varies from 40 m in summer to 100 m in winter to (Eccles 1974; Vollmer *et al* 2005). This is not represented in the tuned model (effective depth of 60 m), where the mixed layer depth indicates that the lake continually mixes (no thermal stratification) as shown in Figure 50a. The untuned model (mean depth of 273 m) produces a more realistic mixed layer depth, Figure 50a, ranging from approximately 60 m in summer to 100 m in winter. This highlights that for lakes where the effective depth is substantially lower than the mean depth, the modelled mixed layer depths is expected to be inaccurate.

5.8.2.2 Salinity and altitude discussion

Primary metrics	Saline versus freshwater		High versus low altitude	
	Saline (26 lakes)	Freshwater (58 lakes)	> 1500 m a.s.l. (10 lakes)	< 1500 m a.s.l., (74 lakes)
MAD (°C)	1.06± 0.67	0.91± 0.64	1.03± 0.82	0.95± 0.64
mth_{max} (°C)	-0.31± 1.90	-0.16± 1.24	-0.40± 2.12	-0.18± 1.37
mth_{min} (°C)	-0.25± 1.74	-0.01±1.33	-0.14± 1.30	-0.07± 1.50
Secondary metrics				
$bias_{mth}$ (°C)	-0.17± 1.27	0.08± 0.97	-0.12± 1.24	0.02± 1.07
$bias_{max}$ (°C)	0.10± 2.01	0.17± 1.39	0.02± 2.33	0.17± 1.49
$bias_{min}$ (°C)	-0.51± 2.09	-0.28± 1.42	-0.49± 1.51	-0.33± 1.68
$inter_{max}$ (R^2_{adj})	0.22± 0.56	0.33± 0.65	0.18 ± 0.62	0.31 ± 0.63
$inter_{min}$ (R^2_{adj})	0.23± 0.49	0.27± 0.50	0.14± 0.44	0.27± 0.50
var_{max} (K^2)	0.25	0.47	0.29	0.42
var_{min} (K^2)	0.53	0.39	0.24	0.46

Table 28 Metric results for saline, freshwater and high and low altitude lakes with the spread of differences across lakes, 2σ

Twenty six (26) of the 84 lakes are saline and have salinity values ranging from < 3 g/l to 285 g/l. Freshwater parameter values were maintained throughout the tuning of *FLake* for all lakes. Table 28 (column 1 and 2) compares saline and freshwater metric results. Similar to the metric results for seasonally ice covered lakes, the average daily MAD of saline non-seasonally ice covered lakes is higher (0.15 °C) than the MAD of freshwater lakes and the spread of differences for all metric results is wider for the saline lakes. Fifty eight per-cent (58%) of saline lakes have MAD values < 1 °C, while 76% of freshwater lakes have MAD values < 1 °C. Although the freshwater lakes metric results are better, the tuning of the saline lakes still yield good results. Figure 51a show the observed and tuned modelled LSWTs for a highly saline lake (145 g/l), Lake Chiquita, Argentina, demonstrating the good observed and modelled agreement.

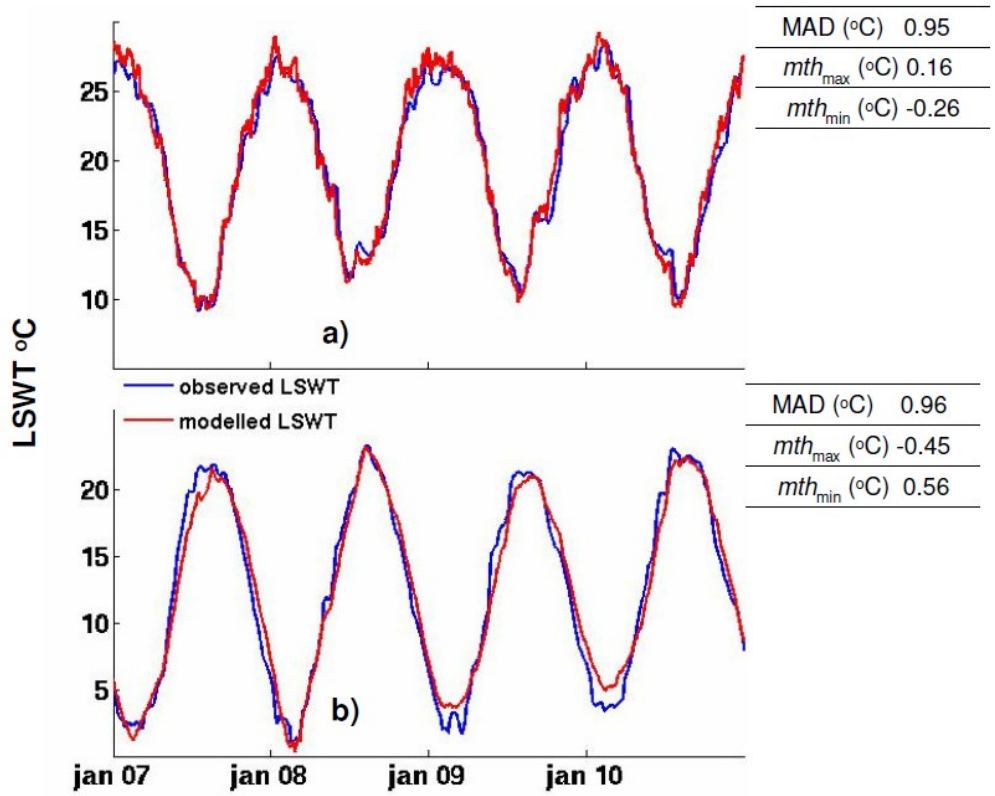

Figure 51 Observed LSWT versus tuned model LSWT for saline and high altitude lakes a) Lake Chiquita, Argentina (31° S, salinity 145 g/l) b) Lake Van, Turkey (38° N, 1638 m a.s.l., salinity 22 g/l)

Ten (10) of the 84 lakes are located at altitudes of 1500 to 3827 m a.s.l. (8 of which are below 2000 m a.s.l.). Seven (7) of the 10 high altitude lakes are also saline. Although the metric results for the low altitude lakes are slightly better, the tuning of the high altitude lakes yield good results. Figure 51b demonstrates the good observed and modelled agreement for Lake Van, a high altitude lake in Turkey, 1638 m a.s.l.

The high altitude lakes show less inter-annual variability in the observed maximum and minimum month (var_{max} = 0.29 K^2 and var_{max} 0.24 K^2) compared to low altitude lakes (0.42 K^2 and 0.46 K^2) and as a result of the correlation between observed variance and the fraction of observed variance explained by the model, the $inter_{max}$ and $inter_{min}$ are lower for high altitude lakes. This shows that the modelled LSWTs of low altitude lakes are more representative of the observed LSWTs than for high altitude lakes. Although, var_{max} and var_{min} have no statistically significant relationship with lake altitude, the annual range of monthly LSWTs (which is lower for high altitude lakes), explain 0.38 and 0.36 (p = 0.000) of the variation in var_{max} and var_{min}. This indicates that where the range in the annual cycle is smaller the variability in the cycle extremes will also be smaller. This also explains the lower var_{max} and var_{min} values for tropical lakes as shown in Table 26; indicating that the modelled LSWT are less representative in lakes where the annual range is lower.

The comparability of the results between the low and high altitude lakes indicates that the geo-potential height of the ERA model forcing is representative. It also implies that any bias or error that occurs as a result of lake altitude not being considered in *FLake* is small or minimised by the tuning process.

The saline lakes and higher altitude lakes (most of which are also saline) show a larger spread of differences for the mth_{max} then for the non-saline and low altitude lakes. Similarly, for secondary metrics there is a larger spread of differences for the $bias_{max.}$ This could be because the k_d value which was shown to be strongly linked with correcting the maximum LSWTs, is also being used by the model to compensate for not considering salinity, as is the case for Lake Bras d'or, Figure 43.

5.8.2.3 Tuned values for LSWTs regulating properties

Similar to the findings in chapter 4 for seasonally ice covered lakes, the tuned values for the LSWT regulating properties for the 84 lakes show that deep lakes are tuned to shallower depths, shallow lakes are tuned to deeper depths and that κ_{d4} and κ_{d5} are the most used tuned light extinction coefficient values. This reinforces the suggested guidance (in chapter 4, section 4.6.3), for getting more accurate LSWTs from *FLake*.

On average deep lakes (> 40m) are tuned to depths of 0.4 times their mean depth and shallow lakes (< 4 m) to twice their mean depth, Figure 52. Excluding the Dead sea which was showed poor tuning results, the inter-lake variation in the effective depths strongly reflect of the variation in the mean depth, showing a correlation of 0.84 (p= 0.000). For light extinction coefficients, 40% of the lakes are tuned with 2 of the 10 κ_d values. The 19 of the 84 lakes are tuned with κ_{d4} have an average depth of 32 m and the 15 lakes tuned with κ_{d5} have an average depth of 9 m. The less transparent κ_{d5} value, used for shallower lakes is sensible, as the water clarity of a shallower lake is more affected by the lake bottom sediments than a deeper lake.

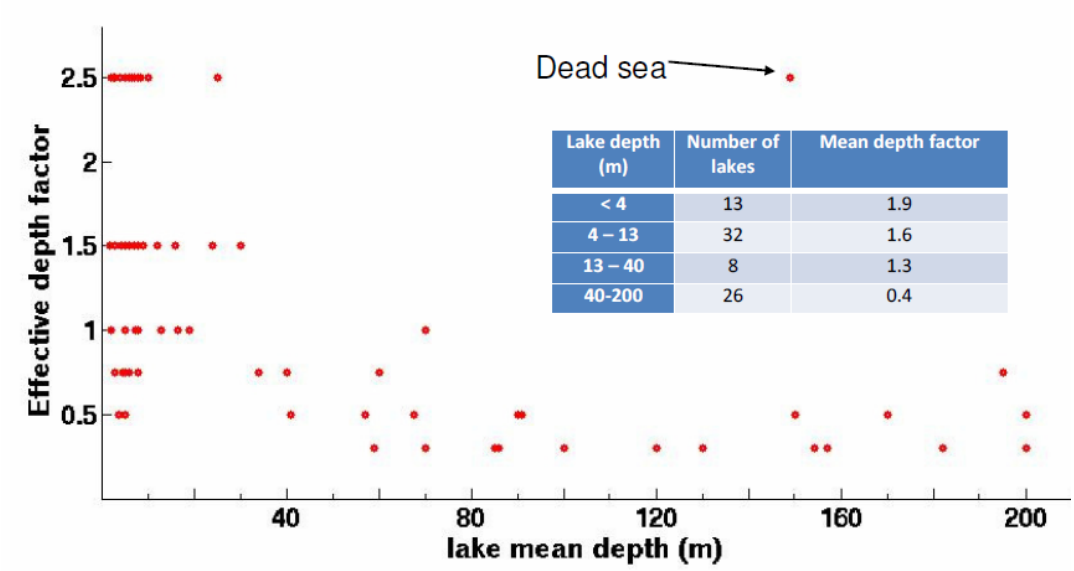

Figure 52 Tuned effective depth factor versus lake-mean depth, demonstrating that shallower lakes are tuned to a higher depth factor and deep lakes to a lower depth factor.

5.9 Independent evaluation of tuned model

I use observational LSWTs for 2011 to test the tuned LSWT regulating properties for approach 3. The year 2011 is the last available year of observed LSWTs and is not used in the tuning process. The primary and secondary metrics from 2011 are compared with metrics from the tuning period; 1996 (first full year from ATSR2) and 2010 last tuned year from AATSR), Table 29.

The mean MAD and dispersion of errors is slightly higher for the untuned year, 2011. However, overall the metrics are very comparable to the metrics from two example years within the tuned period, 1996 and 2010.

Primary Metrics	2011 Untuned	1996 Tuned (ATSR2)	2010 Tuned (AATSR)
MAD (°C)	1.07±0.91	0.98±0.82	0.97±0.81
mth_{max} (°C)	-0.23±2.40	-0.32±1.86	-0.31±2.20
mth_{min} (°C)	-0.02±2.04	-0.23±1.73	+0.11±2.15
Secondary metrics			
$bias_{mth}$ (°C)	+0.05±1.31	-0.19±1.22	+0.09±1.27
$bias_{max}$ (°C)	-0.23±2.18	+0.12±1.56	+0.05±2.26
$bias_{min}$ (°C)	-0.26±1.91	-0.63±2.07	-0.13±2.10

Table 29 Results of the independent test for tuning approach 3 with the spread of differences across lakes, 2σ, showing the untuned year (2011) with the first full year of data from ATSR2 (1996) and the last year of tuned data from AATSR (2010)

5.10 Conclusion

The primary metric results for the 84 non-seasonally ice-covered are highly comparable with the results for the 14 trial lakes, showing that lakes used in the trial and the approach taken resulted in the successful LSWT tuning of the non-seasonally ice covered lakes. The average daily MAD is 0.96$\pm$ 0.66 $^{\circ}$C across the 84 lakes, achieving the aim of reducing the average daily MAD to below 1.0 $^{\circ}$C.

There is no evidence of compensation between depth and wind speed (trial 2), as was shown for the seasonally ice covered trial lakes. This is most possibly due to the greater range of lake classifications, mixing regimes and LSWT annual ranges of non-seasonally ice covered lakes. A compensatory effect was shown between light extinction coefficient and wind speed (trial 3). For 8 of the 14 trial lakes (tropical and higher latitude), the cooler surface caused by a higher wind speed is counter-balanced by a less transparent lake surface (higher κ_d) causing more heat to be retained in the surface layer.

The minimum monthly LSWTs is shown to have a 1:1 relationship with the modelled lake bottom stratified temperature (R^2_{adj} 0.97 (p= 0.000). This highlights that the minimum month LSWTs could be used to as a proxy for deep water lake temperatures, as discussed further in chapter 7, section 7.4.

The observed extreme inter-annual variability is lower in both tropical and high altitude lakes, than in temperate lakes. The lower annual range in monthly LSWTs in tropical and high altitude lakes explains 0.38 and 0.36 (p = 0.000) of the variation in maximum and minimum inter-annual variability respectively, demonstrating that the greater the range in the annual LSWT, the greater the variability in the cycle extremes. This indicating that lakes with a larger range of LSWTs may be more responsive to changes in the LSWT extremes due to changes in the climate.

More pertinent to this study is the relationship between the maximum and minimum inter-annual variability and the fraction of observed maximum and minimum variability explained in the model (0.34 and 0.69) across all non-seasonally ice covered lakes. This shows that lakes with a lower variability (tropical and high altitude lakes) may be less well represented in the model then temperate or low altitude lakes.

Two (2) of the 86 lakes, Lake Viedma in South America and the Dead sea in Asia yielded very poor results. I demonstrated how this can be attributed to the altitude associated with the data measurement of the ECMWF meteorological data.

Having demonstrated successful LSWT tuning the LSWTs for 84 of the 86 non-seasonally ice covered lakes, in chapter 6, I evaluate for what purpose the tuned model is effective, examining long term modelled trends.

Chapter 6 Application of the tuned model

6.1 Introduction

In chapters 4 and 5, I showed how *FLake* was tuned for both the seasonally and non-seasonally ice covered lakes and demonstrated that the tuning approaches were suitable for these lakes (including saline and high altitude lakes). Having shown that the tuned model LSWTs are substantially closer to the observed LSWTs by means of the tuning metrics which principally measure biases in various features of the lake annual cycle, it is now relevant to evaluate for what other purpose the tuned model is effective.

In this chapter, I compare the trends from the tuned and untuned model (section 6.3) and investigate how well the tuned model represents the regional long term (33 years; the length of time of available model forcing data) summer trends, section 6.4. Summer LSWTs are defined as shown in chapter 2, section 2.8. I also present lake-specific trends (JAS LSWT for seasonally ice covered lakes and maximum month LSWT for non-seasonally ice covered lakes) for lakes with modelled trends that are shown to be highly supported by observed (ARC-Lake) trends, section 6.5. I use these lake specific trends to assess the meteorological drivers.

For trend comparison, I use lakes with an observed time period of greater than 16 years. There are 150 seasonally ice covered lakes and 80 non-seasonally ice covered lakes (excluding Lake Viedma and the Dead Sea) with an observed period of tuning period of 16 or 20 years (1992/1996 – 2011).

6.2 Data used in evaluation of trends

In this evaluation, observed (IWBP and ARC-Lake) and modelled trends are also compared using subsets of these 230 lakes. The IWBP LSWTs (nighttime lake centre trends) span 27 years; from 1985 to 2011). To assess the meteorological drivers of

LSWT trends (both over the observed period and the 33 year period), I use seasonal ERA air temperature (T2) and shortwave solar downward radiation (SSRD) model forcing trends (ECMWF 2009). To support regional and lake specific modelled trends, I compare the seasonal ERA T2 trends with the seasonal air temperature from a higher resolution gridded dataset, Climatic Research Unit (CRU) timeseries version 3.20 (Jones *et al* 2013). All regional trends are characterised showing the uncertainty in the mean trend, **Equation 18;**

$$\pm \frac{2\sigma}{\sqrt{(N-1)}}$$

The regression results are reported using the adjusted R^2 (R^2_{adj}) and are in decimal format.

6.3 A comparison of the tuned and untuned model

I compare the tuned and untuned modelled trends and find that both regionally and individually, the summer trends are comparable. The regional tuned and untuned model trends for lakes with 20 years of observations (between 1992 and 2011; 119 lakes) are shown in Table 30, column 1 and 2. Individually, the trends show a correlation of 0.87. There is no relationship between the individual trend difference (between the tuned and untuned trends) and depth, demonstrating that while the tuning process substantially improves the absolute values, the effect of tuning the depth does not greatly affect the modelled trends. The average daily MAD for the LSWTs of all lakes from the untuned model (3.38 $\pm$ 2.74 $^{\circ}$C) compares poorly with the MAD for the tuned model 0.85 $\pm$ 0.61 $^{\circ}$C. The similar trends can be attributed to the consistency in the model forcing data applied to the tuned and untuned model. The same air temperature, SSRD, cloud and humidity is applied and the wind speed scaling, where applied to the tuned model, is consistent throughout the timeseries.

6.3.1 Improvements in the untuned model

The untuned model was run using the mean depth and default albedo. In the absence of light extinction data for the majority of lakes, the seasonally ice covered lakes were modelled using the average κ_{sd} (0.82) of the 21 trial lakes and the non-seasonally ice covered lakes were modelled using the average k_{sd} (1.46) of the 14 trial lakes. All other model parameters and properties as outlined in chapter 3, section 3.2.1 were maintained for the untuned model. In chapters 4 and 5, I made several suggestions on how to improve the modelled LSWTs from *FLake*. I suggested that if the light extinction coefficients were unknown, that κ_{d4} and κ_{d5} (the two least transparent light extinction coefficient for open ocean) would be a good estimate of the light extinction coefficient of a large lake. Modifying the untuned model by applying the κ_{d4} value for lakes with a mean depth > 16 m and the κ_{d5} for lakes with a mean depth < 16m, reduces the MAD from 3.38 $\pm$ 2.74 $^{\circ}$C to 2.28 $\pm$ 2.30 $^{\circ}$C, improving the average MAD by 33%. This confirms that the suggested improvement for modelling LSWTs in *FLake* is valid. This change has little effect on regional trends as shown in Table 30, column 2 and 3. Individual trends show a correlation of 0.95.

Region	No. of lakes	Modelled regional trends °C yr^{-1}			Observed regional trends °C yr^{-1}	
		Tuned	Untuned	Untuned (applying k_{d4} / k_{d5} *)	ARC-Lake lake-mean	ARC-Lake lake centre
Africa	10	0.01 ± 0.02	0.00 ± 0.02	0.01 ± 0.02	0.00 ± 0.01	0.01 ± 0.01
Asia	41	0.03 ± 0.01	0.03 ± 0.01	0.03 ± 0.01	0.01 ± 0.01	0.01 ± 0.01
Europe	14	0.05 ± 0.02	0.06 ± 0.02	0.05 ± 0.02	0.05 ± 0.02	0.06 ± 0.02
North America	39	0.04 ± 0.01	0.04 ± 0.01	0.03 ± 0.01	0.03 ± 0.01	0.03 ± 0.01
South America	13	0.02 ± 0.01	0.02 ± 0.02	0.02 ± 0.02	0.01 ± 0.02	0.01 ± 0.02
Oceania	2	0.03 ± 0.03	0.04 ± 0.01	0.04 ± 0.01	0.03 ± 0.04	0.03 ± 0.04

*applying light extinction coefficient values k_{d4} to lakes with depths >16 m and k_{d5} to lake with depth < 16 m

Table 30 Regional modelled summer LSWT trends (tuned, untuned and untuned with recommended k_d values) and ARC-Lake summer LSWT trends (lake-mean and lake centre) for the 119 lakes with 20 years of observed LSWTs, 1992-2011, showing uncertainty of trends with 95% confidence. Comparable regional modelled trends across columns 1 to 3 and a correlation of 0.82-0.95 for individual trends indicate that tuning has little effect on the trends. Highly comparable trends in column 4 and 5 (correlation of 0.96) show that the lake centre trends are representative of lake-mean trends.

6.4 Regional observed summer trends

It was shown in the 'State of the Climate in 2011 report' (Hook *et al* 2012), that there is large uncertainty in relation to the magnitude of regional LSWT trends and in some regions, uncertainty as to whether LSWTs are actually warming. In this section, I attempt to address some of this uncertainty. In section 6.4.1., I assess the level of agreement between the modelled and observed (ARC-Lake and IWBP) regional trends. In section 6.4.2, I present the modelled summer regional trends over the long term (33 years: from Jan 1979 to Dec 2011) for regions where there is good supporting evidence. The 33 trend period is limited to the number of complete years with available ERA model forcing data.

6.4.1 Comparing model and observed trends

In chapter 2, section 2.8.1, I concluded that lake-mean trends were representative of the lake centre trends (and vice versa). On this basis, I infer that the modelled trends are also indicative of the lake centre trends, as *FLake* is used and tuned in a manner which represents the lake–mean LSWTs. Using the tuned modelled summer trends, I now demonstrate this. The ARC-Lake lake-mean day-night average and lake centre day-night average regional summer trends for lakes with 20 years of LSWT observations (119 lakes) are highly correlated (0.96). As a result, they show a similar correlation (0.53 and 0.54) to the corresponding modelled trends. As shown in Table 30, the regional modelled trends (column 1) compare equally well to the ARC-Lake lake centre and lake-mean trends (column 4 and 5) and therefore can be considered representative of both. The ARC-Lake lake-mean and modelled regional trends, shown in Figure 53, are statistically indistinguishable, supporting the validity of all regional modelled trends over the 20 year period.

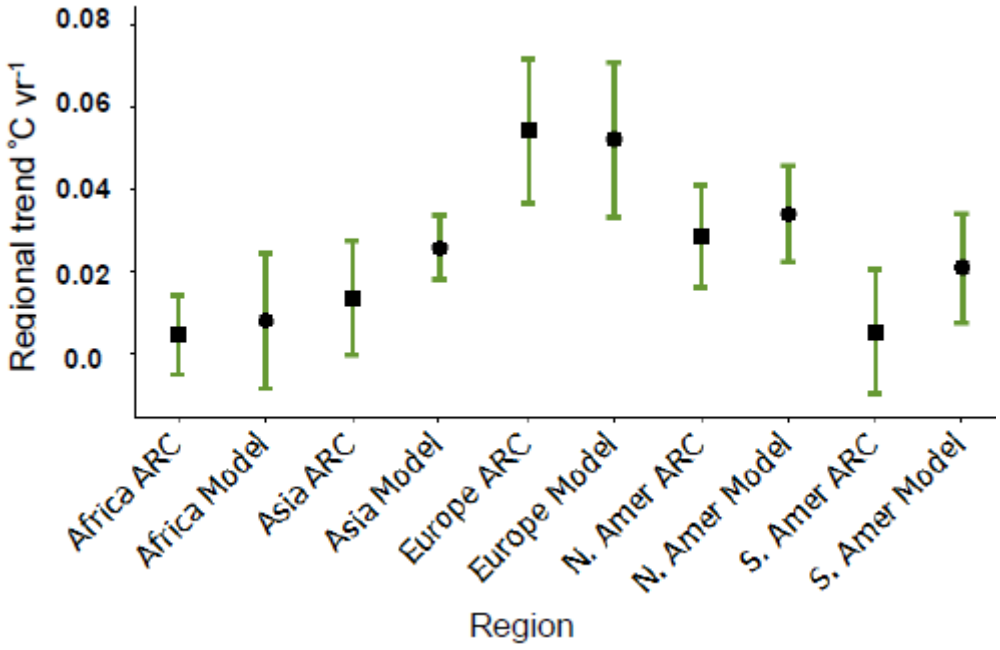

Figure 53 Regional lake-mean LSWT summer trends from ARC-Lake (squares) and tuned modelled trends (circles) determined using 119 lakes with 20 years of observations (from 1992-2011) with the uncertainty (95% confidence level) of the regional trends represented by the error bars. A paired t-test confirmed that the trends are statistically indistinguishable in all regions.

It is valid to compare tuned (lake-mean) *FLake* trends to the IWBP trends, over the 27 years of IWBP observations for the 84 lakes in common, given the good lake centre lake-mean comparability and the high correlation between the ARC-Lake lake centre nighttime and day-night average trends (0.91), established in chapter 2, section 2.8. Although well correlated, the ARC-Lake nighttime trends show slightly stronger warming than the day-night trends in 3 regions, Africa, Asia and North America, and a weaker warming in Europe, as shown in chapter 2, (Table 7 and Figure 23b).

As shown in Figure 54 and Table 31, the IWBP trends are considerably warmer than the modelled trends in 4 regions (and statistically different in 2 regions), indicating that the observed trends may be unrealistically high, particularly in Europe (where the ARC-Lake nighttime trends were shown to be cooler than day-night trends). The

overestimation of the IWBP trends in Europe can be inferred from the comparison of the ARC-Lake and IWBP nighttime lake centre trends, chapter 2, Figure 22.

Individually, the modelled summer trends for the 71 common lakes over the 20 period are also more strongly comparable with the ARC-Lake summer nighttime trends (correlation = 0.50) than the IWBP summer nighttime trends (correlation = 0.40), as shown in Figure 55. The untuned model trends also show a stronger correlation with ARC-Lake trends (0.48), than with the IWBP trends (0.35), demonstrating that the process of tuning using the ARC-Lake LSWTs is not the cause of the stronger correlation between *FLake* and ARC-Lake LSWT trends.
I conclude that the ARC-Lake regional and individual trends are more comparable with the modelled (tuned and untuned) trends than the IWBP trends. For the remainder of this chapter, all modelled trend comparisons with observed LSWTs refer to ARC-Lake lake mean (day-night average) LSWTs. The slightly better trend comparison between ARC-lake and the tuned model (0.50) than between ARC-lake and the untuned model (0.48) indicates that tuning process and use of wind scaling produces slightly more representative modelled trends.

Region	Number of lakes	Trend $^{\circ}C$ /yr^{-1}	
		Tuned Model	IWBP
Africa	9	0.01± 0.01	0.03± 0.01
Asia	29	0.03± 0.01	0.03± 0.01
Europe	11	0.05± 0.01	0.07± 0.03
North America	31	0.03± 0.01	0.04± 0.01
South America	4	0.01± 0.02	0.01± 0.01

Table 31 Regional modelled summer LSWT trends and IWBP trends comparison for the 84 lakes with 27 years of IWBP observations (from 1985-2011), showing uncertainty of trends with 95% confidence

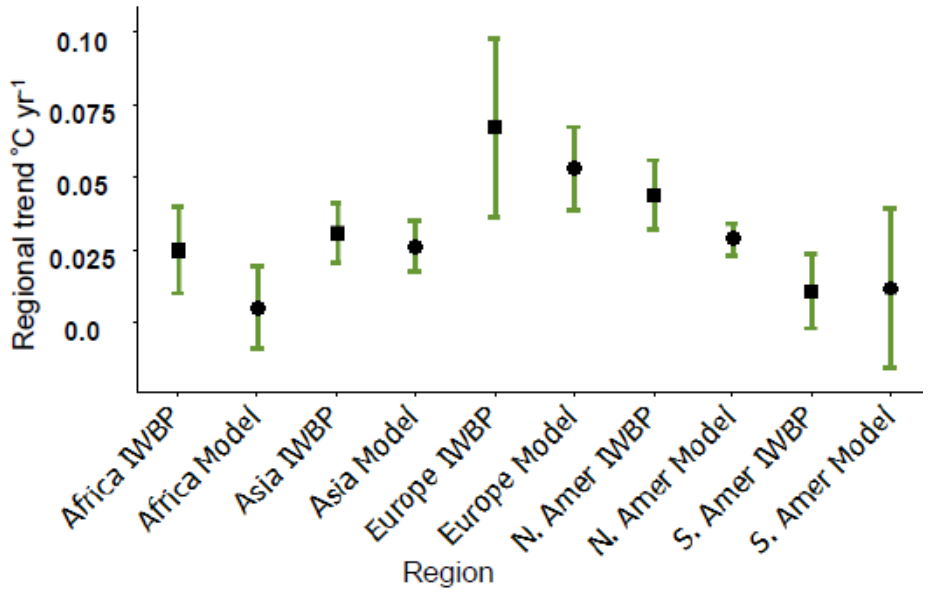

Figure 54 Regional IWBP LSWT summer trends (squares) and tuned modelled trends (circles) comparison for the 84 lakes with 27 years of IWBP observations (from 1985-2011), and the uncertainty (95% confidence level) represented by the error bars. IWBP trends show stronger warming in most regions and are statistically different (paired t-test) in Africa (p = 0.03) and North America (p = 0.02)

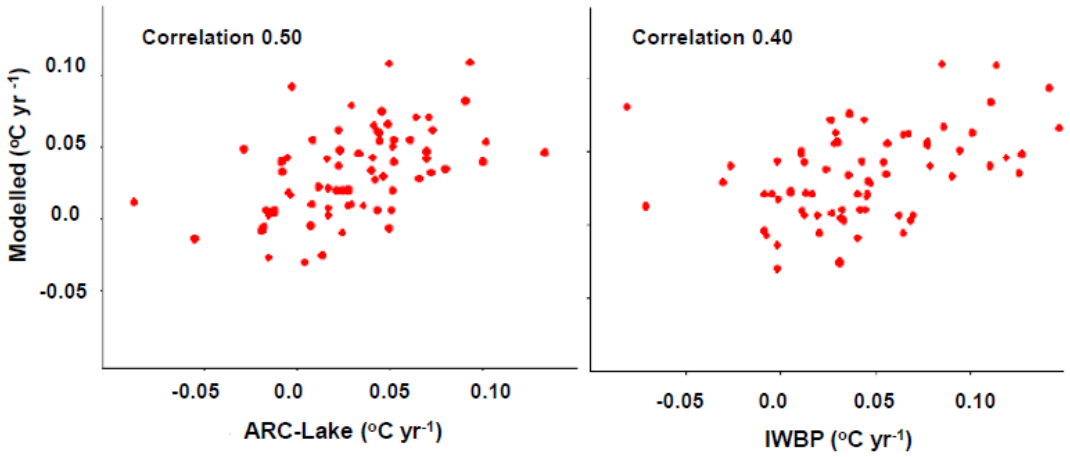

Figure 55 The modelled summer trends versus the observed (nighttime) summer trends over the 20 year period, from 1992-2011 (71 lakes) a) modelled versus ARC-Lake trends b) modelled versus IWBP trends, showing a better correlation with ARC-Lake (0.50) than IWBP (0.40)

6.4.2 Regional modelled long term trends

I present the modelled regional summer trends over the 33 year period (the length of time of available model forcing data). Modelled trends for regions are shown only where they are supported. Trends are presented where the observed and modelled regional trends over the observed period, are statistically indistinguishable (Europe, Asia, Africa and Oceania) or where the ERA T2 and CRU seasonal trends are comparable over the 33 year period (North America).

Regional modelled warming over the 33 year period is shown in Figure 56 and Table 32. The strongest warming has occurred in Europe, (1.35 ºC) and the least in Africa and Oceania (0.30 ºC) from 1979 to 2011 years. Oceania (2 lakes) is not shown in Figure 56 as there is a large uncertainty. In the next 2 subsections, 6.4.2.1 and 6.4.2.2, I explain the approach taken in determining the regional 33 year modelled trends.

Region	Number of lakes	Trend $^{\circ}C\ yr^{-1}$	Average LSWT warming from 1979 -2011 ($^{\circ}C$)
Africa	21	0.01 ± 0.01	0.30
Asia	57	0.02 ± 0.01	0.56
Europe	28	0.04 ± 0.00	1.35
North America	118	0.02 ± 0.00	0.70
Oceania	2	0.01 ± 0.02	0.30

Table 32 Regional modelled summer LSWT trends and warming from 1979-2011 (33 years) for regions supported by comparable modelled and observed trends over the 16-20 year period or comparable long term (33 year) CRU and ERA T2 air temperature trends. Trends show strongest warming in Europe of 1.35 $^{\circ}C$ from 1979-2011

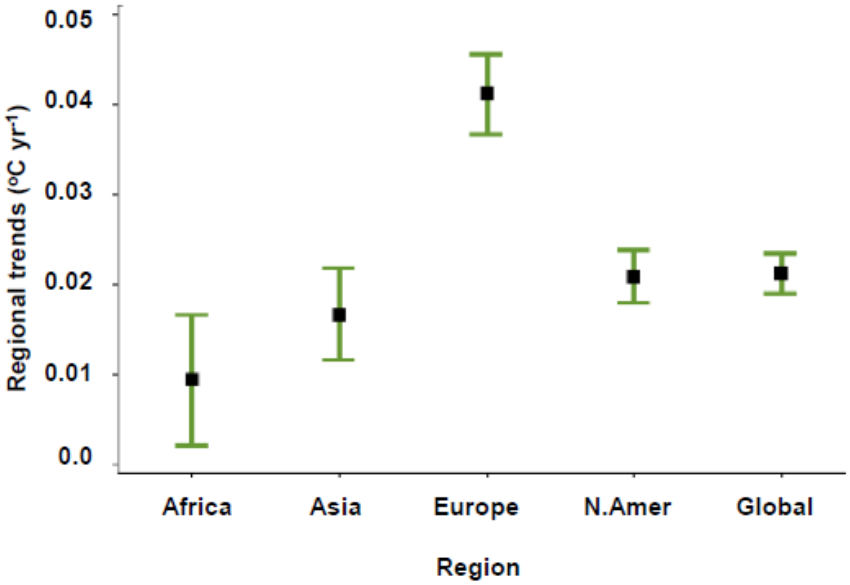

Figure 56 Regional modelled summer LSWT trends from 1979-2011 (33 years) and the uncertainty of the trends (95% confidence level) for regions supported by comparable modelled and observed trends over the 16-20 year period or comparable long term (33 year) CRU and ERA T2 air temperature trends. Oceania (2 lakes) is not shown due to the large uncertainty. In all regions except Oceania summer LSWT show warming with certainty

6.4.2.1 Statistically and non-statistically significant regional trends

Regional summer LSWT trends are more extreme when determined using only statistically significant trends than when determined using all trends within a region. This is attributable to the lower signal (trend) to noise ratio (inter-annual variation) for lakes with a less extreme trend. Figure 57 compares the regional trends determined using an average of the statistically significant trends and an average of all trends in a region. For both modelled (Figure 57a) and observed (Figure 57b) trends, the regional trends determined using an average of statistically significant trends are more extreme in all regions. The statistically significant trends show stronger warming in all regions with exception to the modelled LSWTs in Europe and the observed LSWTs in North America, where the statistically significant trends show stronger cooling. This shows without exception that lakes with weaker (either

warming or cooling) trends are less likely to have statistically significant trends. I determine the regional trends, using all trends within a region as it possibly gives a more realistic overall trend for the region.

6.4.2.2 Support for the regional trends

The modelled and observed regional trends in Europe, Asia, Africa and Oceania are statistically indistinguishable over the 16-20 year period, as shown in Table 33, indicating that the model forcing data are realistic at lake locations in these 4 regions. On this basis, I consider the long term modelled trends in these 4 regions to be reliable. In North and South America, the trends are statistically different, Table 33.

Region	All lakes (230)				Statistically significant trends			
	No. of lakes	Modelled Trend $^{\circ}C\ yr^{-1}$	Observed Trend $^{\circ}C\ yr^{-1}$	Paired t-test *P*	No. of lakes (102)	Modelled Trend $^{\circ}C\ yr^{-1}$	No. of lakes (49)	Observed Trend $^{\circ}C\ yr^{-1}$
Africa	20	0.01 ± 0.01	0.00 ± 0.01	0.096	8	0.02 ± 0.02	3	0.01 ± 0.03
Asia	51	0.02 ± 0.01	0.02 ± 0.01	0.158	23	0.04 ± 0.01	11	0.07 ± 0.03
Europe	27	0.06 ± 0.01	0.04 ± 0.02	0.119	26	0.04 ± 0.00	9	0.07 ± 0.06
North America	113	0.02 ± 0.01	0.00 ± 0.01	**0.001***	38	0.04 ± 0.00	22	-0.03 ± 0.04
South America	19	0.02 ± 0.01	0.00 ± 0.01	**0.043***	7	0.04 ± 0.01	3	0.02 ± 0.05
Oceania	2	0.03 ± 0.03	0.03 ± 0.04	0.610				

Table 33 Regional modelled and ARC-Lake summer LSWT trends over the 16-20 years for all lakes and for statistically significant lakes showing the uncertainty of the trends (95% confidence level). The paired t-test results shown for the modelled and observed regional trends (all lakes), shows statistically different trends in North and South America

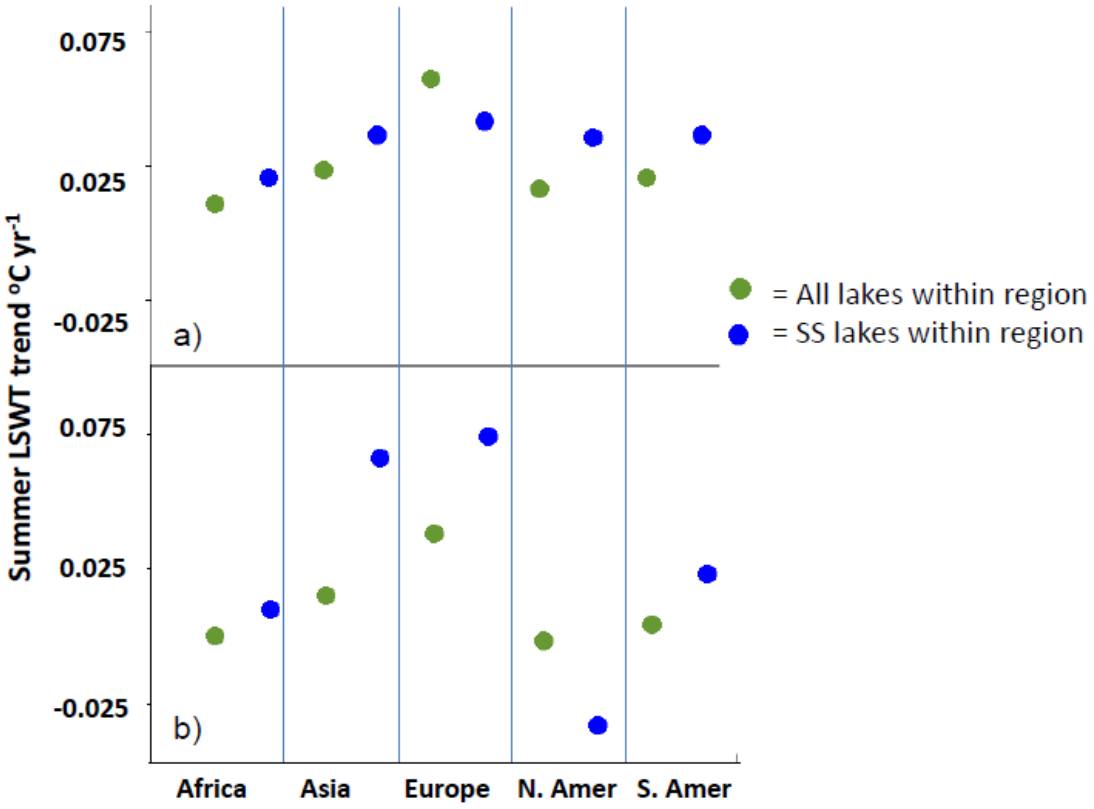

Figure 57 Regional modelled and ARC-Lake summer LSWT trends over the 16-20 years for all lakes (green circle) and for lakes with statistically significant trends (blue circle) a) Modelled trends and b) ARC-Lake trends

The observed summer cooling of many Canadian lakes (northern and western Canada) over the 16-20 year period is not detected in the model, causing the statistically different trends in North America. This disparity is greater for the statistically significant trends in North America, with the model showing strong warming trends, while the observed trends show strong cooling, Table 33 and Figure 57. In North and South America, I compare the ERA T2 and the higher resolution CRU air temperature seasonally trends over the 16-20 year period and over the 33 year period, for all lake locations, Table 34. The level of agreement between the two temperature dataset trends is an indication of how much of the air temperature changes are reflected in the model forcing data. The European regional trends are included in this table as a benchmark, as the modelled and observed trends for Europe are statistically indistinguishable.

	16-20 year trends ºC yr^{-1}						33 year trends ºC yr^{-1}				
	Observed summer LSWT	Modelled summer LSWT	summer CRU	summer ERA T2	winter CRU	winter ERA T2	Modelled summer LSWT	summer CRU	summer ERA T2	winter CRU air temp	winter ERA T2
North America	0.00 ± 0.01	0.02 ± 0.01	-0.02 ± 0.01	0.00 ± 0.01	0.00 ± 0.01	0.04 ± 0.02	0.02± 0.00	0.03 ± 0.00	0.03 ± 0.00	0.05 ± 0.01	0.05 ± 0.01
Europe	0.04 ± 0.02	0.06 ± 0.01	0.04 ± 0.02	0.06 ± 0.02	-0.01± 0.03	0.00 ± 0.02	0.04± 0.01	0.05 ± 0.01	0.05 ± 0.01	0.06 ± 0.01	0.04 ± 0.01
South America	0.01 ± 0.01	0.02 ± 0.01	0.02 ± 0.01	0.04 ± 0.01	0.02 ± 0.01	0.04 ± 0.02	0.02 ± 0.01	0.01 ± 0.01	0.02 ± 0.01	0.00 ± 0.01	0.01 ± 0.01

Table 34 Observed and modelled summer LSWT trends, and seasonal air temperature (CRU and ERA T2) trends for North America, Europe and South America over the 16-20 year and 33 year period, showing the uncertainty of the trends (95% confidence level)

In Europe, over the 16-20 year period, the ERA T2 and the CRU summer air temperature trends show comparable warming in both summer and in winter, with the ERA T2 and the CRU summer trends explaining a similar amount, 0.21 and 0.27 (p= 0.000), of the observed LSWT trends, showing the good agreement between the two air temperature datasets in Europe. In North America, over the same period, the model forcing air temperature (ERA T2) trends shows no change while the corresponding CRU temperature shows cooling of 0.02 ^{o}C yr^{-1}, Table 34, with the ERA T2 summer trend explaining 0.48 (p= 0.000) of the modelled LSWT trends. This explains the warmer modelled trends in North America. In winter there is also poor agreement in North America. The CRU air temperature shows no change while over the same period, the ERA T2 shows warming of 0.04 ^{o}C yr^{-1}, Table 34. The disparities between the CRU air temperature the ERA T2 trends in North America disappears in the longer datasets.

Over the 33 year period the ERA T2 and the CRU air temperature trends show very good agreement in North America (and in Europe). The regional ERA T2 summer 33 year trends explain a similar proportion (0.46 and 0.51) p = 0.000, of the 33 modelled year trends in Europe and North America respectively, and in both cases are highly comparable to the regional CRU air temperature trends. On this basis, the 33 year modelled trends in North America are considered to be realistic.

Considering only lakes with 20 years of observations, the modelled and observed LSWT trends in North America were shown to be comparable, Figure 53. In North America 74 of the 113 lakes have only 16 years of observations. As a result, it is possible that the 16 year period is not long enough to be robust relative to inter-annual variation. Although as shown in Figure 58, the statistically significant modelled trends do not reflect the cooling in northern and western Canadian lakes, a comparison of the modelled an observed trends for all lakes show that the modelled trends detect some of the observed cooling in Canadian lakes (also in Africa and Asia in that period, in that period) Figure 59.

In South America, the ERA T2 summer and winter trends show approximately twice the warming of the CRU summer and winter trends over the 16-20 year period and the 33 year period, Table 34. Although, there is no statistically significant relationship between the ERA T2 and the modelled trends over the 33 year period, (possible due to a lower magnitude of change), the stronger ERA T2 warming trends may result in more rapid modelled warming over the longer period. Over the 20 year period, although the modelled and observed LSWTs are statistically indistinguishable in South America, Figure 53, the modelled trends show considerably stronger warming, 0.02 + 0.01 $^{\circ}$C yr^{-1}, than the observed trends 0.01 + 0.02 $^{\circ}$C yr^{-1}. On the basis, I conclude that the magnitude of warming in the modelled trends over the longer period may be unrealistically high and therefore are not wholly representative of warming in South America.

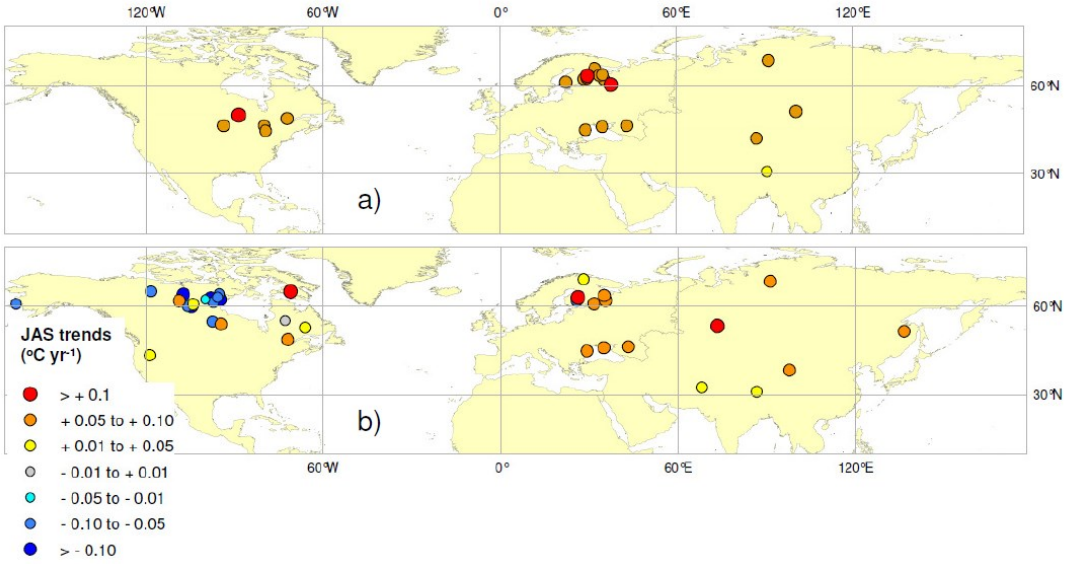

Figure 58 Statistically significant modelled and observed JAS LSWT trends over the 16-20 year period. a) Modelled trends b) ARC-Lake trends, showing that the observed cooling of Canadian lakes is not detected in the statistically significant modelled trends

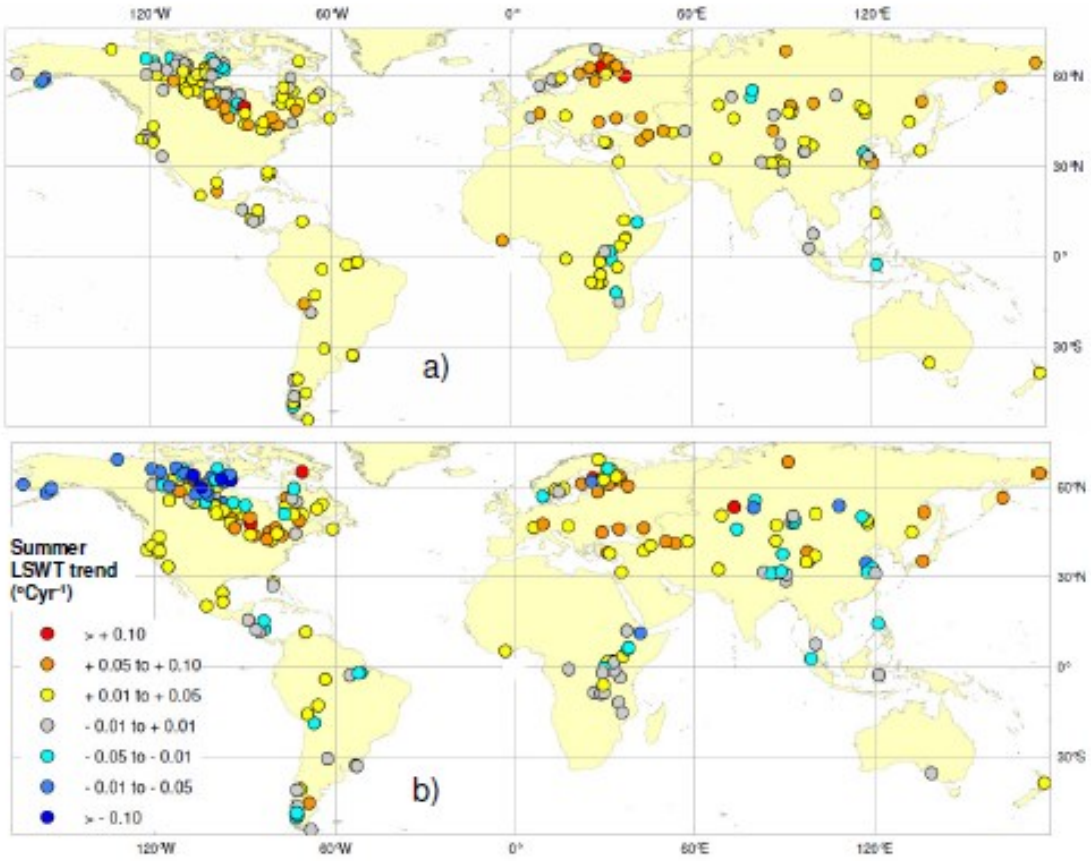

Figure 59 Modelled and observed summer trends for all lakes over the 16-20 year period. a) Modelled trends b) ARC-Lake trends, showing that the model captures some of the observed summer cooling in Canadian lakes

6.4.2.3 Cooling summer trends in Canadian lakes

The same factors explain the observed and modelled summer trends in Canadian lakes. In chapter 2, section 2.9, I showed that the 4 °C warming day explains 0.50 (R^2_{adj}, p = 0.000) of the inter-lake variation in the summer trends of lakes in Canada (79 lakes) and latitude explains 0.26 (p = 0.000) of the variation. Similarly, the modelled 4 °C warming day trends and latitude explain 0.34 and 0.30 (R^2_{adj}, p = 0.000) of the variation in the modelled summer trends.

6.5 Lake specific trends

In the previous section, I addressed some of the uncertainty in relation to the magnitude of regional LSWT trends by presenting modelled summer trends over the 33 years for regions where there is good supporting evidence. I now assess lake specific modelled trends over the 33 year period. I present statistically significant lake trends over the 33 year period, which capture a high fraction of the observed inter-annual variability and show good agreement with observed trends over the 16-20 year period. For seasonally ice covered lakes, I present the JAS (summer) LSWT trends and maximum month LSWT trends for non-seasonally ice covered lakes.

For the JAS LSWTs of seasonally ice covered lakes, the observed and modelled trends over the 16-20 year period are well-correlated for all lakes where the observed JAS LSWT inter-annual variability explained by the model ($inter_{jas}$) is ≥ 0.70. On this basis, I apply 0.70 as the cut-off for the fraction of inter-annual variability explained by the model when considering long term trends for the maximum month LSWT for non-seasonally ice covered lakes. For the maximum month (non-seasonally ice covered lakes) and JAS (seasonally ice covered lakes) LSWTs there is a respective correlation of 0.69 and 0.31 between the fraction of the observed inter-annual variability explained by the model and the amount of true (observed) inter-annual variability. For lakes with greater observed inter-annual variability, the model explains more (proportionally) of the variation, indicating that the factors that drive the observed variance are captured by the model. For this reason, I investigate the meteorological drivers of these lake specific LSWT trends. To assess the drivers, I use seasonal ERA SSRD and T2 trends at the lake locations. I also compare the ERA T2 trends with the CRU air temperature trends at lake locations, over the 33 year period, as agreement between the two temperature datasets further supports the modelled trends.

6.5.1 JAS LSWT trends for seasonally ice covered lakes

There are 150 seasonally ice covered lakes which have $\geq$ 16 years of observations. The average fraction of observed JAS LSWT inter-annual variability explained by the model ($inter_{jas}$) for the 150 lakes is 0.49. Figure 60 and Figure 61 demonstrate that the $inter_{jas}$ fraction is higher for lakes where the observed JAS LSWT inter-annual variability (var_{jas}) is higher. The $inter_{jas}$ and var_{jas} are correlated (Pearson) (0.31, p = 0.000) across the 150 lakes. The observed and modelled trends for these lakes are correlated (0.49, p = 0.010) as shown in Figure 60. Of these 150 lakes, 49 have a high $inter_{jas}$ fraction ($\geq$ 0.70, averaging 0.82). The observed and modelled trends for these 49 lakes are highly correlated (0.80), Figure 60 (insert). Nineteen of these 49 lakes have statistically significant JAS LSWT trends over the 33 years. The trends and lake geographical details of these 19 lakes are presented in Table 35 and Figure 62. Latitude explains 0.35 (p = 0.005) of the variation in the JAS LSWT trends of all lakes (44° N-65° N) in Table 35 (excluding Lake Har-us, a high altitude lake, 1191 m a.s.l.). All other 18 lakes are located from 1 - 540 m a.s.l. Lakes at higher latitudes, 56° N-65° N show greater warming rates (averaging 0.04 °C yr^{-1}, equivalent to 1.41 °C from 1979 to 2011) than lakes at lower latitudes, 44° -49° N (averaging 0.03 ºC yr^{-1}, equivalent to 1.01 °C from 1979 to 2011).

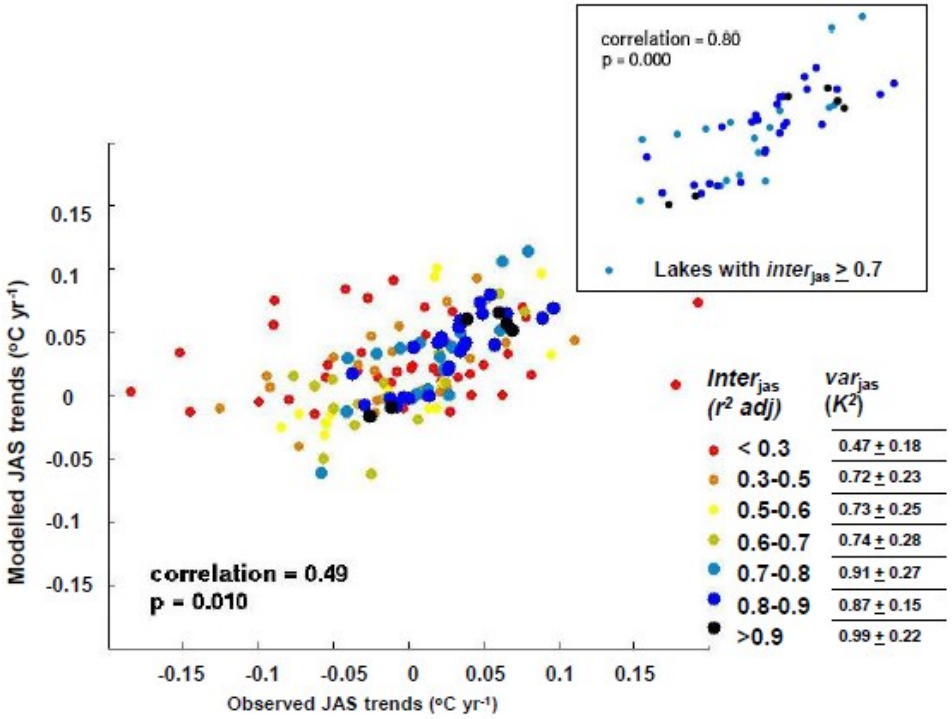

Figure 60 The modelled versus the observed summer LSWT trends for all 150 seasonally ice covered lakes over the 16-20 year period, showing a correlation of 0.49, with the insert showing the correlation for the 49 lakes with $inter_{jas}$ fractions $\geq$ 0.70. The legend shows that lakes with a higher var_{jas} value have a proportionally higher $inter_{jas}$ fraction (correlation = 0.31)

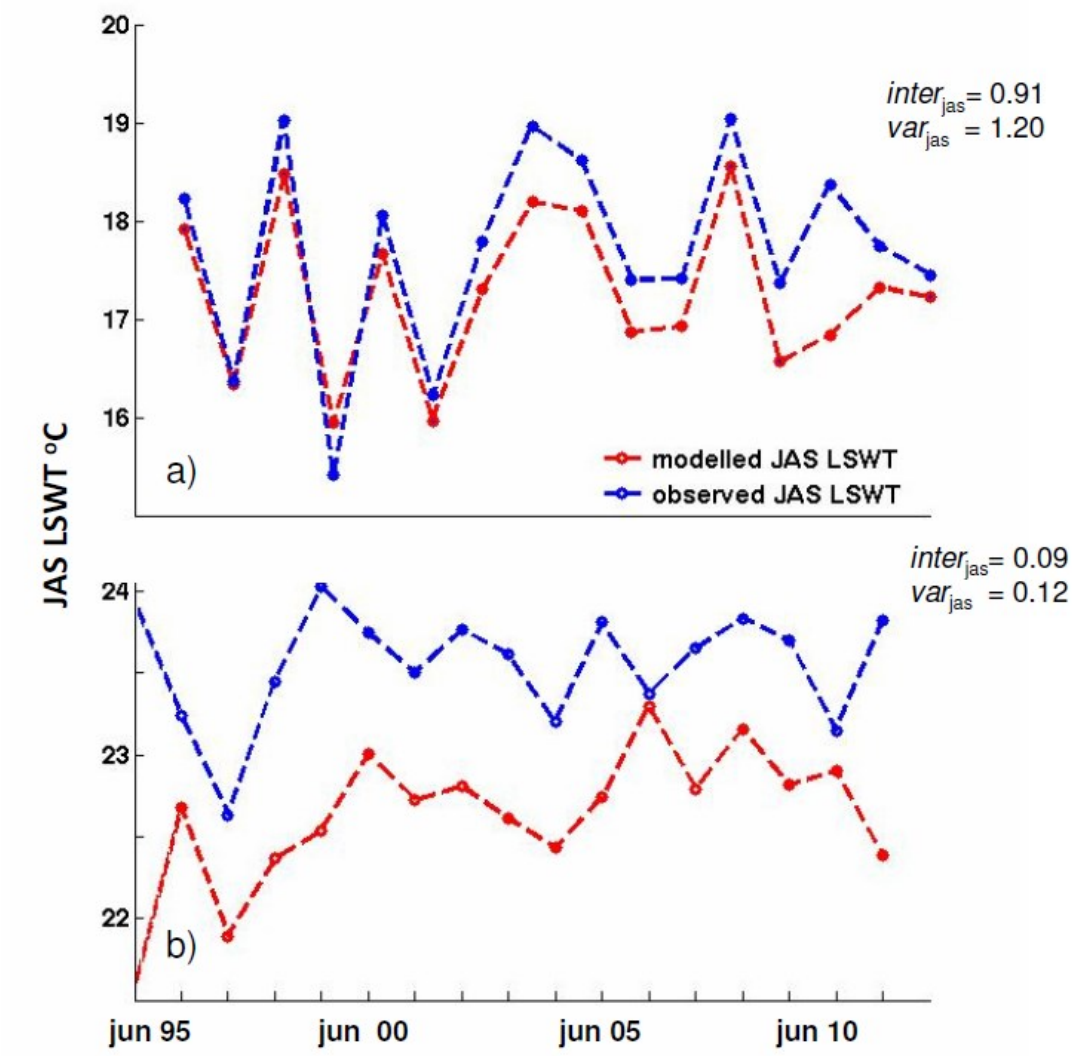

Figure 61 Observed and modelled LSWT timeseries for two lakes where there is a large difference in the observed JAS variability (var_{jas}), demonstrating the relationship between var_{jas} the fraction of inter-annual variation in the JAS LSWT explained by the model ($inter_{jas}$) a) Lake Limfjorden, Denmark (high var_{jas}) and b) Lake Baghrash, China (low var_{jas})

ARC id	Lake	Lat	Lon	Altitude	Country	Continent	P –value	MSD	Constant	trends ºC yr^{-1}
160	Beloye	60.18	37.64	122	Russia	Europe	0.001	0.747	-0.0976	**0.06**
142	Har-us	48.06	92.3	1191	Mongolia	Asia	0.000	0.427	-0.0846	**0.05**
128	Eauclaire	56.15	-74.4	251	Canada	N. Am.	0.013	0.974	-0.0809	**0.05**
50	Peipus	58.41	27.59	29	Russia; Estonia	Europe	0.005	0.702	-0.0787	**0.05**
29	Vanern	58.88	13.22	45	Sweden	Europe	0.014	0.892	-0.0764	**0.05**
140	Limfjorden	56.78	9.17	3	Denmark	Europe	0.006	0.634	-0.0734	**0.04**
264	Kamllukuak	62.28	-101.73	266	Canada	N. Am.	0.017	0.693	-0.0655	**0.03**
344	Krasnoe	64.53	174.44	2	Russia	Asia	0.036	0.957	-0.0665	**0.03**
85	Syvash	45.96	34.74	2	Ukraine	Europe	0.000	0.262	-0.0651	**0.03**
95	Vattern	58.33	14.57	91	Sweden	Europe	0.030	0.791	-0.0627	**0.03**
236	Simcoe	44.47	-79.42	35	Canada	N. Am.	0.020	0.576	-0.058	**0.03**
191	Bras d'or	45.95	-60.83	233	Canada	N. Am.	0.003	0.343	-0.0583	**0.03**
310	Balaton	46.88	17.83	126	Hungary	Europe	0.008	0.398	-0.0557	**0.03**
358	Razelm	44.83	28.97	1	Romania	Europe	0.003	0.304	-0.0552	**0.03**
163	Malaren	59.44	16.19	18	Sweden	Europe	0.044	0.671	-0.0533	**0.03**
250	Manychgudilo	46.26	42.98	15	Russia	Europe	0.003	0.23	-0.0472	**0.03**
198	Nipissing	46.24	-79.92	212	Canada	N. Am.	0.043	0.538	-0.0481	**0.03**
45	Khanka	44.94	132.42	64	Russia; China	Asia	0.016	0.348	-0.0466	**0.03**
75	Hulun	48.97	117.38	539	China	Asia	0.028	0.268	-0.0371	**0.02**

Table 35 Statistically significant modelled JAS LSWT 33 year trends (from 1979-2011) and lake geographical details for 19 seasonally ice covered lakes with $inter_{jas} \geq 0.7$

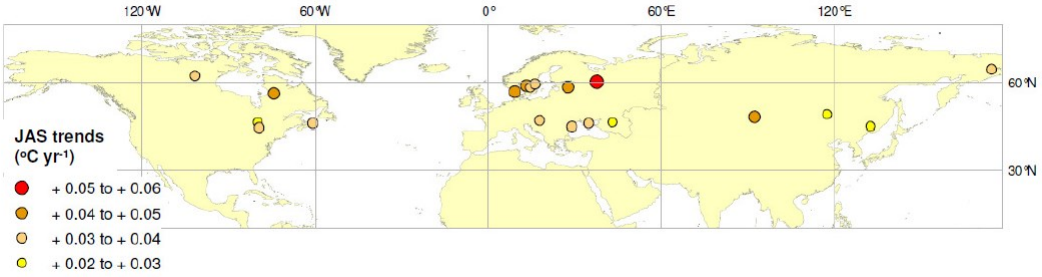

Figure 62 Statistically significant modelled JAS LSWT 33 year trends (from 1979-2011) for seasonally ice covered lakes for the 19 lakes with $inter_{jas} \geq 0.7$

6.5.1.1 Meteorological drivers of JAS LSWT trends

As explained in section 6.5.1, the factors that drive the observed inter-annual LSWT variability are captured in the model where the fraction of $inter_{jas}$ is high. This provides a good basis for assessing the meteorological drivers of the 33 year LSWT trends of 19 lakes with $inter_{jas}$ fractions ≥ 0.70. The winter and summer ERA T2 and CRU air temperature trends and the corresponding 33 year summer modelled LSWT trends are shown in Table 33. This table compares temperature trends only, the ERA SSRD trends are not shown. The winter ERA SSRD trend, explains 0.19 (R^2_{adj}, $p = 0.042$; statistically marginal) of the inter-lake variation of the modelled JAS LSWT trends for the 18 lakes (omitting Lake Har-us, 1191 m a.s.l.). Increasing winter ERA SSRD trends result in warming JAS LSWT trends. There is no statistically significant relationship between the summer ERA (SSRD and T2) trends and JAS LSWT trends. This may be due to the wide range of ice-off dates for these lakes. The observed climatological lake-mean 1 °C warming day (indicative of ice-off) for these 18 lakes range from beginning of March to mid-June (chapter 2, section 2.7.1). As a result, the inter-lake variation in the length of the warming period may mask the variation in the response of the JAS LSWT trends to the summer ERA trends. For higher latitude lakes (9 lakes ranging from 56° N- 65° N), the time span of the observed climatological lake-mean 1 °C warming day is narrower (mid-April to mid-June). The winter and summer ERA T2 and

CRU air temperature trends and the corresponding 33 year summer modelled LSWT trends are compared in Table 33 (first row). For these 9 lakes, the summer ERA SSRD trends explain 0.44 (p = 0.031) and the ERA T2 trends explain 0.35 (with borderline statistical significance, p = 0.050) of the inter-lake variation in the JAS LSWT trends. For the lower latitude lakes (9 lakes ranging from 44° N -49° N), there is no statistically significant relationship with the ERA model forcing trends. This is presumed to be due to the narrow range of latitudes and therefore little change in the maximum shortwave solar downward radiation and air temperature.

The modelled summer trends, summer and winter ERA T2 and CRU air temperature trends for the 18 lakes over the 33 year period are shown in Table 36. Trends are also shown by latitude bands, 56° N-65° N and 44° N-49° N. At both high and low latitudes, the summer ERA trends are warming at a similar rate, while lakes from 56° N- 65° N, show considerably greater winter ERA T2 warming trends (0.04 $\pm$ 0.03 °C yr^{-1}) than for lakes from 44° N- 49° N (0.01 $\pm$ 0.03 °C yr^{-1}). Having shown that there is a relationship between the winter ERA SSRD and the JAS LSWTs (0.19, p = 0.042), it is possible that the stronger winter air temperature warming at higher latitudes may be contributing to the stronger JAS LSWT warming trends at higher latitudes (0.04 $\pm$ 0.01 °C yr^{-1}) than at lower latitudes (0.03 $\pm$ 0.00 °C yr^{-1}). Although, there is no statistically significant relationship between the JAS LSWT and the 4 °C warming days trends for these 18 lakes, in North America the earlier 4 °C warming day trends cause warming JAS LSWT trends. For all lakes in North America, both the modelled and observed the 4 °C warming day trends show a relationship with the JAS LSWT trends, 0.37 (p = 0.001) for the modelled trends over the 33 year period and 0.45 (p = 0.000) for the observed trends over the 16-20 year period. This also demonstrates that the modelled relationship between the 4 °C warming day and the JAS LSWT trends is representative, as it reflects observations. It is possible that this relationship is only evident in North America, as there is a greater concentration of lakes and the limnic ratio is higher than for Asia and Europe. As shown in Table 36, the winter ERA T2

trends for all 18 lakes, show less warming than the winter CRU air temperature trends. Given the relationship between the 4 °C warming day trends and the JAS LSWT trends, this may indicate that the modelled JAS LSWT warming is underestimated.

In this section, using lakes with statistically significant modelled 33 trends with $inter_{jas}$ fractions ≥ 0.70, I demonstrated that both the timing of ice-melt and the summer ERA SSRD are the meteorological drivers of JAS LSWTs.

Trends ºC yr^{-1}	Modelled JAS LSWT	summer ERA T2	summer CRU air temp	winter ERA T2	winter CRU air temp
High latitude (9 lakes, 56° N -65° N)	0.04 ± 0.01	0.05 ± 0.01	0.05 ± 0.01	0.04 ± 0.03	0.05 ± 0.04
Low latitude lakes (9 lakes, 44° N -49° N)	0.03 ± 0.00	0.05 ± 0.02	0.05 ± 0.02	0.01 ± 0.03	0.03 ± 0.01
All 18 lakes (44° N -65° N)	0.04 ± 0.00	0.05 ± 0.01	0.05 ± 0.01	0.03 ± 0.03	0.04 ± 0.02

Table 36 Modelled JAS LSWT, winter and summer ERA and CRU air temperature 33 year trends for the 18 lakes with statistically significant JAS LSWT trends, showing the uncertainty of the trends (95% confidence level). The winter ERA trends show less warming than the winter CRU trends, indicating that the warming JAS LSWT trends may be underestimated in the model

6.5.2 Trends in the month of maximum LSWTs for non–seasonally ice covered lakes

Assessing trends in the month where the LSWT is at the maximum in the annual cycle, is the most appropriate means for detecting changes in warmest part of the LSWT cycle of all non-seasonally ice covered lakes. I refer to the month where the LSWT is at the maximum, as the 'maximum month LSWT'. Non-seasonally ice covered lakes span a wide range of latitudes (55° S to 48° N) from tropical lakes with an annual LSWT range as low as 2-3 °C to temperate lakes with strong seasonal cycle. Use of summer LSWTs (JAS or DJF) is not entirely suitable for

assessing the changes in the maximum month LSWTs for tropical lakes. Many tropical lakes do not have a defined seasonal cycle and have a twice year maximum LSWT in March and September, as shown in chapter 2, section 2.5.2. For lakes where the fraction of the observed maximum month LSWT inter-annual variability explained by the model ($inter_{max}$) $\geq$ 0.70 (R^2_{adj}), I evaluate the long term statistically significant modelled trends. The observed and modelled trends across all non-seasonally ice covered lakes are correlated (0.38, p = 0.000) as shown in Figure 63. There are 14 lakes with an $inter_{max} \geq 0.70$ (average $inter_{max}$= 0.81). The correlation between the observed and modelled trends for these 14 lakes is 0.60, as shown in the insert in Figure 63. Ten (10) of these 14 lakes have statistically significant trends over the 33 years.

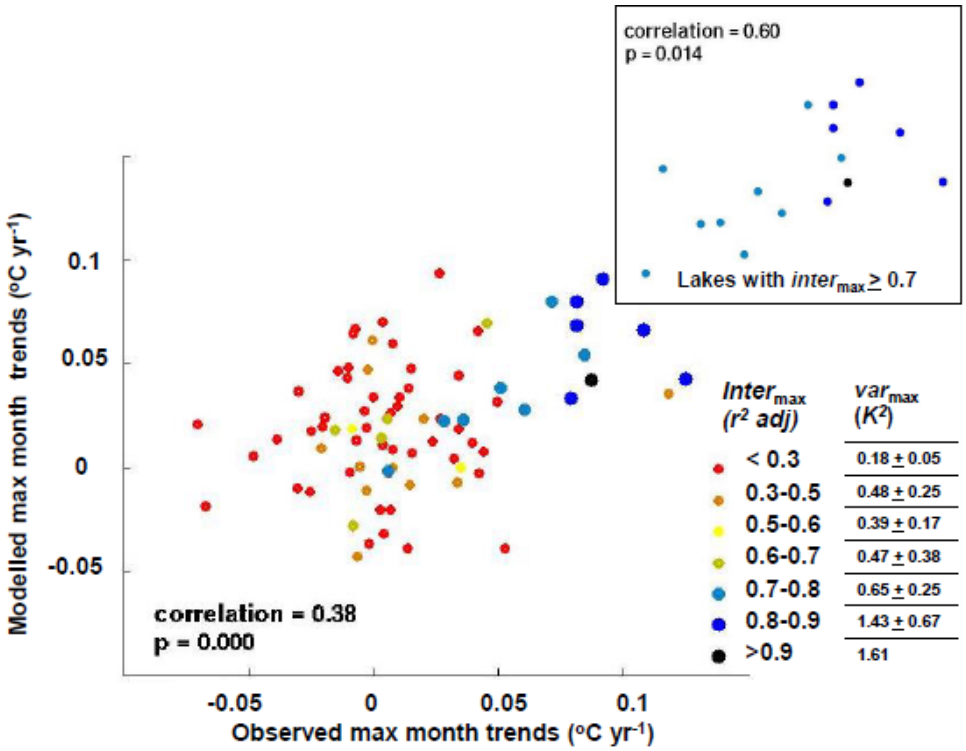

Figure 63 The modelled versus the observed maximum month LSWT trends for 80 seasonally ice covered lakes over the 16-20 year period, showing a correlation of 0.38, with the insert showing the correlation (0.60) for the 14 lakes with $inter_{max}$ fractions $\geq$ 0.70. The legend shows that lakes with a higher var_{jas} value have a proportionally higher $inter_{jas}$ fraction (correlation = 0.69)

The 33 year trends and lake geographical details of the 10 lakes with $inter_{max}$ fractions $\geq$ 0.70 are detailed in Table 37 and illustrated in Figure 64. The average maximum month LSWT warming rate of these lakes is 0.04 $\pm$ 0.02 $^{\circ}$C yr^{-1}. All 10 lakes are located in the northern temperate region from 28° N to 45° N.

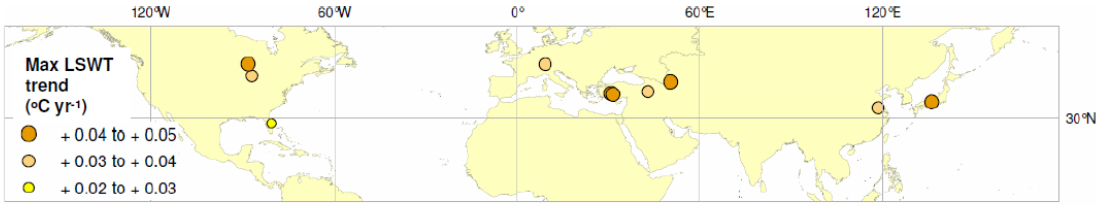

Figure 64 Statistically significant modelled maximum month LSWT 33 year trends (from 1979-2011) for the 10 non-seasonally ice covered lakes with $inter_{jas} \geq$ 0.7.

ARC ID	Lake	Lat	Lon	Country	Continent	P - value	MSD	Constant	trends °C yr^{-1}
268	Biwa	35.25	136.08	Japan	Asia	0.001	0.560	-0.0816	**0.05**
1	Caspian	41.85	50.36	Several; Asia, Europe	Asia; Europe	0.001	0.475	-0.0801	**0.05**
2	Superior	47.72	-88.23	Canada; US	N. Am.	0.016	0.902	-0.0756	**0.04**
267	Beysehir	37.78	31.52	Turkey	Asia	0.006	0.669	-0.0755	**0.04**
390	Egridir	38.07	30.85	Turkey	Asia	0.002	0.454	-0.0725	**0.04**
51	Van	38.66	42.98	Turkey	Asia	0.006	0.550	-0.0678	**0.04**
6	Michigan	43.86	-87.09	US	N. Am.	0.023	0.800	-0.0666	**0.04**
352	Constance	47.65	9.28	Germany; Austria Switzerland;	Europe	0.036	0.758	-0.0592	**0.04**
109	Hungtze	33.34	118.53	China	Asia	0.025	0.576	-0.0554	**0.03**
293	Indian river	28.24	-80.64	US	N. Am.	0.003	0.148	-0.0392	**0.02**

Table 37 Statistically significant maximum month LSWT 33 year trends (from 1979-2011) and lake geographical details for non-seasonally ice covered lakes with $inter_{max} \geq$ 0.7

6.5.2.1 Driver of Maximum month trends

The model explains proportionally more of the observed maximum LSWT variation for lakes where the observed variance is greater, as shown in the legend of Figure 63. For lakes with greater inter-annual observed variability in the maximum LSWT (var_{max}) a greater proportion of the variability is detected in the model than for lakes with a lower $var_{max.}$ This provides a good basis for assessing the meteorological drivers of trends for the 10 lakes with high $inter_{jas}$ fractions (> 0.70).

Trends ºC yr^{-1} for 10 lakes (28° -45° N)	Modelled Max trend	Max ERA T2	Max CRU air temp	summer ERA T2	Summer CRU air temp
	0.04 ± 0.01	0.05 ± 0.02	0.04 ± 0.02	0.05 ± 0.01	0.04 ± 0.02

Table 38 Modelled maximum month LSWT, maximum month and summer ERA and CRU air temperature 33 year trends for the 10 lakes with statistically significant maximum month LSWT 33 year trends, showing the uncertainty of the trends (95% confidence level).

Almost half of the inter-lake variation in the maximum month LSWT trends of the 10 lakes is explained by the variation in the maximum month ERA T2 (0.46, p = 0.020). The summer ERA SSRD trends explain 0.41 (p = 0.030) of the variation. The CRU air temperatures show a slightly lower rate of warming than the ERA T2 trends, which could indicate that the *FLake* may be slightly overestimating the warming trend.

6.5.3 Trends in the month of minimum LSWTs for non–seasonally ice covered lakes

For non-seasonally ice covered lakes, I refer to the month where the LSWT is the lowest in the annual cycle, as the 'minimum month LSWT'. For seasonally ice covered lakes, the presence of ice cover limits the lowest lake-mean winter LSWT to 0 °C. Therefore, evaluating the winter LSWT trends for these lakes is not

meaningful. For non-seasonally ice covered lakes, only 5 lakes have a fraction of observed minimum month variance explained by the model ($inter_{min}$) $\geq$ 0.70. Although, across all non-seasonally ice covered lakes, the observed and modelled minimum month LSWT trends show a correlation of 0.43 ($p < 0.001$), Figure 65, the trends for the 5 lakes (with $inter_{min} \geq 0.70$) do not compare well. For this reason, I do not present any long term minimum month LSWT modelled trends.

I compare the observed and modelled minimum month LSWT trends over the 16-20 year period for northern region (20° N-47° N), equatorial (20° N-20° S) and southern region (20° S-55° S), Table 39. To assess where there may be good agreement in minimum month LSWT trends, I also compare the corresponding ERA T2 and CRU air temperature trends, to find a possible cause for how well the observed and modelled trends compare in these 3 regions. In the southern region the modelled and observed trends show the best comparison, showing a weak warming trend. Comparable trends may be attributed to closely comparable ERA T2 and CRU air temperature minimum month trends. In this region, the ERA T2 trends explain 0.50 ($p = 0.006$) of the variation in the minimum month LSWT trends. In both the northern and equatorial regions, the modelled LSWT trends are warmer than the observed LSWT trends. The corresponding ERA T2 trends are also warmer than the CRU air temperature trends, giving a plausible explanation for the warmer modelled trends. In the southern region, where the modelled and observed trends show best agreement, the average $inter_{min}$ fraction is also higher (0.49) compared to 0.33 in the northern region and 0.24 in the equatorial region. This shows that the factors that drive the inter-annual variation in the minimum month LSWT are better represented in the southern region. In the northern region, the minimum month ERA T2 trends explain 0.27 ($p = 0.001$) of the variation in the corresponding modelled LSWT trends.

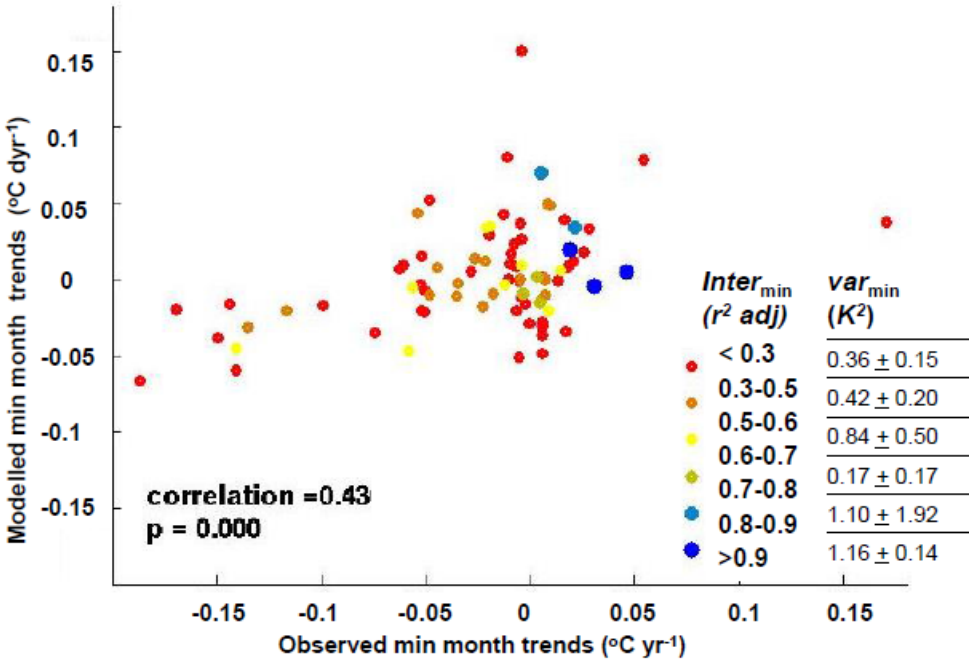

Figure 65 The modelled versus the observed minimum month LSWT trends for 80 seasonally ice covered lakes over the 16-20 year period, showing a correlation of 0.43. The legend shows that lakes with a higher var_{min} value have a proportionally higher $inter_{min}$ fraction (correlation = 0.38)

	16-20 year trends °C yr^{-1}			
Region	Observed Min month	Modelled Min month	Min month CRU air temp	Min month ERA T2
Northern region 20°- 47° N 31 lakes	-0.06± 0.02	-0.01± 0.01	-0.02± 0.02	0.00± 0.02
Equatorial region 20° N- 20° S 37 lakes	-0.01± 0.02	0.01± 0.01	0.01± 0.01	0.02± 0.02
Southern region 20°- 55° S 12 lakes	0.00± 0.02	0.01± 0.01	0.04± 0.03	0.04 ± 0.03

Table 39 Minimum month trends (observed, modelled, CRU air temp and ERA T2) of all non-seasonally ice covered lakes per region (northern, equatorial and southern), over the 16-20 year period, showing a good comparison between CRU and ERA trends in the southern region

6.6 JAS and maximum month LSWT changes, 1979-2011

The lake specific trends from January 1979 to December 2011 are shown in Figure 66. The 19 seasonally ice covered lakes with JAS LSWT changes over this 33 year period are marked with circles and the 10 non-seasonally ice covered lakes with maximum month trends with triangles. The magnitude of the change is indicated by colour. These lakes cover an expansive area of the northern hemisphere; at latitudes from 28° N - 65° N and longitudes from 122° W to 174 ° E. Two thirds of the lakes shown in Figure 66, have warmed by >1.20 °C from 1979 to 2011.

The correlations between observed variance and the fraction of observed variance detected in the model indicates that the modelled LSWTs are less representative where the observed variability is low. In chapters 4 and 5, I established that the observed variability is lower for high altitude seasonally ice covered lakes (which have a lower annual range than low altitude lakes) and where the annual range of non-seasonally ice covered lakes is lower. This shows that low latitude (tropical) or high altitude lakes are less well represented in *FLake*. This also explains why the lake specific trends (which reflect a high fraction of the true inter-annual variability in the model) are at relatively low altitudes or in high latitude northern regions and not in the southern hemisphere. The average annual LSWT range of the 10 non-seasonally ice covered lakes (28° N-48° N) is much higher, 18.8 °C, compared to the annual range of LSWTs of southern hemispheric lakes at corresponding latitudes, 10.1 °C.

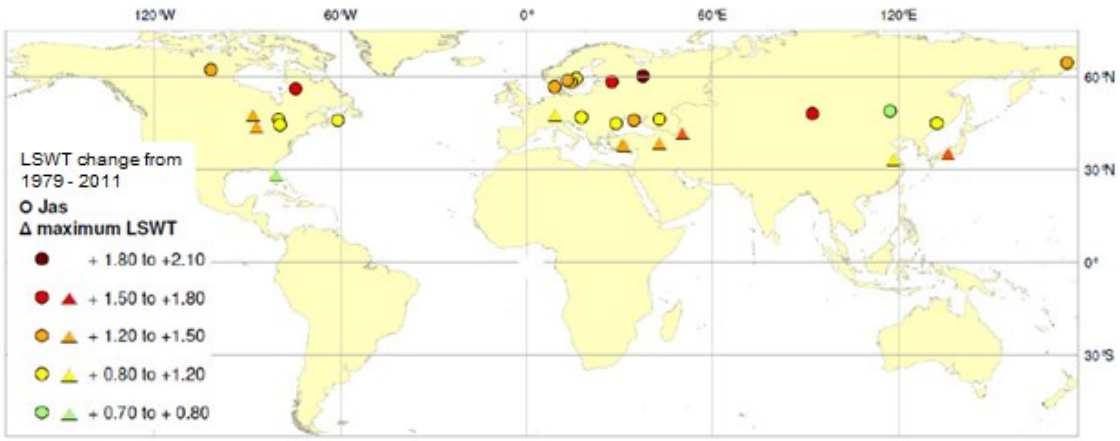

Figure 66 Statistically significant modelled JAS and maximum month LSWT changes from 1979 to 2011. JAS LSWT changes are marked with a circle and maximum month LSWT with a triangle.

6.7 Conclusions

In this chapter, I demonstrate that the modelled summer trends are more comparable with the observed trends from ARC-Lake than from IWBP, both individually (tuned and untuned model) and regionally. I demonstrate that the process of tuning using the ARC-Lake LSWTs is not the cause of the stronger correlation between *FLake* and ARC-Lake LSWT trends. Over the common period, while, the ARC-Lake and modelled trends are statistically indistinguishable in all regions, the IWBP and modelled trends show statistically different trends in Africa and North America and show stronger regional warming in most regions. The IWBP nighttime summer regional trends also show stronger warming than the corresponding ARC-Lake trends, particularly in Europe.

Regionally, the summer modelled LSWTs from1979-2011 shows greatest warming in Europe (1.35 ºC) and least in Africa and Oceania (0.30 ºC), with North American and Asian lakes showing moderate warming of 0.70 ºC and 0.56 ºC, respectively. This warming is supported by statistically indistinguishable observed (ARC-Lake) and modelled regional trends (Europe, Asia, Africa and Oceania) and/or by highly

comparable ERA T2 and CRU summer and winter trends over the 33 year period (North America). The 33 year JAS LSWT warming of the seasonally ice covered lakes occurred faster at higher latitudes than mid latitudes, with latitude explaining 0.35 (p = 0.005) of the inter-lake variation in the warming. The JAS LSWTs from 56° N -65° N (9 lakes) have warmed by 0.04 $\pm$ 0.02 °C yr^{-1} and from 44° N -49° N (10 lakes) by 0.03 $\pm$ 0.02 °C yr^{-1}. For these 18 lakes, (with exception to Lake Har-us), it can be inferred that the winter ERA SSRD trends cause JAS LSWT warming, R^2_{adj} = 0.19 (p = 0.041), by means of an earlier ice-melt. This is supported by the relationship (observed and modelled) between the JAS LSWT and 4 °C warming day trends (0.37 and 0.45) for all lakes in North America, also demonstrating that the factors affecting the JAS LSWT changes are represented in the model. For the higher latitude lakes (56° N -65° N), the summer ERA SSRD trend is the dominant driver of the inter-lake variation in the JAS LSWT trends 0.44 (p = 0.031). The stronger average winter ERA T2 warming trends for the 9 higher latitude lakes (approximately 4 times stronger than the 10 low altitude lakes), are possibly the cause of the stronger modelled JAS LSWT warming at higher latitudes. Furthermore, as the winter ERA T2 trends show less warming than the corresponding winter CRU air temperature trends, the model may be underestimating JAS LSWT warming.

The modelled changes in the JAS LSWTs of the 19 seasonally ice covered lakes and the maximum month LSWTs of the 10 non-seasonally ice covered lakes, are well supported by observations over the16-20 year period, giving a high degree of confidence to the presented results. These 29 lakes cover an expansive area of the northern hemisphere; at latitudes from 28° N - 65° N and longitudes from 122° W to 174 ° E. Two thirds of the lakes in Figure 66 show warming of greater than 1.20 °C from 1979 to 2011. The greatest warming has occurred in northern Europe.

In chapters 4 and 5, the observed inter-annual LSWT (JAS, maximum and minimum) variance was shown to be lower for lakes where the annual LSWT range

is lower. Having shown that there is a relationship between this observed variance and the fraction of observed variance detected in the model, I conclude that the *FLake* is more representative in regions where the annual range is larger, as is evident from the lake locations, Figure 66.

Chapter 7 Discussion, conclusions and further work

In this final chapter, I draw together the findings from the study (section 7.1), demonstrating how the aims of the study were met (section 7.2), discuss the limitations of the study (section 7.3) and outline further work arising from the findings (section 7.4).

7.1 Discussion

In this section, I discuss the practical findings of my research, for example, I discuss how ARC-Lake observations inform us about LSWT behaviour and how the tuning process adds to our understanding of LSWT behaviour. I emphasise the practical benefits of using a tuned model. I discuss the outcome of the modelled LSWT trends and how they are affected by meteorological forcing and lake depth.

7.1.1 Global climatology of LSWTS of large lakes

In chapter 2, I demonstrated the suitability of applying ARC-Lake observations in global scale studies, both adding to and supporting the current understanding of the LSWT climatological behaviour.

7.1.1.1 Net surface solar irradiance

I demonstrated how net surface solar irradiance (netSSI) can be used to estimate several features of the LSWT cycle of lakes globally. The minimum month netSSI (which factors in the reduction of shortwave radiation to the earths' surface due to cloud cover in addition to seasonal Earth-Sun geometry) strongly predicts the minimum month LSWTs and is a stronger predictor of various features in the LSWT annual cycle than latitude. The minimum month netSSI can be used to estimate if a lake surface has a seasonally ice covered period; at the minimum

month netSSI value of $\leq$ 60 W/m^2, the minimum monthly LSWT is approximately 0 $^{\circ}$C. It can also be used to estimate the length of the cold phase. In North America, the minimum month netSSI explains more of the inter-lake variation in the length of the cold phase (0.73) than latitude (0.67). Where the minimum month netSSI exceeds 60 W/m^2, it explains $\geq$ 0.88 (R^2_{adj}) of the inter-lake variation of minimum month LSWTs for non-seasonally ice covered lakes in both hemispheres. Additionally, netSSI is strongly reflected in tropical lakes where there is a lack of seasonality. The LSWT annual cycle shows a good relationship with time lag to the netSSI annual cycle and reflects the twice annual peak of netSSI. The climatological range in the annual monthly LSWTs is at a minimum at 2°S, reflecting the latitude of the minimum netSSI climatological range.

7.1.1.2 Air temperature

LSWTs were shown to closely track air temperature. Across 10° zones containing lakes without a seasonal ice cover period (40°S to 30°N), the zonal LSWT climatological extremes exceed air temperature climatological extremes. The maximum month LSWTs track maximum month air temperatures more closely at higher altitudes. The LSWT-air temperature difference in the tropics showed a decrease of 1.9 $^{\circ}$C from 500 to 1800 m.a.s.l., similar to the rate of decrease found in a study of summer LSWT-air temperature differences in small temperate lakes in the Swiss plateau (Livingstone and Lotter, 1998).

Air temperature is globally a better estimator of the LSWT phase transition days (1 $^{\circ}$C and 4 $^{\circ}$C cooling and warming days) than latitude, for seasonally ice covered lakes. Globally, the air temperature transition days (through 0 $^{\circ}$C) explain 0.69 to 0.80 of the inter-lake variation in the LSWT phase transition days, while latitude explains only 0.42 to 0.54 of the variation.

Globally and regionally (with the exception to Europe), air temperature shows a stronger relationship with LSWT warming (1 $^{\circ}$C and 4 $^{\circ}$C warming days and the

warming intervening phase) than with LSWT cooling (1 °C and 4 °C cooling days and the cooling intervening phase). This supports findings from Williams et al (2004), which showed that air temperature explained more of the inter-lake variation in ice-off than in ice-on, chapter 1, section 1.5.

As the LSWT phase transition days are lake-mean values, at a lake-mean LSWT of 1 °C parts of a large lake are ice free and responding to ambient air temperatures while other parts of lake will be ice covered. The extent of lake ice cover at a lake-mean of 1 °C varies from lake-to-lake, confounding the inter-lake relationship between the 1 °C days and air temperature. The presence of ice and the inter-lake variability in the extent of ice is the possible reason why the air temperature transition days in North American and Asian lakes explain more of the variation in the 4 °C cooling and warming days than in the 1 °C cooling and warming days.

Globally and regionally (Asia and North America), the 0 °C air temperature transition days have approximately a 1:1 relationship with the 4 °C phase transition days. The equations outlined in chapter 2, Table 3 -6 are suitable for the prediction of the LSWT transition days and phases of large non-saline lakes < 700 m a.s.l. in North America, Europe and Asia, lying within 42 °N to 69° N, with depths from <1 to 680 m and within surface areas of 100 to 32,000 km^2.

7.1.1.3 Lake depth

In Europe, where air temperature is a poor predictor of the inter-lake variation in the LSWT phase transition days (0.30-0.32), lake depth explains 0.24-0.25 of the variation in the 1 °C and 4 °C cooling days, re-enforcing the findings, that depth is a good indicator of the heat storage capacity. Globally and regionally, deeper lakes consistently caused later cooling and later warming days, generally showing a stronger relationship with cooling. Additionally, depth explains more of the variation in the intervening cooling phase (from 4 °C to 1 °C), than in the intervening warming phase.

7.1.2 What can ARC-Lake observations tell us about LSWT behaviour?

7.1.2.1 Lake centre versus lake-mean LSWTs

The lake centre summer LSWT trends and absolute values are representative of the lake-mean summer LSWT trends and absolute values, for the majority of the observed lakes (93%). With the exception to a few very small or sinuous lakes (13 lakes), the lake centre trends are representative of the lake mean trends. Sixty nine per-cent (69%) of all lakes have lake centre trends within $\pm$ 0.01 $^{\circ}C\ yr^{-1}$ of the lake-mean trends.

The absolute summer LSWT values are representative of the lake-mean values (for all lakes with the exception to 4 very large lakes; Caspian Sea, Lake Michigan, Lake Superior and Lake Huron), yielding daily MADs below 0.6 $^{\circ}C$ and an average MAD of 0.18 $^{\circ}C$ across all lakes. The daily MADs for the 4 very large lakes range from 0.8 to 1.3 $^{\circ}C$. The lake centre and lake-mean daily MAD increases with surface area (correlation = 0.51), as shown in chapter 2, Figure 18. This demonstrates that with the few exceptions, the LSWT absolute values and trends determined from lake centre buoys, can be considered representative of entire lake. This representation can be extended to *FLake*, as the modelled trends showed a similar correlation to the observed lake centre (0.53) and lake-mean (0.54) trends.

7.1.2.2 Minimum month LSWTs; A proxy for lake bottom temperatures

Changes in the minimum month LSWTs have the potential to be used as a proxy for determining changes to lake bottom (hypolimnion) temperatures for stratified non-seasonally ice covered lakes. The minimum monthly climatological ARC-Lake LSWTs explain 0.97 (R^2_{adj}) of the variation in the temperatures of the stratified bottom layer, obtained from *Flake* lake model (based on a perpetual hydrological year, 2005/2006) and have a 1:1 relationship, as shown in chapter 5, Figure 47.

Although, changes in other factors affect hypolimnion temperature, such as influx of cooler water, the minimum month observed LSWTs offer a good indication of the hypolimnion temperature in cases where this temperature can't be or isn't observed directly.

This relationship is applicable to deep non-seasonally ice covered lakes during the stratification period only. At the minimum LSWT for these lakes, the water is at its densest in the annual cycle. Surface water, when at the minimum temperature will therefore sink to the lake bottom. For deep lakes, stratification buffers the hypolimnion from heat flux and mixing of the upper water layer, explaining why the lake hypolimnion temperature of deep non-seasonally ice covered lakes can reflect the minimum LSWT during the stratification period.

Having demonstrated that the observed minimum month LSWT is reflected in the lake bottom (*FLake*) temperature, further work could be carried out using the same lakes, to confirm if the same relationship is found between the observed minimum month LSWT and *in situ* bottom temperature (where available). This would validate the use of the minimum month LSWTs as a proxy for lake bottom temperature (and it would also serve to validate the *FLake* model bottom temperature, as discussed in the next section; section 7.1.3). Furthermore, a study could be carried out on several deep non-seasonally ice covered lakes to assess how sensitive the modelled minimum LSWT (or, *in situ*, if available) are to more subtle changes in minimum month LSWT. A suggestion for this work is outlined in section 7.4.4.

7.1.2.3 LSWT annual range and observed inter-annual variability

Non-seasonally ice covered lakes with a larger LSWT annual range have more observed inter-annual variability in their LSWT extremes, highlighting that the extreme LSWTs for these lakes may be more responsive to rapid fluctuations in extreme air temperature than lakes with a low annual range. This conclusion is

drawn on the basis of a correlation between the observed minimum and maximum variability and the annual range of LSWTs of 0.36 and 0.38 (R^2_{adj}) for non-seasonally ice covered lakes. There is no such correlation between the annual LSWT range and the observed variability in the JAS LSWT for seasonally ice covered lakes, possibly because the inter-lake variation in the annual range of monthly LSWTs is almost 3 times greater (62 K^2) in non-seasonally ice covered lakes than in seasonally ice covered lakes (22 K^2). However, the observed JAS LSWT inter-annual variability for seasonally ice covered lakes in Asia, decreases with increasing altitude (-12 to 5000 m a.s.l.), $R^2_{adj} = 0.26$. The low variability in high altitude lakes may be due to the lower annual LSWT range of higher altitude lakes. This highlights that the JAS LSWT of seasonally ice covered lakes with a large annual range may also be more responsive to rapid fluctuations and changes in summer air temperature than lakes with a low annual range.

Lakes with greater inter-annual variability in the maximum month / JAS LSWT are more susceptible to ecological damage, for the reasons outlined in chapter 1, section 1.1. Increases in the summer LSWTs, a time when the winds are generally low and the LSWTs are relatively high, can result in rapid decrease in dissolved oxygen, leading in fish kills and fish migration, reducing the fish stocks.

7.1.2.4 Nighttime versus day-night LSWT trends

The diurnal LSWT range in lakes is generally modest, though subtle changes have occurred in the diurnal range in most regions. From 1992-2011, the ARC-Lake LSWT nighttime trends have warmed more rapidly than day-night trends in Africa, Asia and North America and less rapidly in Europe, chapter 2, Figure 23. Individually, 75% of these lakes show more rapid nighttime trends over the same period. There is much evidence to suggest that while nighttime air temperatures have warmed since the 1900's, recent decades show comparable minimum and

maximum air temperature changes (section 2.8.2.1). This suggests that the LSWT diurnal extreme trends may not be reflecting air temperature diurnal extreme trends.

Changes in the LSWT diurnal range over time have important ecological and climate feedback implications. A very useful and informative application of the ARC-Lake observations is to investigate if the inter-lake variability diurnal extreme LSWTs reflect the variation in the diurnal extreme air temperatures at the lake locations and if other factors (climatic or lake characteristics) may explain the inter-lake variability. Further work on this area is suggested in section 7.4.1.

There is relatively good agreement between the observed nighttime individual summer trends from IWBP and ARC-Lake from 1992 - 2011 (correlation = 0.62). Though, regionally, the IWBP trends show stronger warming in all regions than ARC-Lake and are statistically different in Europe, where the IWBP trends show twice the warming of the ARC-Lake trends.

7.1.2.5 Trending period

There is enough evidence to suggest that evaluating observed LSWTs over a minimum of 20 years may be long enough to filter out much of the inter-annual variability, yielding reasonably meaningful trends. Ideally, changes in temperatures are assessed over a typical climate period (30 years). This length of time however is not currently available for observed LSWTs. A comparison of the modelled and observed (ARC-Lake) trends with 20 years of observations, show the average regional trends to be statistically indistinguishable, chapter 6, Figure 53. Extended to include lakes with 16 years of LSWTs, the same comparison shows statistically different trends in 2 of the 5 regions. Similarly, the ARC-Lake and IWBP observed trends over the 20 year period (71 lakes) are statistically indistinguishable in all regions except in Europe, where the trend is marginally statistically distinguishable (paired t-test $p = 0.049$). The same comparison, extended to include trends over the

16 year period (a total of 84 lakes), yielded statistically different trends in Europe, North America and Africa. The better comparison in LSWTs trends over the 20 year period, indicates that 20 years may be long enough to filter out much of the inter-annual variability, establishing reasonably meaningful LSWT trends.

7.1.3 Can the tuning process add to our understanding of LSWT behaviour?

The tuning of 244 seasonally and non-seasonally ice covered lakes greatly reduced the biases in several features of the LSWT annual cycle, as shown in Table 40. The post-tuning metrics for all lakes are highly representative of the post-tuning metrics for the trial lakes, demonstrating that the trial lakes are well representative of all lakes in the ARC-Lake database. Many important aspects of LSWT behaviour were demonstrated throughout the tuning process in chapter 4 and chapter 5.

Seasonally ice covered lakes				Non-seasonally ice covered lakes			
Primary metrics	Pre-tuning (21 trial lakes)	Post-tuning (21 trial lakes)	Post-tuning (160 lakes)	Primary metrics	Pre-tuning (14 trial lakes)	Post-tuning (14 trial lakes)	Post-tuning (84 lakes)
MAD (°C)	3.07 ±2.25	0.84 ± 0.51	0.80 ± 0.56	MAD (°C)	3.55 +3.20	0.96 ±0.63	0.96 ± 0.66
Mean JAS LSWT bias (°C)	3.71 ±3.51	-0.12 ± 1.09	-0.06 ± 1.15	mth_{max} (°C)	1.92 +5.05	-0.44 ±1.52	-0.21 ± 1.47
1 °C cooling day bias (days)	12.0 ±39.6	-1.6 ± 12.8	-1.08 ± 8.5	mth_{min} (°C)	3.71 +4.33	-0.03 ±1.48	-0.08 ± 1.47
1 °C warming day bias (days)	- 27.1 ±29.7	-0.2 ± 10.7	+0.3± 12.3				

Table 40 Summary of the pre and post-tuning results for the trial seasonally and non-seasonally ice covered lakes and the post-tuning results for all seasonally and non-seasonally ice covered lakes showing the spread of differences across lakes, 2σ

7.1.3.1 The effect of depth on the whole LSWT cycle

The whole LSWT annual cycle of deep high latitude (or very deep) seasonally ice covered lakes is strongly affected by changes in the timing of ice-off, demonstrating that LSWTs of these lakes are more sensitive to climatic changes than shallow lakes. Mean depth and latitude account for 0.50 (R^2_{adj}, p= 0.001) of the modelled JAS LSWT decrease resulting from an later 1 $^{\circ}$C warming day, with depth alone accounting for 0.35 (p= 0.003) of the JAS LSWT decrease. The longer time required for a deep lake to heat becomes more critical at higher latitudes or altitudes, primarily because the lake doesn't heat to its full heat storage capacity during the relatively short warming period. As a result, any change to the length of the warming period will directly affect the JAS LSWT. The modelled decrease in the JAS LSWT in turn shortens the cooling period, causing an earlier 1 $^{\circ}$C cooling day in deep lakes. Depth was shown to explain 0.42 ($R^2_{adj,}$ p= 0.001) of the inter-lake variation in the difference of the 1 $^{\circ}$C cooling day, resulting from the JAS LSWT decrease. A separate study using *in situ* data, carried out on Lake Superior, depth 147 m (Austin and Colman 2007), supports these findings, attributing the JAS LSWT warming trend to the earlier ice-off day trend. The length of the LSWT warming period of deep high latitude lakes may also be the reason for the different LSWT response to changes in air temperature between deep high latitude and deep low latitude lakes. Observations on Lake Superior indicated that LSWT warming was approximately double the air temperature warming, while LSWT changes for tropical Lake Malawi correlated with air temperature warming.

7.1.3.2 The variable effect of wind on the LSWTs

Wind speed is demonstrated to have a consistent effect on the modelled LSWT of seasonally ice covered lakes, with the highest wind speed scaling, *u3* (U_{water} = 1.62 + 1.17 U_{land}), causing earlier cooling and later warming, lengthening the ice cover period. The higher wind speed causes more rapid mixing and heat exchange

between the surface and atmosphere, resulting in an earlier modelled 1 °C cooling day. As wind promotes ice growth, higher wind speeds also causes a later modelled 1 °C warming day, which as demonstrated in section 7.1.3.1, affects the JAS LSWT for deep high latitude lakes. For the 21 trial lakes (without tuning), the higher wind speed scaling, *u3*, in place of the unscaled wind speed, halved the average modelled biases; reducing the average JAS LSWT bias from +3.71 to +1.87 °C and the cold phase bias from -39 days to -21 days. This demonstrates the modelled effect of wind speed on the whole LSWT cycle of seasonally ice covered and highlights the importance of using a representative over-water wind speed scaling. It can inferred that all seasonally ice covered lakes will generally show improved modelled LSWTs with *u3,* as all 21 trial seasonally ice covered lakes showed improved LSWTs with this wind speed scaling.

As higher wind speeds were shown to cause a later modelled 1 °C warming day for the 21 trial lakes, it is possible that the high wind scaling is compensating for the under-estimated default albedo which was shown to cause an earlier 1 °C warming day and over-estimated JAS LSWT biases in the untuned model.

There is no optimal wind speed scaling for all non-seasonally ice covered lakes. This is attributed to the highly variable range of LSWTs and of mixing regimes of non-seasonally ice covered lakes. Seasonally ice covered lakes are predominantly dimictic, while the mixing regimes of non-seasonally ice-covered lakes are highly variable (for example, permanently stratified, warm-monomictic and continuous warm polymictic). The range of mixing regimes most possibly confounds the compensatory effect between depth and wind speed that is evident in seasonally ice covered lakes.

The wider range of mixing regimes and annual cycles of non-seasonally ice covered lakes, also highlights the dynamic nature of these lakes. Unlike seasonally ice covered lakes, there is no physical restriction on the minimum LSWT and thus the

water is directly exposed to air temperature and solar radiation fluctuations all year round. As a result, the ecological state of non-seasonally ice covered lakes may therefore be more susceptible to fluctuations or changes.

The optimal wind speed scaling for non-seasonally ice covered lakes shows some relation to the latitude. For 5 of 7 trial lakes located at latitudes > 35° N/ S the higher wind speed scaling (*u3*) is optimal and for 5 of the 7 trial lakes located at latitudes < 35° N/ S the lowest wind speed (*u1)*is optimal. The remaining 4 lakes, showing better results with *u2* are dispersed across the tropics and higher latitudes, highlighting that the most appropriate wind speed cannot be predicted using latitude alone. The density difference between maximum LSWT and the bottom layer temperature (determined using the minimum LSWT during stratification) is indicative of a buffering effect against wind induced mixing and may be factor in determining an appropriate wind speed scaling for non-seasonally ice covered lakes. The density difference between maximum LSWT and the bottom layer of stratified lakes is larger (1.49 $x10^{-3}$ kg m^3) at high latitudes (> 35° N/ S) than in low latitude lakes (< 35° N/ S), 0.65 $x10^{-3}$ kg m^3. Furthermore, using the density differences to determine an appropriate wind speed scaling considers depth, as depth influences the bottom temperature. Further work could be carried out to investigate if the optimal modelled wind speed scaling for deep non-seasonally ice covered lakes can be better predicted by assessing density differences than latitude alone, section 7.4.2.

7.1.3.3 Validation of lake bottom temperatures modelled in *FLake*

The 1:1 relationship between the observed minimum month LSWTs and the modelled lake bottom temperatures from *FLake* for deep non-seasonally ice covered lakes, show that the minimum LSWT is reflected in the bottom temperatures (during stratification) across a wide range of latitudes. Discussed in section 7.1.2.2, a comparison of the minimum month LSWT with *in situ* bottom temperature (where available) could confirm the relationship between the observed

minimum month LSWTs and the lake bottom temperatures and would also validate the bottom temperature modelled in *FLake*. A suggestion for this work is outlined in section 7.4.4.

This validation can also be extended to the *FLake* model available from Kirillin (2010), as the same lake physics are applied to model versions. The LSWTs from both versions, are based on a two-layer parametric representation of the lake temperature. Although the models do not calculate the depth of the hypolimnion layer, the bottom modelled temperature is representative of the hypolimnion temperature, which remains constant with depth.

7.1.4 Benefits of using a tuning approach

The tuning approach undertaken in this study, overcomes the problem of the lack of available lake characteristic information for individual lakes. This approach resulted in highly representative modelled LSWTs for 244 lakes (including saline and high altitude lakes). The improvement on the untuned results are evident from pre and post-tuning metric results for the trial for both seasonally and non-seasonally ice covered lakes Table 40. The tuned values for depth, albedo and light extinction coefficients for the 244 lakes are a well-founded basis for providing practical guidance on improving the modelled LSWTs using *FLake.*

7.1.4.1 Overcoming the lack of available lake information

Gathering lake characteristic information for 100's of lakes, where the basic lake characteristics are not readily available, is difficult and resource intensive. The tuning approach used in this study, overcomes this obstacle, by allowing values for depth, albedo and light extinction coefficients to be assigned to the 244 individual lakes. Choosing an appropriate light extinction coefficient value was achieved by fitting between a range of up to 10 optical water types which essentially describe

the attenuation process of oceans (Jerlov 1976). This approach caters for the lack of available information on Secchi disk depth data (often used to estimate light extinction coefficient) and lake optical properties.

Of the 244 lakes, 45 have no available mean and maximum depth information, For the tuning of these 45 lakes, the range of depth factors were applied to an initial depth of 5 m, allowing a range of relatively shallow depths to be assessed. Where the results indicated that the depth was too low, the initial depth was increased and lakes were re-tuned. The strong correlation between the mean lake depth and the effective (tuned) depth for all 244 lakes (0.75 for seasonally ice covered lakes and 0.84 for non-seasonally ice covered lakes) indicates that the applied depth factors and the approach taken for lakes with unavailable depth information produced sensible results. For both types of lakes (seasonally and non-seasonally ice covered) the trials also show a compensatory effect between depth and light extinction coefficients. Given the sensible effective depth values for depth, this indicates that the tuned light extinction coefficients are also sensible. This signifies that the 1 $^{\circ}$C cooling day metric exerts good control over the effective depth and the maximum month/ JAS LSWT metrics exerts control over the tuned κ_d values.

As the default albedo in *FLake* caused an earlier 1 $^{\circ}$C warming day and over-estimated JAS LSWTs for all the trial seasonally ice covered lakes, I included 3 other albedo values (all higher than the default) in the LSWT tuning process. Only 19% of the lakes were tuned to the default (lowest) albedo. Sixty four per-cent (64%) of lakes were tuned to the two highest albedos $\alpha 2$ or $\alpha 3$ (snow and white ice = 0.80 and melting snow and blue ice = 0.60 for $\alpha 2$ or 0.40 for $\alpha 3$). The $\alpha 3$ albedo value is comparable to albedo values obtained on a Lake in Minnesota (Henneman and Stefan 1999) and may be a more appropriate default value for *FLake*. The findings also showed that the tuned albedo value exerts good control over 1 $^{\circ}$C warming day metric. The earlier 1 $^{\circ}$C warming day, shorter cold phase and over-estimated open water temperatures obtained using the *FLake* model default albedo

shown in two other *FLake* studies, further supports the need for a higher default value in *FLake.*

7.1.4.2 How can modelling LSWTs in *FLake* be improved?

The sensible tuned values for depth, light extinction coefficients and albedo, shown in the previous section (section 7.1.4.1) provides a well-founded basis for practical guidance on improving the modelled biases that appear to be a feature of *FLake*.

As discussed in chapter 4, section 4.6.3, the tuning of deep lakes to a shallower depth and shallow lakes to a deeper depth is sensible under the *FLake* run conditions. Figure 67 shows the relationship between the lake-mean depth and the effective depth for all 244 successfully tuned lakes, colour coded by the depth factor optimised in the tuning process. The figure legend shows the effective depth factor with the corresponding average lake-mean depth. The relationship between the two is shown in the figure insert, providing a means to estimate an appropriate effective depth for any lake with a mean depth from 4-124 m.

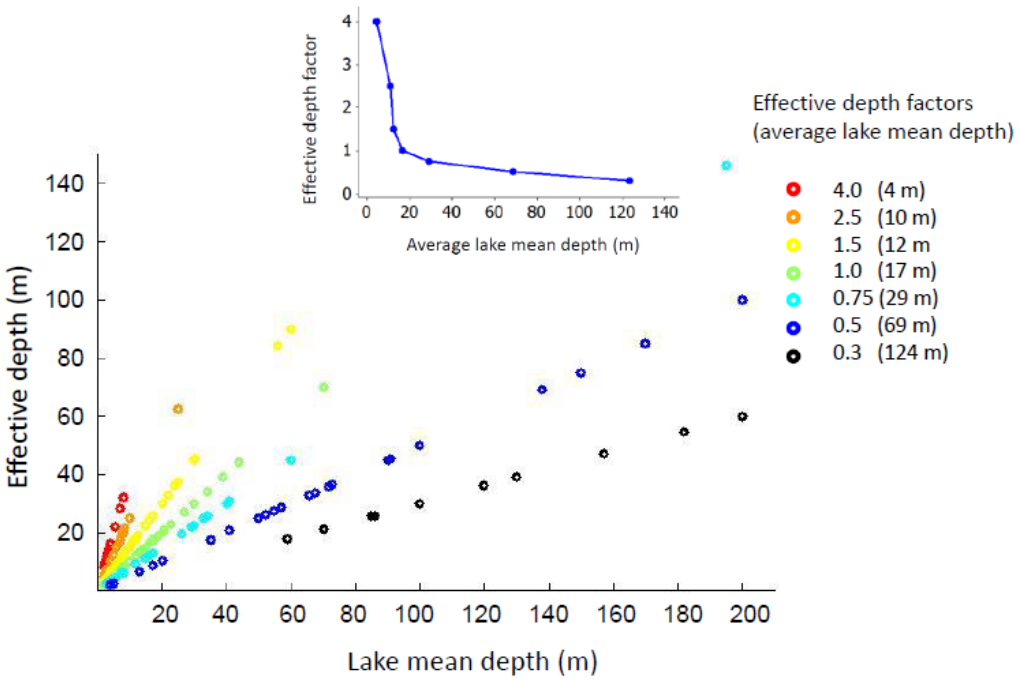

Figure 67 The lake mean depth versus the modelled effective depth for 244 tuned lakes, colour coded by the effective depth factors and the average lake depth for each effective depth factor used in the tuning process (insert), demonstrating that deeper lakes are tuned to a lower effective depth and shallower lakes to a greater effective depth.

Across all lakes, a total of 57% were tuned with light extinction coefficient values κ_{d4} and $\kappa_{d5,}$ showing an average depth of 21 m for κ_{d4} and 13 m for κ_{d5}. Where the values are unknown, applying κ_{d4} for lakes > 16 m in depth and κ_{d5} for lakes < 16 m in depth provides a good estimation of the light extinction coefficient. Tuning of deeper lakes to the more transparent κ_d value (κ_{d4}) and shallower lakes to the less transparent κ_d value (κ_{d5}) makes sense as the water clarity of a shallower lake is more affected by the lake bottom sediments than that of deeper lake. κ_{d4} and κ_{d5} values, applied to the untuned model for all seasonally and non-seasonally ice covered lakes reduced the daily MAD 3.38 $^{\circ}$C $\pm$ 2.74 $^{\circ}$C to 2.28 $\pm$ 2.30 $^{\circ}$C, chapter 6, section 6.3.1, demonstrating the suggested modelled LSWT improvements.

For seasonally ice covered lakes, to obtain a more timely (later) ice-off and to help address the over-estimated JAS LSWTs, the albedo value *α3* is recommended in place default value (*α1*), as discussed in section 7.1.4.1.

As shown throughout the trials, the good estimation of the most appropriate wind speed scaling for all seasonally ice covered lakes and non-seasonally ice covered lakes > 35° N/ S is *u3* and for lakes < 35° N/ S is *u1*. For a better estimation of wind speed scalings for non-seasonally ice covered, further work is suggested, as outlined in section 7.4.2.

7.1.5 Modelled LSWT trends

7.1.5.1 Regional trends

The lower signal (trend) to noise ratio (inter-annual variation) for lakes with a relatively small trend may explain why regional trends (modelled and observed) determined using all lakes show less extreme warming, than when determined using statistically significant trends. Regional modelled long term summer LSWT trends are determined using all lakes within a region, presenting a more realistic representation of regional warming.

The modelled trends over the 33 year period are presented for regions where the modelled and observed (ARC-Lake) trends for all lakes over the 16-20 year period are statistically indistinguishable (Europe, Asia, Africa and Oceania) or where ERA T2 and CRU air temperature summer and winter trends over the 33 year period are closely comparable (North America). The level of agreement in trends between the ERA T2 and the higher resolution CRU air temperature trends indicate how much of the air temperature changes are reflected in the ERA data. Over the 33 year period, the summer LSWT trends show that the most warming has occurred in

Europe, 0.04 $^{\circ}$C yr^{-1}, equivalent to 1.35 $^{\circ}$C and the least in Africa and Oceania, 0.09 $^{\circ}$C yr^{-1}, equivalent to 0.30 $^{\circ}$C, Figure 68 and Table 41. The global average LSWT warming is 0.02 $^{\circ}$C yr^{-1}, equivalent to 0.69 $^{\circ}$C from 1979 to 2011.

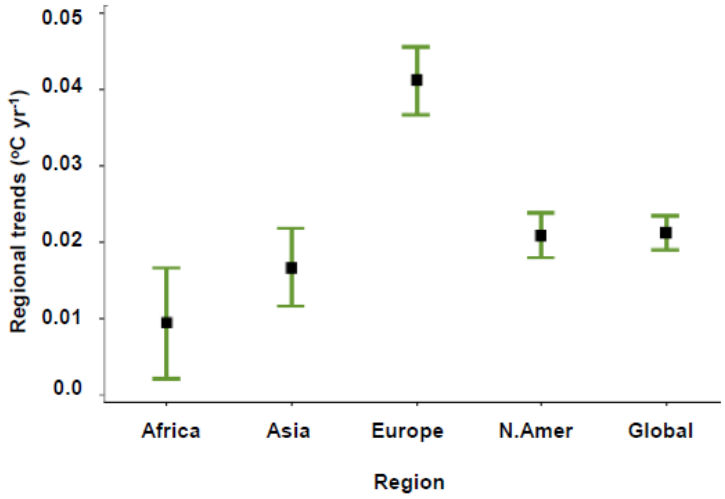

Figure 68 Regional modelled summer LSWT trends from 1979-2011 (33 years) and the uncertainty of the trends (95% confidence level) for regions supported by good short term (16-20 year) modelled and observed trend comparison or good long term (33 year) CRU and ERA T2 air temperature trend comparison. Oceania (2 lakes) is not shown due to a large range of uncertainty (reproduction of figure 57 from chapter 6)

Region	Number of lakes	Summer Trend $^{\circ}$C yr^{-1}	Average warming from 1979 -2011 ($^{\circ}$C)
Africa	21	0.01 $\pm$ 0.01	0.30
Asia	57	0.02 $\pm$ 0.01	0.56
Europe	28	0.04 $\pm$ 0.00	1.35
North America	118	0.02 $\pm$ 0.00	0.70
Oceania	2	0.01 $\pm$ 0.02	0.30

Table 41 Regional modelled summer LSWT trends and warming from 1979-2011 (33 years) for regions supported by good short term(16-20 year) modelled and observed trend comparison or good long term (33 year) CRU and ERA T2 air temperature trend comparison (reproduction of table 32 from chapter 6)

7.1.5.2 Lake specific trends

I present statistically significant modelled trends over the 33 year period, for 19 seasonally ice covered lakes (JAS LSWT) and 10 non-seasonally ice covered lakes (maximum month LSWT), as shown in Figure 69. Trends are presented for lakes where the observed and modelled JAS LSWT/ maximum month LSWT trends over the 16-20 year period compare well and the modelled LSWTs detected a high fraction (≥ 0.70) of observed LSWT inter-annual variability. These lakes cover an expansive area of the northern temperate region; spanning latitudes from 28 $^{\circ}$N - 65° N and longitudes from 102° W to 174° E. The LSWTs show an average warming of 0.04 $^{\circ}$C yr^{-1}, equivalent to 1.26 $^{\circ}$C from 1979 to 2011. The greatest warming has occurred in northern Europe, averaging 1.42 $^{\circ}$C, over the 33 year period. North America, Asia and the remainder of Europe show warming of 1.10 to 1.30 $^{\circ}$C, over the same period.

I discussed in chapter 1, section 1.1, the importance of understanding LSWT changes for commercial (fishing and transportation), recreational and ecological reasons. While the effect of LSWTs changes on transport and recreational activities may be more easily ascertained, for example by the presence or absence of lake ice, the ecological effect of LSWT changes requires more in depth investigation. The substantial warming in summer LSWTs shown for northern hemispheric lakes (Figure 69), are likely to be of great ecological importance and highlights lakes where the ecological effect of LSWT warming could be further investigated.

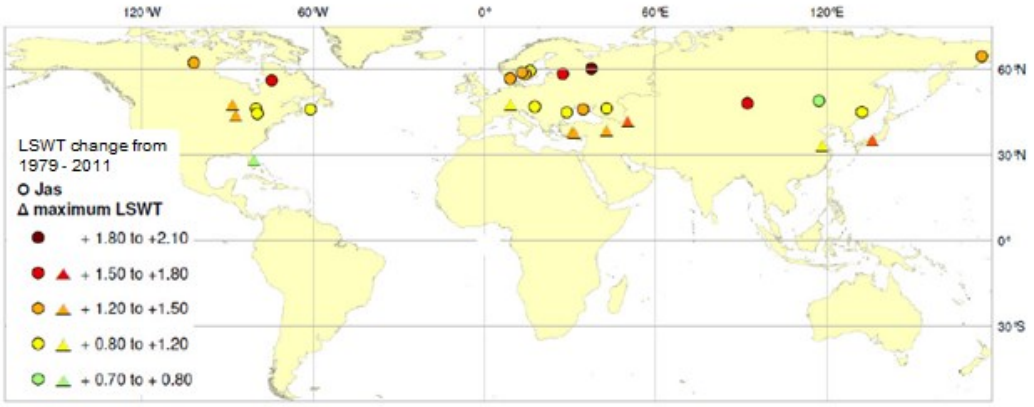

Figure 69 Statistically significant modelled JAS and maximum month LSWT changes from 1979 to 2011. Circles indicate JAS LSWT trends and triangles indicate maximum month LSWT trends (reproduction of figure 68 in chapter 6)

7.2 Conclusions

The conclusions are discussed in relation to the aims of this study, as outlined in section 1.3 of this thesis; 'LSWT climatological behaviour' and 'Expanding our knowledge of LSWTs worldwide by tuning a 1-dimensional model'.

7.2.1 LSWT climatological behaviour

My first research aim was to use the ARC-Lake LSWT observations to add to the understanding of the LSWT climatological behaviour of large lakes worldwide. This aim was met by quantifying the global scale responses of the LSWT annual cycle of the large lakes to annual cycles of air temperature and solar radiation, demonstrating useful findings. For example, netSSI can be used to estimate several features of the LSWT cycle of lakes globally and air temperature can strongly estimate the start and end of the open water phase. In a comparison between LSWT observations and LSWTs from a parametric fit, I showed that where they differed that *in situ* LSWTs from various sources supported the ARC-Lake observations.

This analysis demonstrates the suitability of using ARC-Lake observations in global scale studies, meeting the first research aim.

7.2.2 Expanding our knowledge of LSWTs worldwide using a 1-dimensional model

My second research aim was to develop a means of tuning a 1-dimensional model with ARC-Lake LSWT observations and then to use the tuned model to expand our knowledge on LSWT behaviour, both in terms of the LSWT climatology and changes over time. I achieved the second research aim by using the ARC-Lake lake-mean LSWT time-series to tune *FLake* and by assessing the tuned results, as discussed in section 7.1.3 to 7.1.5. The modelled biases for several features of the annual LSWT cycle demonstrate the level of improvement on the untuned model, as shown in Table 40. The aim of achieving an average MAD of < 1 ˚C was met; 0.80 ˚C $\pm$ 0.56 and 0.96 ˚C $\pm$ 0.66 for seasonally and non-seasonally ice covered lakes, respectively. There are many useful findings from this tuning study, for example, I demonstrated the how the LSWT regulating properties (depth, light extinction coefficient and albedo) and wind affect the modelled LSWT, highlighting that the whole annual cycle of deep and high latitude seasonally ice covered lakes are highly affected by a change in albedo. Additionally, I showed how the LSWT regulating properties (lake depth, albedo and light extinction co-efficient) optimised in the tuning process could be used to improve the LSWT modelling in *FLake* (untuned). Regionally and where justifiable, lake specific modelled trends over the 33 year period, 1979-2011 were reported. These demonstrated substantial warming in summer LSWTs northern hemispheric lakes, particularly those in northern Europe.

Several factors were encountered that placed limitations on the conclusion that can be drawn from this study. These are discussed in section 7.3.

7.3 Limitations

In this section, the limitations of the tuned model are discussed in relation to lakes with a relatively low LSWT annual range. I outline the limited conclusions that can be drawn from the relatively short ARC-Lake LSWT observational period (16-20 years) and from comparing IWBP nighttime LSWTs and the modelled LSWTs. The use of a latitudinal boundary to apply wind scaling to non-seasonally ice covered lakes is also discussed.

7.3.1 Modelling tropical, high altitude or southern hemisphere lakes

The modelled LSWTs capture less of the true (observed) inter-annual variability in lakes where the annual LSWT range is low, as discussed in section 6.5. It is for this reason that lakes with a low annual range are less well-represented in the model.

This also explains why there are no very high altitude lakes or low latitude lakes meeting the criteria for lake specific lake trends ($inter_{max}$ and $inter_{jas}$ fractions $\geq$ 0.70) in the northern hemisphere and no non-seasonally ice covered lakes meeting the criteria in the southern hemispheric. The 10 non-seasonally ice covered lakes, shown in Figure 69, are located from 28° N-48° N and have an average annual LSWT range of 18.8 °C, which is substantially higher than the average annual range of LSWTs of southern hemispheric lakes at corresponding latitudes, 10.1 °C.

This is possibly not directly due to the *FLake* model itself but moreso the difficulty in modelling the cycle in a system where the range is low. While the observed variance in the maximum and minimum LSWTs of temperate lakes is 4-5 times greater than in tropical lakes, the metrics results for the tropical and temperate lakes are comparable, Table 26. This indicates that the approach taken to tune the model for tropical lakes is not the cause of the poor representation of the inter-annual variability in the maximum and minimum LSWTs.

7.3.2 Comparing modelled and IWBP LSWTs

It is difficult to ascertain how meaningful it is to compare the IWBP and modelled LSWTs in this study, as the ARC-Lake LSWTs show a better comparison with the tuned and untuned model than the IWBP LSWTs (section 6.4.1). Additionally, given that the relationship between the ARC-Lake nighttime and day-night LSWT trends are not consistent across all lakes and regions (section 7.1.2.4), comparing IWBP nighttime LSWTs and the modelled LSWTs (representative of day-night average) may be less meaningful. An alternative approach would have been to tune *FLake* using the nighttime ERA meteorological forcing data. This would provide a better basis for comparing all 3 (model, IWBP and ARC-Lake) LSWTs sources. Furthermore, this would allow for a comparison of modelled and observed (IWBP) LSWTs over a longer period (27 years; from 1985-2011).

7.3.3 Trending period

In this study, the time series of ARC-Lake LSWTs is relatively short in terms of filtering out inter-annual variability. For almost half the lakes, the time series is ~16 years. As concluded in section 7.1.2.5, 20 years of LSWTs may be long enough to filter out much of the inter-annual variability, establishing reasonably meaningful LSWT trends.

This implies that where the trend comparisons (modelled v's observed ARC-Lake LSWTs) over the shorter 16 year period didn't agree well, it may be attributable to the length of time of the comparison period. On this basis, it is possible that if the time span of the observed data were longer than 16 years, there would have been a greater number of lakes with supported (modelled versus observed trends over the observed period) lake specific LSWT trends, than those shown in Figure 66.

7.3.4 Wind

For non-seasonally ice covered lakes, no wind speed scaling (*u1*) was applied for the tuning of lakes < 35° N/S and the highest scaling (*u3*) was applied for tuning lakes > 35° N/S. The scaling was applied due to the findings from trials 1-4, although some of the trial lakes didn't fall into the </>35° N/S boundary, as discussed in section 7.1.3.2. On this basis, it is possible that the applied wind scaling was not suitable for all non-seasonally ice covered lakes. The greater density difference between the maximum LSWT and the bottom layer during stratification for lakes at high latitudes than lake at low latitude lakes, is an indication of the buffering effect against wind. In section 7.4.2, I suggest investigating if the optimal wind speed scaling for modelling deep non-seasonally ice covered lakes can be better predicted by assessing density differences than latitude alone. This approach would also take lake depth into consideration, as depth has a bearing on the bottom temperature.

7.3.5 Regional analysis of results; an alternative approach

Within this study, the LSWTs are assessed regionally: for example, the climatologies of seasonally ice covered lakes (section 2.7) and LSWT summer trends for all lakes (section 6.4). Additionally, the model was tuned on the basis of seasonally and non-seasonally ice covered lakes.
In chapter 2, section 2.6.2, I highlighted that regional differences in LSWT behaviours are expected due to localized climate systems and regional variability in the limnic ratio. An alternative approach would be to assess LSWTs on the basis of ecoregion (regions defined by environmental conditions, in particular climate, landforms, and topography characteristics). For example, Olsen et al (2001) defines 14 biomes and 8 biogeographic (terrestrial) realms globally. However, with a greater number of eco-regions (and fewer number of lakes within each region), the assessment of lake characteristic influences within each region may be less detectable than if assessed by geographical region. Additionally, as previous LSWT

studies have been assessed on a geographical regional basis, the approach used in this study allows for a better comparison with previous studies. However, analysis on an eco-regional basis may allow for a more characterised approach to the assessment of trends. For example, it would be worth assessing, if the modelled and observed (ARC-Lake and IWBP) LSWT trends show better agreement in certain eco-regions. Analysis on the basis of eco-region may also be helpful in determining regions where lakes are more susceptible to ecological damage.

In section 7.1.2.3, I suggested that lakes with a greater LSWT annual range (and greater inter-annual variability in the maximum month / JAS LSWT) may be more susceptible to ecological damage than lakes with a smaller LSWT annual range. This also highlights a practical interpretation of the modelled results, var_{jas} and var_{max}. Though the inter-annual variability is generally low in tropical lakes and higher in temperate, analysing the lakes on the basis of eco-region may highlight specific regions where lakes are more susceptible to ecological damage.

7.4 Further work

On the basis of the findings and limitations of this research, further work is suggested. In this section, I suggest investigative work that may result in a better understanding of the LSWT diurnal range and in the application of a more suitable wind speed scaling for non-seasonally ice covered lakes. An approach for modelling smaller ARC-Lake lakes in *FLake* and for validating if ARC-Lake LSWTs can be used to assess changes in lake bottom temperatures is also discussed.

7.4.1 LSWT diurnal temperature range

As suggested in section 7.1.2.4, the LSWT diurnal extreme trends in the past two decades may not be reflecting air temperature diurnal extreme trends.

With the availability of both daytime and nighttime ARC-Lake LSWT observations, investigating the causes of the inter-lake variability in changes in the diurnal LSWT extremes would be a very useful and informative application of the ARC-Lake observations. This work could answer climate response questions, for example, do diurnal LSWT extreme changes reflect diurnal air temperature extreme changes in some regions? Other meteorological factors such as cloud cover, wind and nighttime air temperature-LSWT differences could be considered. Having shown that lakes with a larger LSWT annual range show greater observed inter-annual variability in the extremes, it is worth investigating if there is any relationship between the LSWT diurnal temperature range and the variability in the diurnal LSWT extremes, as this could have ecological implications.

Lake characteristics such as altitude and depth could also be considered. This could answer questions, such as, are diurnal LSWT extreme changes more strongly related to diurnal air temperature extreme changes in shallow lakes than in deep lakes or in low altitude lakes than in high altitude lakes?

7.4.2 Model wind speed for non-seasonally ice covered lakes

As discussed in chapter 3, section 3.4, wind speed over large areas of water it can be considerably stronger than wind measured over land. For non-seasonally ice covered lakes, I applied a wind scaling for lakes > 35° N/S. For lakes < 35° N/S, no scaling was applied. To investigate if the optimal wind speed scaling for the modelled LSWTs of all non-seasonally ice covered lakes can be better predicted by factors other than a latitudinal boundary, modelling of LSWTs using all 3 wind speed scalings (a repeat of trial 1 applied to all 84 lakes) could be carried out. Light extinction coefficient (if unknown) and lake depth as recommended in section 7.1.4.2, should be applied in this study. It is expected that evaluating the density difference between maximum month LSWT and the minimum month LSWT for deep lakes (indication of the buffering effect against wind induced mixing) would

allow for a good prediction of wind speed scaling. If this is the case, the optimal modelled wind speed scaling of shallow lakes should be better represented using the unscaled wind speed, as there will be little or no density gradient in shallow lakes and therefore there will be no buffering effect.

Wind speed could also be a factor in optimised wind speed. It is worth expanding the relationship between density difference between maximum and minimum month LSWT of deep lakes and the optimised wind speed scaling to include the average annual wind speed or wind speed during stratification. A good estimate of the stratification period could be determined using *FLake* (perpetual hydrological year). The wind speed during this period could be extracted from the ERA model forcing wind speed data. It is possible that for a lake where the wind speed is relatively low and density gradient is high, modelling with a higher scaling may result in more representative LSWTs than with a lower or no wind speed scaling. This work would allow for a greater understanding of the role that wind plays in non-seasonally ice covered lakes and would also validate the most suitable wind speed scaling for modelling the LSWTs of non-seasonally ice covered lakes in *FLake*.

7.4.3 Modelling smaller lakes in *FLake*

Under the ARC-Lake project, the techniques have now been developed to derive the LSWTs of smaller lakes (surface area < 100 km^2). The final list of target lakes is expected to be in the order of 1000 lakes, improving the global coverage, as shown in Figure 70. While the LSWTs in analysed in this study were derived a fixed (in time) land mask, a temporally varying lake mask was derived and used in determining the LSWTs of the smaller lakes (Figure 70). This was carried out using the visible channels of the ATSRs in a water detection algorithm.

Modelling the LSWTs of these smaller lakes has the potential to provide long term trends for ~1000 small lakes, expanding on the insights gained on LSWT behaviour

in this study of large lakes. The tuning process in this study used for the large lakes, could be applied to the small lakes. This would allow for like-for-like comparisons to be made between large and small lakes.

Alternatively, a simpler approach (without tuning) could be used for modelling the smaller lakes in *FLake*. Applying the depth factors, light extinction coefficients and albedo values suggested in section 7.1.4.2, may result in lower modelled LSWT biases, than if modelled using the default/ recommended modelled setting. Irrespective of the approach, the biases can be quantified using the observational LSWTs, as was done for this study, Appendix III. For these smaller lakes, the fetch will be less than 16 km, in which case, as discussed in chapter 3, a wind speed scaling of 1.2 is considered a reasonable wind speed scaling. Alternative wind speed scaling for these smaller lakes could be investigated as outlined in section 7.4.2.

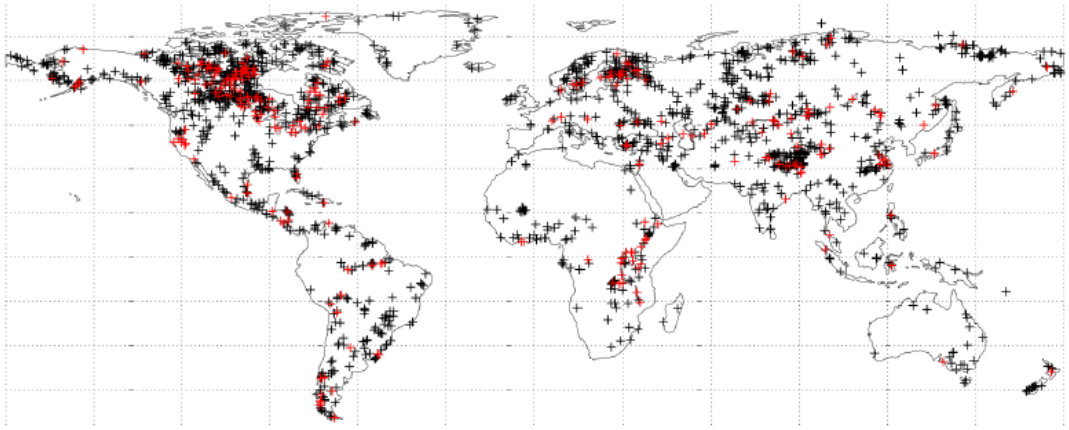

Figure 70 Locations of ARC-Lake target lakes showing lakes > 500 km^2 (red symbols) and additional targets for lakes < 100 km^2 (black symbols)

7.4.4 Using ARC-Lake LSWTs to assess changes in lake bottom temperatures

I demonstrated that the observed minimum month LSWT climatology (1992-2011) is strongly reflected in the modelled lake bottom temperature of *FLake*, during stratification. This indicates that LSWT observations could be used to infer lake bottom temperatures of stratified lakes, negating the need to carry out *in situ* lake bottom measurements.

Further validation work is being suggested, to assess (for the same lakes used in the analysis) if this relationship is applicable to *in situ* bottom temperature (where available). This will demonstrate if the *in situ* bottom temperatures reflect the climatological minimum month LSWTs, and would also in the process validate the bottom temperatures modelled in *FLake.*

The comparison between the minimum month LSWT climatology (1992-2011) and modelled lake bottom temperatures, encompassed a wide range of temperatures (from 4 $^{\circ}$C - 27 $^{\circ}$C), as shown in chapter 5, Figure 47. This comparison does not assess how accurately the modelled bottom temperature or the observed minimum month LSWT may infer subtle lake bottom changes over time. For this assessment, a comparison between the observed minimum month LSWTs and the modelled and *in situ* lake bottom temperatures over a 20 year period is required. It would be suffice to demonstrate this using a few lakes at varying latitudes.

7.5 The final word

Through the course of this research, I have generated wholly new climatological analysis of LSWTs worldwide, systematically quantifying the relationship between many features in the meteorological and LSWT annual cycle. I developed an approach to tuning model LSWTs where basic information is lacking or difficult to find. Through the systematic tuning approach, I showed that the tuned values for the LSWT regulating properties are sensible and greatly improve the modelled LSWTs in *FLake*, a lake model that is important in the scientific community. This also gives a precedent that can inform the evaluation and tuning of other lake models in future.

I demonstrated that certain characteristics of lakes are indicators of lake sensitivity to climate change or variability. For example, the whole LSWT cycle of very deep lakes or deep high latitude lakes are strongly affected by changes in ice-off and lakes with a large annual LSWT range show more variability in their extremes. These more sensitive lakes may be at increased risk of ecological damage, resulting in wider societal impacts. This is particularly relevant in remote areas where large riparian communities depend on lakes for their livelihood and for freshwater.

The potential exists to use these findings to influence policy-makers in areas of environmental regulation. For example, more rigorously enforced pollution control policies and measures are of particular importance for lakes that are already at risk from algae blooms from increased summer LSWTs. The reduction in the dissolved oxygen content of warming lakes is exacerbated by the effects of pollution (and vice versa) further increasing the risk of algae blooms in summer. Furthermore, given the well-established link between climate change and the increase in greenhouse gases (GHG) emissions, stricter policies for the reduction of GHG emissions may provide long term protection of sensitive lakes.

References

Armengol, J., L. Caputo, M. Comerma, C. Feijoó, J. C. García, R. Marcé, E. Navarro and J. Ordoñez, 2003. Sau reservoir's light climate: relationships between Secchi depth and light extinction coefficient. *Limnetica 22(1-2): 195-210 (2003) Asociación Española de Limnología, Madrid. Spain. ISSN: 0213-8409* 22:195-210.

Arst, H. and A. Reinart, 2009. Application of optical classifications to North European lakes. *Aquatic Ecology* 43:789-801.

Ashton, G. D., 1986. River and Lake Ice Engineering. Water Resources Publication, Littleton, CO, p. pp 355.

Austin, J. and S. Colman, 2008. A century of temperature variability in Lake Superior. *Limnology and Oceanography 53:* 53, DOI: 10.4319/lo.2008.53.6.2724

Austin, J. A. and S. M. Colman, 2007. Lake Superior summer water temperatures are increasing more rapidly than regional air temperatures: A positive ice-albedo feedback. *Geophysical Research Letters* 34.

Benson, B. and J. Magnuson, 2000. Global lake and river ice phenology database, updated 2007. Boulder, CO: National Snow and Ice Data Center/World Data Center for Glaciology. Digital media.

Bernhardt, J., C. Engelhardt, G. Kirillin and J. Matschullat, 2012. Lake ice phenology in Berlin-Brandenburg from 1947-2007: observations and model hindcasts. *Climatic Change* 112:791-817.

Boehrer, B. and M. Schultze, 2008. Stratification of lakes. *Rev. Geophys.* 46, DOI: 10.1029/2006rg000210.

Brown, L. C. and C. R. Duguay, 2010. The response and role of ice cover in lake-climate interactions. *Progress in Physical Geography* 34, DOI: 10.1177/0309133310375653

Bukata, R. P., J. H. Jerome and J. E. Bruton, 1988. Relationships among secchi disk depth, beam attenuation coefficient, and irradiance attenuation coefficient for great-lakes waters. *J. Gt. Lakes Res.* 14

Carlson, R. E., 1977. Trophic State Index for Lakes. *Limnology and Oceanography* 22:361-369.

Carvalho, L., A. G. Solimini, G. Phillips, O.-P. Pietilainen, J. Moe, A. C. Cardoso, A. L. Solheim, I. Ott, M. Sondergaard, G. Tartari and S. Rekolainen, 2009. Site-specific chlorophyll reference conditions for lakes in Northern and Western Europe. *Hydrobiologia* 633:59-66.

Crosman, E. T. and J. D. Horel, 2009. MODIS-derived surface temperature of the Great Salt Lake. *Remote Sens. Environ.* 113:73-81.

Descy, J.-P., F. o. Darchambeau, M. Schmid and A. WÃ¼est, 2012. Stratification, Mixing and Transport Processes in Lake Kivu. *In*: *Lake Kivu.* Springer Netherlands, pp. 13-29.

Donat, M. G., L. V. Alexander, H. Yang, I. Durre, R. Vose, R. J. H. Dunn, K. M. Willett, E. Aguilar, M. Brunet, J. Caesar, B. Hewitson, C. Jack, A. M. G. K. Tank, A. C. Kruger, J. Marengo, T. C. Peterson, M. Renom, C. Oria Rojas, M. Rusticucci, J. Salinger, A. S. Elrayah, S. S. Sekele, A. K. Srivastava, B. Trewin, C. Villarroel, L. A. Vincent, P. Zhai, X. Zhang and S. Kitching, 2013.

Updated analyses of temperature and precipitation extreme indices since the beginning of the twentieth century: The HadEX2 dataset. *Journal of Geophysical Research-Atmospheres* 118:2098-2118.

Donlon, C. J., P. J. Minnett, C. Gentemann, T. J. Nightingale, I. J. Barton, B. Ward and M. J. Murray, 2002. Toward improved validation of satellite sea surface skin temperature measurements for climate research. *Journal of Climate* 15:353-369.

Duguay, C. R., T. D. Prowse, B. R. Bonsal, R. D. Brown, M. P. Lacroix and P. Menard, 2006. Recent trends in Canadian lake ice cover. *Hydrological Processes* 20, DOI: 10.1002/hyp.6131

Dutra, E., V. M. Stepanenko, G. Balsamo, P. Viterbo, P. M. A. Miranda, D. Mironov and C. Schaer, 2010. An offline study of the impact of lakes on the performance of the ECMWF surface scheme. *Boreal Environ. Res.* 15:100-112.

Eccles, D. H., 1974. Outline of Physical Limnology of Lake Malawi (Lake-Nyasa). *Limnology and Oceanography* 19:730-742.

ECMWF, 2009. European Centre for Medium-Range Weather Forecasts. ECMWF ERA-Interim Re-Analysis data, [Internet]. . NCAS British Atmospheric Data Centre. 2009-, Sep - Nov 2012. Available from http://badc.nerc.ac.uk/view/badc.nerc.ac.uk__ATOM__dataent_12458543158227759. Sep - Nov 2012.

Francis-Floyd, R. and S. Florida Cooperative Extension, 1992. *Dissolved Oxygen for Fish Production*, Cooperative Extension Service, University of Florida, Institute of Food and Agricultural Sciences.

Gibbs, M., 2010. *Lake Taupo long-term monitoring programme 2008-2009.* Hamilton, National Institute of Water & Atmospheric Research Ltd

Haynes, W. M., 2013. *CRC Handbook of Chemistry and Physics, 94th Edition*, Taylor & Francis Limited.

Henneman, H. E. and H. G. Stefan, 1999. Albedo models for snow and ice on a freshwater lake. *Cold Regions Science and Technology* 29:31-48.

Herdendorf, C. E., 1982. Large Lakes of the World. *J. Gt. Lakes Res.* 8:379-412.

Holmes, R. W., 1970. Secchi Disk in Turbid Coastal Waters. *Limnology and Oceanography* 15:688.

Hook, S. J., F. J. Prata, R. E. Alley, A. Abtahi, R. C. Richards, S. G. Schladow and S. O. Palmarsson, 2003. Retrieval of lake bulk and skin temperatures using Along-Track Scanning Radiometer (ATSR-2) data: A case study using Lake Tahoe, California. *J. Atmos. Ocean. Technol.* 20:534-548.

Hook, S. J., R. C. Wilson, S. N. MacCallum and C. J. Merchant, 2012. : [Global Climate] Lake surface Temperature [in "State of the Climate in 2011"]. *Bulletin of the American Meteorological Society* 93 (7):S18-S19.

Horita, J., 2009. Isotopic Evolution of Saline Lakes in the Low-Latitude and Polar Regions. *Aquat. Geochem.* 15, DOI: 10.1007/s10498-008-9050-3.

Horne, J. and C. Goldman, 1994. *Limnology*. Singapore, McGraw-Hill Book Co.

Hsu, S. A., 1988. *Coastal Meteorology*. San Diego, USA, Academic Press Inc.

Hutchinson, G. E. and H. Loffler, 1956. The Thermal Classification of Lakes. *Proceedings of the National Academy of Sciences of the United States of America* 42:84-86.

ILEC, 1999. World Lake Database. International Lake Environment Committee Foundation

Imerito, A., 2013. *Dynamic reservoir simulation model DYRESM (User guide)* Centre for Water Research, Australia.

IPCC, 2012. *Summary for Policymakers. In: Managing the Risks of Extreme Events and Disasters to Advance Climate Change Adaptation*.

Jerlov, N. G., 1976. *Marine Optics*, Elsevier Scientific Publishing Company.

Jones, P. and I. Harris, 2008. CRU Time Series (TS) high resolution gridded datasets, [Internet].NCAS British Atmospheric Data Centre, . University of East Anglia Climatic Research Unit (CRU). April 2012 Available from http://badc.nerc.ac.uk/view/badc.nerc.ac.uk__ATOM__dataent_1256223773328276.

Jones, P. D., D. E. Parker, T. J. Osborn and K. R. Briffa, 2013. Global and hemispheric temperature anomalies-land and marine instrumental records. In Trends: A Compendium of Data on Global Change. . *Carbon Dioxide Information Analysis Center, Oak Ridge National Laboratory, U.S. Department of Energy, Oak Ridge, Tenn., U.S.A.*

Kamari, J., 2001. *Benchmark Models for the Water framework directive*, Finnish Environment Institute.

Kang, K. and C. R. Duguay, 2011. Monitoring ice phenology on Great Bear and Great Slave Lakes, Canada, from the synergy of spaceborne microwave and optical measurements. *In*: *American Geophysical Union, Fall Meeting 2011.* abstract #C21B-0471, San Francisco, CA.

Kirillin, G., 2010. FLAKE and deep lakes (email discussion), A. Layden. p. 1 page 26th July.

Kirillin, G., J. Hochschild, D. Mironov, A. Terzhevik, S. Golosov and G. Nutzmann, 2011. FLake-Global: Online lake model with worldwide coverage. *Environmental Modelling & Software* 26:683-684.

Kourzeneva, E., H. Asensio, E. Martin and S. Faroux, 2012. Global gridded dataset of lake coverage and lake depth for use in numerical weather prediction and climate modelling. *Tellus Series a-Dynamic Meteorology and Oceanography* 64.

LakeNet, 2003. LakeNet's global lake database. http://www.worldlakes.org Accessed Mar - May 2011.

Launiainen, J. and B. Cheng, 1998. Modelling of ice thermodynamics in natural water bodies. *Cold Regions Science and Technology* 27:153-178.

Layman, K. L., 2001. The dependence of freshwater lake ice covers on climate, lake morphology, and geographic location. *MS thesis , Univ. of Minnesota, Minneapolis (1955- 1996)*.

Lehner, B. and P. Doll, 2004. Development and validation of a global database of lakes, reservoirs and wetlands. *J. Hydrol.* 296, DOI: 10.1016/j.jhydrol.2004.03.028

Lenormand, F., C. R. Duguay and R. Gauthier, 2002. Development of a historical ice database for the study of climate change in Canada. *Hydrological Processes* 16, DOI: 10.1002/hyp.1235

Lerman, A., D. Imboden and J. Gat, 1995a. *Physics and Chemistry of Lakes*. Verlag berlin Heidelberg, Springer.

Lerman, A., D. Imboden, J. Gat and S. W. Hostetler, 1995b. Hydrological and Thermal Response of Lakes to Climate: Description and Modeling. *In*: *Physics and Chemistry of Lakes.* Springer Berlin Heidelberg, pp. 63-82.

Lewis, W. M., 1983. A revised classification of lakes based on mixing. *Can. J. Fish. Aquat. Sci.* 40:1779-1787.

Lewis, W. M., 1987. Tropical Limnology. *Annu. Rev. Ecol. Syst.* 18:159-184.

Lewis, W. M., 1996. Tropical lakes: How latitude makes a difference. *Perspectives in Tropical Limnology*:43-64.

Livingstone, D. M. and R. Adrian, 2009. Modeling the duration of intermittent ice cover on a lake for climate-change studies. *Limnology and Oceanography* 54, DOI: 10.4319/lo.2009.54.5.1709

Livingstone, D. M. and A. F. Lotter, 1998. The relationship between air and water temperatures in lakes of the Swiss Plateau: a case study with palaeolimnological implications. *J. Paleolimn.* 19, DOI: 10.1023/A:1007904817619

Livingstone, D. M., A. F. Lotter and I. R. Walker, 1999. The decrease in summer surf are water temperature with altitude in Swiss Alpine lakes: A comparison with air temperature lapse rates. *Arct. Antarct. Alp. Res.* 31, DOI: 10.2307/1552583

Loeb, N. G., B. A. Wielicki, D. R. Doelling, G. L. Smith, D. F. Keyes, S. Kato, N. Manalo-Smith and T. Wong, 2009. Toward Optimal Closure of the Earth's Top-of-Atmosphere Radiation Budget. *Journal of Climate* 22:748-766. DOI: 710.1175/2008JCLI2637.1171.

Long, Z., W. Perrie, J. Gyakum, D. Caya and R. Laprise, 2007. Northern lake impacts on local seasonal climate. *Journal of Hydrometeorology* 8:881-896.

MacCallum, S. N. and C. J. Merchant, 2010. *ATSR Reprocessing for Climate Lake Surface Temperature: ARC-Lake - Algorithm Theoretical Basis Document - v1.0*, School of GeoSciences, The University of Edinburgh.

MacCallum, S. N. and C. J. Merchant, 2012. Surface Water Temperature Observations of Large Lakes by Optimal Estimation. *Candian Journal of Remote Sensing* 38(1):25-45. DOI:10.5589/m5512-5010.

MacIntyre, S., J. R. Romero and G. W. Kling, 2002. Spatial-temporal variability in surface layer deepening and lateral advection in an embayment of Lake Victoria, East Africa. *Limnology and Oceanography* 47:656-671.

Magnuson, J. J., D. M. Robertson, B. J. Benson, R. H. Wynne, D. M. Livingstone, T. Arai, R. A. Assel, R. G. Barry, V. Card, E. Kuusisto, N. G. Granin, T. D. Prowse, K. M. Stewart and V. S. Vuglinski, 2000. Historical trends in lake and river ice cover in the Northern Hemisphere. *Science* 289, DOI: 10.1126/science.289.5485.1743

Manabe, S. and R. J. Stouffer, 1980. Sensitivity of a Global Climate Model to an Increase of Co2 Concentration in the Atmosphere. *Journal of Geophysical Research-Oceans and Atmospheres* 85:5529-5554.

Matishov, D., T. Orlova, Y. Gargopa and E. Pavel'skaya, 2007. Long-term variability in the hydrochemical regime of the Manych-Chograi hydrological system. *Water Resources* 34

Merchant, C. J., D. Llewellyn-Jones, R. W. Saunders, N. A. Rayner, E. C. Kent, C. P. Old, D. Berry, A. R. Birks, T. Blackmore, G. K. Corlett, O. Embury, V. L. Jay, J. Kennedy, C. T. Mutlow, T. J. Nightingale, A. G. O'Carroll, M. J.

Pritchard, J. J. Remedios and S. Tett, 2008. Deriving a sea surface temperature record suitable for climate change research from the along-track scanning radiometers. *Adv. Space Res.* 41:1-11.

Milius, A. and H. Starast, 1997. A three-parameter trophic state index for small lakes. *Proceedings of the Estonian Academy of Sciences Biology Ecology* 46:27-39.

Mironow, D. V., 2008. Parameterization of Lakes in Numerical Weather Prediction, Description of a Lake model. *In,* Editor (Editor)^(Editors). German Weather Service, Offenbach am Main, Germany.

Monson, B., 1992. A primer on limnology. Water Resources Center , University of Minnesota, St Paul, MN.

Muhindo, M. W. and A. Gidudu, 2012. Montoring the surface temperature of lake victoria using MODIS imagery. *In*: *The first Conference on Advances Geomatics Research.* Makerere University Kampala, Uganda. .

Palecki, M. A. and R. G. Barry, 1986. Freeze-up and Break-up of Lakes as an Index of Temperature-Changes during the Transition Seasons - a Case-Study for Finland. *Journal of Climate and Applied Meteorology* 25, DOI: 10.1175/1520-0450(1986)025<0893:FUABUO>2.0.CO;2.

Poole, H. H. and W. R. G. Atkins, 1929. Photo-electric measurements of submarine illumination throughout the year. *Jour Marine Biol Assoc United Kingdom* 16:297-324.

Pour, H. K., C. R. Duguay, A. Martynov and L. C. Brown, 2012. Simulation of surface temperature and ice cover of large northern lakes with 1-D models: a comparison with MODIS satellite data and in situ measurements. *Tellus Series a-Dynamic Meteorology and Oceanography* 64:DOI: 10.3402/tellusa.v3464i3400.17614

Reijmer, C. H., R. Bintanja and W. Greuell, 2001. Surface albedo measurements over snow and blue ice in thematic mapper bands 2 and 4 in Dronning Maud Land, Antarctica. *Journal of Geophysical Research-Atmospheres* 106:9661-9672.

Reinart, A. and M. Reinhold, 2008. Mapping surface temperature in large lakes with MODIS data. *Remote Sens. Environ.* 112:603-611. DOI: 610.1016/j.rse.2007.1005.1015

Resio, D. T., S. M. Bratos and E. F. Thompson, 2008. Meteorology and Wave climate. *In*: *Coastal Engineering Manual.* U.S. Army Corps of Engineers.

Revadekar, J. V., S. Hameed, D. Collins, M. Manton, M. Sheikh, H. P. Borgaonkar, D. R. Kothawale, M. Adnan, A. U. Ahmed, J. Ashraf, S. Baidya, N. Islam, D. Jayasinghearachchi, N. Manzoor, K. H. M. S. Premalal and M. L. Shreshta, 2013. Impact of altitude and latitude on changes in temperature extremes over South Asia during 1971-2000. *International Journal of Climatology* 33:199-209.

Riley, M. and H. Stefan, 1987. *Dynamic lake water quality simulation model 'MINLAKE'*. Minnesota, University of Minnesota.

Ritter, M. E., 2006. The Physical Environment: an Introduction to Physical Geography.

Saloranta, T. and T. Andersen, 2007. MyLake - A multi-year lake simulation model code suitable for uncertainty and sensitivity analysis simulations. *Ecological Modelling* 207:45-60.

Schneider, P. and S. J. Hook, 2010. Space observations of inland water bodies show rapid surface warming since 1985. *Geophysical Research Letters* 37.

Schneider, P., S. J. Hook, R. G. Radocinski, G. K. Corlett, G. C. Hulley, S. G. Schladow and T. E. Steissberg, 2009. Satellite observations indicate rapid warming trend for lakes in California and Nevada. *Geophysical Research Letters* 36.

Sherwood, I., 1974. *On the Universality of the Poole and Atkins Secchi Disk-light Extinction Equation*, U.S. Water Conservation Lab.

Stephens, A., 2000. Long-term variability in offshore wind speeds. University of East Anglia.

Strahler, A. N. and A. H. Strahler, 1989. *Elements of Physical Geography*, Wiley.

Straskraba, M., 1980. The Effects of Physical Variables on Fresh Water Production Analyses Based on Models. *In*: *The Functioning of Freshwater Ecosystems,* E. D. Le Cren and R. H. Lowe-Mcconnell (E. D. Le Cren and R. H. Lowe-Mcconnell(E. D. Le Cren and R. H. Lowe-Mcconnells). Cambridge University Press, Cambridge, pp. P13-84.

Sun, D., Y. Li, Q. Wang, C. Le, H. Lv, C. Huang and S. Gong, 2012. Specific inherent optical quantities of complex turbid inland waters, from the perspective of water classification. *Photochemical & Photobiological Sciences* 11:1299-1312.

Thompson, R., M. Ventura and L. Camarero, 2009. On the climate and weather of mountain and sub-arctic lakes in Europe and their susceptibility to future climate change. *Freshw. Biol.* 54, DOI: 10.1111/j.1365-2427.2009.02236.x.

Vadineanu, A., S. Cristofor, G. Ignat, G. Romanca, C. Ciubuc and C. Florescu, 1997. Changes and opportunities for integrated management of the Razim-Sinoe Lagoon System. *International Journal of Salt Lake Research* 6:135-144.

Vincent, W., 2009. Effects of Climate Change on Lakes. *Pollution and Remediation*.

Vollmer, M. K., H. A. Bootsma, R. E. Hecky, G. Patterson, J. D. Halfman, J. M. Edmond, D. H. Eccles and R. F. Weiss, 2005. Deep-water warming trend in Lake Malawi, East Africa. *Limnology and Oceanography* 50, DOI.

Voros, M., V. Istvanovics and T. Weidinger, 2010. Applicability of the FLake model to Lake Balaton. *Boreal Environ. Res.* 15:245-254.

Vose, R. S., D. R. Easterling and B. Gleason, 2005. Maximum and minimum temperature trends for the globe: An update through 2004. *Geophysical Research Letters* 32.

Vyverman, W. and K. Sabbe, 1995. Diatom-Temperature Transfer-Functions Based on the Altitudinal Zonation of Diatom Assemblages in Papua-New-Guinea - a Possible Tool in the Reconstruction of Regional Paleoclimatic Changes. *J. Paleolimn.* 13, DOI: 10.1007/BF00678111

Wessel, P. and W. H. F. Smith, 1996. A global, self-consistent, hierarchical, high-resolution shoreline database. *J. Geophys. Res.-Solid Earth* 101:8741-8743.

Wetzel, R., 1975. *Limnology*. Holt, Saunders college Publishing.

Weyhenmeyer, G. A., M. Meili and D. M. Livingstone, 2004. Nonlinear temperature response of lake ice breakup. *Geophysical Research Letters* 31, DOI: 10.1029/2004GL019530

Williams, G. P., 1965. Correlating freeze-up and break-up with weather conditions. *Candian Geotechnical Journal* II:313-326.

Williams, S. G. and H. G. Stefan, 2006. Modeling of lake ice characteristics in North America using climate, geography, and lake bathymetry. *Journal of Cold Regions Engineering* 20, DOI: 10.1061/(ASCE)0887-381X(2006)20:4(140)

Williams, W. D., 1962. A contribution to lake typology in Victoria, Australia. *Int Ver Theor Angew Limnol Verh* 15:158-168.